SAN ONOFRE NUCLEAR GENERATING STATION (SONGS)
SONGS MEAN SEA LEVEL RISE IMPACT ASSESSMENT

Technical Report for
CSLC Special Provision 14 in Lease No. PRC 6785.1

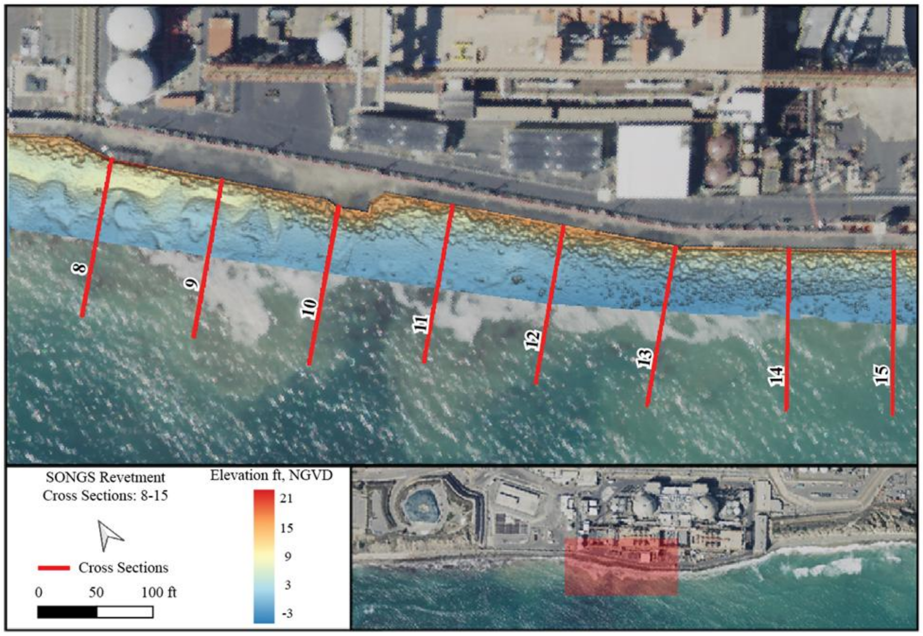

by

Hany Elwany, Ph.D.
Reinhard E. Flick, Ph.D.
Frederico Scarelli, Ph.D.

for

Southern California Edison
2244 Walnut Grove Avenue
Rosemead, CA 91770

Coastal Environments, Inc.
2166 Avenida de la Playa, Suite E
La Jolla, CA 92037

CE Reference No. 21-07
25 March 2021

TABLE OF CONTENTS

LIST OF APPENDICES

LIST OF TABLES

LIST OF FIGURES

LIST OF PHOTOGRAPHS

EXECUTIVE SUMMARY

This report is being written to comply with California State Lands Commission Special Provision 14 for standards addressing sea level rise that may be required or adopted by local, state, or federal agencies related to the Lease Premises. The report presents the current information about sea level rise projections from the state and federal agency guidelines, assessments for San Onofre beach and the San Onofre Nuclear Generating Station (SONGS) revetment walkway and seawall, and the impacts of Mean Sea Level Rise (MSLR) on SONGS, including the premises located east of the seawall, such as the Independent Spent Fuel Storage Installation (ISFSI) and its Security Building, and the adaptive capacity of the Lease Premises and facilities therein. The report presents:

a. MSLR and beach profile assessments, site photographs taken in 2020 of shoreline structures such as riprap, walkways, and seawalls, and descriptions of repair and maintenance operations of shoreline structures. The sea level rise vulnerability information considered the Medium-High Risk Aversion (0.5% probability) projection scenarios from the most recent state guidance (issued by the Ocean Protection Council [OPC] every five years), as well as the extreme H++ projection scenario, in combination with the annual and 20-year events, as well as extreme high tide heights ("King Tides"). Pertinent information may be sourced from Southern California Edison (SCE) or any other research conducted within the region that is relevant to conditions at the Lease Provision 14(a).
b. Quarterly groundwater elevation data collected from onsite monitoring wells relevant to conditions at Lease Provision 14(b).

Chapter 1 presents the overall structure of this report and provides a summary of the key information presented in this study with emphasis on the main points outlined in Special Provision 14.

Projections of future MSLR are evolving continuously as the understanding of key climate change processes improves (Chapter 2). In Sections 2.1.1 to 2.1.3, we summarize the currently existing guidelines, which are so far unchanged from last year. Recent global and regional studies published in reviewed papers in 2020 are discussed in Section 2.1.4. In Section 2.1.5, we have reviewed four new California state agency documents that provide updated MSLR policy and plans or other information that potentially affects future projections of MSLR.

The beach prevents toe scouring, which can undermine the revetment and cause rock units to settle. When the beach is narrow or water level unusually high, or both, waves breaking on the revetment can cause dislocation of individual rocks, which contributes to revetment instability. Section 3.7 gives a summary of San Onofre Beach assessments based on SCE's beach monitoring program at San Onofre Beach from 1964 to the present, with gaps, presented in Appendix E. Selected photographs of the beach taken in 2020 are also presented in Appendix D. These insights will be valuable assuming sea level rise accelerates in the future. Elwany et al. (2017) have addressed the impacts of sea level rise on San Onofre Beach.

The assessment of the SONGS revetment is reviewed in Chapter 3. Revetment maintenance carried out in 2018 and 2019 is summarized in Section 3.1.1. In Section 3.2 and Appendices A, B, C, and D, we gauge the current revetment condition and describe the characteristics of the riprap, namely rock, and dimension and weight distributions, based on a site inspection carried out on 25 February 2021. Sections 3.3-3.6 discuss factors influencing revetment stability. We evaluate the revetment stability based upon these observations and standard coastal engineering criteria (Sections 3.8-3.10).

During November 2020 and the period between 25 January 25 and 21 February 2021, the revetment was subject to large waves with heights varying between 2 m (6.6 ft) and 4.34 m (14.2 ft) and short periods of about 8 seconds. The observed 4.34 m waves were higher than the previously estimated wave height for the 100-year-return period, which is 3.8 m (12.5 ft). Despite the long duration of these large waves, the damage to the revetment and walkway was minimal. This study finds that the revetment, in its present condition, is likely to tolerate wave forces with acceptable rock movement that will not affect the integrity of the revetment as a whole. The study found that, as designed and with regular maintenance, the revetment will withstand wave forces over the next 30 years (Sections 3.9 and 3.10). The revetment, retaining wall, and walkway also provide additional protection to the SONGS seawall. Appendix C presents historical aerial photographs of the revetment for the period from 2003 to 2020. Photographs taken during the 25 February 2021 site visit are shown in Appendix D.

Section 3.10 addresses the maintenance and adaptive capacity of the Lease Premises. The major threats to revetment stability in the future include wave storms, or clusters of wave storms, such as those that occurred from 1981 to 1983. In this respect, the revetment's adaptive capacity to MSLR is high, in the sense that its current stable condition, along with occasional maintenance, will allow it to continue functioning as intended.

Effects of groundwater on the ISFSI based on quarterly measurements of the groundwater from 9 coastal wells out of 16 total wells are presented in Appendix F. The OPC (2018) medium-high (0.5%) and H++ SLR scenarios for groundwater elevation for 2050 are 4.43 and 5.23 ft National Geodetic Vertical Datum (NGVD) (Section 2) and are 1.54 and 0.74 ft lower than the bottom of the ISFSI support foundation, respectively. The ISFSI support foundation is 3 ft thick. Therefore, the data shows that there are no impacts from the groundwater on the ISFSI support foundation. The values obtained from the measurements obtained in 2020 are 0.19 ft lower than the values for 2019. Next reports will start trending the changes of groundwater elevation to monitor the transitory high groundwater levels at the bottom of the ISFSI support foundation.

The analysis of vulnerability of the revetment to wave run-up and overtopping of the revetment is presented in Chapter 4. This study considers the Medium-High Risk Aversion projection (0.5%) and extreme H++ projection scenarios from the most recent state guidance issued by the OPC (2018) in combination with the annual, 2-, 5-, 10-, 25-, 50-, and 100-year wave return period wave and high water events, which include storm surges and King Tides. Our conclusions are stated in Chapter 5, where we found that the revetment in its present condition, and with regular maintenance, is likely to tolerate wave forces with acceptable rock movement that will not affect its integrity as a whole over the next 30 years.

SAN ONOFRE NUCLEAR GENERATING STATION (SONGS) SONGS MEAN SEA LEVEL RISE IMPACT ASSESSMENT

Technical Report for CSLC Special Provision 14 in Lease No. PRC 6785.1

1.0 INTRODUCTION

This report has been prepared per Special Provision 14 in the California State Lands Commission (CSLC) Lease No. PRC 6785.1 for the use, maintenance, and decommissioning of existing offshore improvements associated with the San Onofre Nuclear Generating Station (SONGS). Special Provision 14 requires, as part of compliance with applicable provisions or standards addressing sea level rise that may be required or adopted by local, state, or federal agencies related to and affecting the lease premises, that the Lessee provide an annual summary, including information related to sea level rise vulnerability, structural integrity, and adaptation capacity of the Lease Premises and the facilities therein.

The information in this report includes sea level rise discussion and beach profile assessments, annual site photographs of shoreline facilities (i.e., riprap, pedestrian walkway, and seawall), and description of repair and maintenance operations for shoreline protection structures. Sea level rise vulnerability information considers the Medium-High Risk Aversion (0.5% probability) projection scenarios from the most recent state guidance (updated by the Ocean Protection Council [OPC] every five years), as well as the extreme H++ projection scenario, in combination with the annual, 20-year, and 100-year storm events, as well as with extreme high tide heights (King Tides). Pertinent information has been sourced from Southern California Edison (SCE), surveys and study by Coastal Environments, Inc. (CE), scientific and state agency literature review, water level and wave data, and quarterly groundwater elevation data collected from onsite monitoring wells, and other research conducted within the region that is relevant to conditions at the Lease Provision 14(b).

In Chapter 2 of this report, we summarize the present knowledge of mean sea level rise (MSLR), which is constantly evolving due to the rapid pace of data acquisition and scientific understanding, especially concerning the long-term consequences of accelerating ice sheet melt in Greenland and Antarctica. We present agency guidance current as of 2018 with the associated MSLR projections to determine impacts on the SONGS shoreline and cliffs, and the likelihood of wave overtopping of the seawall described in Elwany et al. (2016 and 2017).

The SONGS revetment and retaining wall is essential to maintaining the walkway that enables safe lateral access for beach users. The revetment and retaining wall shelter the walkway from most wave run-up and overtopping, thus preventing or reducing negative impacts to lateral beach access due to flooding and other hazards of high water levels and waves. These also eliminate almost all wave impacts on the SONGS seawall.

The assessment of the SONGS revetment is reviewed in Chapter 3. In Chapter 3, we also determine the current revetment, retaining wall, and walkway exposure and vulnerability to waves and high water level events by gauging their present condition. We describe the characteristics of the riprap, namely rock, and dimension and weight distributions, based on a site inspection in February 2021. We evaluate its stability based upon these observations and standard coastal engineering criteria. The importance of the sand beach fronting the revetment is discussed in Section 3.7, along with the recent characteristics of the beach nearby SONGS and observed short- and long-term erosion and accretion patterns based on the ongoing beach profile surveys carried out in 2017-2020 (CE, 2020).

Additionally, in Section 3.10, we discuss the adaptive capacity of the Lease Premises and present an adaptive management plan to maintain the facilities, including the revetment, walkway, and seawall shoreline protection structures, and the Independent Spent Fuel Storage Installation (ISFSI) and its Security Building in good condition during the lease agreement.

MSLR will likely increase both the wave forces on the rocks (due to greater water depth and wave height fronting the revetment), and sand scour undermining that could lower and destabilize the revetment (due to beach retreat). This study considers the Medium-High Risk Aversion projection (0.5%) scenarios from the most recent state guidance (OPC, 2018), as well as the extreme H++ projection scenario, in combination with the annual, 2-, 5-, 10-, 25-, 50-, and 100-year return period wave and high water events, which include King Tides. The vulnerability of the revetment to wave run-up and overtopping are presented in Chapter 4.

Our study finds that the revetment in its present condition, and with regular maintenance, is likely to tolerate wave forces with acceptable rock movement that will not affect its integrity as a whole over the next 30 years.

The walkway at elevation 14 ft (National Geodetic Vertical Datum [NGVD]) behind the revetment and retaining wall is relatively low and likely will be flooded under large wave conditions, especially if these occur during extreme high water levels. However, the impact of wave run-up and overtopping on the walkway itself or on public access is limited and temporary, since the beach will not be accessible during such conditions, and floodwater has adequate drainage from the site and off the public walkway. Our major conclusions are stated in Chapter 5.

Chapter 6 provides a reference list, followed by six Appendices (A-F). Appendices A, B, C, and D provide information regarding the 25 February 2021 survey carried out at the SONGS revetment, including the location of the transects, the profiles analyzed along the riprap, and the photographs taken during the survey. Appendix E presents our assessment of the San Onofre Beach and the results of the beach profile surveys carried out at San Onofre Beach from 2017-2020. Appendix F is written in compliance with Provision 14b; this Chapter discusses the groundwater elevations measured quarterly in 2020 and the MSLR impacts on the ISFSI up to 2050. The 2020 quarterly groundwater elevation monitoring program was carried out by SONGS Decommissioning Solutions (SDS).

2.0 MEAN SEA LEVEL RISE IMPACT ASSESSMENT

2.1 MEAN SEA LEVEL RISE GUIDANCE

Projections of future MSLR continue evolving as understanding of key climate change processes improves. Of special concern are the possible ranges and rates of glacial ice loss in Greenland and Antarctica (e.g., DeConto and Pollard, 2016). Future MSLR is highly uncertain, especially after about 2050, for several reasons. The largest unknown is what mitigation strategies humans will employ to decrease the rates and amounts of greenhouse gas (GHG) emitted and ultimately resident in the atmosphere. Second, the climate sensitivity, or amount and rate of warming for a given increase in GHGs is not precisely known. Third, polar ice response to warming is not yet accurately predictable.

This section provides a discussion of MSLR vulnerability of the revetment fronting SONGS and an update of the sea level information presented in Elwany et al. (2020). This includes a summary of existing State of California guidance, 2020 mean sea level (MSL) data and the relation of measurements and projections of future MSLR since 2000, 2020 monthly peak total water level data, a review of recently published scientific literature potentially influencing future MSLR projections (and therefore state guidance), and an update of 2020 California state agency developments with respect to MSLR that may impact SONGS deconstruction. A short discussion of possible MSLR-related changes in groundwater level appears at the end of this section.

2.1.1 Mean Sea Level Rise Vulnerability

CE has updated the vulnerability, structural integrity, and adaptive capacity assessment of the revetment, retaining wall, and walkway to MSLR impacts as defined by the CSLC Lease provided in the previous report in this mandated SONGS sea level rise impact assessment series (Elwany et al., 2020). The revetment provides partial protection to the SONGS sea wall, is essential to maintaining the walkway enabling safe lateral access for beach users, and shelters the walkway and the SONGS seawall from wave run-up and overtopping preventing or reducing flooding and other hazards from high water levels and waves.

This update was carried out by conducting a physical inspection of the revetment and walkway on 25-26 February 2021 and gauging their present condition to assess current exposure and vulnerability to design wave and high water level events (including King Tides). CE has continued our inspection surveys using Terrestrial Laser Scanning (TLS) annually to track changes in the integrity of the revetment and the walkway. CE will continue close cooperation with the Decommissioning Environmental Strategy Team (DEST), SCE engineers, and maintenance crews at SONGS.

2.1.2 California State MSLR and Guidance Summary

With one important caveat concerning a potential increase in the maximum MSLR guidance target value from 2.8 ft to 3.5 ft by 2050 that is discussed in detail in Section 2.1.5 below, the currently existing guidance, so far unchanged from last year, is summarized herein.

Current MSLR guidance values and their associated probability ranges are contained in OPC (2018) and California Coastal Commission (CCC, 2015; updated 2018). Table 2-1 lists the MSLR projections for La Jolla, CA (relevant for conditions at SONGS) to 2050 from OPC (2018). For additional details, please refer to Elwany et al. (2020).

The projections in Table 2-1 have probability range estimates associated with them. These originated from IPCC AR5 (2013) by calculating probabilities of "representative concentration pathways" (RCP) scenarios. Each RCP has a numerical designation condensing a host of factors into a final average global radiation imbalance in Watts/m^2 by 2100. The full range was RCP2.6 to RCP8.5, respectively from low to high. Thus "RCP4.2" represents a (moderate) GHG trajectory that results in a net radiative imbalance of 4.2 Watts/m^2 by 2100. The probability estimates use the framework of Kopp et al. (2014).

From 2000-2050, only the "High" MSLR trajectory is considered in OPC (2018). This is based on two factors: first, there are no ambitious global GHG emissions reduction plans presently apparent; and second, even if emissions immediately dropped to net-zero, warming and MSLR are assumed to continue for at least several more decades owing to climate inertia. In effect, both High and Low trajectories produce near-identical projections between 2000 and 2050, and only begin to differ after mid-century.

Table 2-1 shows five columns (Columns 2-6) headed with percentage probability numbers, and one (Column 7) indicated as H++. Column 2 titled "50%" indicates the median projected MSLR each year (Column 1) relative to 2000. That means, for example, there is a 50:50, or "even" chance that MSLR will be less than or greater than 0.9 ft by 2050. Columns 3-4 titled "> 67% <" bracket the 2/3 probability that MSLR will fall between these numbers. In other words, it is 2/3 likely that MSLR will reach between 0.7-1.2 ft by 2050. Columns 5 and 6, respectively, provide the MSLR that has a 5%, or "1 in 20," and a 0.5% or "1 in 200" chance of being exceeded. This means there is only a 1 in 200 chance that MSLR will reach or exceed 2 ft by 2050. The H++ scenario (Column 7) is included in OPC (2018) to account for the now still remote possibility that *"...rapid ice sheet loss on Antarctica could drive rates of sea level rise in California above 50 mm/year (2 inches/year) by the end of the century, leading to potential sea level rise exceeding 10 feet. This rate of sea level rise would be about 30-40 times faster than the sea level rise experienced over the last century."*

CE calculated annual MSL elevation for 2020 from monthly measurements at La Jolla, CA, routinely compiled and published by the National Oceanic and Atmospheric Administration's (NOAA) National Ocean Service (NOS) for all U.S. tide stations.[1] Figure 2-1 illustrates the OPC (2018) trajectories described above, along with the actual average annual and monthly MSL data measured at the La Jolla tide gauge (941-0230) located at the end of Scripps Institution of Oceanography (SIO) pier where data collection begin in 1925. The observations shown were adjusted so that their average over the 19-year epoch (1991-2009) centered on year

[1] https://tidesandcurrents.noaa.gov/waterlevels.html?id=9410230

2000 was zero to facilitate comparison with projections beginning in 2000 (see Flick et al., 2013).

The all-time maximum annual average sea level 2015 value (circled) of 0.4 ft above 1991-2009 mean resulted from the 2015-16 El Niño. Figure 2-1 shows that all annual average, except 2015, so far fall close to or below the 50-50 trajectory (blue broken line). This could be interpreted to mean that the projections since 2000 overestimate MSLR. However, as Figure 2-1 indicates, the natural inter-annual variability range is about 0.5 ft, while the seasonal and other variations in monthly means ranges about 1.2 ft, which is larger than the current difference between the highest and lowest scenarios (~0.4 ft). Which trajectory MSLR is actually on should become more apparent approaching mid-century (2030-2050), when projected values increase significantly and their range broadens to 1-2 ft.

2.1.3 Sea Level Extremes

It is important to remember that water elevation at or around MSL generally does not cause flooding, erosion, or infrastructure damage. Damages almost always occur during times of extreme high water levels that, on the California coast, are driven mainly by coincidence of peak high tides and large storm waves. Elevated water levels due to El Niño and other large-scale oceanographic phenomenon also raise maximum water levels for months to several years. Of course, continued and likely accelerated MSLR will continuously worsen these effects causing them to become more severe and last longer. For further details, see Elwany et al. (2020).

Observed maximum monthly water levels published by NOAA-NOS for La Jolla are presented in Figures 2-2A and 2-2B, which are updated from Elwany et al. (2020). Figure 2-2A shows the data plotted relative to the NAVD88 datum, which is the official national standard supported by NOAA's National Geodetic Survey (NGS), and used by surveyors and engineers. Figure 2-2B shows the same data plotted relative to the legacy NGVD (also called NGVD29 or MSL29), which lay close to MSL in the past. While NGVD is no longer supported by NGS or routinely employed by surveyors and engineers, it is still beneficial because of its extensive and long use for coastal measurements and studies, including many at SONGS. NGVD lies 0.43 ft below current MSL (as defined by the 1983-2001 epoch).

It is apparent from Figures 2-2A and 2-2B, that monthly maxima are increasing as sea level rises. This is expected to continue in the future. Table 2-2 lists the six highest maximum monthly water levels observed at La Jolla relative to NAVD88 and NGVD. The all-time maximum reading occurred on 25 November 2015 during the 2015-16 El Niño warming event, which also produced the highest-ever annual average level observed at La Jolla. Note that the four highest events exceeding the previous record elevations of 1983 occurred in only 18 years, from 1997-2015.

NOS also provides statistics of extreme sea levels based on the observations discussed. Their current estimates of "return period," or the probability of exceeding a given value in any year are summarized in Table 2-3 relative to NAVD88 and NGVD. Note the relatively small spread of less than 1 ft between the 1% (100-yr) and 99% (1-yr) extreme high water level events. This illustrates the dominant influence of the astronomical tide on extreme water levels along the

California coast. The highest tide is about 7 ft above NAVD88, less than about 0.5 ft below the 100-yr return event. It also illustrates the exceedingly rare coincidence of peak high tides with extraordinary storm surges or other water level enhancing processes, such as El Niño, which can raise MSL up to about 1.5 ft over time scales of days to a year.[2]

2.1.4 Developments in Climate Change Science

The already large number of research papers published in peer-reviewed journals concerning MSLR and the closely related issue of extreme water levels, continues to grow at a rapid pace. This of course reflects the importance of better understanding these processes as Earth continues warming. CE has compiled and summarized papers and reports not previously considered that present relevant global, state, regional, and local findings that may in time impact state policies, or may inform decisions by SCE concerning SONGS deconstruction.

The relevant research papers reviewed below fall into three broad categories, with some overlap, which include: (1) Global MSLR projections; (2) Regional MSLR projections; and (3) Regional or local total maximum water level projections. Complete citations for the papers reviewed under each category are given in the References section.

Studies relevant to global MSLR:

The IMBIE Team (2020) considered changes in the mass balance of the Greenland Ice Sheet from 1992-2018 in which time it lost 3,902 ± 342 billion tonnes of ice after being nearly stable into the 1990s. This contributed a global MSLR of 10.8 ± 0.9 mm, or about 0.42 mm/yr of the total estimated to be about 3.4 mm/yr. A key conclusion is that the MSLR contribution from Greenland tracked the upper (highest) IPCC (2013) AR5 scenario projections since the mid-1990s. There is also evidence that ice loss rates in Greenland slowed beginning about 2012. However, if high rates of ice loss resume, it is possible that the now relatively low probabilities of occurrence of the highest MSLR projections could be revised upwards.

Slater et al. (2020) in a follow-up to the IMBIE Team (2020) findings, determined that Antarctica contributed about 7.2 mm/yr to global MSLR between 1992 and 2018. Together, Greenland and Antarctica provided about 17.8 mm of global MSLR, or 0.7 mm/yr. This total likewise tracked the IPCC (2013) high AR5 scenario through at least 2017.

Hofer et al. (2020) show that the MSLR contribution from Greenland Ice Sheet runoff expected by 2100, previously estimated at about 10 cm, may be closer to about 18 ± 8 cm owing to a +1.3 °C greater "Arctic Amplification" and associated cloud and sea ice feedbacks.

Sun et al. (2020) compared an ensemble of 15 ice-sheet model responses over the next 500 years to a decrease in buttressing to determine total and sustained loss of ice in Antarctic ice shelves. While admittedly unrealistic, this enables gauging the sensitivity of ice sheet models to a

[2] See Flick (2016) for details exemplified by the 2015-16 El Niño winter.

total loss of buttressing and, therefore, exhibit the full potential of marine ice sheet instability. All models led to multi-meter (1-12 m) sea level rise, of the approximately 58 m of global MSLR stored in Antarctica's ice sheets. It was found that collapse of the West Antarctic Ice Sheet (WAIS) alone leads to 1.9-5.1 m of MSLR over 500 years. The upper limit is higher than the previous estimate of about 3.3 m.

Jevrejeva et al. (2020) review recent developments in assessing the uncertainty of probability estimates of MSLR scenarios through 2100. The paper illustrates the substantial quantitative differences in MSLR probability distributions owing to which (imperfectly understood) physical processes are included and how they are modeled, as well as the variation between regions of the world. The paper also deals with the scarcely considered subject of how global, open ocean MSLR will manifest on the continental shelves and to the world's coasts. Another valuable contribution from this work comes from the clear discussion of how planners, engineers, officials, and the public who must use the MSLR projections to make land use and infrastructure planning decisions may approach the uncertainties of the MSLR enterprise. An example, *"Instead of trying to identify a single probabilistic sea level projection corresponding to a "best estimate", coastal adaptation practitioners may choose to consider all existing probabilistic sea level projections or a set of projections that span the range of probability distributions… the challenge is to identify the particular probabilistic projection that is best aligned with their level of risk aversion… For example, managers of critical infrastructures with long lifetimes (e.g., nuclear power stations) may consider the most pessimistic probabilistic projection in order to test their resilience to the full range of future possible sea level changes. …and developing structured contingency plans to follow as the fate of future sea level becomes clearer."*

Studies relevant to regional MSLR projections:

Hamlington et al. (2020) is a comprehensive process-based review paper that addresses how the satellite global sea level record that started in about 1993 can separate climate change forced MSLR acceleration from both the upward trend in sea level and the natural "internal" variability, which has strong regional differences. Previous studies to address this crucial problem relied on the much longer records of sea level measured by tide gauges, which are not well suited to answer these questions. The paper also discusses uncertainties in future MSLR projections.

Thomas and Lin (2020) analyze regional MSLR hazards using probabilistic total sea level rise distributions created from a set of radiative forcing scenarios and a prediction model sampling process. Simulations of thermosteric sea level rise, glacier melt, and ice sheet mass balance using different models facilitates aggregation of sources of MSLR producing estimates of exceedance probability. Resulting hazard maps demonstrate how the fingerprints of different sources of MSLR combine into distinct regional patterns and their uncertainty.

Studies relevant to maximum total water levels, especially regionally, are now becoming much more detailed and numerous because of the wide recognition that flooding, erosion, land loss, and coastal infrastructure damage occurs when high tides, storm waves, and temporary enhanced water levels coincide. The chief effect of MSLR is to make these flooding events more common, more intense, and longer lasting. The latest contributions to this growing body of scientific literature emphasize so-called "nuisance flooding" defined as occasional, minor, short-term, non-destructive events that are nevertheless inconvenient and cumulatively costly.

Studies relevant to maximum total water levels include:

Haigh et al. (2019) provide a comprehensive review of mechanisms that contribute to changing tide amplitudes around the world. A growing number of studies have identified widespread, sometimes regionally coherent, positive and negative trends in tidal range since the 19^{th} century. MSLR and climate change will continue to alter tides over the next several centuries, with regionally coherent modes caused by alterations to coastal morphology and ice sheet extent. Better understanding of the causes and consequences of tidal variations will help assess the implications for coastal protection, risk assessment, and ecological change.

Kirezci et al. (2020) use global models of tide, storm surge, and wave setup to obtain projections of episodic coastal flooding over the coming century. Global "hotspots" where significant changes in episodic flooding are expected by 2100 are identified. These are concentrated in northwestern Europe and Asia. Results for the "mean" RCP8.5 scenario show that without coastal protection or adaptation, an additional 48% of the world's land area, 52% of the global population, and 46% of global assets will become at risk for flooding by 2100. A total of 68% of the global coastal area flooded will be caused by tide and storm events, with 32% due to projected regional sea level rise.

Muis et al. (2020) present a novel global dataset of extreme sea levels (Coastal Dataset for the Evaluation of Climate Impact) that is used to accurately map the impact of climate change on coastal regions around the world. They also apply a global tide and surge model, with a coastal resolution of 2.5 km (1.25 km in Europe), to simulate extreme sea levels for the ERA5 climate re-analysis from 1979-2017, as well as for future climate scenarios from 2040-2100. Average increases in the occurrence of 1:10 probability water level events range around 0.4 m. However, results are not summarized in a way to be readily compared to Kirezci et al. (2020).

Sida et al. (2021), published in early March 2021, is the latest and most comprehensive analysis of nuisance flooding (NF) along the U.S. coast. While sea level rise is the main driver for the observed increase in NF events in the U.S., the study shows that secular changes in tides also contribute. An analysis of 40 tidal gauge records from U.S. coasts finds that NF increased at 18 locations and decreased at 11. Estuaries show the largest changes in NF attributable to tide changes, which can often be traced to anthropogenic alterations such as dredging. The total number of NF days caused by tidal changes has increased at an exponential rate since 1950, adding ~27% to the total number of NF events observed in 2019 across locations with tidal amplification.

2.1.5 Developments in California Agency Guidance

CE has reviewed four new California state agency documents that provide updated MSLR policy, plans, or other information that potentially affects SONGS deconstruction activity. These were issued since preparation of our last report in March 2020 (Elwany et al., 2020), which relied on CCC (2015; updated 2018), and OPC (2018). The new documents include: CCC (2020a), CCC (2020b), OPC (2020), and CNRA-CEPA (2020). Complete citations and website availability are provided in the list of references.

Both CCC (2020a) and OPC (2020) re-committed to *"Update the State of California's Sea-Level Rise Guidance in 2023 and every five years thereafter to incorporate best available science and projections, and continually improve integration of changing ocean conditions into California's state government policies, planning, and operations."* This would continue to be led by OPC and can be anticipated to change the existing MSLR guidance by 2023, depending heavily on current and future scientific findings.

CCC (2020a) is the updated CCC 2020-2025 Strategic Plan issued in November 2020. It presents nine goals:

1. *Enhance Agency Capacity and Maintain an Effective and Diverse Workforce*
2. *Maximize Public Access and Recreation for All*
3. *Protect and Enhance Coastal Resources*
4. *Support Resilient Coastal Communities in the Face of Climate Change and Sea Level Rise*
5. *Advance Diversity, Equity, Environmental Justice, and Tribal Relations*
6. *Continue to Enhance the LCP Planning Program and Refine Implementation of the Regulatory Program*
7. *Expand and Enhance the Enforcement Program*
8. *Continue to Develop and Maintain Partnerships and Enhance Public Presence*
9. *Enhance Information Management and E-Government*

Together, these contain 50 objectives with 199 specific actions.

Importantly, CCC (2020a) "*…accounts more fully for the dynamic imperatives of climate change and sea level rise (Goal 4), which are already adversely affecting marine and terrestrial ecosystems and threatening the safety and economic health of our coastal communities. Building resilient communities while preserving public beaches and open space in the face of climate change is essential if the coast is to endure as a vital part of California's social and cultural fabric, and the coastal economy is to remain strong throughout the 21st Century and beyond."*

This emphasizes the State's interest in building coastal "resiliency" in the face of sea level rise, especially with respect to coastal access.

In particular, CCC (2020a) finds that, "*…climate change and sea level rise could jeopardize access and availability of state beaches, trails and other coastal access opportunities. The Strategic Plan focuses on several areas for achieving the goal of maximizing public access and recreation. First, there is an on-going need to ensure that public access easements and other public access ways are open and available to the public (Objective 2.1) and to protect all other existing public access and recreational opportunities (Objective 2.2). Ensure Continued Public Access in Light of Changing Shoreline Conditions and Sea Level Rise. (See also Climate Change Objective 4.4) 2.6.1 Identify locations where public access ways, the CCT or roadways that* *facilitate access to these areas may be limited or eliminated in the future due to sea level rise and increased storm events."*

The major threats to revetment stability continue to arise from wave storms, or clusters of wave storms, especially when these occur during times of high total water levels. Storm waves can damage the revetment in two ways: First, they can cause offshore sand movement (i.e., beach erosion) that undermines the revetment and causes rocks to move and settle. Second, sufficiently powerful waves can displace rocks. The extent and severity of damages depend on the height and period of waves and their duration, the initial state of the beach, and the condition of the revetment, including the rock size and placement. Large waves also cause wave run-up and potential revetment and retaining wall overtopping, which can lead to water, sand, and debris on the walkway, all at least temporarily hindering lateral access.

CCC (2020b) issued in July 2020, is a student-produced publicity "planning" piece aiming to explain and present sea level rise in a broadly popular fashion with summary technical findings and illustrative photos. The web document begins, *"With more than 1,270 miles of coastline in California's coastal zone, sandy beaches and scenic bluffs are an essential part of what makes this state so special. Our coast is home to 26.3 million people, a draw for visitors from around the world and the reason for our $44 billion coastal economy. It is important, now more than ever, that we Californians begin to plan for a future that includes sea level rise."*

This document summarizes sea level rise history, the effects on flooding and beach and cliff erosion, how California is preparing, which includes references to policy and CCC (2015; updated 2018) guidance, local coastal program development, how to become personally involved, and mentions resources that can be accessed to do this.

CCC (2020a) and CCC (2020b) contain no changes to the previously evaluated MSLR scenarios presented in Elwany et al. (2020). Neither document alters or expands on the sea level rise projections contained in OPC (2018) and CCC (2015; updated 2018). This suggests that CCC MSLR policy and guidance remains unchanged.

OPC (2020) is the Ocean Protection Council 2020-2025 Five-Year Strategic Plan update finalized in February 2020. It sets goals to meet and specific actions to take over the next five years. In the climate change realm most relevant to SONGS, these plans are focused on preparation and facilitation of resiliency and access adaptation to the negative effects of MSLR for state and local agencies and other entities.

The "Call to Action" letter introduction to the document states that, among other climate change effects, *"Warming seas and rapidly melting ice sheets are projected to increase sea levels by 3.5 feet or more by the end of century."*

We note that the OPC (2018) summary Table 31 for MSLR at La Jolla, which is applicable to SONGS, shows that MSLR by 2100 (for the high emissions scenario) could be greater or less than 3.5 ft, depending on the chosen probability of occurrence. However, it is currently highly unlikely that MSLR reaches 3.5 ft by 2050. For example, the "median" 50% probability value is 2.6 ft by 2100, while the 66% probability range is 1.8-3.6 ft. These are lower than or barely exceed 3.5 ft. The 5% probability reaches 3.5 ft between 2080 and 2090. The 0.5% probability hits 3.6 ft in 2070. Even the extreme "H++" scenario only reaches 2.8 ft by 2050, but accelerates rapidly to 3.9 ft by 2060. We conclude based on the best available science contained in OPC (2018), that it is not impossible, but highly unlikely that MSLR reaches 3.5 ft by 2050 or shortly thereafter.

Overall, OPC (2020) presents four goals:

1. *Safeguard Coastal and Marine Ecosystems and Communities in the Face of Climate Change*
2. *Advance Equity Across Ocean and Coastal Policies and Actions*
3. *Enhance Coastal and Marine Biodiversity*
4. *Support Ocean Health through a Sustainable Blue Economy*

OPC (2020) Goal 1 encompasses MSLR and lists numerous action items. Goal 1, Objective 1 emphasizes building *"Resiliency to Sea-Level Rise, Coastal Storms, Erosion, and Flooding."*

Target 1.1.1 seeks to: *"Ensure California's coast is resilient to at least 3.5 feet of sea-level rise by 2050, as consistent with the State's Sea-Level Rise Guidance Document as appropriate for a given location or project. This target will be modified periodically based on the best available science and updates to the State's Sea-Level Rise Guidance Document."*

Target 1.1.1 suggests a new interpretation of existing policy potentially changing the guidance previously published, which implies taking steps that consider that projects can weather MSLR *up to 2.6 ft* by 2050 where the extreme H++ scenario is applicable.

OPC (2020) Target 1.1.2 of the same goal and objective states, "*In conjunction with ongoing efforts, develop a site-specific infrastructure resiliency plan focused on state roads, railroads, wastewater treatment plants, water supply facilities, ports, and power plants by 2023."*

Specific action proposed under this target includes, *"By 2022, develop more protective baseline (greater than 3.5 feet of sea-level rise) 2050 and 2100 adaptation strategies and targets for vulnerable and critical infrastructure (state roads, railroads, wastewater treatment plants, water supply facilities, ports, power plants, etc.)"*

CNRA-CEPA (2020) published in April 2020, is a result of high-level meetings of 17 state entities convened by the Governor's Natural Resources Agency (NRA) and California Environmental Protection Agency (CEPA) Cabinet Secretaries to develop and approve state-wide sea level rise principles for planning, policy setting, project development, and decision-making. The overall objective is to *"align state action"* so that it is more consistent among agencies, less duplicative, more efficient and effective, and ultimately less costly.

The document opens with, *"California's coast, bays, estuaries, and ocean are facing an immediate threat from sea-level rise. To improve effectiveness in addressing the immediate challenge of adapting our state to sea-level rise, California state agencies with coastal, bay, and shoreline climate resilience responsibilities, including for coastal infrastructure and Californians' safety, endorse the following Principles for Aligned State Action. These Principles will guide unified, effective action toward sea-level rise resilience for California's coastal communities, ecosystems, and economies around: Best Available Science, Partnerships, Alignment, Communications, Local Support, Coastal Resilience Projects, and Equity."* These six principles provide the document outline.

Under Principal 1, which promotes use of the best available science, states in part, "*Utilize SLR targets based on the best available science and a minimum of 3.5 feet of SLR by 2050. Develop and utilize more protective baseline 2050 and 2100 targets for road, rail, port, power plants, water and waste systems, and other critical infrastructure."*

This principle echoes OPC (2020) Targets 1.1.1 and 1.1.2 and seems to call for using 3.5 ft of MSLR by 2050 in project planning for "*critical infrastructure."* As in OPC (2020), this document, which is intended to be applied by all State agencies, would seem to require a higher than anticipated MSLR scenario of at least 3.5 ft by 2050.

Similar to the previously described State efforts, CNRA-CEPA (2020) promotes adaptation through building "resilience." Specifically, Principles 5 and 6 provide suggestions about how to accomplish this, again stressing avoiding negative impacts on public coastal access as follows:

5. *Strengthen alignment around coastal resilience: Agencies should develop and apply agreed-upon baseline SLR terms, projections, and targets. They should ensure alignment on vulnerability assessments and best-practice coastal resiliency strategies. They should collaborate on developing funding sources. And they should avoid unnecessary duplication of effort or authority.*
6. *Implement and learn from coastal resilience projects: Agencies should protect natural coastal resources and biodiversity as well as critical water-dependent infrastructure, including ports and harbors. They should prioritize nature-based adaptation strategies, where appropriate. They should increase the number of adaptation projects and streamline high-need coastal restoration projects, while ensuring that the implementation of these projects will not shift hazards elsewhere. And they should work to prevent SLR from impacting public access to coastal areas.*

2.1.6 Groundwater

Our focus here is the current and nearly certain higher future elevations of groundwater due to MSLR, particularly under the ISFSI. Groundwater levels at SONGS were measured quarterly by SDS at 16 wells in 2019 and 2020. Nine of these wells are located along the western edge of SONGS inside the seawall, suggesting they may reflect coastal oceanographic influences (e.g., Raubenheimer et al., 1999). Data are presented in Appendix F.

The average groundwater elevation readings from the coastal wells were 2.62 ft (NGVD) for 2019, and 2.43 ft (NGVD) for 2020, 0.19 ft lower. We note that local MSL offshore SONGS as determined by the La Jolla tide gauge lies about 0.43 ft above MSL (averaged over the current 1983-2001 NOAA 19-year tidal datum epoch). This means that the coastal groundwater at SONGS is about 2.1 ft above MSL.

Since only two years of groundwater data are available, it is not possible to discern a meaningful trend. Further, the sampling protocol precludes any determination of tidal or other short or intermediate time-scale fluctuations in groundwater levels. Finally, any influences from inland water sources or processes such as rainfall changes, are likewise uncertain.

To estimate possible future groundwater elevation increases due to MSLR, we assume that near-coastal groundwater will rise by an equal amount. Adding the OPC (2018) 0.5% (medium-high) and H++ SLR scenarios, which respectively elevate MSL 2 ft and 2.8 ft by 2050, to the current elevation of 2.43 ft (NGVD), results in groundwater elevations of 4.43 ft and 5.23 ft (NGVD) at that time. These values are 0.74 ft to 1.54 ft below the 3-ft thick concrete support foundation, which lies at 5.97 ft (NGVD), as shown in Figure 2-3. Continued monitoring of groundwater will enable future assessments of trends and fluctuations and improved estimation of the likelihood of interaction with the ISFSI support foundation.

Table 2-1. Ocean Protection Council (2018) MSLR Guidance (ft)

1	2	3	4	5	6	7
Year	**50%**	**> 67% <**		**5%**	**0.5%**	**H++**
2000	0.0	0.0	0.0	0.0	0.0	0.0
2030	0.5	0.4	0.6	0.7	0.9	1.1
2040	0.7	0.5	0.9	1.0	1.3	1.8
2050	0.9	0.7	1.2	1.4	2.0	2.8

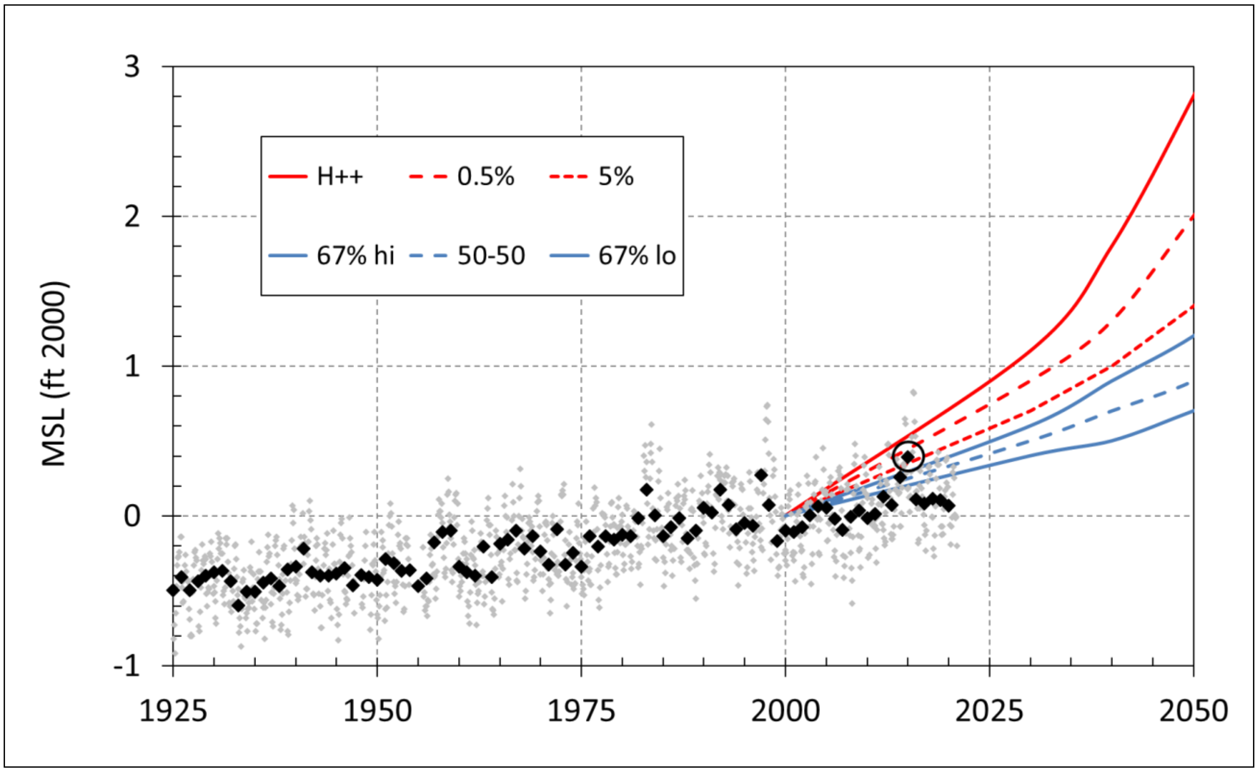

Figure 2-1. Average MSL at La Jolla, 1925-2020 – annual (black symbols), monthly (light grey), adjusted to zero over 1991-2009 epoch centered on 2000. OPC (2018) MSLR projections (colored lines). Maximum annual average 0.4 ft (circle) during 2015 El Niño. Future MSLR projection lines: H++ (solid red); 1 in 200 chance or 0.5% (long broken red); 1 in 20 or 5% (short broken red); 2/3 or 67% upper and lower limits (solid blue); even chance or 50-50 (broken blue).

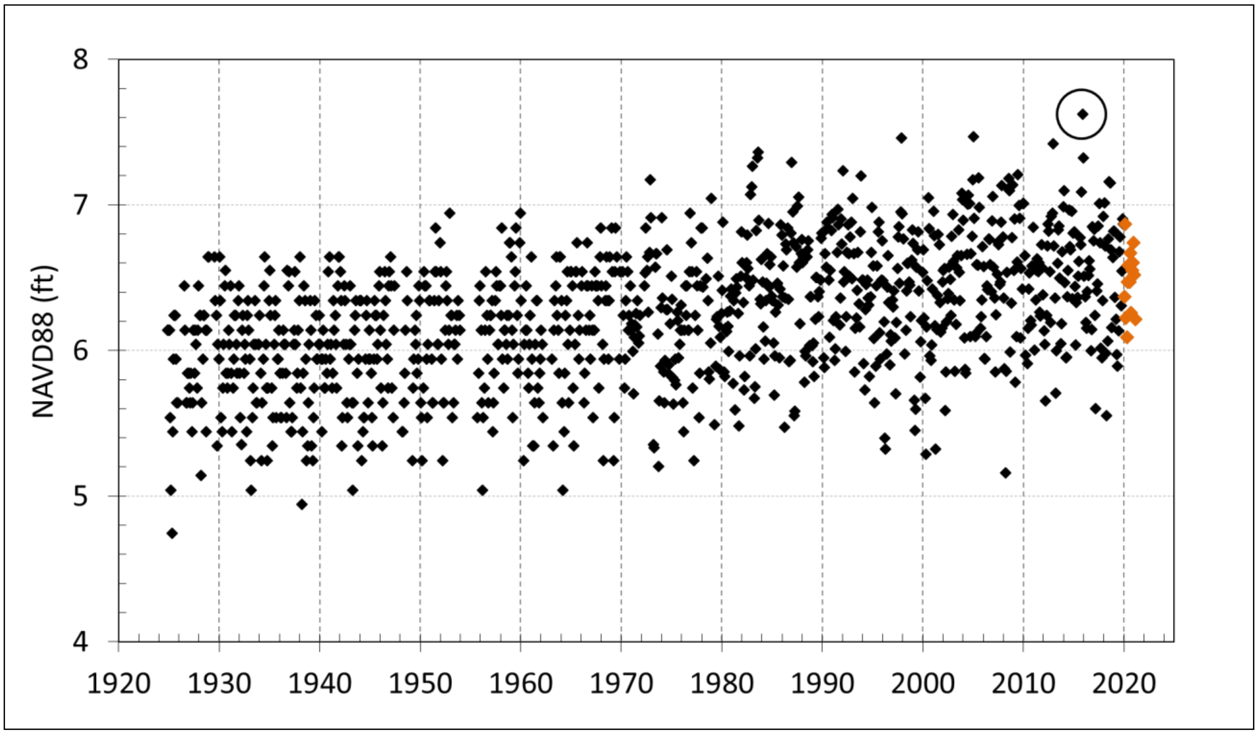

Figure 2-2A. Monthly maximum sea level at La Jolla relative to NAVD88 datum, 1925-2019 (black symbols), 2020-Feb 2021 (orange symbols). Maximum observed 7.62 ft height (circled) on 25 November 2015 during 2015-16 El Niño. Note 2020 to early 2021 well below historical maxima.

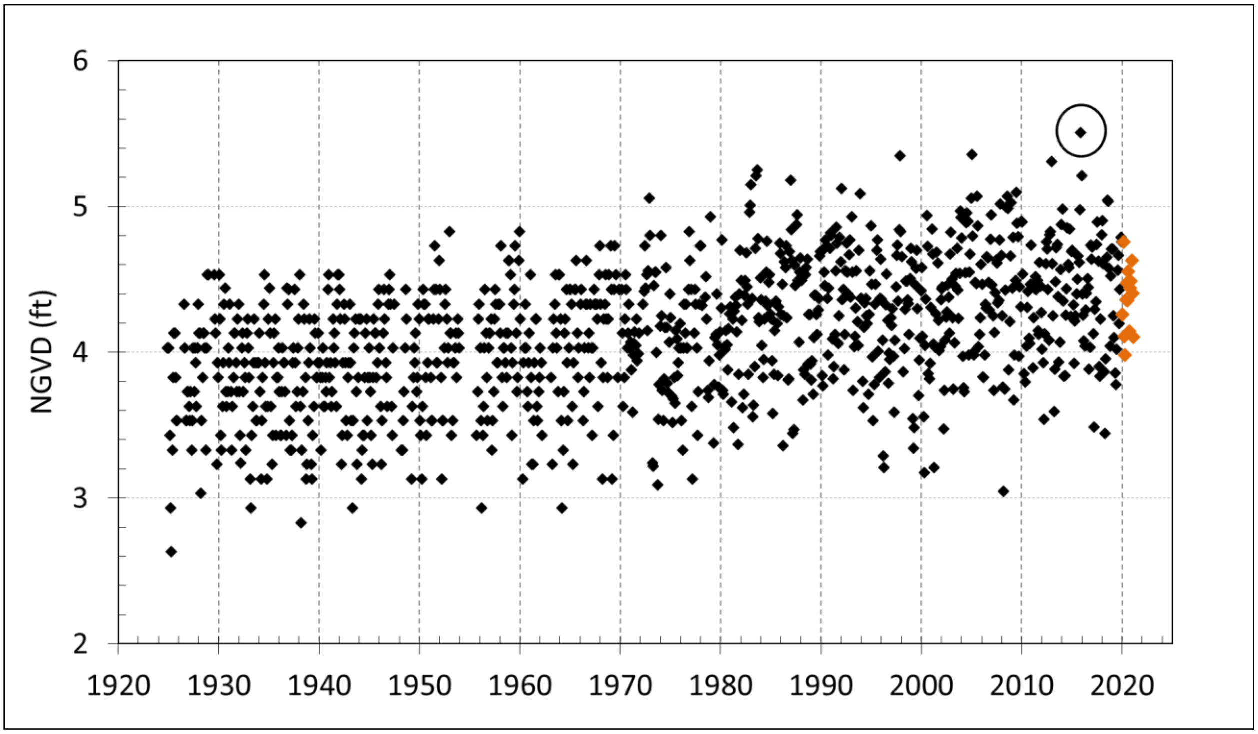

Figure 2-2B. Same as Figure 2-2A, but relative to NGVD datum.

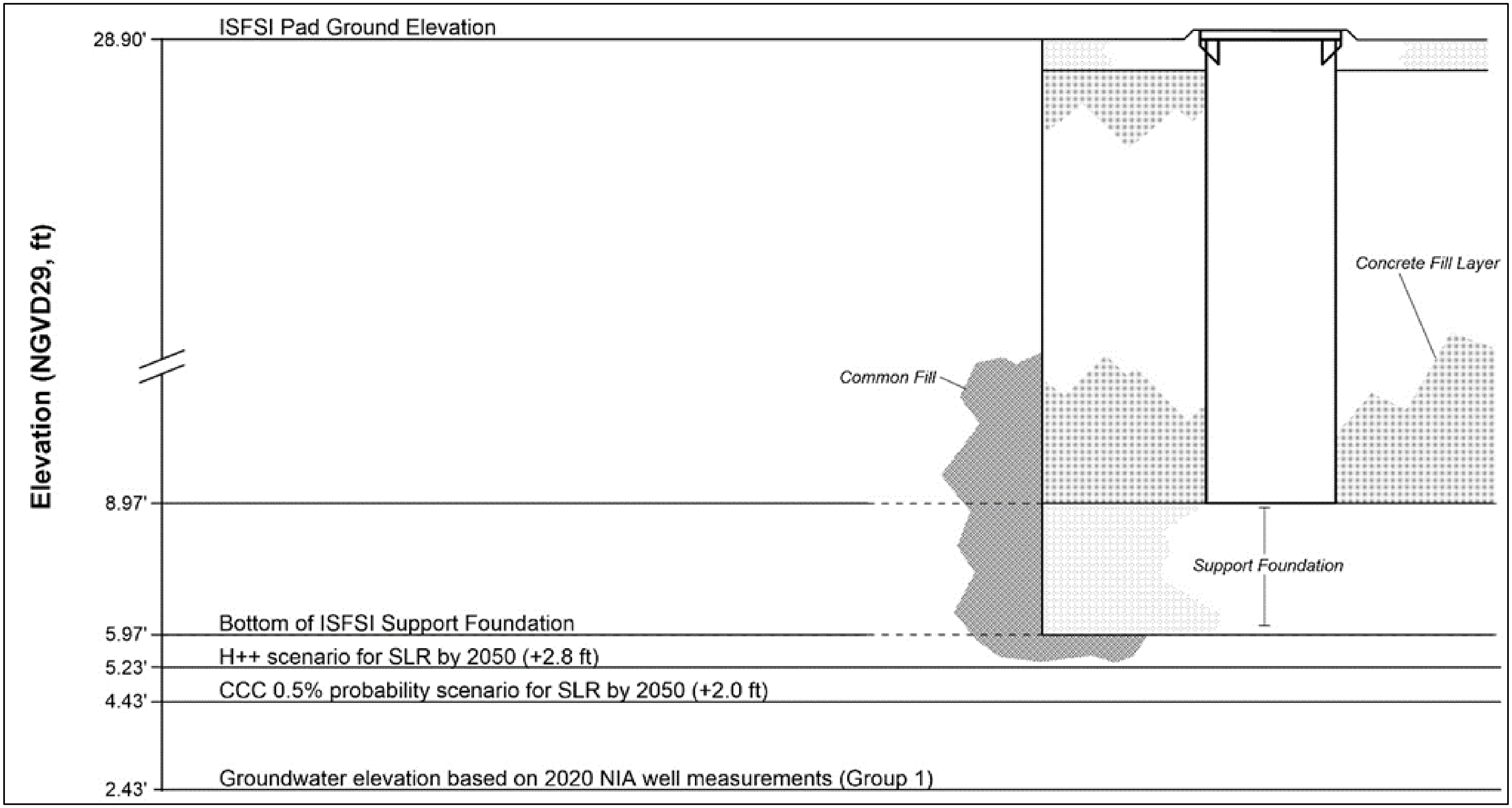

Figure 2-3. Groundwater elevations in 2020 and 2050 based on the CCC and H++ SLR projections (OPC, 2018).

Table 2-2. Highest Maximum Observed Total Water Levels, La Jolla (ft).

Year Month	NAVD88	NGVD
2015 Nov	7.62	5.51
2005 Jan	7.47	5.36
1997 Nov	7.46	5.35
2012 Dec	7.42	5.31
1983 Aug	7.36	5.25
1983 Jan	7.26	5.15

Table 2-3. NOAA-NOS La Jolla Extreme Water Level Statistics (ft).

Percent/Yr	Return (Yrs)	NAVD88	NGVD
1%	100	7.43	5.32
10%	10	7.20	5.09
50%	2	6.94	4.82
99%	1	6.51	4.40

3.0 SONGS REVETMENT

3.1 DESCRIPTION OF THE SONGS REVETMENT

The SONGS revetment, retaining wall, and access walkway provide partial front-line protection for the SONGS seawall; and SCE continues to maintain the walkway for safe lateral access for beach users. The revetment shelters the retaining wall and walkway from most wave run-up and overtopping, thus preventing or reducing negative impacts to lateral beach access due to flooding and other hazards from high water levels and waves.

Figure 3-1 is an aerial photograph showing the revetment, which extends along the entire length of SONGS on the beach fronting the walkway. Figure 3-2 is a close-up of the revetment at its southern end. The revetment is about 2,200 ft long, extending from the north end of Unit 1 to the south end of Units 2 and 3. The revetment is constructed of multiple layers of placed riprap consisting of quarry rock "rubble." A well-known desirable characteristic of placed rubble structures is their ability to adjust and re-settle under wave attack. The advantage of using rock riprap is that it is highly durable and readily available in Southern California. Furthermore, due to their roughness, rock revetments dissipate more wave energy and thus produce less wave run-up and overtopping, as opposed to smoothed-faced structures.

3.1.1 Revetment and Walkway Maintenance 2018-2019

Recent repairs of the SONGS revetment (fronting Units 2 and 3) were done in two phases. Phase 1 started on 7 May 2018 and ended on 10 October 2018, and Phase 2 started on 15 October 2019 and ended on 16 December 2019. No substantial repairs were carried out in 2020.

During Phase 1, SCE: (1) placed imported rock riprap along 500 linear ft at the southern portion of the public access walkway (Figure 3-3); and (2) elevated the access ramp of the southern public walkway using imported cobbles and sand.

Elevating of the south public access ramp was necessary to compensate for the sand lost due to wave action, which resulted in an approximately 10 ft lowering of the beach at the south end of the walkway, and scouring of the revetment riprap that protects the sheet pile seawall. The riprap had been undermined and eventually, if not corrected, the revetment would have no longer been effective. The repairs successfully addressed these issues.

During Phase 2, SCE: (1) placed an additional 150 linear ft of imported rock riprap north of that previously placed, for a total of 650 linear ft of revetment repair; (2) added 70 ft of riprap in front of the sheet pile seawall closure section at the south end of the public walkway, and (3) re-installed the Vehicle Barrier System at the south end of the public walkway. Figure 3-4 shows the south end of the walkway before and after these repairs.

3.2 SITE VISIT

CE conducted an inspection of the revetment for this study on 25 and 26 February 2021. During this visit, CE took photos of the seaward front of the revetment at all 21 cross-section ranges used for this work. These photos are presented in Appendix D. A laser scan survey was also carried out in order to construct a digital elevation model (DEM) of the revetment.

3.2.1 Rock Measurements

The size of individual rocks is expressed by the dimensions of their three axes. The long axis, ‘a’, is the maximum length of the stone (Figure 3-5); the intermediate axis, ‘b’, is the maximum width perpendicular to the long axis; and the short axis, ‘c’, is the height of the stone perpendicular to the plane of the a-axis and b-axis. The size of an individual rock is usually expressed as its b-axis dimension, or alternatively by its calculated or actual weight. Rock weight estimates, which are needed to evaluate riprap stability, are discussed in Section 3.3 below. Histograms of the lengths, widths, and heights of the 80 sample rocks measured at SONGS are presented in Figure 3-6, and their cumulative distributions in percentage are shown in Figure 3-7.

3.2.2 Revetment Laser Scanner Survey

A laser scanner survey was carried out using a Trimble SX10 scanning total station (Figure 3-8) for the purpose of creating a DEM to visualize the spatial characteristics of the revetment. Control points were established to aid in subsequent station setups. The revetment was scanned from the beach with scanner location determined from control points. The system scanned in a vertical direction and slowly rotated horizontally to cover the areas of the revetment at a high resolution. A total of 14 scans were carried out to capture the entire SONGS revetment.

Tide was a limiting factor in obtaining complete coverage from the beach at the southern portion of the revetment. Therefore, some scans were carried out from the top of the revetment near the walkway to fill data gaps.

The survey on 25-26 February 2021 acquired over 47 million data points, assembled in a “point cloud.” The data set was pre-processed using “Global Mapper” software that enables outlier points, and points likely reflected from the walkway wall, to be removed. The processed data were then graphically presented to show the revetment and adjacent beach. The model results at each of the transects are presented in Appendix A.

An advantage of creating a DEM is that the model can be “re-sampled” to show cross-sections and contour maps that would otherwise be difficult or impossible to derive in a reliable way. Twenty-one cross-section transects were generated from the DEM at locations shown in Figure 3-9. Results of the revetment laser scanner survey are shown in Figures 3-10 through 3-12 for the 21 transects. For clarity, Appendix A shows the DEM comparison between 2021 and 2020 for each transect. Representative cross-sections are shown in Figure 3-13; all 21 transect cross-sections are presented in Appendix B. Table 3-1 provides riprap height, walkway wall height, and the revetment slope β for each transect.

The DEM was also used to determine the height of the revetment along its upper edge adjacent to the walkway retaining wall (Figure 3-14). The height of this upper edge varies from about 8 ft to 12 ft (NGVD), a few feet lower than the upper edge of the retaining wall, which lies at about 14 ft.

3.3 RIPRAP ROCK UNIT WEIGHT

Riprap rock unit weights and their variations are essential to estimating the stability of a revetment. Individual rock weight is proportional to volume and specific weight (or density) of the stone. The estimation of weight is complicated by the fact that each rock unit is not a simple geometric form, such as a sphere or rectangular shape, like a brick.

Individual rock weight, W(x), was estimated from Equation 3-1, which assumes each rock (x) is equivalent to a sphere with diameter D(x) = b(x), the maximum width perpendicular to the long axis, as described in Section 3.2 above. Dimension ‘b’ is often referred to as rock “diameter.” Then:

$$W\ x\ =\ \frac{\pi \gamma_s\ D(x)\ ^3}{6} \qquad (3\text{-}1)$$

Where:

γ_s = Specific weight of revetment rock.

Table 3-2 gives the dimensions and weights of each sampled rock. The mean and standard deviations for the length, width, and weight of the rocks are presented in Table 3-3. Percent distribution of rock weights and the cumulative distribution of estimated rock weights are shown in Figure 3-15.

A key design parameter for any revetment is the median rock weight, designated W_{50}. Half of the rocks are heavier, and the other half are lighter than W_{50}. We estimated W_{50} in two different ways using standard coastal engineering practice (U.S. Army Corps of Engineers [USACE] 1994a,b). These gave nearly identical results.

First, we determined the individual rock weight estimates from each rock diameter, D(x), as described above in equation 3-1. The result was W_{50} = 600 kg. Second, we calculated the median diameter of the 80 sampled rocks, D_{50}. The result was D_{50} = 2.5 ft. We then used this number in place of D(x) in Equation 3-1, which resulted in W_{50} = 580 kg.

3.4 DESIGN WATER LEVEL

Water surface elevation is dependent on tides, storm surge, and MSLR. These factors are discussed in Section 2.1.3, and the values of observed extreme water levels are given in Table 2-3. Table 2-3 gives the NOAA estimates for the extreme water level for various return estimates. The 100-year return period for surface water elevation at La Jolla is 5.32 ft, NGVD

(7.43 ft NAVD88) while the maximum observed water surface elevation of 5.5 ft occurred on 25 November 2015 during the 2015-16 El Niño warming event.

These estimations include astronomical tide, storm surge, and sea level fluctuations due to normal seasonal heating and cooling, as well as El Niño condition enhancements. They do not include wave setup caused by breaking waves, since tide gauges are located offshore of the surf zone, and their water level sampling system filters out relatively high-frequency fluctuations such as wave surges. The design water level used for this study is the extreme thus far observed: 5.5 ft (1.7 m) NGVD, or 7.6 ft (2.3 m) NAVD88 (rounded to one decimal).

3.5 DESIGN WAVE ESTIMATION

Wave run-up can be the dominant contribution to high water levels on beaches, depending on the state of the tide, and the height, direction, and period of the waves, especially during storms. The wave record for San Onofre, estimated from measurements at SONGS and a comparison with the Oceanside wave array data between 1978 through 1994, were used to calculate wave height return periods for San Onofre (see Section 5.2 in Elwany et al., 2016).

The Seasonal Maxima Distribution Model (SMDM), developed by L. E. Borgmann and published in USACOE (1988), was selected as the appropriate analysis method to estimate the design wave height at a range of return periods. Monthly wave maxima were extracted from the wave data and split into seasonal sets. The seasonal maximum wave-height distribution functions were calculated for each season and then multiplied together to produce the annual maximum distribution. This distribution function was used to estimate extreme wave-height return periods.

The design wave analysis shown in Figure 3-16 was used to identify the significant wave heights associated with 5-, 10-, 25-, 50-, and 100-year wave events at San Onofre. Wave spectra matching those wave heights were selectively extracted from the record. The wave spectra from these storms (Figure 3-17) were extracted from the Coastal Data Information Program (CDIP) database (https://cdip.ucsd.edu/) and used to estimate the peak period associated with wave-height return period. A typical wave storm on this Southern California coast has a wave height of about 6.9 ft (2.1 m). Extreme-values for the 5-, 10-, 25-, 50-, and 100-year return period wave heights at San Onofre are given in Table 3-4.

The historical largest storm on record between 1980 and 2016 occurred on 18 January 1988. The deepwater wave height was 16 ft (4.9 m) with a period of 17 sec (as measured at the Oceanside buoy). The corresponding wave height at San Onofre was about 12.5 ft (3.8 m) approaching the shore from the west. Table 3-5 represents the highest significant wave heights at San Onofre in descending order estimated from the Oceanside measured wave data for summer, winter, and all data.

3.6 SONGS REVETMENT STABILITY ESTIMATION

As outlined above, the median rock weight W_{50} is a key parameter in assessing the stability of a revetment. Hudson's formula (Ahrens, 1981a,b; USACOE, 1984 and 1994a,b; BCMELP, 2000) is the standard practice method used to estimate W_{50} necessary for revetment stability:

$$W_{50} = \frac{\gamma_r H^3}{K_D \left(\frac{\gamma_r}{\gamma_w} - 1\right)^3 \cot\alpha} \quad (3\text{-}2)$$

Where:

W_{50} = required median armor unit weight,
γ_r = specific weight of the rock unit, Kg/m^3,
H = wave height at the toe of the revetment,
K_D = stability coefficient,
γ_w = specific weight of water at the site, and
α = revetment slope angle from horizontal.

K_D values vary primarily with the shape of the rocks, surface roughness, sharpness of edges, and degree of interlocking. Typically, K_D = 2.1. Wave height H at the structure is estimated by shoaling the design waves to the breaking point (H_b). If H_b is less than the wave height at the toe, H_{toe}, of the revetment, we use H_b; otherwise, H_{toe} is used.

The height of the wave at the toe of the revetment is depth limited. The extreme water depth at the toe of the SONGS revetment (Ds) is 5.5 ft + 2.29 = 7.79 ft, MLLW, where 5.5 ft, NGVD is extreme water level (Section 3.4) and 2.29 is the difference in elevation between datums NGVD and MLLW.

The water depth at the toe of the structure (Ds) varies as the sea level rises. In 2050, the water depth at the toe of the structure is projected to be between 9.79 ft, MLLW (OPC, 2018, Medium-High Scenario) and 10.59 ft, MLLW (OPC, 2018 H++ Scenario). A calculation of the wave height (H) was made from the equation H = 0.56 x Ds (Thornton and Guza, 1982 and 1983).

Equation 3-2 is used to compute the minimum W_{50} required for revetment stability under the given wave conditions. Table 3-6 gives the calculated values of W_{50} for the MSLR projections (medium-high and H++ at 2020 and 2050).

3.7 ASSESSMENT OF SAN ONOFRE BEACH

The condition of the beach fronting SONGS is significant since it prevents or buffers wave attack of the revetment and retaining wall, which in turn protect the walkway required for lateral beach access, as well as the SONGS seawall. The stability of the SONGS revetment depends on the rock size (i.e., W_{50}), and the condition of the beach. Presence of a healthy beach causes waves to break farther seaward of the revetment, thus reducing wave run-up, splashing, and overtopping. The beach also prevents toe scouring that can undermine the revetment and cause rock units to settle or move. When the beach is narrow, or water level unusually high, or both, waves breaking on the revetment can cause dislocation of individual rocks, contributing to revetment instability.

Recent beach conditions are defined by the 2017 through 2020 quarterly profile measurements (Appendix E), which characterize the beach configuration in autumn, winter, spring, and summer seasons. Comparisons with earlier beach profiles dating back as early as 1964 quantify long-term beach changes. The main factors controlling erosion or accretion are waves and sand supply. Other contributing factors are the nearshore and offshore bathymetry of the region, particularly any wide, flat shelf areas, and the presence of reefs, all of which limit wave height. Structures, particularly the SONGS temporary laydown pads used for Units 1, 2, and 3 construction, have influenced beach width and stability. In the future, MSLR will cause beaches worldwide to migrate landward and upward. Depending on the state of the backshore, especially its erodibility, beaches may or may not continue to exist. Appendix E documents the complex history and context of beach condition changes at SONGS.

Two surveys each year include the offshore portion of the beach at SONGS. The results of each recent survey have been presented in reports by CE (2017, 2018, 2019, and 2020). Longer-term beach change patterns are characterized by comparing beach widths from these recent surveys to comparable measurements from 1985-1993 sponsored by SCE. Earlier directly comparable data were taken in May 1985, just after the removal of the SONGS Units 2 and 3 laydown pad (Flick and Wanetick, 1989), and from 1990-1993 (Elwany et al., 1994), 2000 (CE, 2000), and 2016 (Elwany et al., 2016).

Appendix E presents an analysis of SONGS beach width data. In Sections 2 and 3 of Appendix E, we present an overview of the data and how it was collected. In Section 4, we then discuss the characteristics of SONGS beach profiles and how these relate to typical Southern California beaches. Beach width changes and shoreline trends are discussed in Sections 5 and 6. In Section 7, we utilized the available historical information to better understand beach width fluctuations over a long time scale and shoreline changes at San Onofre. Our conclusions are detailed in Section 8. For convenience, Figures 3-18 and 3-19, and Table 3-7 are reproduced from Appendix E in this section to show the long-term decrease in beach width.

The beach profile surveys and photography programs sponsored by SCE since 1964 have provided valuable information and understanding of the response at San Onofre to beach filling and the construction of stabilizing structures (Flick and Wanetick, 1989; Flick et al., 2010). This insight will be valuable as MSLR accelerates in the future. Elwany et al. (2017) addressed the impacts of MSLR on San Onofre Beach.

3.8 EVALUATION CRITERIA

A "stable" rock revetment must perform satisfactorily in the sense that it functions as designed even though individual rocks may move, or that portions or the entire revetment settles or changes slope. Such changes are expected in rock revetments, and as previously noted, are accounted for in the original design. In short, a revetment is functioning properly if it provides protection as designed and is considered stable if no damage exceeds ordinary maintenance needs. At a minimum, the design must withstand conditions that have a 50% probability of being exceeded during the revetment's economic life.

Revetment failure can be caused by: (1) large dislocation of individual rocks such that they become sufficiently separated as to no longer function as a unit to dampen wave attack; or (2) extreme settlement where the height is no longer sufficient to prevent excessive overtopping. In addition, failure of the project during probable maximum conditions should not result in loss of life or unreasonable cost.

3.9 REVETMENT STABILITY FROM FEBRUARY 2020 TO FEBRUARY 2021

Wave data (wave height, period, and direction) from wave buoy number 46224, located offshore of the City of Oceanside in 238 m water depth, were used to estimate the wave heights and periods in 10 m water depth seawards of the SONGS revetment from 1 January 2020 through 28 February 2021. These computed wave heights and periods are shown in Figure 3-20. The waves during this period were generally calm except for the periods from 7 November to 9 November 2020 and from 25 January to 21 February 2021 (Figure 3-20).

The November 2020 wave event lasted three days and had an average wave height of about 3.45 m (11.3 ft) (Figure 3-21). The period from 1 January to 28 February 2021 (Figure 3-22) was characterized by a series of large wave storms having an average wave height of about 2 m (6.6 ft) with maximum wave height of 4.34 m (14.2 ft) observed between 25 January to 26 January 2021 as shown in Figure 3-23. The wave period during the wave storms varied between 8 to 12 secs. These wave events offered a good opportunity to examine the stability of the revetment using actual wave storm events.

The damage to the revetment was minor; it occurred at two locations, noticeably Ranges 1 and 10. The damages to the revetment were limited to a few rock locations. The revetment damage at Transect 1 occurred at the drainage structure. These wave events impacted the beach fronting SONGS by removing the thin layer of sand covering the cobble. Some of the cobble was pushed inshore to the toe of the revetment and between the rocks at even higher elevations. Cobble was thrown onto the walkway in few locations near Transect 10 by waves splashing over the revetment. No damages were observed in the walkway, indicating that the revetment protected the walkway from wave run-up and overtopping.

It is notable from the DEM (Appendix A) and the photographs (Appendix D) that most of the changes in the revetment occurred at the toe. These changes were: (1) movement of a limited number of small rocks by a few feet; (2) exposure of the revetment rocks that had previously been under the sand; and (3) pushing cobbles inshore towards and over the revetment. Movement of large rocks that constitute the main revetment were insignificant and did not negatively impact revetment stability.

In February 2020, the north portion of the revetment was covered by beach sand. Large waves in early 2021 removed this sand, exposing cobble and more of the revetment rocks under the sand (Figure 3-24). The changes in the San Onofre beach caused by the January and February

2021 large wave storms were normal and expected. They were typical of what has been observed at other Southern California beaches, such as Camp Pendleton, Oceanside, and the City of Del Mar.

The photographs taken during the 25-26 February 2021 site visit (Appendix D) are important to this study; they complement the laser scanner survey and show the beach conditions at each of the 21 ranges after the January-February 2021 wave storms. The laser scanner survey clearly described the rock shape (sizes) while the photographs highlighted the sand and cobble areas on the beach. Aerial photographs of the revetment for the period from 2003-2020 are presented in Appendix C.

3.10 MAINTENANCE AND ADAPTIVE CAPACITY

As described in Section 3.9, the SONGS revetment is currently in good condition and can likely provide wave protection to the retaining wall and walkway through at least 2050. The major threats to revetment stability in the future include wave storms, or clusters of wave storms, such as those that occurred from 1981 to 1983. As described above, potential revetment damages depend on the height of waves and the duration of wave attack, as well as the condition of the beach. Large waves can cause dramatic narrowing and lowering of the beach fronting the revetment, leading to rock settlement and displacement, wave run-up, and overtopping.

Section 3.9 of this study showed that the revetment was capable of withstanding both a single large wave event of 2-4 days and a series of large wave storms. It should be pointed out that the revetment is expected to occasionally sustain future damages larger than were observed during January and February 2021; and, therefore, the revetment will continue to require occasional maintenance in the future. It is not expected to collapse or fail in a way that would prevent its function if properly maintained. As previously noted, some rock movement and settlement are expected in rock revetments, and are accounted for in the original design such that no damage exceeds ordinary maintenance needs. In this respect, the revetment’s adaptive capacity to MSLR is high in the sense that it is currently in a stable condition and has lately been tested by the January-February 2021 waves. Occasional maintenance will allow it to continue functioning as intended.

For these reasons, it is important to continue monitoring the cross-sections of the revetment at various locations by surveys and photographs (Sections 3.2.1 and 3.2.2), especially before and after large wave storms. Similarly, it is also important to continue monitoring the beach fronting as well as north and south of the revetment, as described in Section 3.7 and Appendix E.

The revetment, retaining wall, and walkway provide protection for the main SONGS seawall, which is indispensable to protect the ISFSI and its Security Building. It is crucial that the seawall remain in place at least until the deconstruction efforts of Units 2 and 3 are completed to avoid exposing these and other critical facilities to wave action or flooding and any resulting damages. The seawall prevents any wave impact or ocean water flooding of the ISFSI site and the Security Building and avoids erosion and storm surge flooding of these and other SONGS facilities. The revetment and retaining wall structures fronting the walkway and seawall serve as a protective buffer, preventing almost all direct wave impact on the seawall. They are essential to maintain lateral access along the walkway.

Continued maintenance of the SONGS revetment is necessary (Section 3.1.1), as is maintaining the main SONGS seawall. These structures substantially decrease exposure and risk to SONGS from future MSLR, and therefore increase the resilience and adaptive capacity of all SONGS facilities and the Lease Premises in compliance with the SCE lease agreement. Additionally, as discussed in section 3.6, the designed rock weight used on SONGS' revetment likely can provide protection until 2050. Since the mean weight of the rocks used in the revetment is 849 kg (Table 3-3), and the median armor unit weight (W_{50}) to keep the stability of the revetment in 2050, under the H++ scenarios, was calculated to be 685 kg, as shows Table 3-6.

Figure 3-1. Photograph taken on 20 August 2018, showing the SONGS revetment. Notice the north part of the revetment is covered by beach sand.

Figure 3-2. The revetment at its southern end.

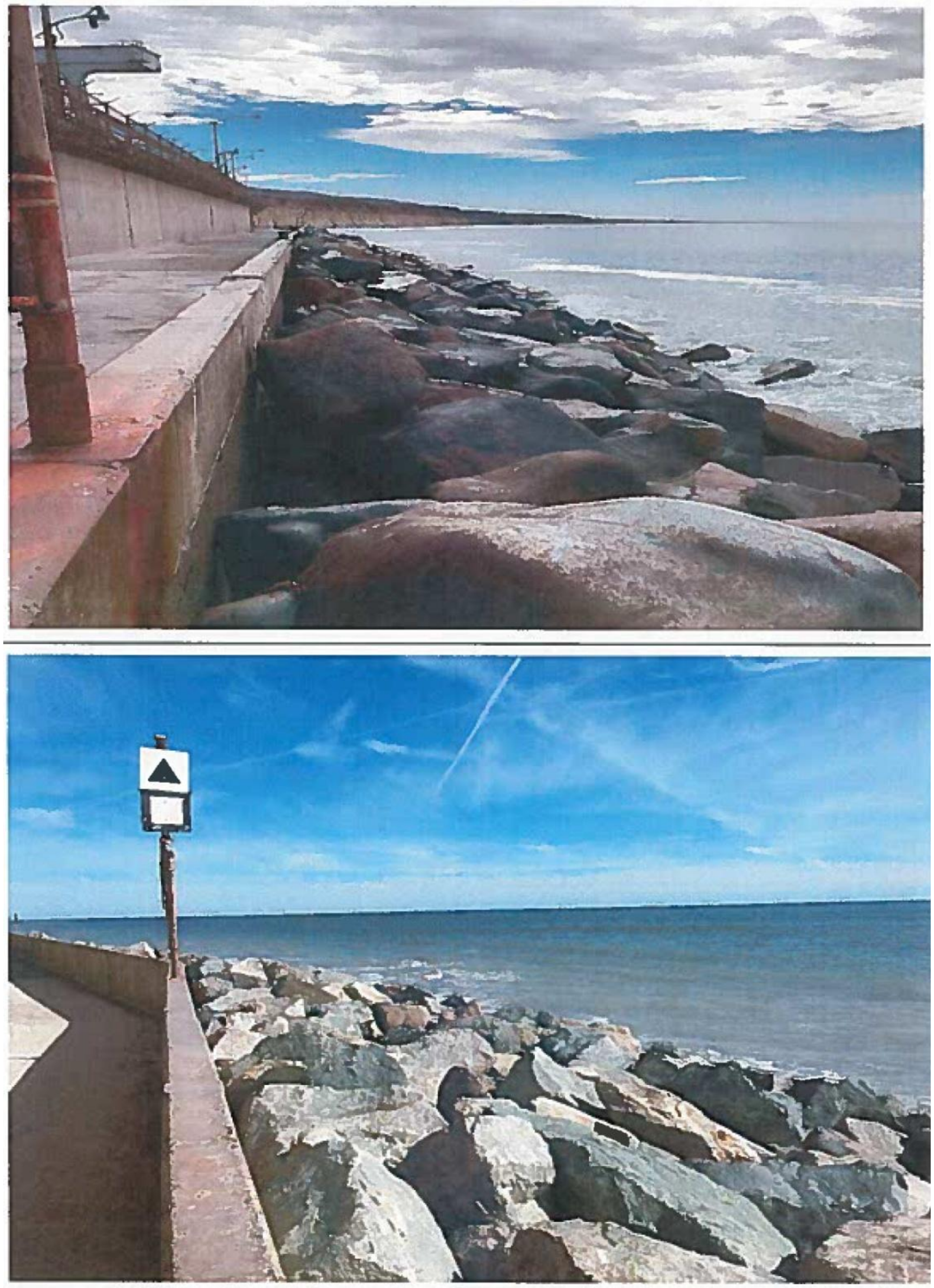

Figure 3-3. Top photograph taken on 20 March 2018, before placement of maintenance riprap seaward of retaining wall. Bottom photograph taken on 17 December 2019, after placement of riprap within gaps and depredated areas of the revetment. Direction of the photograph taken towards the south.

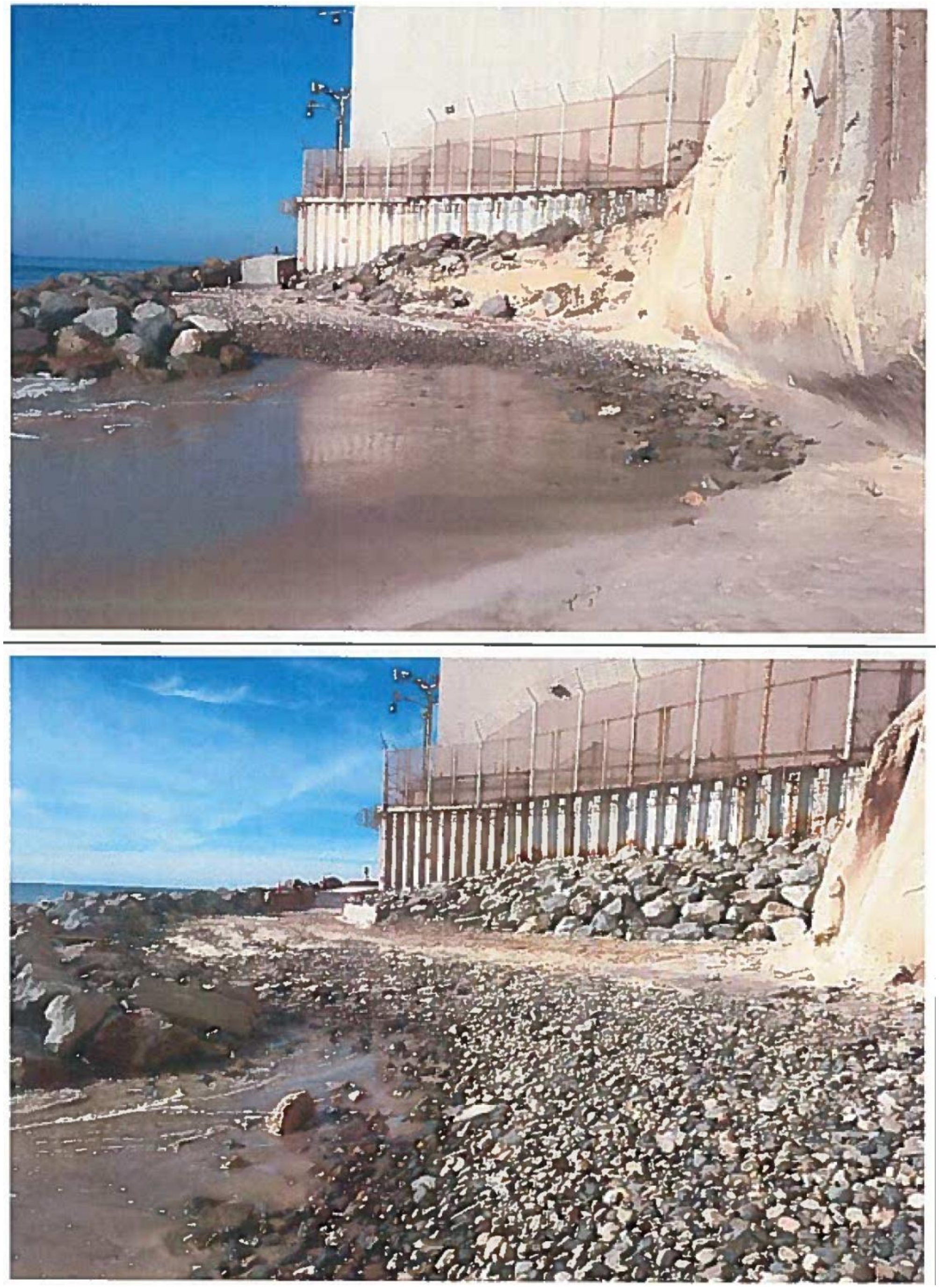

Figure 3-4. Top photograph taken on 15 October 2019, showing the sheet pile seawall before repairing the south end of the walkway. Bottom photograph taken on 17 December 2019, showing the sheet pile seawall after repairing the south end of the walkway.

Figure 3-5. Measurements of the long axis of the rock (length).

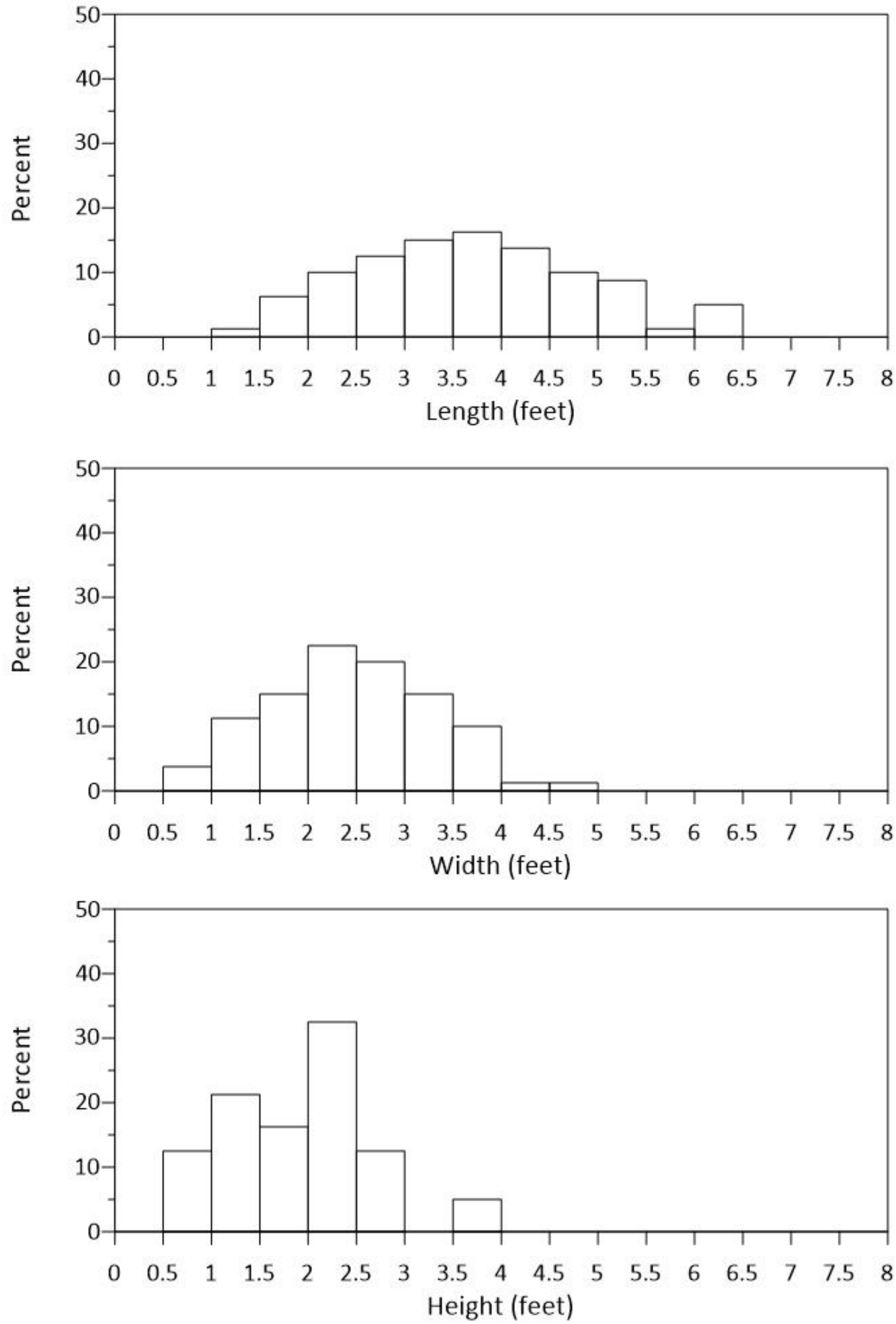

Figure 3-6. Histograms of rock length, width, and height.

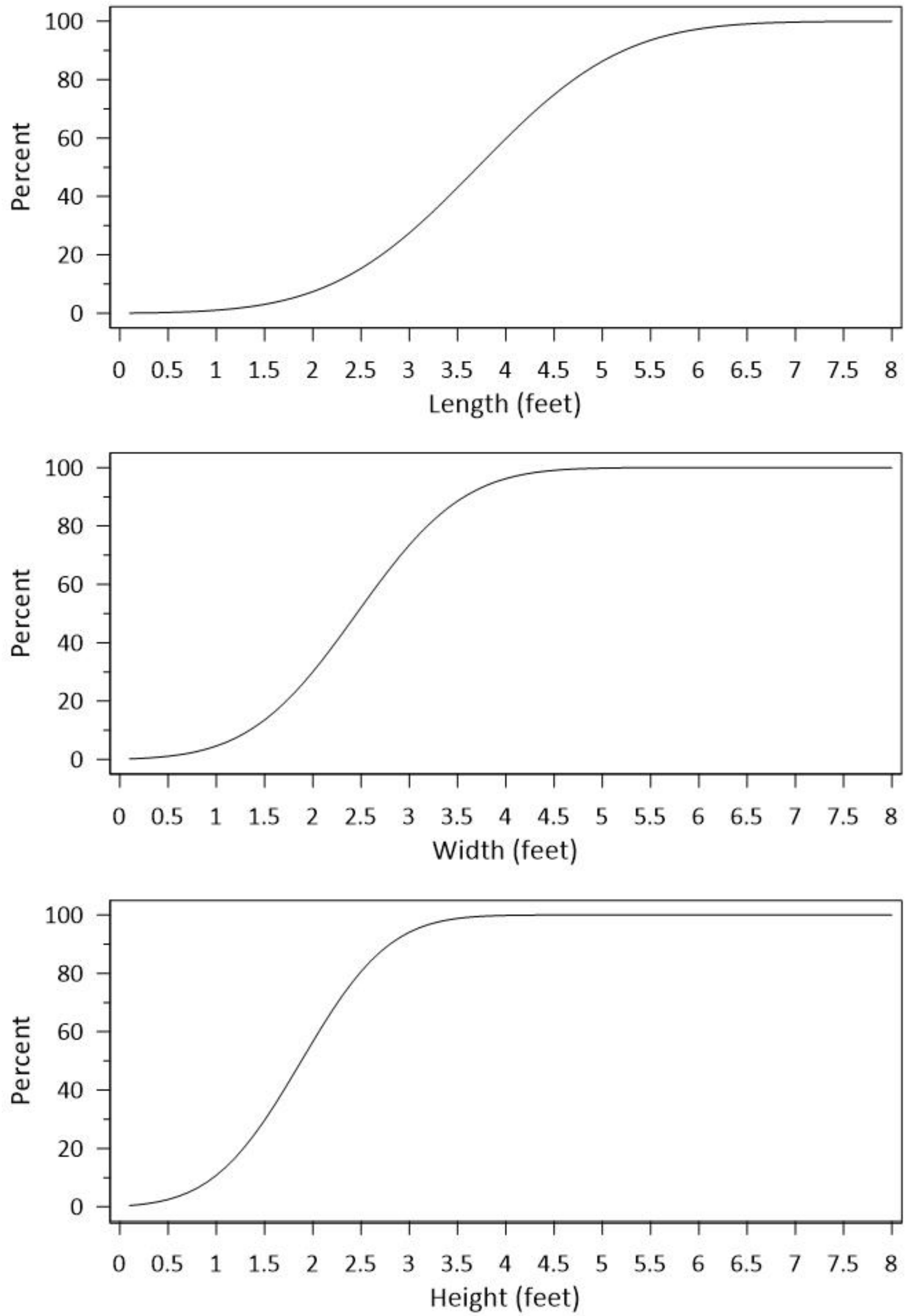

Figure 3-7. Cumulative distributions of rock length, width, and height.

Figure 3-8. Trimble SX10 scanning total station.

Figure 3-9. Location of 21 transects along the revetment, spaced 100 ft apart.

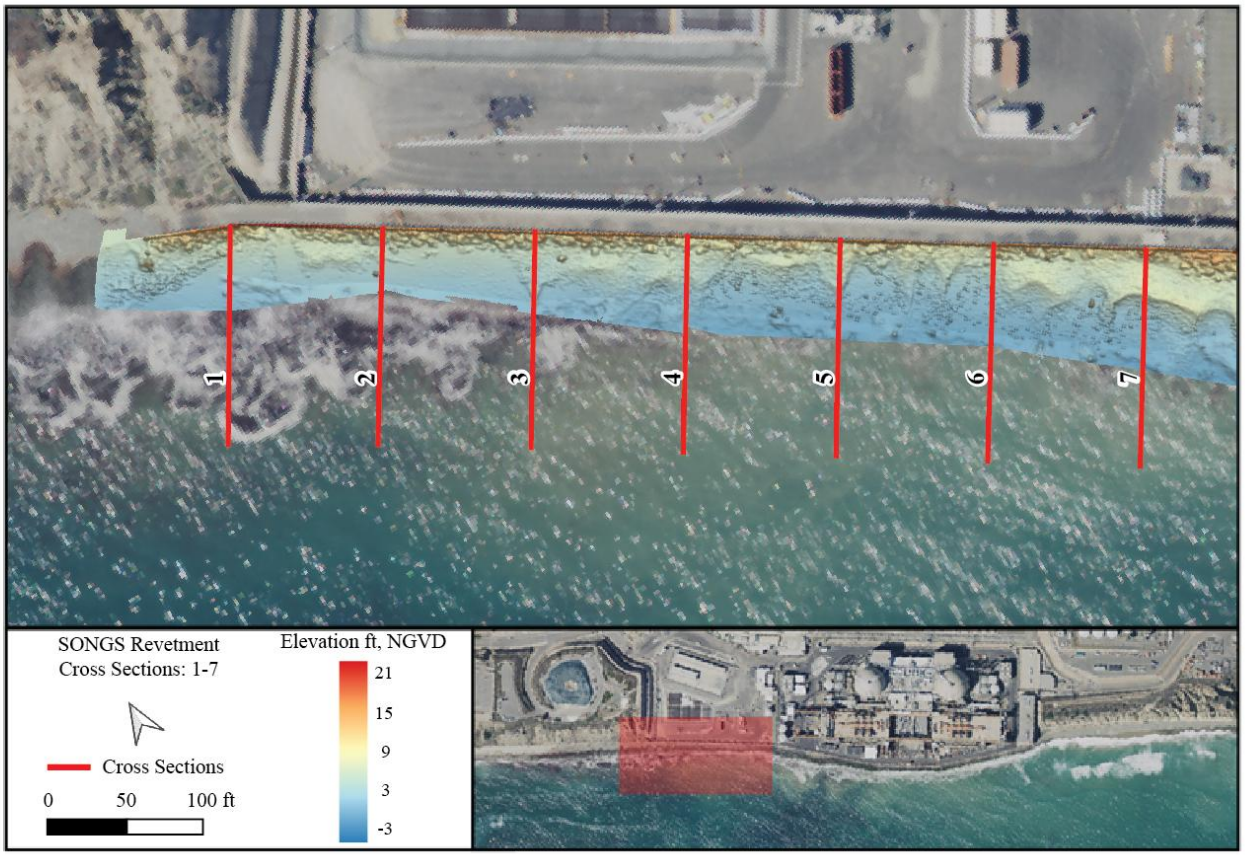

Figure 3-10. Elevation model of SONGS revetment from laser scanner for transects 1 to 7.

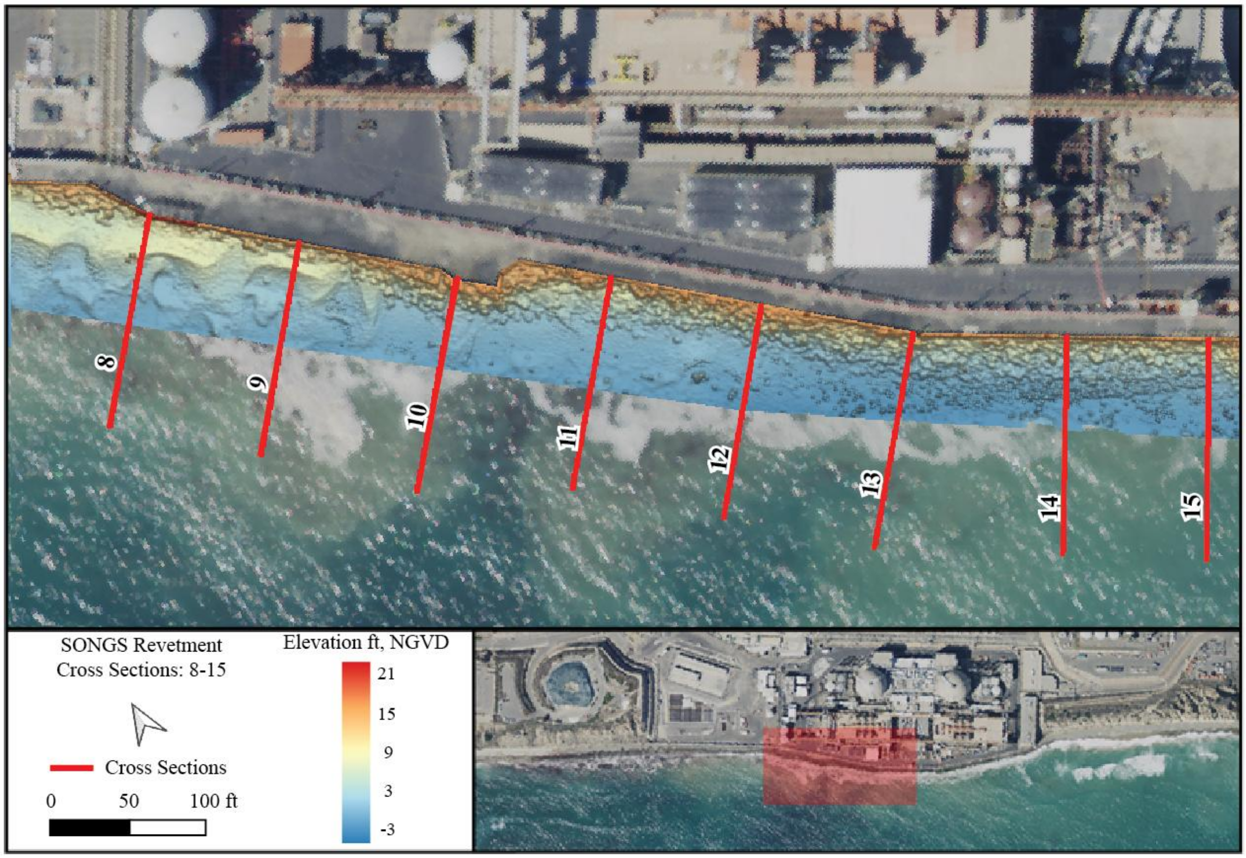

Figure 3-11. Elevation model of SONGS revetment from laser scanner for transects 8 to 15.

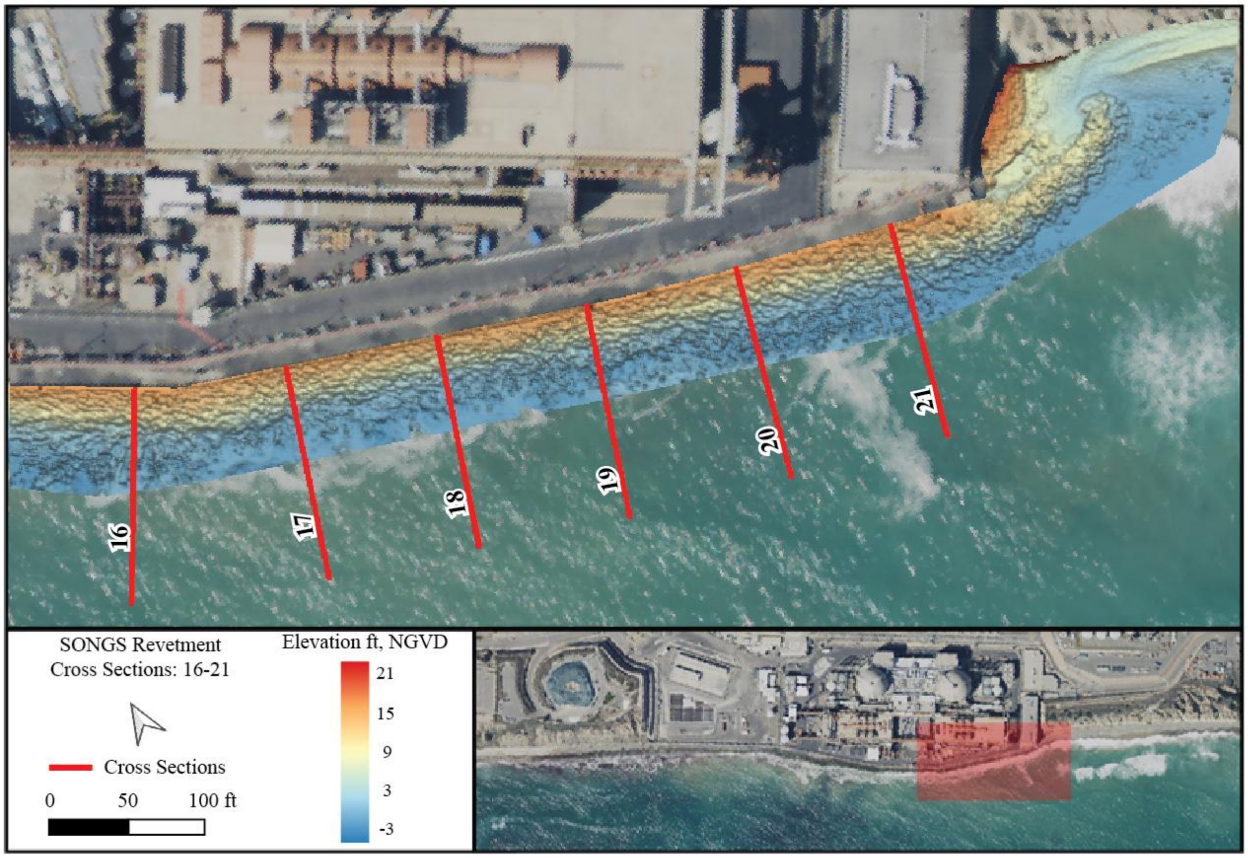

Figure 3-12. Elevation model of SONGS revetment from laser scanner for transects 16 to 21.

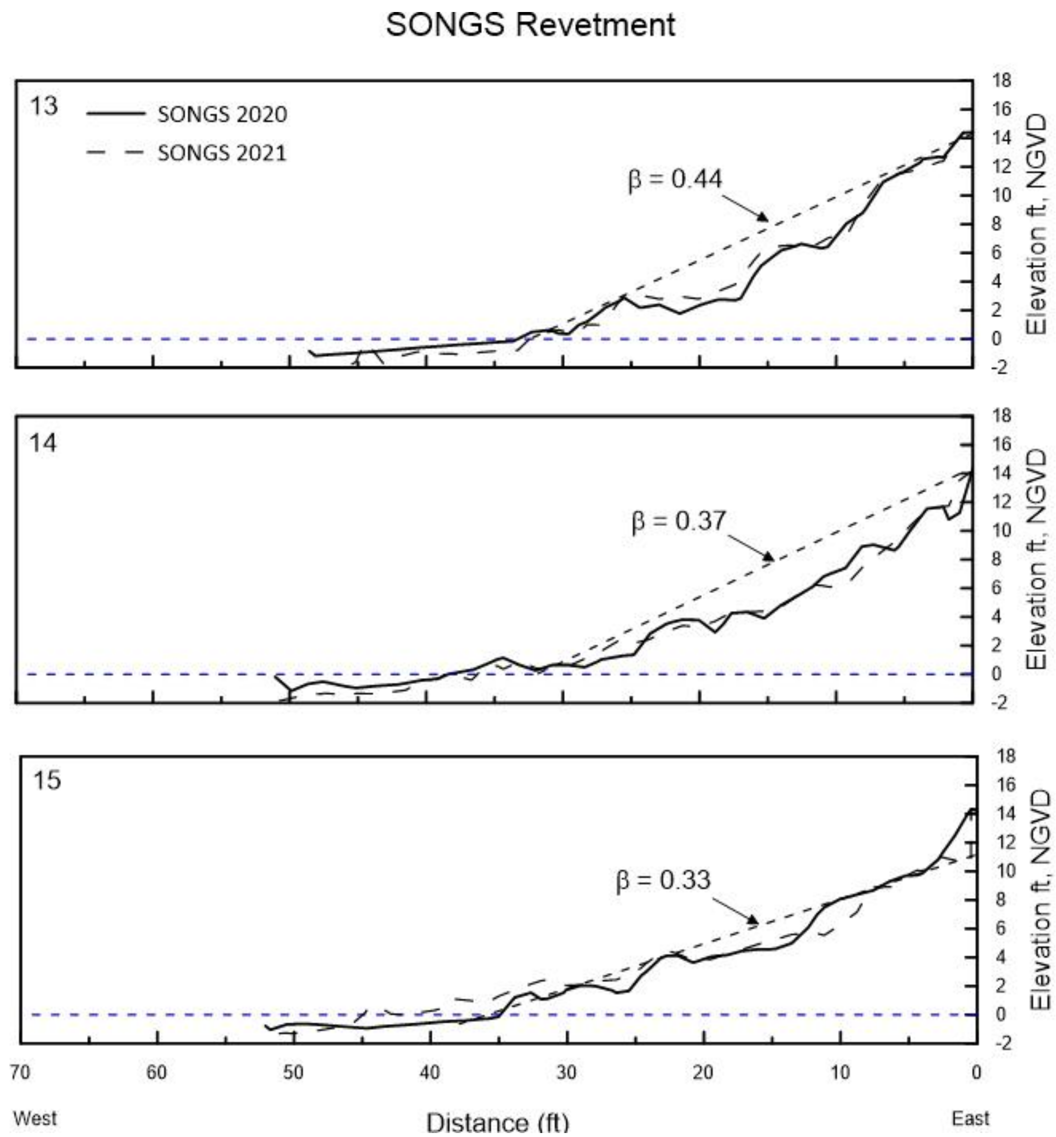

Figure 3-13. Typical revetment cross-sections showing slope "β" at the indicated transect (transect numbers in upper left corner of figures).

Table 3-1. Riprap and walkway wall heights and revetment slope (β).

Transect #	Riprap Height ft, NGVD29	Wall Height ft, NGVD29	Slope (β)
1	12.89	16.79	0.90
2	12.27	14.27	0.66
3	12.15	14.27	1.52
4	9.22	14.32	1.13
5	9.44	14.27	0.35
6	10.13	14.2	0.43
7	12.48	14.34	0.67
8	9.55	14.39	0.20
9	10.59	14.29	0.38
10	15.12	14.39	0.46
11	13.69	14.34	0.40
12	13.63	14.39	0.54
13	12.37	14.39	0.44
14	12.34	14.37	0.37
15	10.34	14.34	0.33
16	14.24	14.21	0.42
17	12.98	14.27	0.38
18	13.58	14.22	0.39
19	14	14.31	0.40
20	13.49	14.32	0.37
21	14.4	14.32	0.35

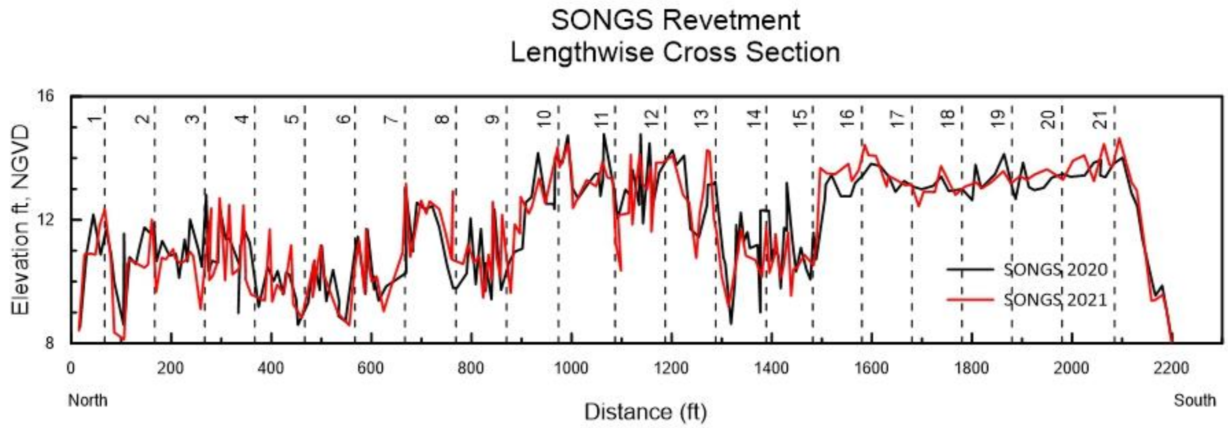

Figure 3-14. Elevation of the top of revetment for the 21 transects.

Table 3-2. Length, width, height, and estimated weight of the measured rocks.

Rock	Length (ft)	Width (ft)	Height (ft)	Weight (kg)
1	2.6	2.1	2	369
2	3.3	2.4	2.7	551
3	3.3	2.9	2.1	973
4	2	1.8	1.4	233
5	4.8	3.9	1.8	2,366
6	3.5	1.7	1.2	196
7	3.2	2.6	2.5	701
8	2.8	1.6	1	163
9	3.2	2.4	1.7	551
10	1.9	1	1	40
11	3.5	1.9	2	274
12	2	1.5	0.9	135
13	2.6	2.3	1.1	485
14	4.3	3.5	2.5	1,710
15	3.8	2.6	1.3	701
16	2.3	1.7	1	196
17	5.2	3	1.4	1,077
18	4.3	3.9	1.2	2,366
19	5.3	3.6	3	1,861
20	4.4	3.2	2.1	1,307
21	4.3	3.5	2.7	1,710
22	4.7	3	2.6	1,077
23	2.6	1.4	1.5	109
24	4.8	3.2	1.8	1,307
25	5.2	2.9	2.3	973
26	3.7	2.5	2.5	623
27	3.4	1.9	1.6	274
28	4.6	2.2	2.1	425
29	4	3.4	2.1	1,568
30	3.4	1.9	1.3	274
31	3.8	2.7	2.1	785
32	4.6	3.9	0.9	2,366
33	4.3	3.2	2.3	1,307
34	4.9	2.4	2.3	551
35	3.5	2.7	2.2	785
36	2.8	2.8	1.5	876
37	3	2.2	1.6	425
38	3.6	1.8	0.9	233
39	4.5	3.8	3.7	2,189
40	3.8	2.2	2	425
41	4.9	4.6	2.4	3,883
42	2.9	2.7	2.4	785

Rock	Length (ft)	Width (ft)	Height (ft)	Weight (kg)
43	3.6	2.1	2.1	369
44	4	2.4	2.6	551
45	4.3	2.7	3.6	785
46	3.8	2.2	3.6	425
47	4.1	3.3	2.1	1,433
48	3.6	2.5	1.5	623
49	3.9	2.4	1.2	551
50	6.3	3.4	2.3	1,568
51	5.1	2.9	2.2	973
52	2.2	1.5	1.1	135
53	2	1.2	0.9	69
54	2.3	1.6	1.6	163
55	4.4	2.7	2.1	785
56	3.3	2.6	1.2	701
57	2.4	2.1	1.1	369
58	2.5	2.1	2.1	369
59	5.5	3.7	2.7	2,020
60	3.4	1.9	2.2	274
61	4.2	1.7	1.9	196
62	2.9	1.4	2.1	109
63	5.4	4.2	2.8	2,955
64	2.9	1.9	2.3	274
65	5	3.2	1.6	1,307
66	5.8	3.3	2	1,433
67	6.1	3.4	3.7	1,568
68	6.4	4	2.8	2,553
69	4.2	3.7	2.9	2,020
70	6.3	3.2	2.2	1,307
71	3	1.1	2.2	53
72	3.4	2.2	1.3	425
73	2.2	1.1	1.3	53
74	1.3	1.1	0.6	53
75	1.6	1	0.8	40
76	3.8	2.7	2.7	785
77	5.4	2.4	2.1	551
78	2.3	1.2	0.7	69
79	2.1	0.7	1.4	14
80	3.8	2.9	2	973

Table 3-3. Mean and standard deviation for rocks parameters.

Rock Parameters	Length (ft)	Width (ft)	Height (ft)	Calculated weight (kg)
Mean	3.8	2.5	1.9	849
Minimum	1.3	0.7	0.6	14
Maximum	6.4	4.6	3.7	3,882
Std Dev	1.2	0.9	0.7	779

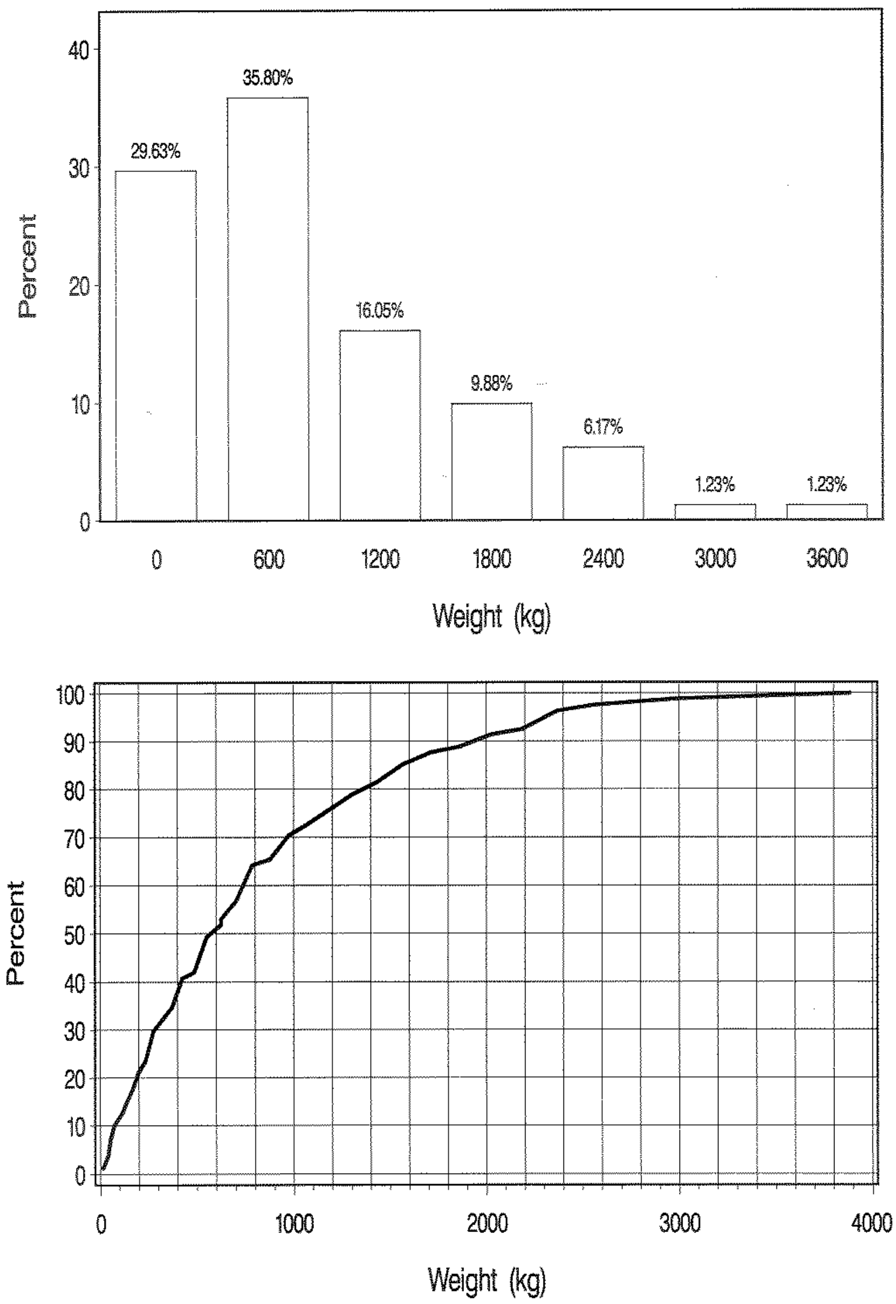

Figure 3-15. Weight distribution of SONGS revetment rocks.

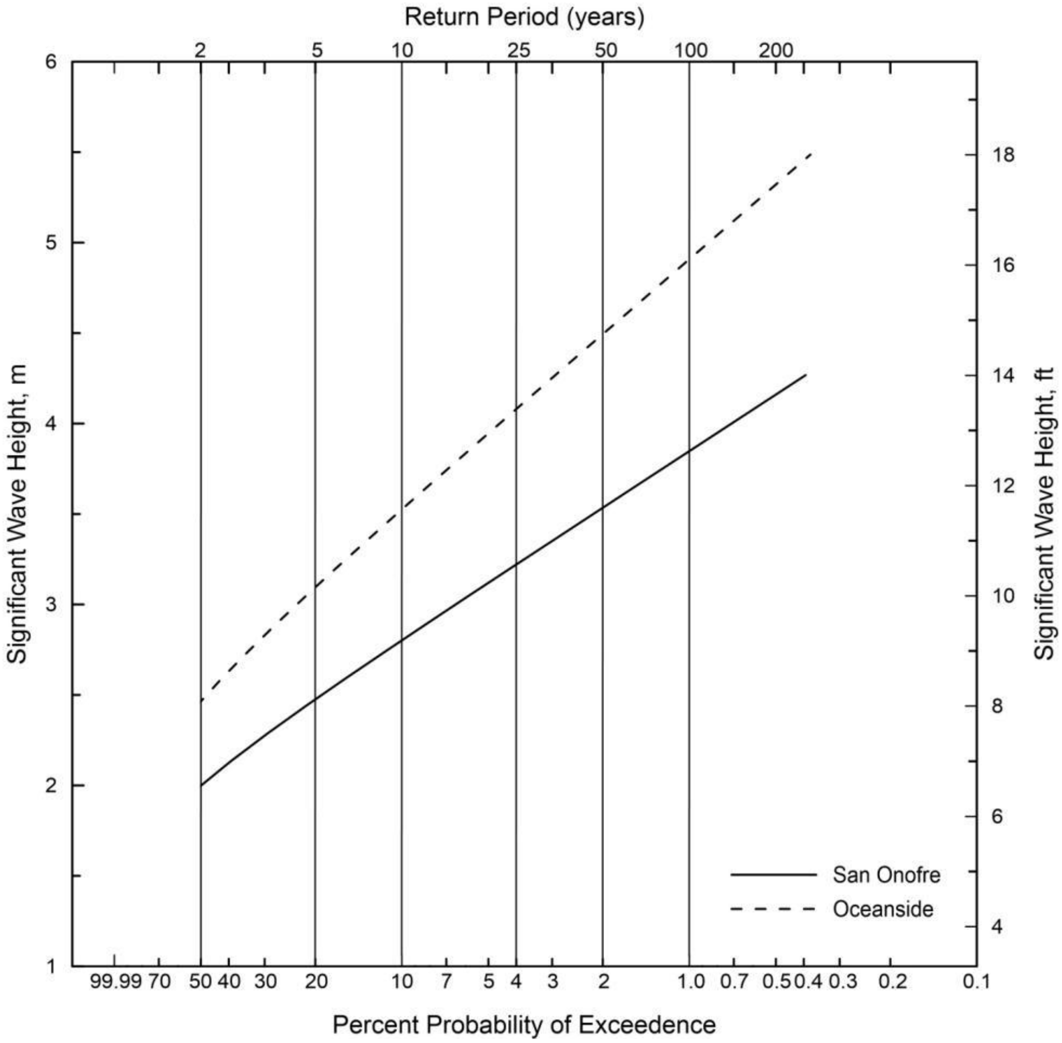

Figure 3-16. Design wave heights for various return periods at San Onofre.

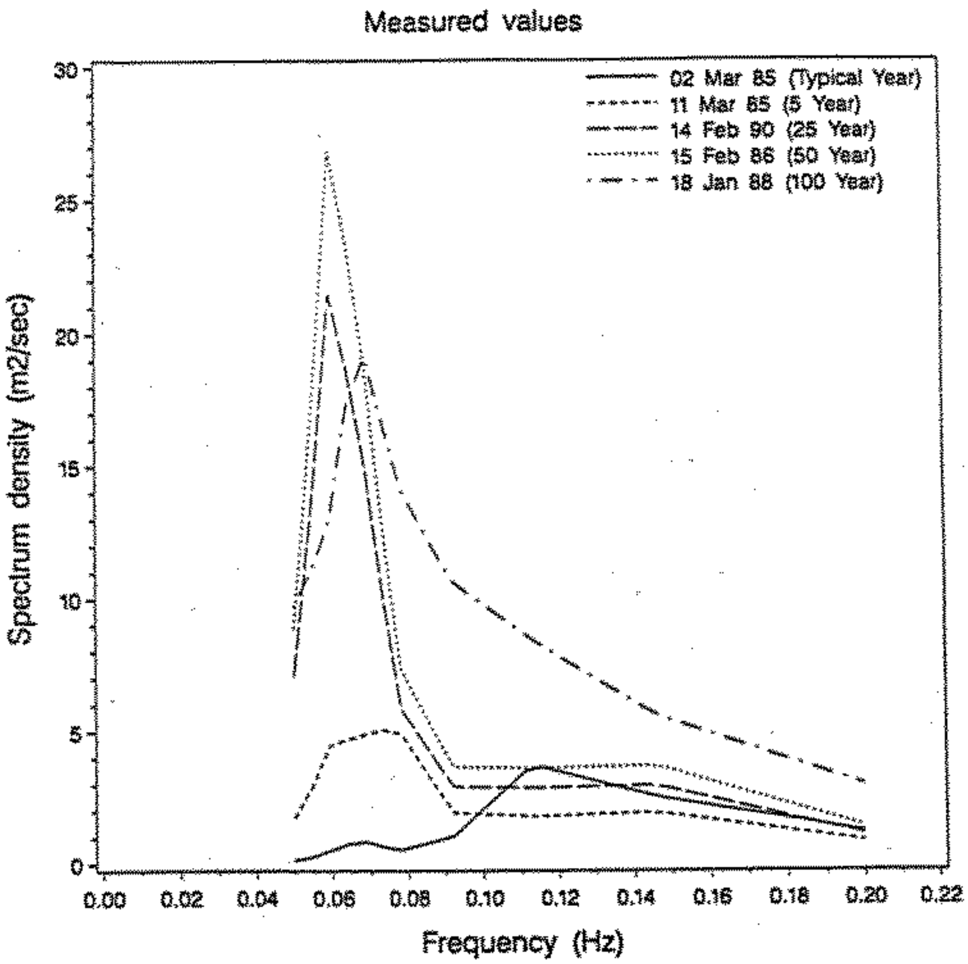

Figure 3-17. Measured spectrum density for various storms.

Table 3-4. Design wave characteristics at San Onofre.

Storm Return Period (yr)	Significant Wave Height, Hs (m)	Peak Period, Tp (sec)
2	2.0	9
5	2.4	12
10	2.8	12
25	3.2	17
50	3.5	17
100	3.8	16

Table 3-5. Largest 40 waves at San Onofre ranked in descending order (1976-1994).

Rank	Winter		Summer		All	
	Hs (m)	Tp (secs)	Hs (m)	Tp (secs)	Hs (m)	Tp (secs)
1	3.85	14.22	2.01	8.00	3.85	14.22
2	3.28	12.80	1.76	8.53	3.28	12.80
3	2.88	14.22	1.73	7.11	2.88	14.22
4	2.88	8.53	1.70	8.53	2.88	8.53
5	2.52	12.80	1.64	16.00	2.52	12.80
6	2.41	8.53	1.64	8.26	2.41	8.53
7	2.36	8.53	1.60	7.53	2.36	8.53
8	2.31	7.53	1.59	7.11	2.31	7.53
9	2.26	6.74	1.52	8.53	2.26	6.74
10	2.25	12.80	1.50	7.53	2.25	12.80
11	2.25	12.80	1.47	8.00	2.25	12.80
12	2.12	12.80	1.47	9.48	2.12	12.80
13	2.06	7.53	1.44	14.22	2.06	7.53
14	2.06	14.22	1.44	7.53	2.06	14.22
15	2.06	12.80	1.42	7.53	2.06	12.80
16	2.05	14.22	1.42	7.53	2.05	14.22
17	2.04	7.53	1.42	16.00	2.04	7.53
18	2.03	9.14	1.41	6.74	2.03	9.14
19	2.03	7.53	1.41	9.85	2.03	7.53
20	2.03	14.22	1.41	16.00	2.03	14.22

Table 3-6. Rock weights (W50) for 2020 and 2050.

Year	Water Depth Ds (ft)	H (ft)	H (m)	W50 (kg)
2020	7.79	4.4	1.33	276
2050 (P .05%)	9.79	5.5	1.67	548
2050 (H++)	10.59	5.9	1.8	685

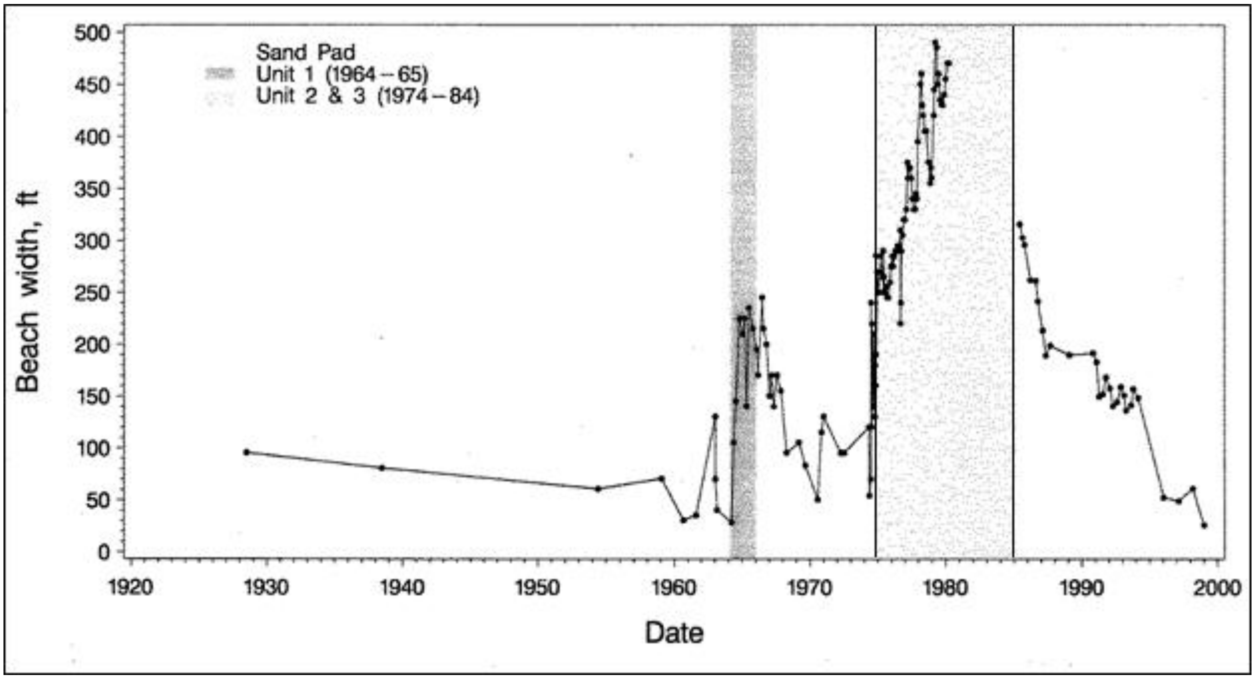

Figure 3-18. Historical beach width adjacent to Unit 1, 1928-2000. Vertical columns show periods when laydown pads were present. From Appendix E (Figure 7-5).

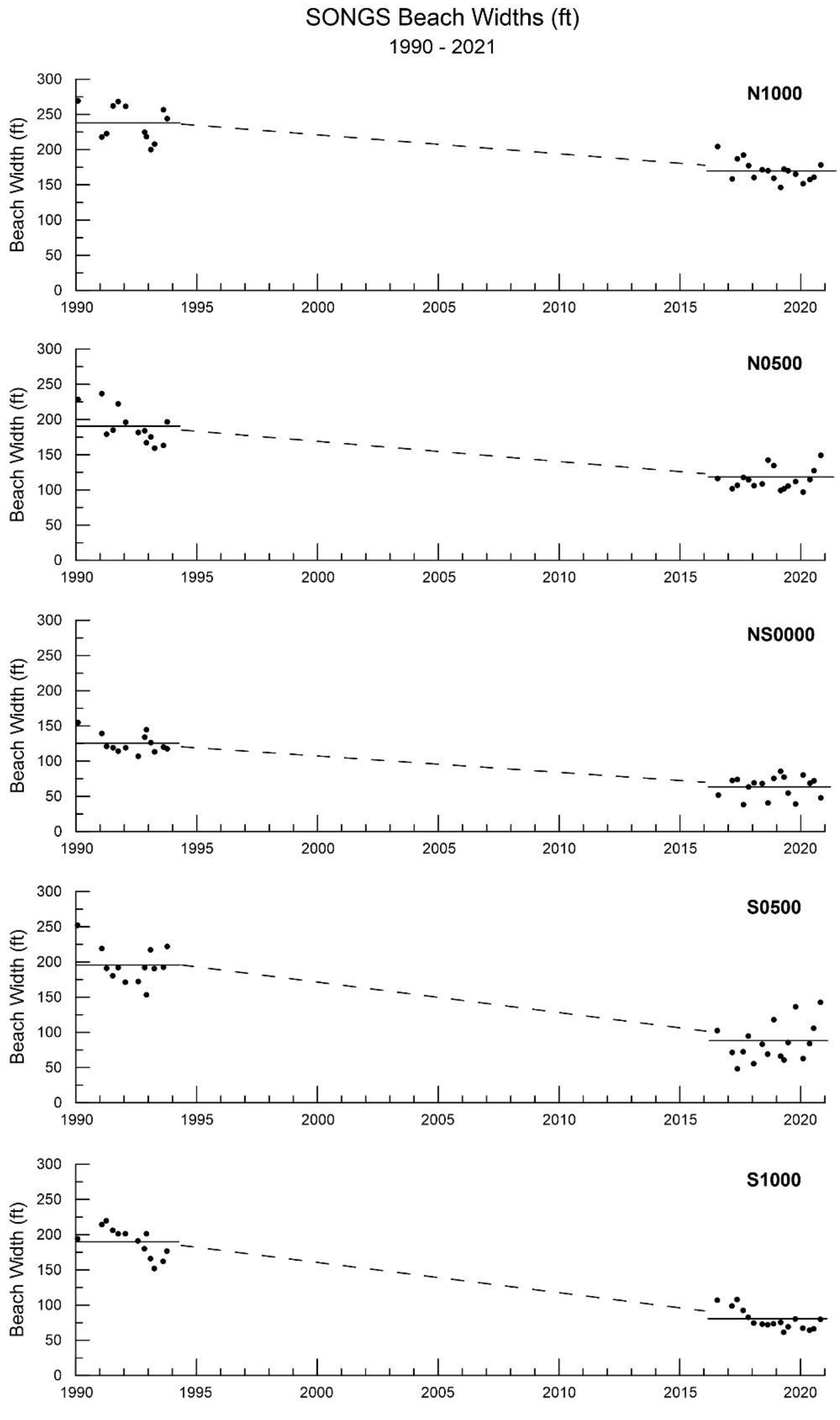

Figure 3-19. Beach width measured between 1991 through 1993 and between 2016 through 2020. Solid lines are the mean of beach width for the referenced periods and dotted lines cover the period where no long-term measurements were carried out. From Appendix E (Figure 7-7).

Table 3-7. Mean beach widths (ft) at San Onofre, 1990-1993 vs. 2017-2020. From Appendix E (Table 7-1).

Profile	1990-1993		2017-2020		Difference in mean	p-value
	Mean	Std. Dev	Mean	Std. Dev		
N1000	237.9	25.1	167.4	12.4	70.5	2.09E-07
N0500	190.4	25.0	114.9	15.6	75.5	1.19E-08
NS0000	125.4	13.9	64.3	15.3	61.1	1.02E-11
S0500	195.8	26.0	84.9	28.0	110.9	2.64E-11
S1000	189.8	20.9	77.5	12.8	112.3	6.05E-13

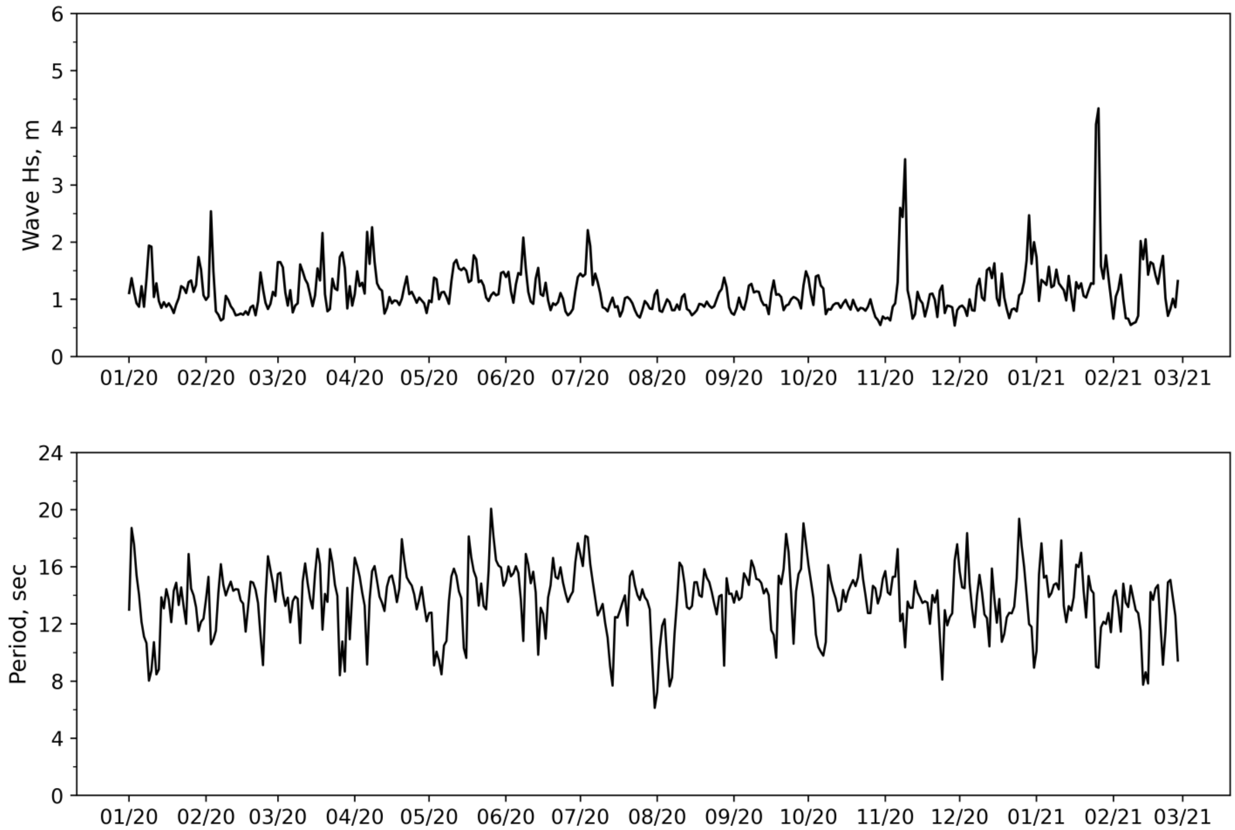

Figure 3-20. Wave height and wave period at SONGS from 1 January 2020 to 28 February 2021, calculated from wave data measured by Buoy 46224.

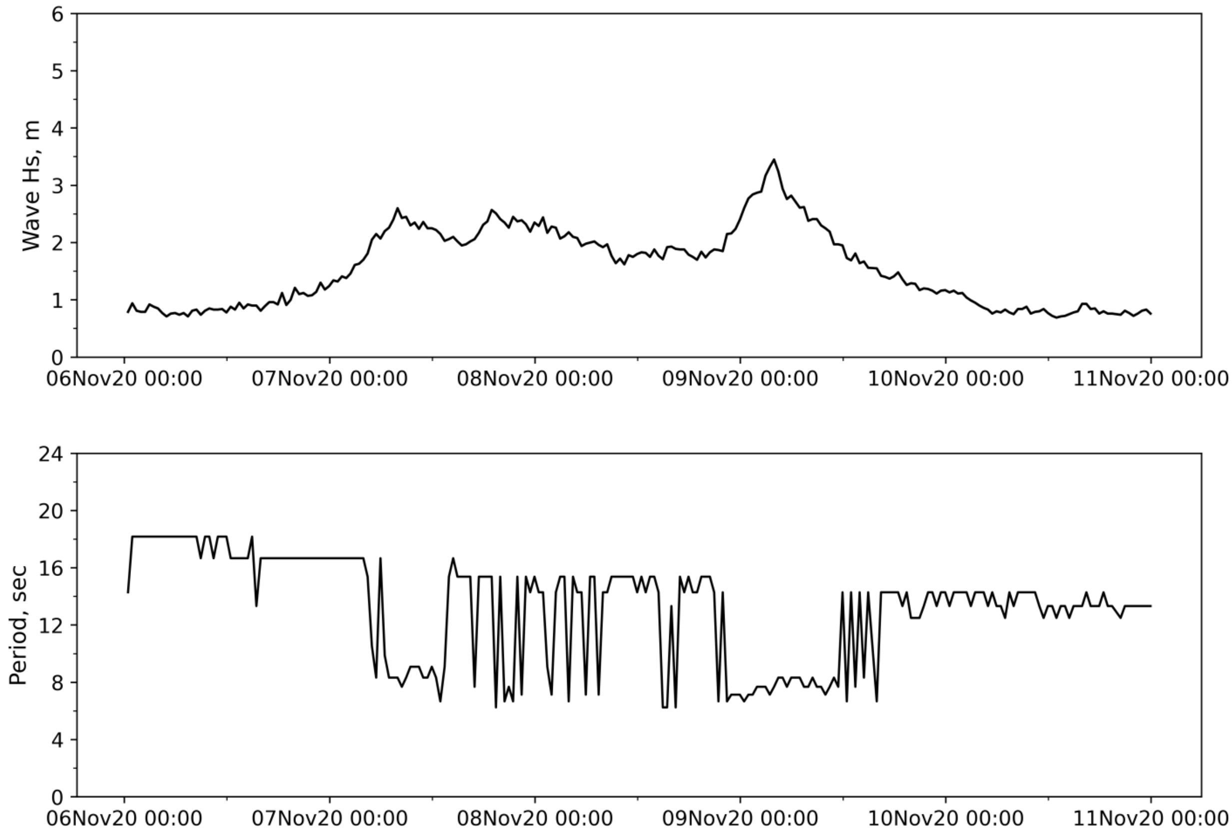

Figure 3-21. Wave height and wave period at SONGS from 6 to 11 November 2020.

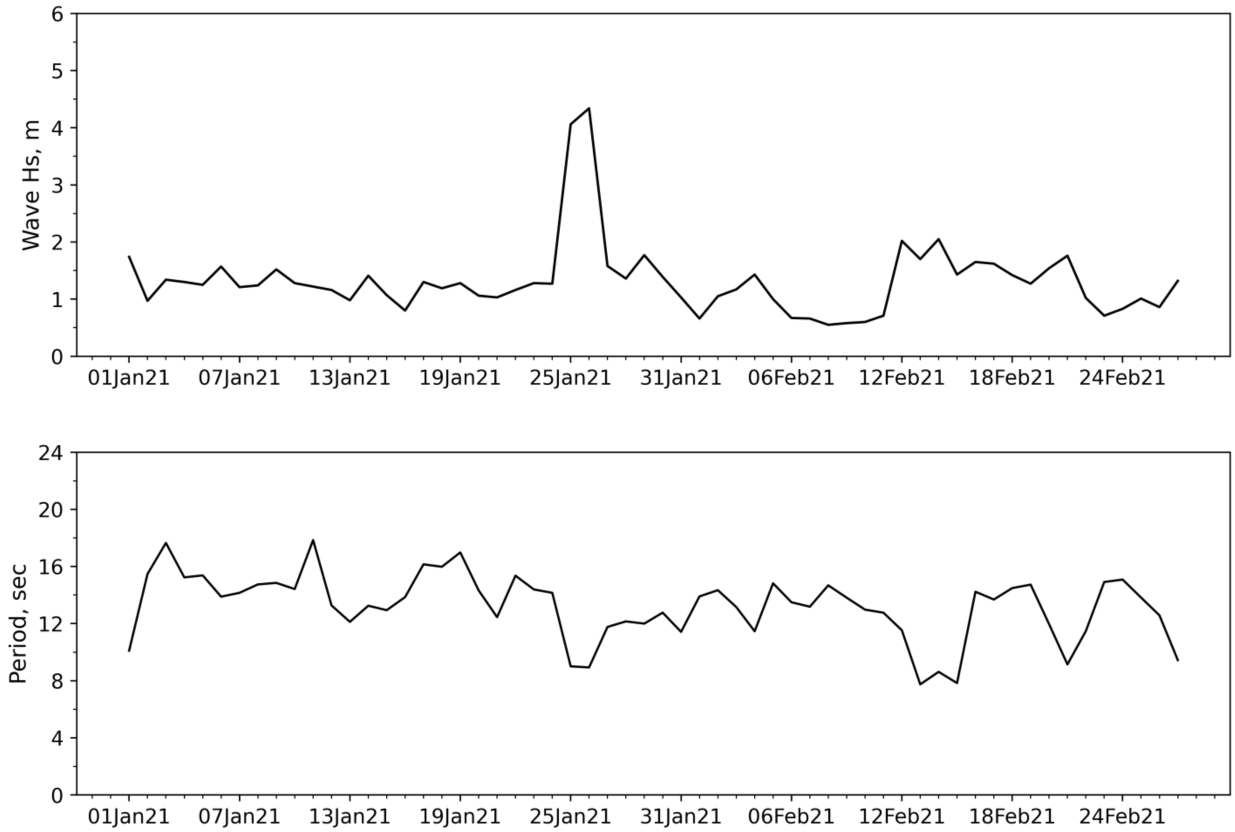

Figure 3-22. Wave height and wave period at SONGS from 1 January 2021 to 28 February 2021.

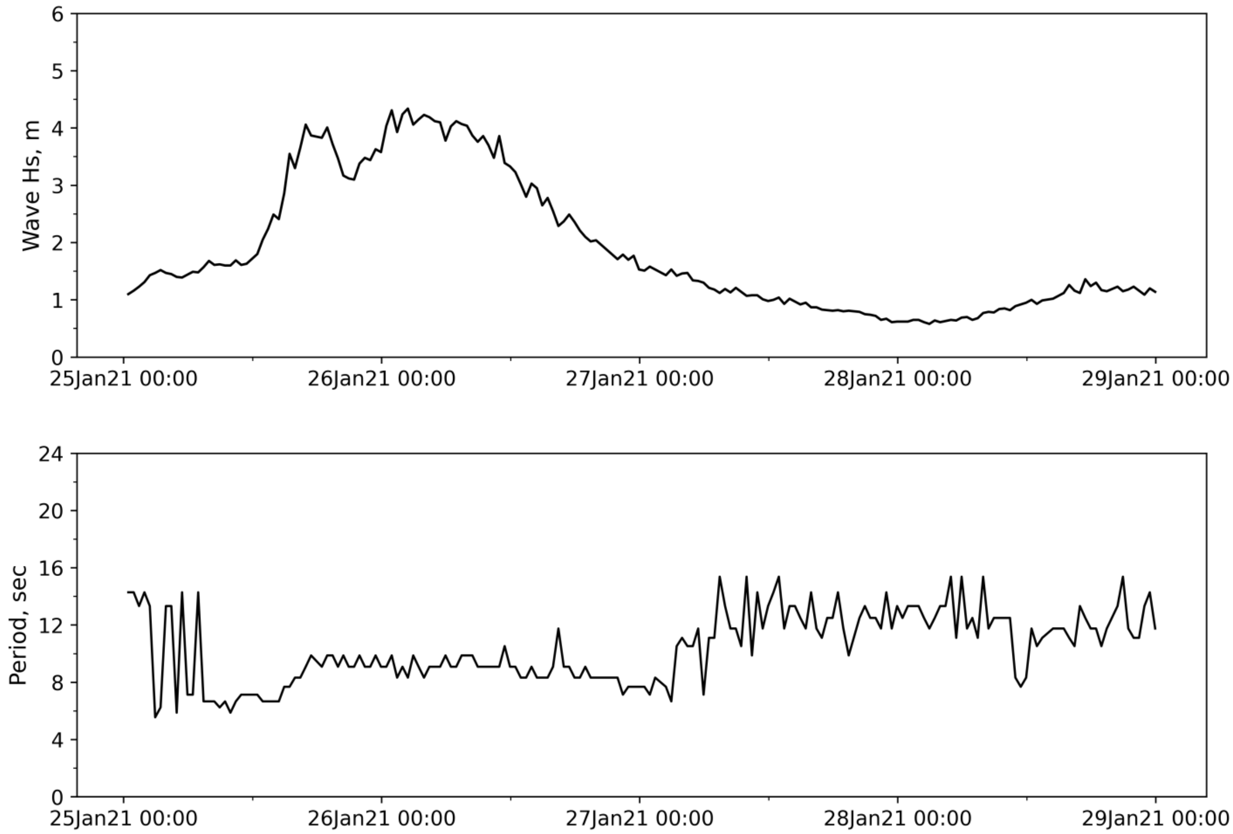

Figure 3-23. Wave height and wave period at SONGS from 25 to 29 January 2021.

Figure 3-24. North portion of the revetment covered by beach sand in 2020 (bottom), now covered with cobble in 2021 (top).

4.0 RUN-UP AND OVERTOPPING ANALYSIS

Wave run-up is defined as the rush of water up a beach or coastal structure caused by, or associated with, wave-breaking. The run-up elevation, designated *R* (Figure 4-1), is the maximum vertical height above still water level that the run-up will reach. If the run-up elevation is higher than the beach berm (or back of the beach) elevation, the excess is then representative of overtopping. Run-up elevation is dependent on the incident wave characteristics, beach slope, and porosity, and if a structure is present, on that structure's shape, slope, roughness, permeability, and water depth at the toe. Run-up analysis is important to assess possible flooding and damage to the SONGS revetment, retaining wall, and walkway. The amount of damage is dependent on the run-up elevation and amount of overtopping, as well as on storm wave duration.

4.1 RANDOM WAVE METHOD

Wave run-up (R) is composed of wave setup and swash run-up. The swash run-up is defined as a super elevation of the mean water level and fluctuation about that mean (S). *R* is given by the equation:

$$R = \acute{\eta} + S/2 \tag{4-1}$$

where ή is the setup and *S* is swash run-up.

Many small- and large-scale laboratory studies have been conducted to measure run-up values for modeled beaches, sloped dikes, and seawalls (e.g., Hunt, 1959; Van der Meer and Jenssen, 1995; Hedges and Reis, 1998). Based on laboratory experiments, Hunt (1959) proposed various formulas for estimating wave run-up, *R*, on a smooth slope as a function of offshore wave height, *H*, and the Iribarren number, ζ, such that:

$$R = kH\zeta, \tag{4-2}$$

where *k* is a constant and ζ is the Iribarren number defined as:

$$\zeta = \frac{tan\beta}{\overline{Ho/Lo}} \tag{4-3}$$

where tan *β* is beach slope, *Ho* is deepwater wave height, and *Lo* is deepwater wavelength.

Fewer studies have centered on run-up on beaches (Holland and Holman, 1993; Raubenheimer et al., 1995; Ruggiero et al., 2004; Stockdon et al., 2006).

Stockdon et al. (2006) considered the contribution from both incident and infra gravity waves, using data from 10 field experiments with varying bathymetries and wave heights. They empirically estimated $R_{2\%}$ by:

$$R_2 = A\left(0.35\,\beta_f\,(H_0 L_0)^{1/2} + \frac{\left[H_0 L_0\,(0.563\beta_r^2 + 0.004)\right]^{1/2}}{2}\right) \qquad (4\text{-}4)$$

where β_f is the foreshore beach slope and H_o is the deepwater significant wave height, A is a coefficient equal to 1.1 as estimated by Stockdon, and $R_{2\%}$ is the 2% exceedance level of run-up for each run. The units of the Equation 4-4 are in meters.

The SONGS revetment reduces wave run-up by factor that varies from 0.5 to 0.6 (USACE, 1994b; Table 7-2) due to slope roughness and permeability, which can be described by a characteristic diameter of the armor unit and the porosity of the layer that is able to decrease the wave run-up on the structure. This is significant since the revetment illuminates at least one-half of the wave run-up that would occur without it, thus reducing overtopping of the retaining wall and related flooding and other negative impacts on the walkway and SONGS main seawall.

4.2 OVERTOPPING

The overtopping rate (Q) is defined as the volume of water that overtops a coastal structure or beach berm along the beach length per unit time and length. The units are volume per second per unit length (ft^3/sec-ft or m^3/sec-m). Overtopping empirical models are based on laboratory studies of structure overtopping. These models are used to test design specifications intended to limit the overtopping of levees and dikes, and they, therefore, give conservative values. A beach berm can act in the same manner as these structures in protecting the backshore development from wave attack and flooding.

Wave overtopping values depend on the ratio of freeboard height and wave run-up height. Freeboard *Rc* is defined as the height of the berm crest above mean water level. In order for waves to overtop a berm, the run-up heights must be greater than the freeboard height. Overtopping is dependent on run-up height and, therefore, dependent on incident wave height and period, and beach slope.

Hedges and Reis (1998) introduced a semi-empirical model (H&R model) based on an overtopping theory for regular waves developed by Kikkawa et al. (1968), which assumed that a seawall or beach berm acted as a weir whenever the incident water level exceeded the seawall level and the described instantaneous discharge by the weir formula. The H&R model extended the concept to random waves. Reis et al. (2008) compared the H&R model with three other methods used to estimate the overtopping rate for various structures subject to random wave action. The slopes of these structures varied from 1:1 to 1:20, and wave steepness varied from 0.01 to 0.3. The models were: (1) Owen model (Owen, 1980); (2) Van der Meer Janssen model (Van der Meer and Janssen, 1995); and (3) AMAZON Numerical Model (Hu, 2000). The results showed good agreement between the H&R model and the data. There was general agreement between the H&R and AMAZON models, while Owen's model systematically over-predicted the discharges. Van der Meer and Janssen's model gave similar results to the H&R model, except that they over-predicted discharges for some conditions, which are outside the ranges of applicability.

The H&R model extending the concept to random waves can be written as:

$$\frac{\mathrm{Q}}{\overline{gR3\mathrm{max}}} = A \quad 1- \frac{Rc}{\gamma rRmax} \quad \mathrm{B} \qquad for 0 \leq \frac{Rc}{\gamma rRmax} < 1 \qquad (4\text{-}5)$$

and

$$\frac{\mathrm{Q}}{\overline{gR3\mathrm{max}}} = 0 \qquad\qquad for \quad \frac{Rc}{\gamma rRmax} \geq 1 \qquad (4\text{-}6)$$

where g is gravitational acceleration, R_{max} is the maximum run-up on smooth slope, and γr is a reduction factor to account for rough slope. In this study, R_{max} is estimated by equation number 9 presented by Reis et al. (2008). Additionally, the coefficients of the HR model were given by Reis et al. (2008) as:

$$A = \begin{matrix} 0.0033 + 0.0025 \ \ 1/\beta & for 0.08 \leq \ \beta \ \leq 1 \\ 0.0333 & for 0.05 \ \leq \ \beta \ < 0.083 \end{matrix} \qquad (4\text{-}7)$$

$$B = \begin{matrix} 2.8 + 0.65 \ \ 1/\beta & for 0.13 \leq \ \beta \ \leq 1 \\ 10.2 - 0.275 \ \ 1/\beta & for 0.05 \ \leq \ \beta \ < 0.13 \end{matrix} \qquad (4\text{-}8)$$

where β is the beach slope.

4.3 RESULTS

Figure 3-13 shows typical cross-sections of the SONGS revetment. The locations of these profiles are shown in Figure 3-9. The slope (β) of the revetment varies from 0.33 to 0.44. The height of the walkway is about 14 ft (NGVD). The design water level is estimated as 5.5 ft (NGVD). Table 4-1 provides run-up and overtopping results for all design wave and water level conditions, including MSLR under the medium-high scenario for 2020, 2030, 2040, and 2050. Table 4-2 shows these results for the extreme H++ MSLR projection. Tables 4-1 and 4-2 suggest that wave overtopping already occurs (in 2020) for storm wave conditions meeting or exceeding a 10-year return period, that is, waves with 10% probability of occurrence in a given year. This is consistent with observations.

As MSLR progresses, overtopping rates are expected to increase. For large storms, rates are projected to reach 0.5 ft^3/sec-ft by 2030 and 1-1.6 ft^3/sec-ft by 2050. There is a short segment in the walkway where the concrete wall has been replaced by rails to provide a flow path for the saltwater cooling system during plant operations. This opening in the wall will increase overtopping on the walkway (Figure 4-2). However, it does not represent a significant hazard to pedestrians since the walkway will be closed during storms and there are no more discharges from the system.

4.4 PROBABILITY ANALYSIS

The probability associated with run-up and overtopping is considered in quantitative terms. This risk is defined as the probability that a “T-year” return-period event will occur at least once during a given “n-year” long time period. The run-up results in Tables 4-1 and 4-2 can be used to estimate the risk for any selected “n-year” long time period. The results can also be used to estimate the probability of run-up of a given size during a specified time period. The probability of a T-year run-up in any one year is $P = 1/T$.

In other words, there is a one-percent chance that the 100-year run-up will occur during a given year. The probability is equal to the sum of the probabilities of having one run-up, two run-ups, or *n* run-up events occurring during *n* years of interest, or to 1 minus the probability of having no run-ups. The risk can be calculated from Equation 4-9:

$$P = 1 - (1 - 1/T)^n \tag{4-9}$$

Equation 4-9 indicates that there is a 63% chance that the 100-year magnitude run-up will occur at least once during any 100-year time interval. Similarly, Equation 4-9 can be used to calculate the risk associated with any T-year run-up during any time period. Figure 4-3 gives the probability of occurrence of T = 25-year, 50-year and 100-year run-ups in an n-year period based on Equation 4-9.

4.5 DISCUSSION

Observations suggest that over the last decade or longer, the SONGS revetment has adjusted to reach an equilibrium configuration. Under its current condition, the revetment is expected to withstand projected wave forces with acceptable minimum damages that will not impact the integrity of the revetment as a whole.

The walkway elevation at 14 ft (NGVD) is relatively low and will continue to be flooded under large wave conditions that overtop the revetment. Occasional walkway flooding will not significantly impact the main SONGS seawall structure, nor seriously affect lateral public beach access since it will be relatively brief and limited to large wave events when beach access will be unsafe in any case. Additionally, it should be noted that the results of run-up and overtopping presented in this study are conservative for the following reasons:

1. The results are based on an extreme high water level of 5.5 ft (NGVD) that includes King Tides, El Niño enhancements, and one-foot storm surges. Observations suggest that it is exceedingly unlikely for large storm waves to occur precisely at the time of peak high (King) tides (e.g., Elwany and Flick, 1999; Flick, 1998 and 2016; Young et al., 2018).
2. Figure 4-4 illustrates the joint probability distribution between significant wave height and water level between 1976-1994, a period characterized by large wave events occurring between 1981 and 1984. Figure 4-3 shows that the probability of 50-year and 100-year waves occurring in the next 30 years is 0.45 and 0.28, respectively. Multiplying these probabilities by the probability of larger waves occurring at high tides will lead to an extremely low probability of occurrence.

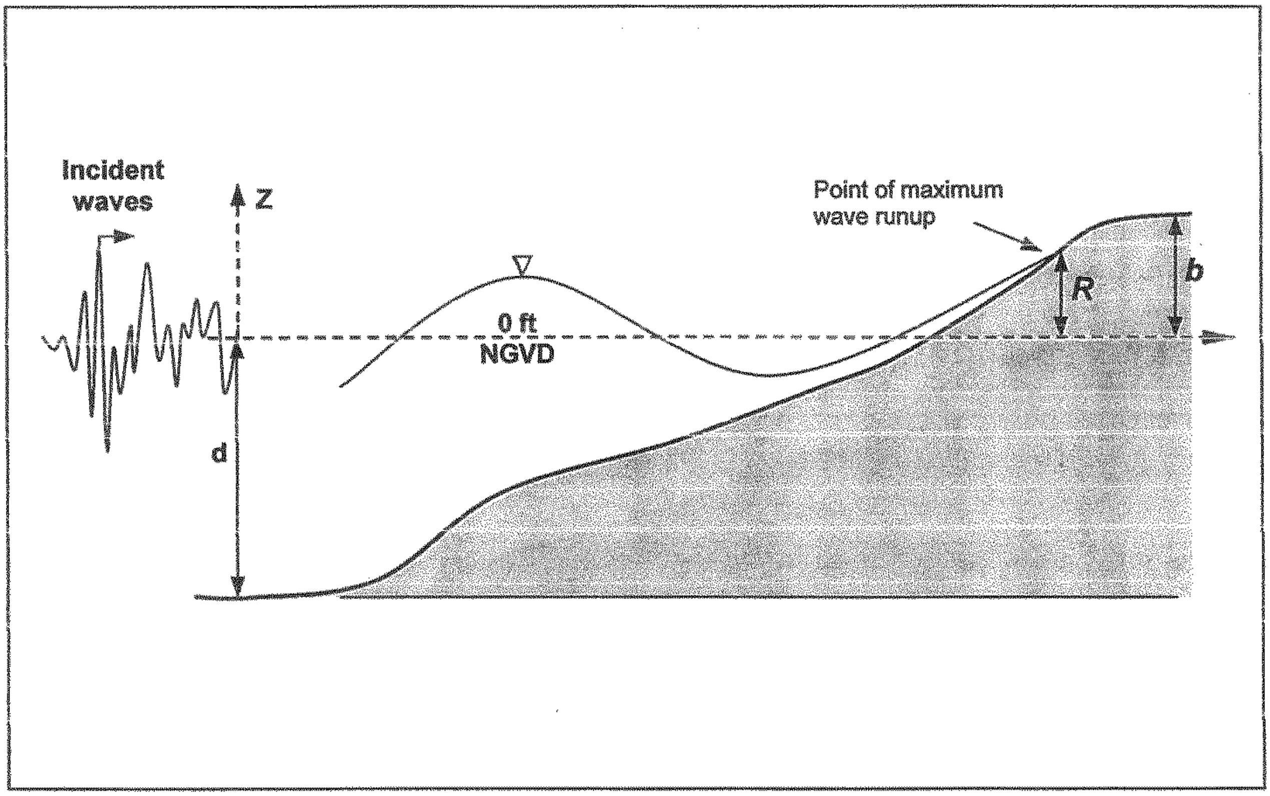

Figure 4-1. Wave run-up on a slope. R is the run-up elevation, b is the height of the beach berm. If R > b, then overtopping will occur.

Table 4-1. Run-up and overtopping summary for Medium-High Risk Aversion.

Year	Return Period (yr)	HS (ft)	Tp (Sec)	Sea Level Rise (ft)	Run-up (ft)	Run-up Elevation (ft)	Overtopping Rate (ft^3/sec-ft)
2020	2	2	9	0	5.27	10.77	0.00
	5	2.4	12	0	7.23	12.73	0.00
	10	2.8	12	0	7.81	13.31	0.01
	25	3.2	17	0	10.58	16.08	0.18
	50	3.5	17	0	11.06	16.56	0.28
	100	3.8	16	0	11.09	16.59	0.32
2030	2	2	9	0.9	5.27	11.67	0.00
	5	2.4	12	0.9	7.23	13.63	0.01
	10	2.8	12	0.9	7.81	14.21	0.04
	25	3.2	17	0.9	10.58	16.98	0.34
	50	3.5	17	0.9	11.06	17.46	0.49
	100	3.8	16	0.9	11.09	17.49	0.56
2040	2	2	9	1.3	5.27	12.07	0.00
	5	2.4	12	1.3	7.23	14.03	0.02
	10	2.8	12	1.3	7.81	14.61	0.06
	25	3.2	17	1.3	10.58	17.38	0.44
	50	3.5	17	1.3	11.06	17.86	0.62
	100	3.8	16	1.3	11.09	17.89	0.71
2050	2	2	9	2	5.27	12.77	0.00
	5	2.4	12	2	7.23	14.73	0.05
	10	2.8	12	2	7.81	15.31	0.12
	25	3.2	17	2	10.58	18.08	0.69
	50	3.5	17	2	11.06	18.56	0.94
	100	3.8	16	2	11.09	18.59	1.05

Table 4-2. Run-up and overtopping summary for Extreme Risk Aversion (H++).

Year	Return Period (yr)	HS (ft)	Tp (Sec)	Sea Level Rise (ft)	Run-up (ft)	Run-up Elevation (ft)	Overtopping Rate (ft^3/sec-ft)
2020	2	2	9	0	5.27	10.77	0.00
	5	2.4	12	0	7.23	12.73	0.00
	10	2.8	12	0	7.81	13.31	0.01
	25	3.2	17	0	10.58	16.08	0.18
	50	3.5	17	0	11.06	16.56	0.28
	100	3.8	16	0	11.09	16.59	0.32
2030	2	2	9	1.1	5.27	11.87	0.00
	5	2.4	12	1.1	7.23	13.83	0.02
	10	2.8	12	1.1	7.81	14.41	0.05
	25	3.2	17	1.1	10.58	17.18	0.39
	50	3.5	17	1.1	11.06	17.66	0.55
	100	3.8	16	1.1	11.09	17.69	0.63
2040	2	2	9	1.8	5.27	12.57	0.00
	5	2.4	12	1.8	7.23	14.53	0.04
	10	2.8	12	1.8	7.81	15.11	0.10
	25	3.2	17	1.8	10.58	17.88	0.61
	50	3.5	17	1.8	11.06	18.36	0.84
	100	3.8	16	1.8	11.09	18.39	0.94
2050	2	2	9	2.8	5.27	13.57	0.01
	5	2.4	12	2.8	7.23	15.53	0.12
	10	2.8	12	2.8	7.81	16.11	0.24
	25	3.2	17	2.8	10.58	18.88	1.12
	50	3.5	17	2.8	11.06	19.36	1.47
	100	3.8	16	2.8	11.09	19.39	1.62

Figure 4-2. Exposed area in the walkway wall.

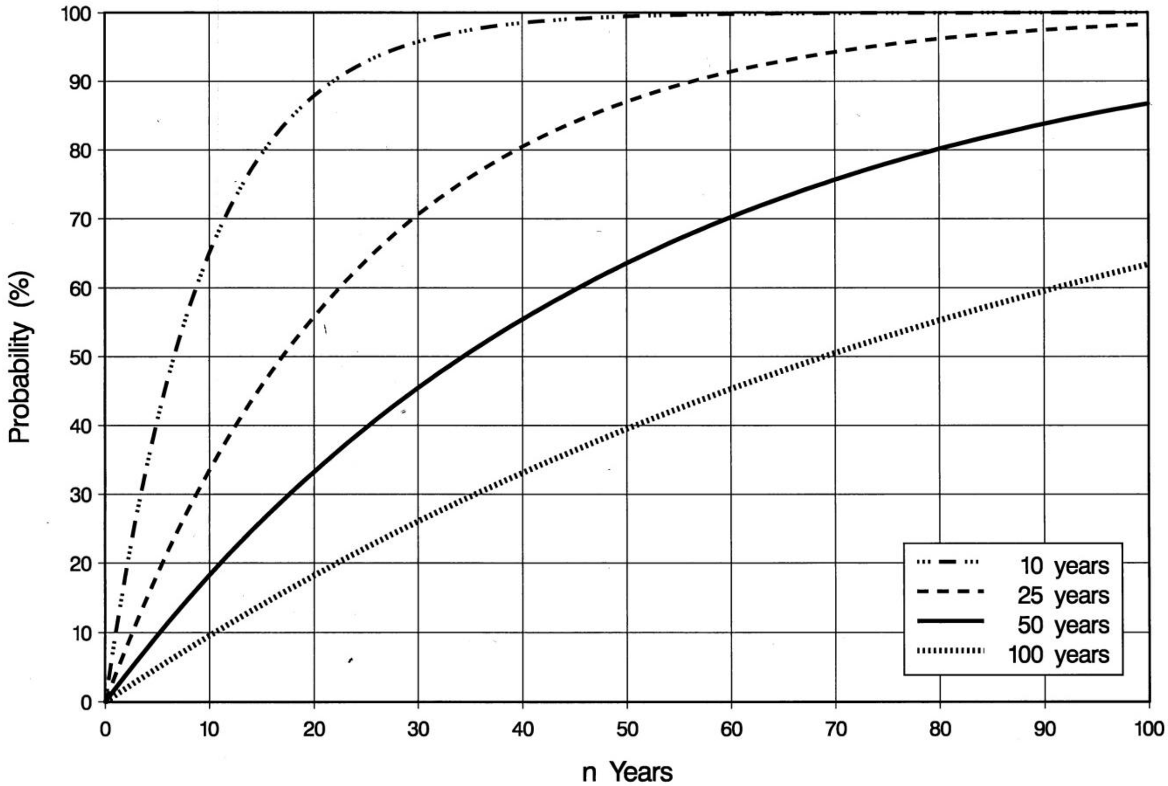

Figure 4-3. Probability of 10-, 25-, 50-, and 100-year waves return period to occur in the next 100 years.

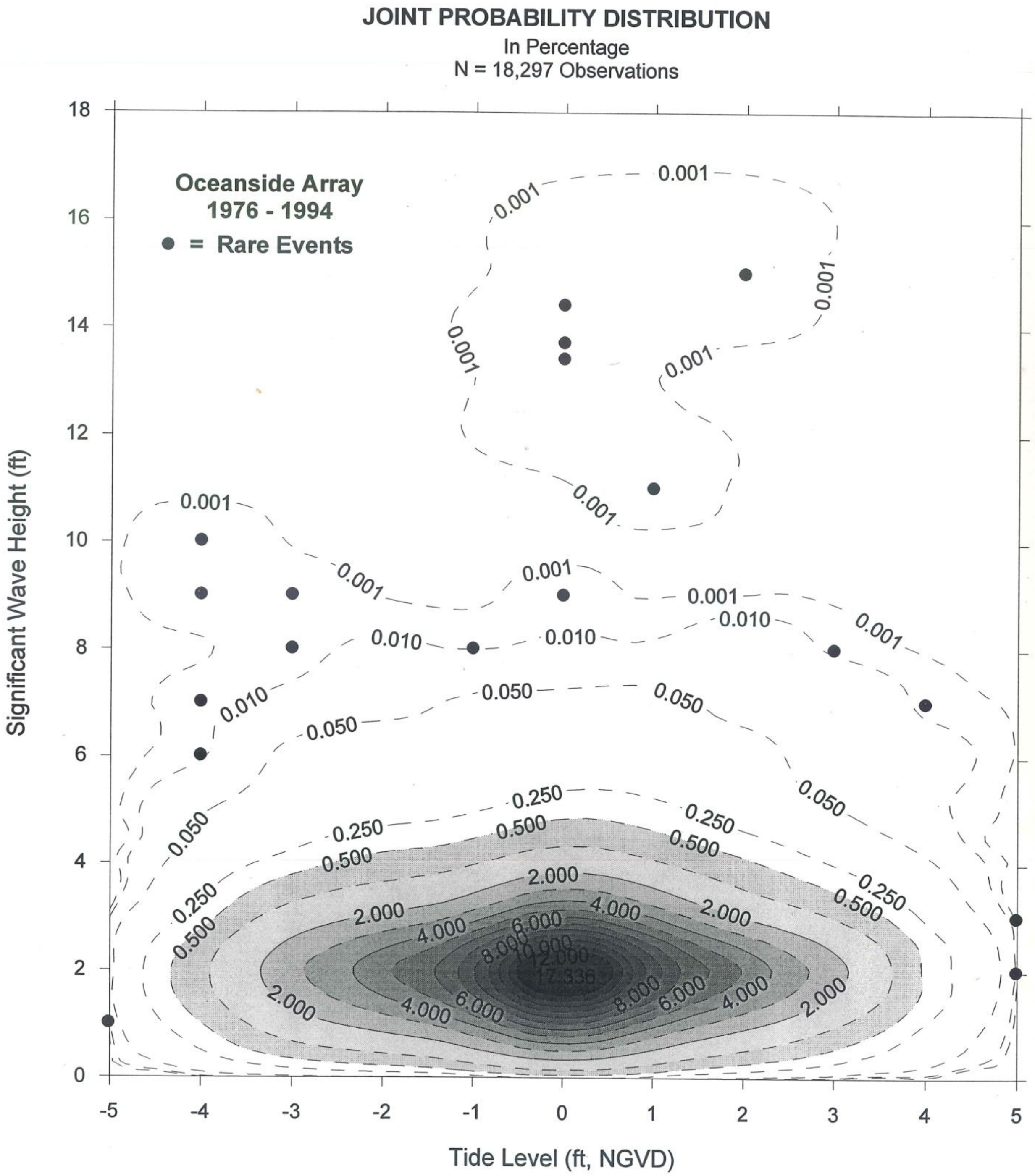

Figure 4-4. Joint Probability distribution between significant wave height and tide level. From Elwany and Flick (1999).

5.0 CONCLUSIONS

The objective of this report is to provide information related to sea level rise vulnerability, structural integrity, and the adaptive capacity of the Lease Premises and the structures therein. We summarize the present knowledge of MSLR using the latest state and federal agency guidelines, especially OPC (2018). We also evaluate the current SONGS revetment and walkway exposure and vulnerability to wave and high water level events by gauging their current condition and examining storm data from the past year. We review the revetment stability by evaluating structure changes within the past year, and comparing the weight of its rocks to the design weight needed to withstand wave forces for various design waves return periods.

The OPC (2018) and CCC (2015; updated 2018) probability-based MSLR scenarios evaluated in this study are unchanged from last year and the most current existing MSLR guidance for the State of California. Projections of future MSLR continue to evolve as understanding of key climate change processes improves. Of notable concern are the possible ranges and rates of glacial ice loss in Greenland and Antarctica (e.g., DeConto and Pollard, 2016). Future MSLR is highly uncertain, especially after 2050, for reasons outlined in Section 2 of this report.

CE has compiled and summarized papers and reports published in 2020 regarding estimations of MSLR that present relevant global, state, regional, and local findings that may in time impact state policies or may inform decisions by SCE concerning SONGS deconstruction (Section 2.1.4). For example, the CCC continued commitment to coastal access suggests that implementing all feasible means to maintain existing lateral access along the beach fronting SONGS will be both necessary and beneficial. Lateral access depends on keeping the revetment and retaining wall in good condition to protect the walkway fronting the main SONGS seawall. The SONGS revetment is currently in good condition and can likely provide adequate wave protection to the retaining wall and walkway through at least 2050, assuming normal maintenance.

During November 2020 and the period between 25 January and 21 February 2021, the revetment was subjected to a series of large wave events with heights varying between 2-4.34 m (6.6-14.2 ft) and short periods of about 8 seconds. The observed 4.3 m waves were higher than the 3.8 m (12.5 ft) previously estimated wave height for the 100-year return period. Despite the long duration of these large waves, our study shows the damage to the revetment and walkway was minimal.

The damages to the revetment were limited to displaced rocks at a few locations. The DEMs (Appendix A) and photographs (Appendix D) show that most of the small damages occurred at the toe of the revetment. These wave events impacted the beach fronting SONGS by removing the thin layer of sand covering the cobble. Some of the cobble was pushed inshore to the toe of the revetment and between the rocks at higher elevations. Cobble was thrown onto the walkway in a few locations near Transect 10 by waves splashing over the revetment. No damages were observed in the walkway, indicating the revetment protected it from wave run-up and overtopping.

Appendix A shows comparisons between revetment conditions in 2021 vs. 2020. The data were obtained by laser scanner system (Section 3.2.2). The photographs taken during February 2021 site visit (Appendix D) were important to this study; they complement the laser scanner survey and show the beach conditions at each of the 21 ranges after the January-February 2021 wave storms. The laser scanner survey clearly described the rock shape (sizes) while the photographs highlighted the sand and cobble areas on the beach.

This study finds that the revetment, in its present condition, is likely to tolerate wave forces with acceptable rock movement that will not affect the integrity of the revetment as a whole. The study found that, as designed and with regular maintenance, the revetment should withstand wave forces over the next 30 years and has a high adaptive capacity to MSLR (Section 3.10).

The beach prevents toe scouring that can undermine the revetment and cause rock units to settle. When the beach is narrow or water level is unusually high, or both, waves breaking on the revetment can cause dislocation of individual rocks, which contributes to revetment instability. A San Onofre Beach assessment based on SCE's beach monitoring program is valuable as sea level rise accelerates in the future. MSLR will likely increase both the wave forces on the rocks (due to greater water depth and wave height fronting the revetment), and sand scour undermining that could lower and destabilize the revetment (due to beach retreat). Elwany et al. (2017) have addressed the impacts of sea level rise on San Onofre Beach.

Wave overtopping and walkway flooding will occur when high wave events coincide with extreme water levels due to the relatively low elevation of the walkway at 14 ft, NGVD. However, occasional flooding is not likely to impact lateral public beach access since this will be normally limited during storms. Furthermore, flood waters will drain from the walkway after each event.

Quarterly measurements of groundwater levels from nine coastal wells at SONGS in 2020 are presented in Appendix F. Adding the OPC (2018) 0.5% and H++ MSLR projection scenarios, which respectively elevate MSL 2 ft and 2.8 ft by 2050, to the 2020 average groundwater elevation of 2.43 ft (NGVD) results in groundwater elevation projection estimates of 4.43 ft and 5.23 ft (NGVD) at that time. This remains 1.54 ft to 0.74 ft below the bottom of the ISFSI 3-ft thick concrete support foundation, which lies at 5.97 ft (NGVD).

6.0 REFERENCES

Ahrens J. P., 1981a. *Irregular Wave Runup on Smooth Slopes.* Coastal Engineering Technical Aid No. 81-17. USACE, 26 pp.

Ahrens J. P., 1981b. *Design of Riprap Revetments for Protection Against Wave Attack.* Technical Paper No. 81-5. USACE, 31 pp.

British Columbia Ministry of Environment, Lands and Parks (BCMELP), 2000. *Riprap Design and Construction Guide.* Public Safety Section Water Management Branch, 12 pp.

California Coastal Commission, 2015; updated 2018. *California Coastal Commission Sea Level Rise Policy Guidance, Interpretive Guidelines for Addressing Sea Level Rise in Local Coastal Programs and Coastal Development Permits*, California Coastal Commission, San Francisco, CA, 307 pp.

California Coastal Commission (CCC), 2020a. *2021-2025, Protecting California's Coast for Present and Future Generations*, CCC, San Francisco, CA, 32 October 2020, 56 pp. https://www.coastal.ca.gov/strategicplan/spindex.html.

California Coastal Commission (CCC), 2020b. *Sea Level Rise in California: Planning for the Future*, *California Coastal Commission*, San Francisco, CA, 17 pp. https://storymaps.arcgis.com/stories/d0c1df224a97418bb4dad129ea4c6d17.

California Natural Resources Agency (CNRA) and California Environmental Protection Agency (CEPA), 2020. *Making California's Coast Resilient to Sea Level Rise: Principles for Aligned State Action*, CNRA and CEPA, Sacramento, CA, 29 April 2020, 6 pp. https://www.adaptationclearinghouse.org/resources/making-california-eys-coast-resilient-to-sea-level-rise-principles-for-aligned-state-action.html.

Coastal Environments, 2000. *SONGS Unit 1 Deconstruction Marine Impacts Study, Phase I.* Unpublished report submitted to Southern California Edison Company, 24 January 2000, CE Ref. No. 2000-03, 44 pp. plus 2 appendices.

Coastal Environments, 2020. 2017-2019 Beach Profile Surveys at San Onofre. Report Submitted to Southern California Edison, Rosemead, CA 91770, 9 March 2020, CE Ref No. 20-03. 41 pp. and 6 Appendices.

DeConto, R., and D. Pollard, 2016. Contribution of Antarctica to past and future sea level rise. *Nature* 531, 591-597.

Elwany, H, R Flick and S. Aijaz, 1994. 1993 Beach Profile Surveys at San Onofre, Final Report. Submitted to Southern California Edison, Rosemead, C A 91770, CE Ref. No. 94-07.32 pp. and 2 Appendices.

Elwany, H., and R. E. Flick, 1999. *Coastal and Oceanographic Conditions in the Vicinity of the Proposed Manchester Resort Development Oceanside, California.* Coastal Environments Reference No. 99-03, prepared for Manchester Resort, 1 Market Place, San Diego, CA, 61 pp. and 4 Appendices.

Elwany, H., R. E. Flick, and A.D. Young, 2016. *Coastal Analysis for End-State Planning of San Onofre Nuclear Generating Station, Phase 1*, Coastal Environments Reference No. 16-26, prepared for Southern California Edison Company, Rosemead, CA, 151 pp.

Elwany, H., R. E. Flick, and A.P. Young, 2017. *Coastal Processes Analysis at San Onofre Nuclear Generating Station, Phase 2*, Coastal Environments Reference No. 17-08, prepared for Southern California Edison, 160 pp.

Elwany, H. and R.E. Flick, and F. Scarelli, 2020. San Onofre Nuclear Generating Station (SONGS) Mean Sea Level Rise Impact Assessment, Summary Report, Report prepared for Southern California Edison by Coastal Environments, Inc. La Jolla, CA, CE-Reference 20-08, 64 pp. and 6 Appendices.

Flick, R.E., and J.R. Wanetick, 1989. *San Onofre Beach Study*. Unpublished report submitted to Southern California Edison Co., Rosemead, CA, October 1989, SIO Ref. No 89-20. 26 pp. and 25 figures.

Flick, R. E., 1998. Comparison of California Tides, Storm Surges, and Sea Level During the El Niño Winters of 1982-83 and 1997-98, *Shore & Beach*, 66(3), 7-11.

Flick, R. E., 2016. California tides, sea level, and waves – Winter 2015-16, *Shore & Beach*, 84(2), 25-30.

Flick, R. E., K. Knuuti, and S. K. Gill, 2013. Matching Mean Sea Level Rise Projections to Local Elevation Datums, *J. Waterway, Port, Coastal and Ocean Eng*., Amer. Soc. Civil Engineers, 139(2), 142-146.

Haigh, I.D., M.D. Pickering, et al., 2019. The tides they are a-changin′: A comprehensive review of past and future nonastronomical changes in tides, their driving mechanisms, and future implications. *Rev. Geophys.*, 58.

Hamlington, B.D., A.S. Gardner, et al., 2020. Understanding of contemporary regional sea-level change and the implications for the future. *Rev. Geophys.*, 58, 39 pp.

Hedges, T.S., Reis, M.T., 1998. *Random wave overtopping of simple seawalls: a new regression model*. Water, Maritime and Energy Journal, 130(1), pp. 1-10.

Hofer, S., Lang, C., Amory, C. et al., 2020. Greater Greenland Ice Sheet contribution to global sea level rise in CMIP6, *Nature Communications* 11**,** 6289, 11 pp.

Holland, K. T., and R. A. Holman, 1993. *The statistical distribution of swash maxima on natural beaches*. J. Geophys. Res.,87, 10,271-10, 278.

Hu, K., 2000. High-Resolution Finite Volume Methods for Hydraulic Flow Modelling. Manchester, U.K.: Centre for Mathematical Modelling and Flow Analysis, Manchester Metropolitan University, Doctoral thesis, 194 pp.

Hunt, I. A., 1959. *Design of Seawalls and Breakwaters*. J. Waterways and Harbors Div., ASCE, Vol. 85, No. WW3.

IMBIE Team., Shepherd, A., Ivins, E., et al., 2020. Mass balance of the Greenland Ice Sheet from 1992 to 2018, *Nature*, 579**,** 233–239.

Intergovernmental Panel on Climate Change, 2013. *Climate Change 2013: The Physical Science Basis, Contribution of Working Group I to the Fifth Assessment Report of the Intergovernmental Panel on Climate Change*, Cambridge University Press, Cambridge, United Kingdom and New York, NY, 1535 pp.

Jevrejeva, S., T. Frederikse, R.E. Kopp, G. Le Cozannet, L. P. Jackson, R.S.W. van de Wal, 2019. Probabilistic Sea Level Projections at the Coast by 2100, *Surv. Geophys.*, 40, 1673–1696.

Kikkawa, H., Shi-igai, H. and Kono, T., 1968. *Fundamental Study of Wave Over-Topping on Levees.* Journal of Coastal Engineering in Japan, 11, 107-115.

Kirezci, E., et al., 2020. Projections of global-scale extreme sea levels and resulting episodic coastal flooding over the 21st Century, *Scientific Reports, Nature Research*, 10, 11629.

Kopp, R. E., R. M. Horton, C. M. Little, J. X. Mitrovica, M. Oppenheimer, D.J. Rasmussen, B. H. Strauss, and C. Tebaldi, 2014. Probabilistic 21st and 22nd century sea level projections at a global network of tide-gauge sites. *Earth's Future*, 2, 383-406.

Muis S, I. Apecechea, et al., 2020. A High-Resolution Global Dataset of Extreme Sea Levels, Tides, and Storm Surges, Including Future Projections, *Front. Mar. Sci.*, 7, 263, 15 pp.

Ocean Protection Council, 2018. *State of California Sea Level Rise Guidance, 2018 Update* (California Natural Resources Agency Ocean Protection Council), 84 pp.

Ocean Protection Council (OPC), 2020. *Strategic Plan to Protect California's Coast and Ocean 2020–2025*, California Natural Resources Agency Ocean Protection Council, 64 pp. https://www.opc.ca.gov/webmaster/ftp/pdf/2020-2025-strategic-plan/OPC-2020-2025-Strategic-Plan-FINAL-20200228.pdf.

Owen, M.W., 1980. *Design of Seawalls Allowing for Wave Overtopping*. Report. EX 924, Hydraulics Research Station, Wallingford, UK.

Raubenheimer, B., R.T. Guza, and S. Elgar, 1999. *Tidal water table fluctuations in a sandy ocean beach*, J. Geophys. Res., 35(8), 2313-2320.

Raubenheimer, B., R.T. Guza, Steve Elgar, and N. Kobayashi, 1995. *Swash on a gently sloping beach*, J. Geophys. Res., 100, 8751-8760.

Reis, M. T., Hu, K., Hedges, T. S., and Mase, H., 2008. *A comparison of empirical, semiempirical, and numerical wave overtopping models*. J. Coastal Res., 24(2A), 250–262.

Ruggiero, Peter & Holman, Robert & Beach, R., 2004. *Wave runup on a high-energy dissipative beach*. Journal of Geophysical Research C: Oceans. 109. 10.1029/2003JC002160.

Sida, L., T. Wahl, S.A. Talke, D.A. Jay, P.M. Orton, X. Liang, G. Wang, and L. Liu, 2021. Evolving tides aggravate nuisance flooding along the U.S. coastline, *Science Advances*, 7(10), 10 pp.

f, T., A.E. Hogg, and R. Mottram, 2020. Ice-sheet losses track high-end sea-level rise projections, *Nature Climate Change*, 10, 877–881.

Stockdon, H. F., Holman, R. A., Howd, P. A., and Sallenger, A. H., 2006. *Empirical parameterization of setup, swash, and runup,* Coastal Engineering, 53, 573–588.

Sun, S., F. Pattyn, et al., 2020. Antarctic ice sheet response to sudden and sustained ice-shelf collapse (ABUMIP), *Jour. Glaciology*, 66(260), 891-904.

Thomas, M.A., and T. Lin, 2020. Illustrative Analysis of Probabilistic Sea Level Rise Hazard, *Jour. Climate,* 33(4), 12 pp.

Thornton, E. B. and Guza, R. T., 1982. *Energy Saturation and Phase Speeds Measured on a Natural Beach*. Journal of Geophysical Research, 87(C12), 9499-9508.

Thornton, E. B. and Guza, R. T., 1983. *Transformation of Wave Height Distribution*. Journal of Geophysical Research, 88 (C10), 5925-5938.

USACOE.1984. Shore Protection Manual. Waterways Experiment Station, Coastal Engineering Research Center, Vicksburg, MS, 2 vols.

USACOE, 1988. *Historic Wave and Sea Level Data Report: San Diego Region*. Coast of California Storm and Tidal Wave Study, Reference No. 88-6.

USACOE, 1994a. *Hydraulic Design of Flood Control Channels*. Department of the Army. CECW-EH-D, Engineer Manual 1110-2-1601.

USACOE, 1994b. *Shore Protection Manual, Volume II.* Department of the Army. Coastal Engineering Research Center.

USACOE, 1995. *Design of Revetments, Seawalls and Bulkheads*. Department of the Army. Coastal Engineering Manual, Engineer Manual 1110-2-1614.

Van der Meer, J.W. and J.P.F.M. Janssen, 1995. *Wave runup and wave overtopping at dikes*. In: Wave Forces on Inclined and Vertical Wall Structures. ASCE. Ed. N. Kobayashi and Z. Demirbilek. Ch. 1, p. 1-27.

Young, A.P., R. E. Flick, T.W. Gallien, S. N. Giddings, R.T. Guza, M. Harvey, L. Lenain, B.C. Ludka, W. K. Melville, and W. C. O'Reilly, 2018. Southern California coastal response to the 2015-2016 El Niño, *J. Geophys. Res: Earth Surface*, 123.

6.1 RELEVANT UNCITED SOURCES

Bedsworth, L., D. Cayan, G. Franco, L. Fisher, and S. Ziaja, 2018. *Statewide Summary Report, California's Fourth Climate Change Assessment*, California Governor's Office of Planning and Research, Scripps Institution of Oceanography, California Energy Commission, and California Public Utilities Commission, Publication Number SUM-CCCA4-2018-013, 133 pp.

Chadwick, B., P. F. Wang, M. Brand, R. Flick, A. Young, W. O'Reilly, P. Bromirski, W. Crampton, R. Guza, J. Helly, T. Nishikawa, S. Boyce, M. Landon, M. Martinez, I. Canner, and B. Leslie, 2014. *A Methodology for Assessing the Impact of Sea Level Rise on Representative Military Installations in the Southwestern United States*, SPAWAR Systems Center Pacific, in Collaboration with TerraCosta Consulting Group, University of California San Diego, San Diego State University, U.S. Geological Survey, U.S. Army Corps of Engineers, and Moffatt & Nichol, Final Report submitted to the Strategic Environmental Research and Development Program (SERDP), 680 pp.

Griggs, G., J. Árvai, D. Cayan, R. DeConto, J. Fox, H. A. Fricker, R. E. Kopp, C. Tebaldi, and E. A. Whiteman, 2017. *Rising Seas in California, An Update on Sea Level Rise Science* (California Ocean Protection Council Science Advisory Team Working Group), 71 pp.

Hall, J. A., S. Gill, J. Obeysekera, W. Sweet, K. Knuuti, and J. Marburger, 2016. *Regional Sea Level Scenarios for Coastal Risk Management: Managing the Uncertainty of Future Sea Level Change and Extreme Water Levels for Department of Defense Coastal Sites Worldwide.* U.S. Department of Defense, Strategic Environmental Research and Development Program, 224 pp.

National Research Council, 2012. *Sea Level Rise for the Coasts of California, Oregon, and Washington: Past, Present, and Future*, Committee on Sea Level Rise in California, Oregon, and Washington. National Academies Press, Washington, DC. 250 pp.

Zetler, B.D. and R. E. Flick, 1985. Predicted Extreme High Tides for Mixed-Tide Regimes, *J. Phys. Oceanog*., 15(3), 357-359.

APPENDIX A

DIGITAL ELEVATION MODELS (DEM) FROM 2021 & 2020 REVETMENT SURVEYS

Figure A-1. Locations of 21 transect ranges along the revetment, spaced 100 ft apart.

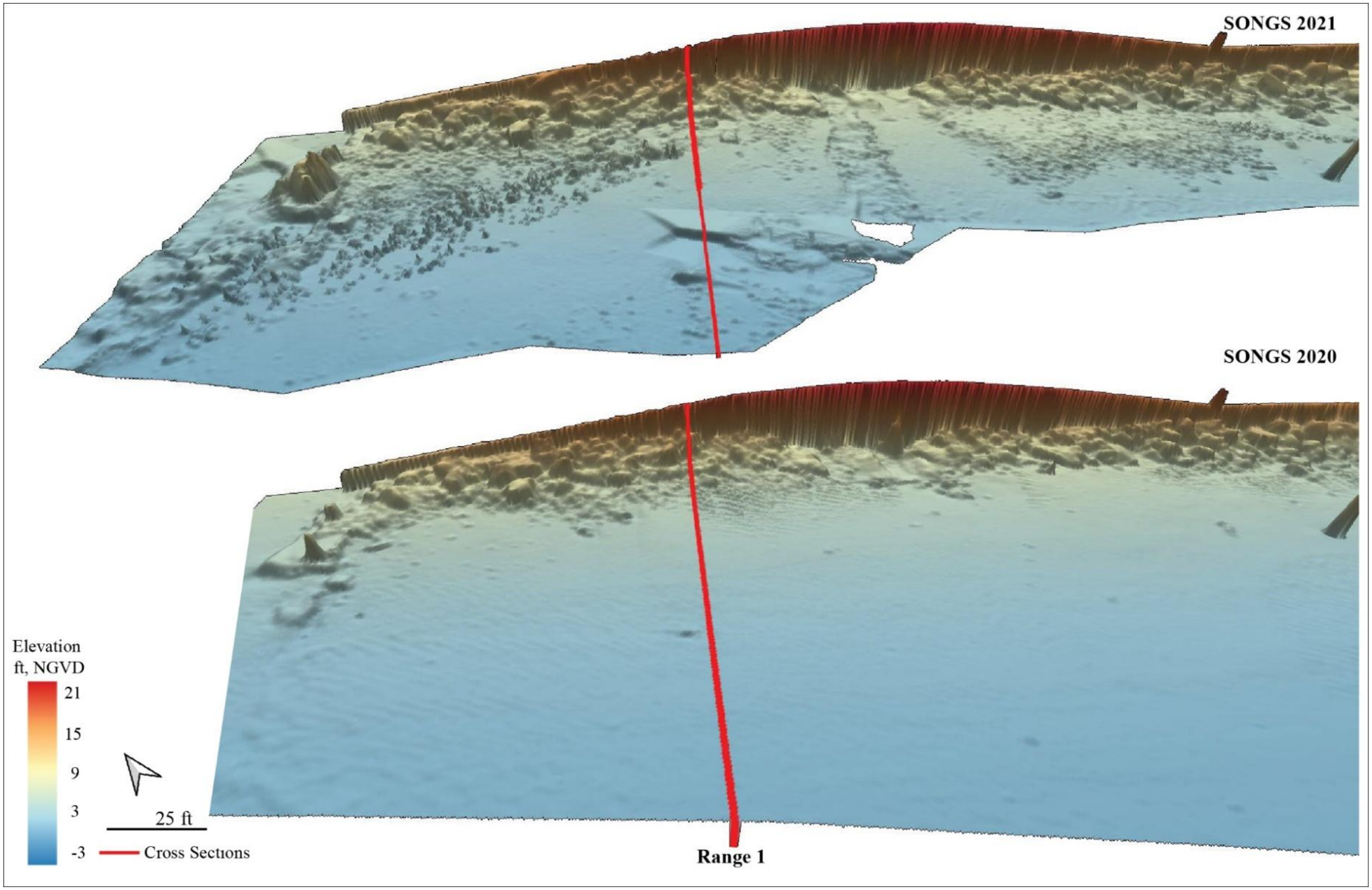

Figure A-2. DEM comparison between 2021 (top) and 2020 (bottom) showing Transect 1 along the SONGS revetment. Notice the increased presence of cobbles in 2021 on either side of Transect 1. There is no noticeable movement of the larger rocks against the wall of the walkway.

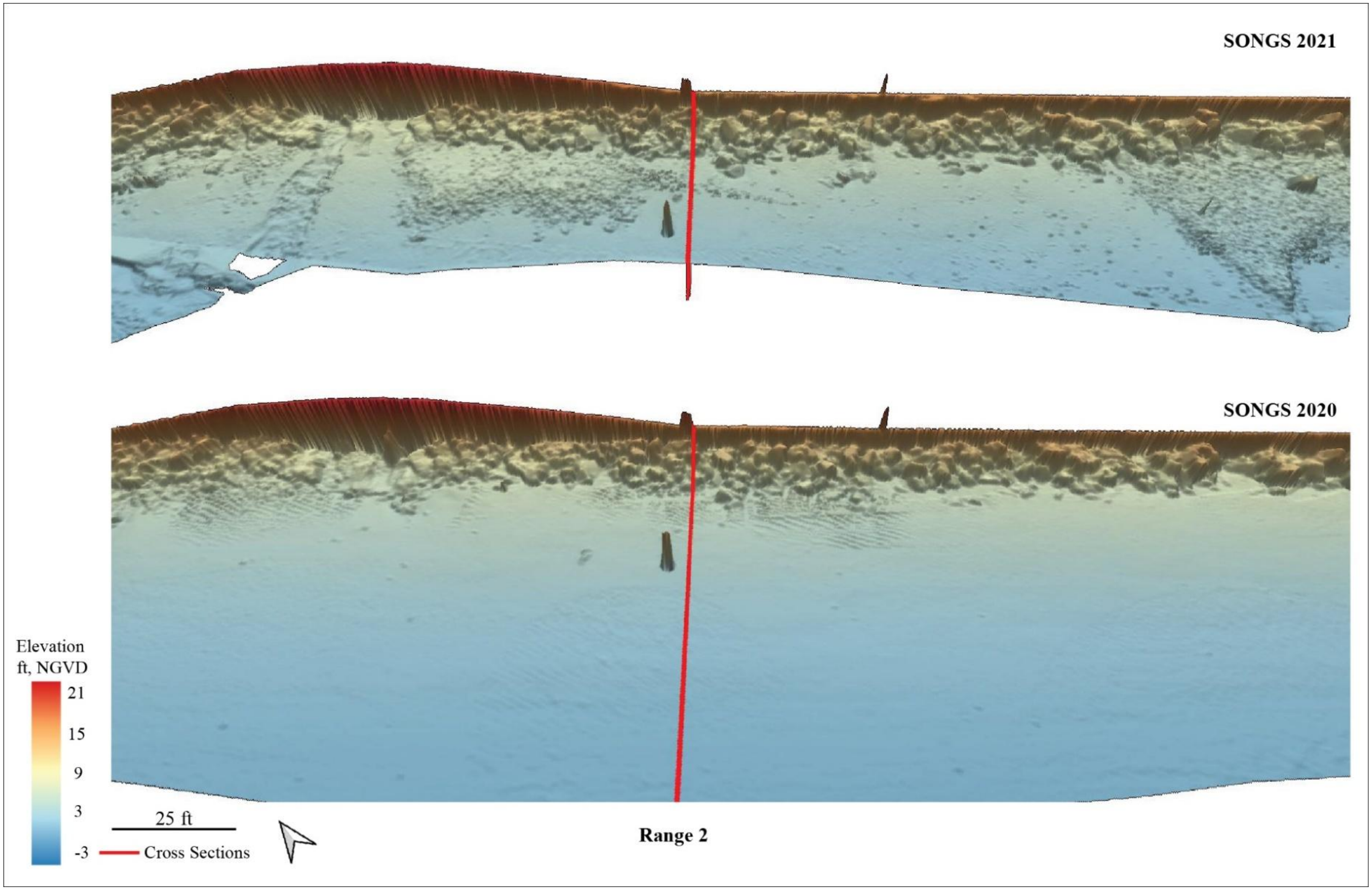

Figure A-3. DEM comparison between 2021 (top) and 2020 (bottom) showing Transect 2 along the SONGS revetment. Notice the increased presence of cobbles in 2021 just north of Transect 2. There is no noticeable movement of the larger rocks against the seawall.

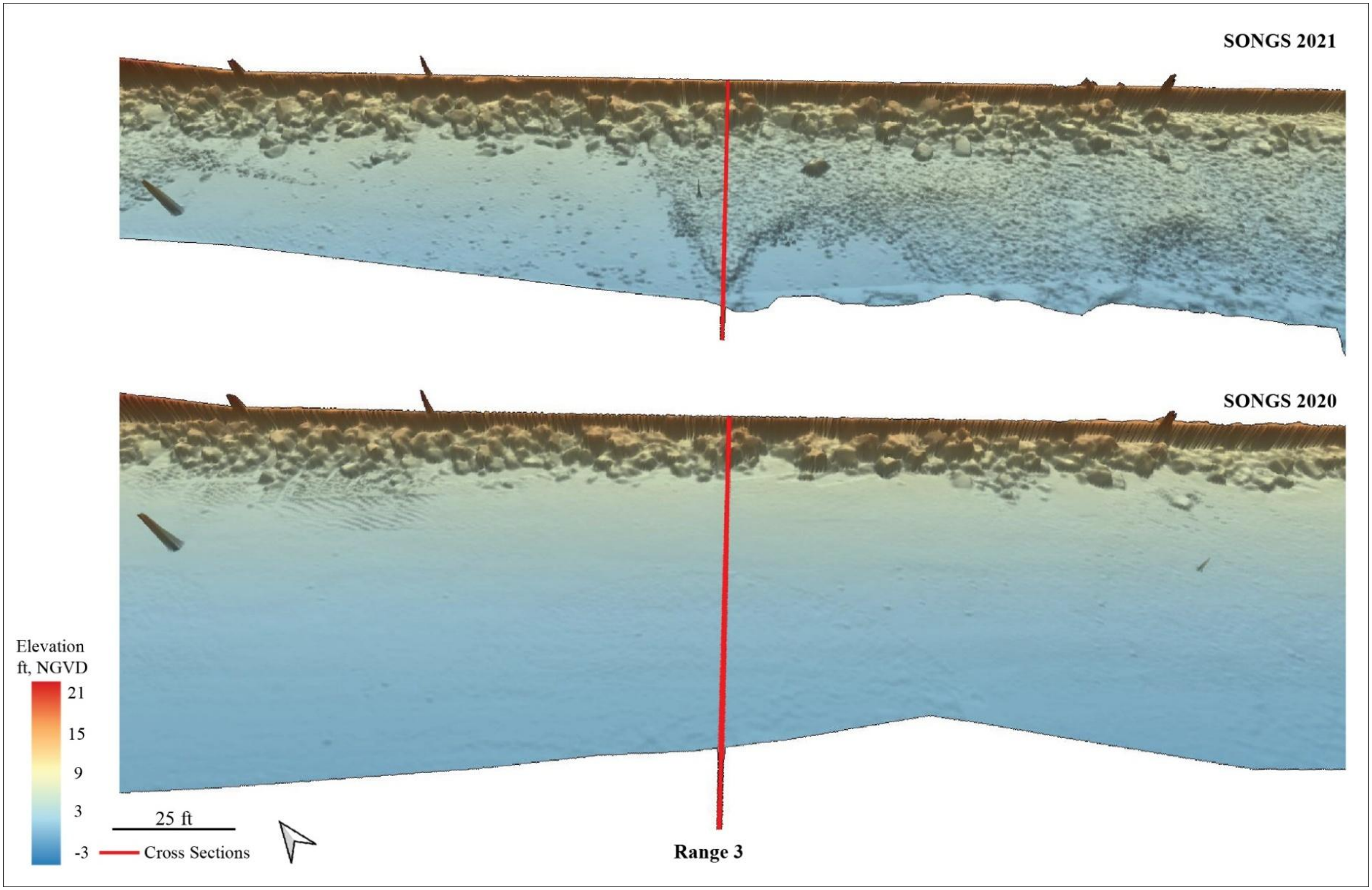

Figure A-4. DEM comparison between 2021 (top) and 2020 (bottom) showing Transect 3 along the SONGS revetment. Notice the increased presence of cobbles in the 2021 survey along and south of Transect 3. There is no noticeable movement of the larger rocks against the walkway wall.

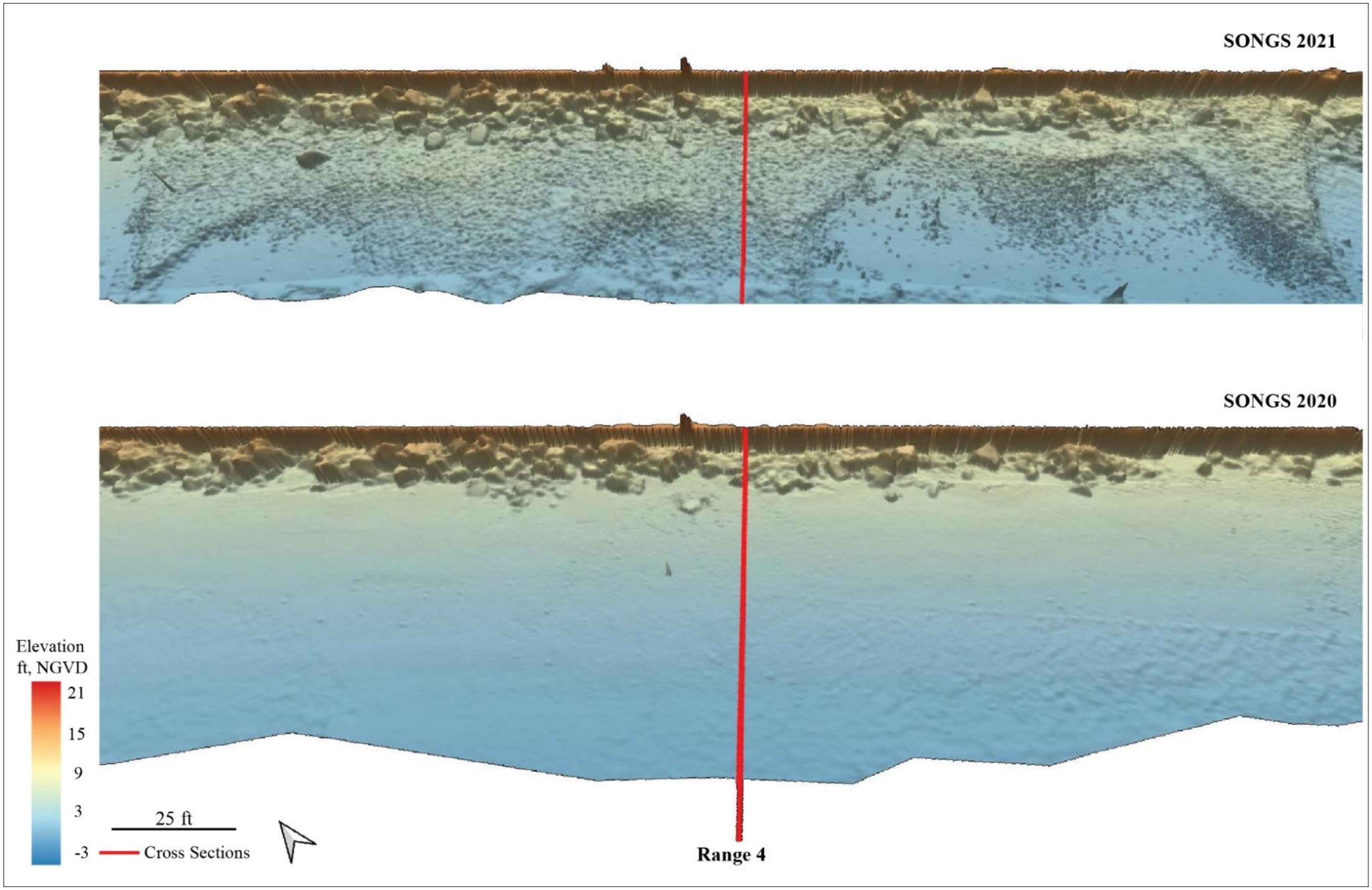

Figure A-5. DEM comparison between 2021 (top) and 2020 (bottom) showing Transect 4 along the SONGS revetment. Notice the increased presence of cobbles along the entire beach in 2021. There is no noticeable movement of the larger rocks against the walkway wall.

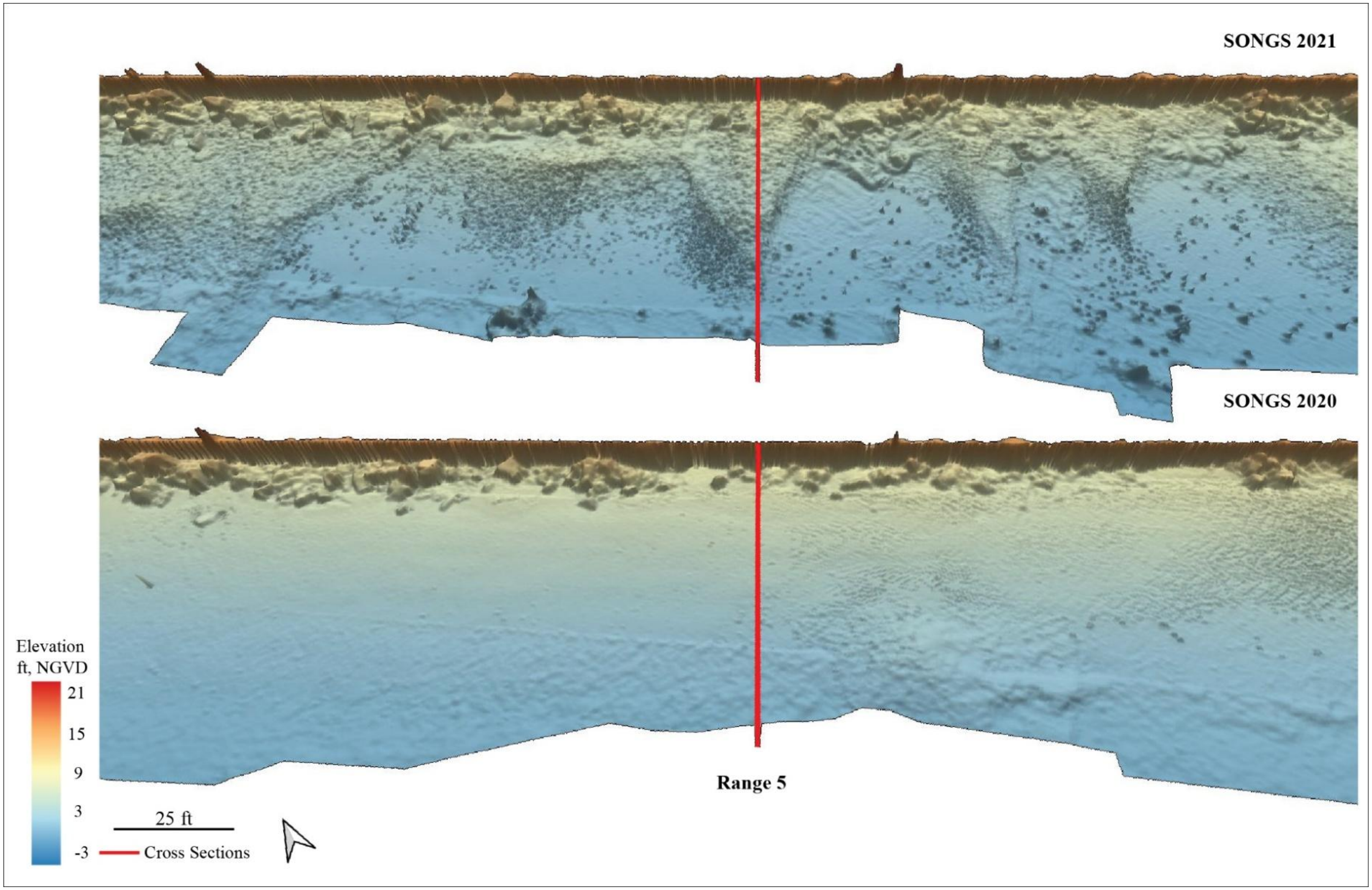

Figure A-6. DEM comparison between 2021 (top) and 2020 (bottom) showing Transect 5 along the SONGS revetment. Notice the increased exposure of cobbles along the beach and larger rocks against the walkway wall just south of Transect 5 in 2021 due to erosion.

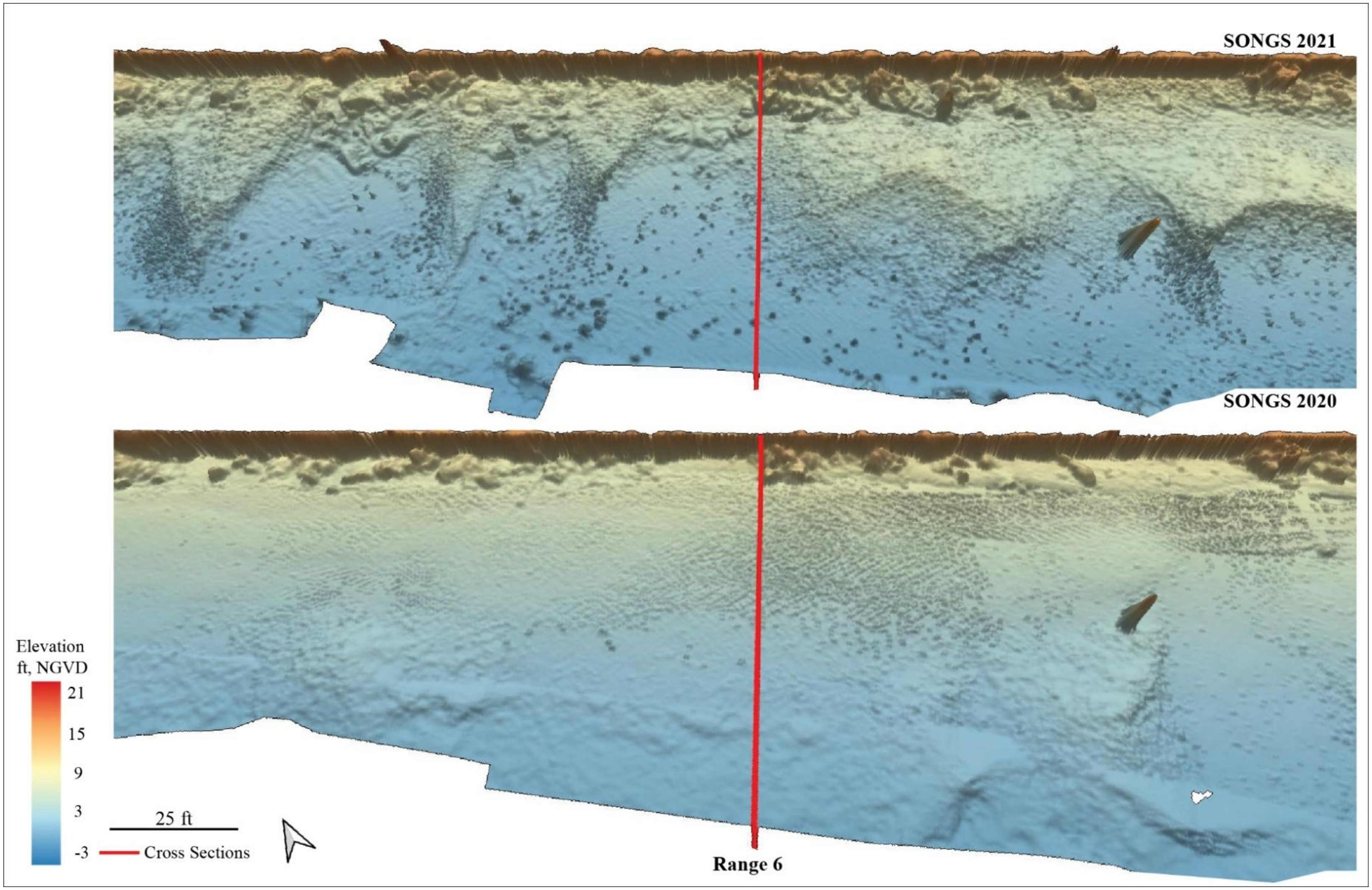

Figure A-7. DEM comparison between 2021 (top) and 2020 (bottom) showing Transect 6 along the SONGS revetment. Notice the increased exposure of cobbles along the beach and larger rocks against the walkway wall just south of Transect 6 in 2021 due to erosion.

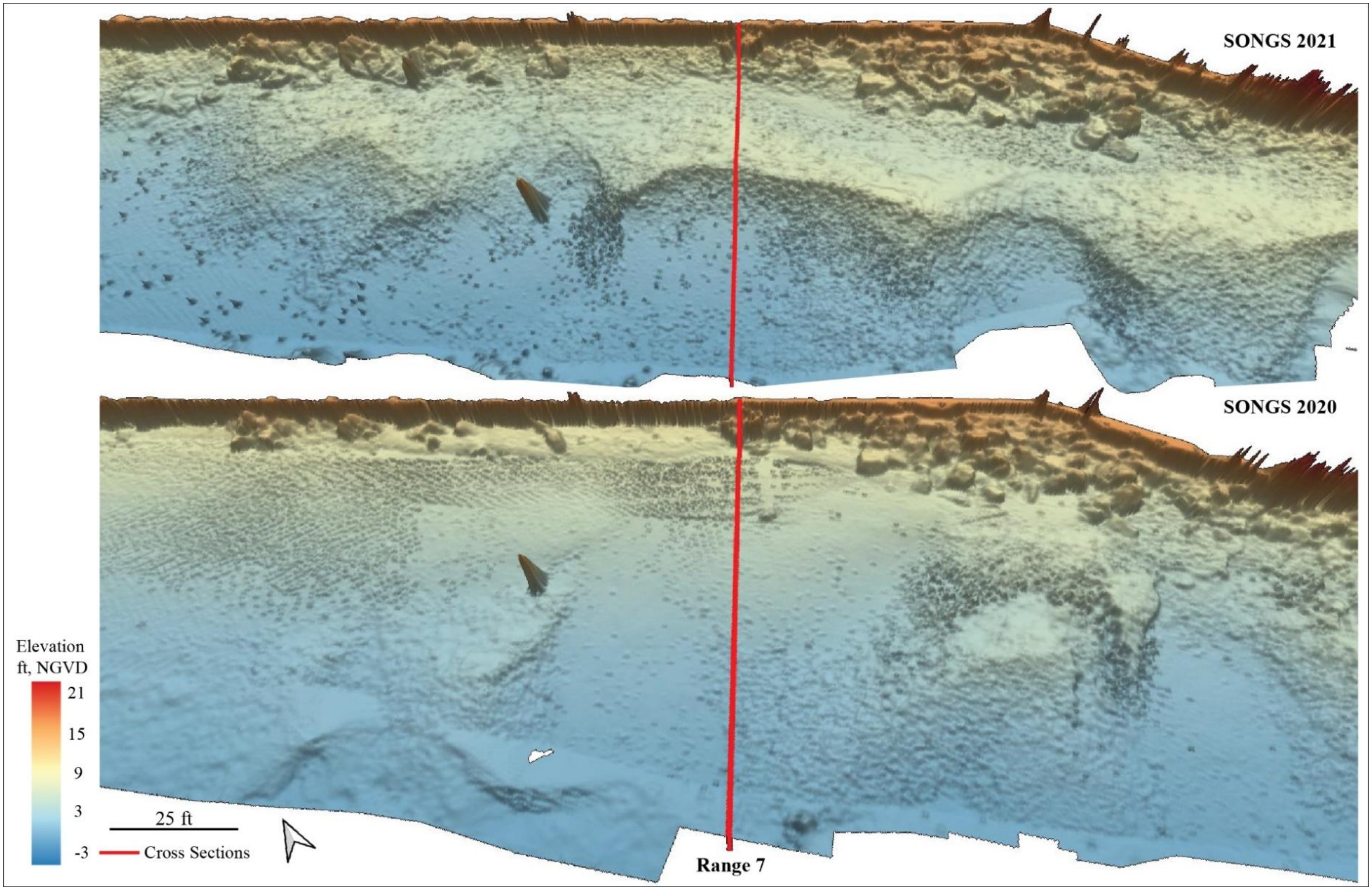

Figure A-8. DEM comparison between 2021 (top) and 2020 (bottom) showing Transect 7 along the SONGS revetment. Notice the presence of both an elevated berm and exposed cobbles along Transect 7 in 2021. There is no noticeable change in the larger rocks against the walkway wall along Transect 7.

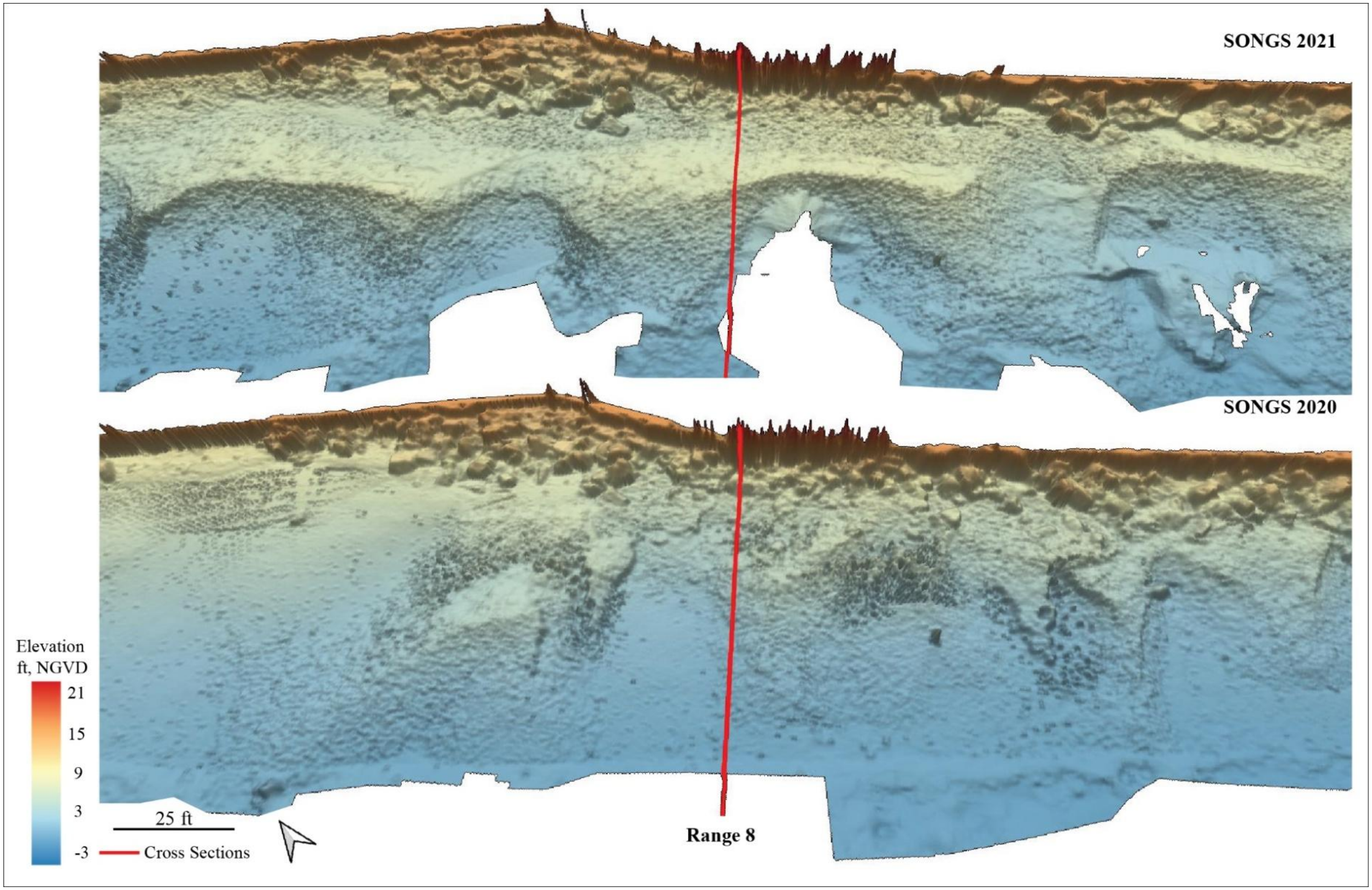

Figure A-9. DEM comparison between 2021 (top) and 2020 (bottom) showing Transect 8 along the SONGS revetment. Notice the elevated sand berm and partial coverage of larger rocks against the walkway wall due to accretion in 2021.

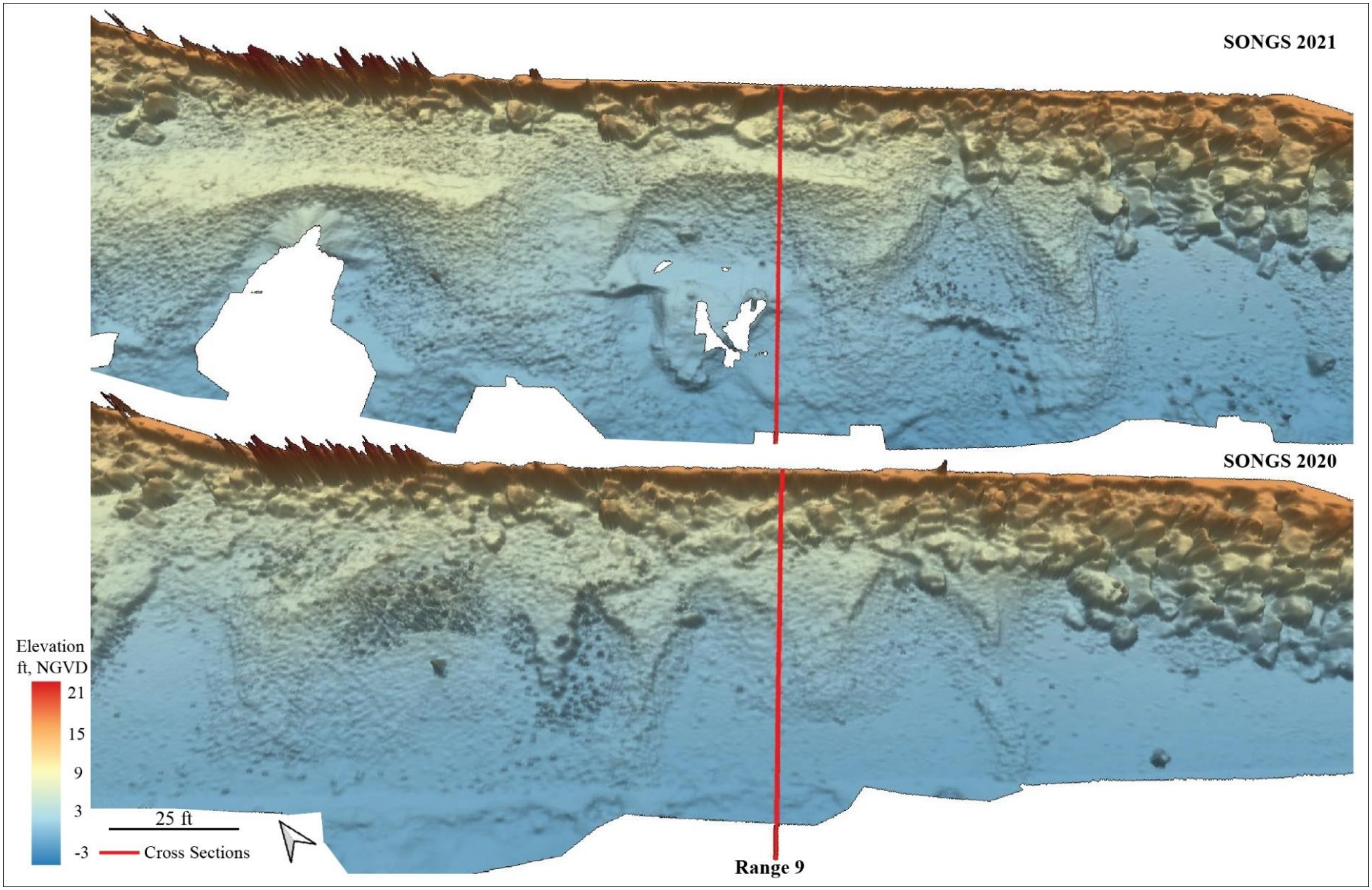

Figure A-10. DEM comparison between 2021 (top) and 2020 (bottom) showing Transect 9 along the SONGS revetment. Notice the elevated berm and partial coverage of larger rocks against the walkway wall due to accretion in 2021.

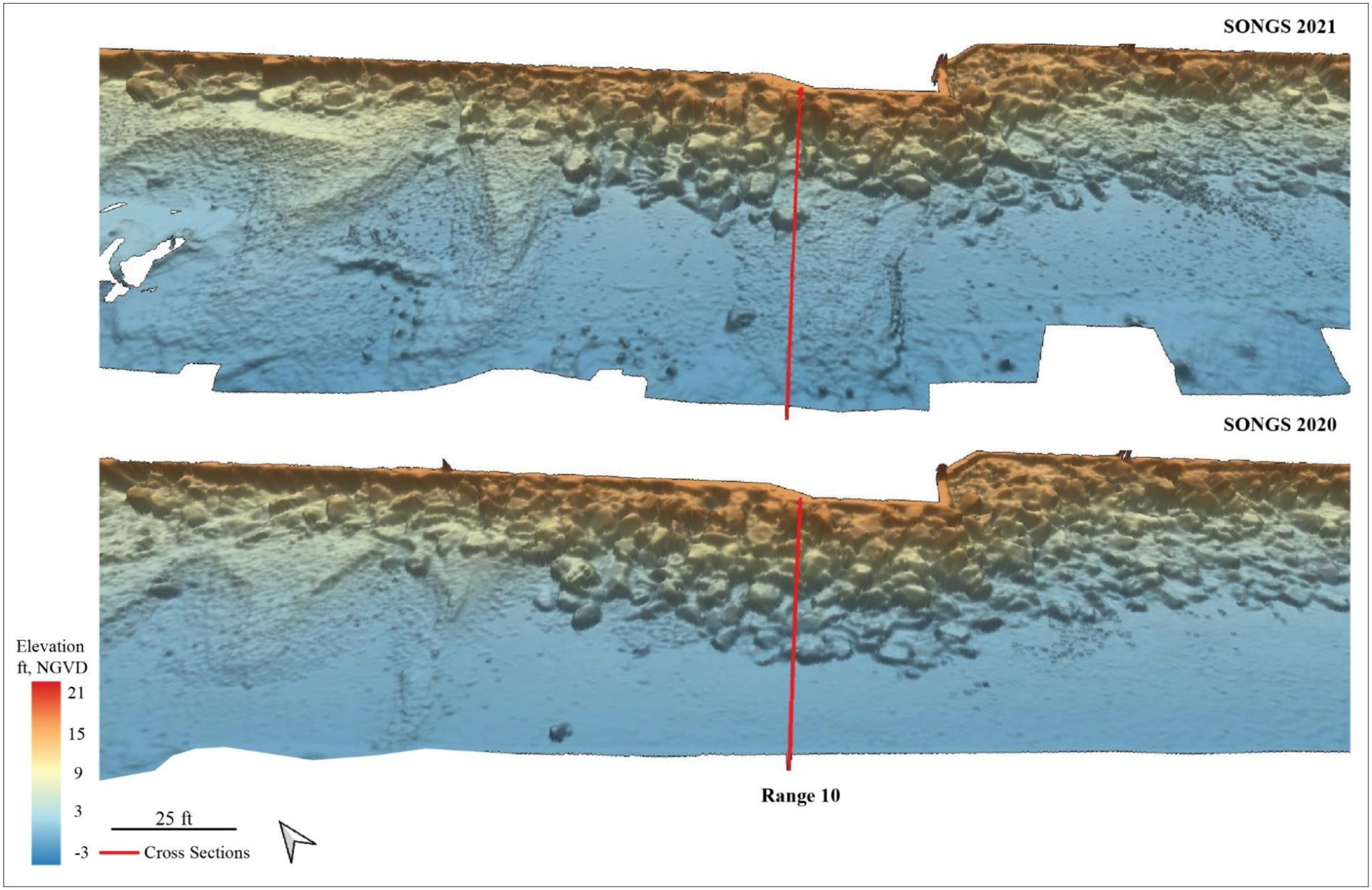

Figure A-11. DEM comparison between 2021 (top) and 2020 (bottom) showing Transect 10 along the SONGS revetment. Notice the movement of large rocks at the midpoint of the revetment along Transect 10 and increased presence of cobbles in 2021.

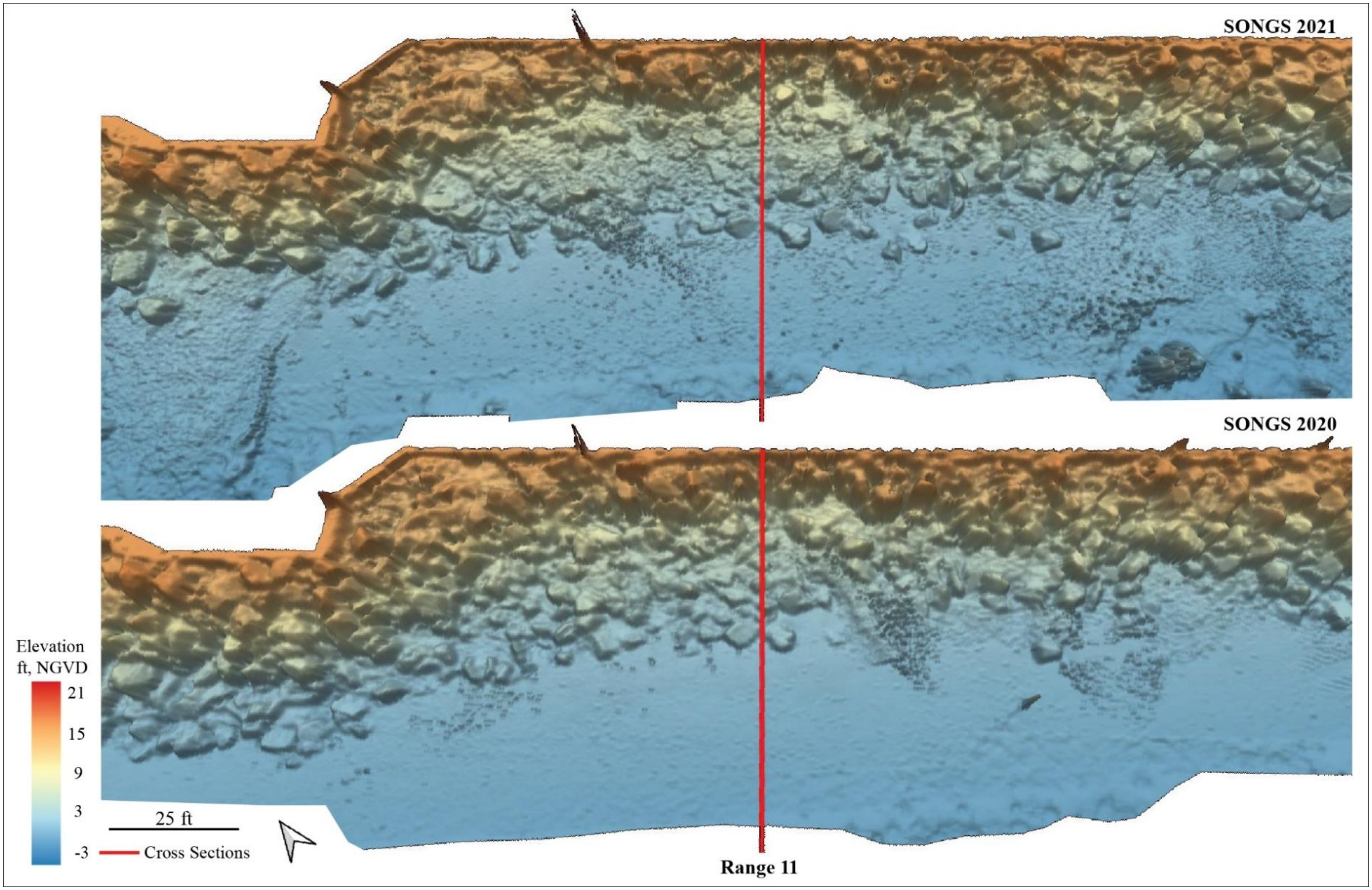

Figure A-12. DEM comparison between 2021 (top) and 2020 (bottom) showing Transect 11 along the SONGS revetment. Notice the partial burial of larger rocks in the middle of the revetment with sand and cobble in 2021.

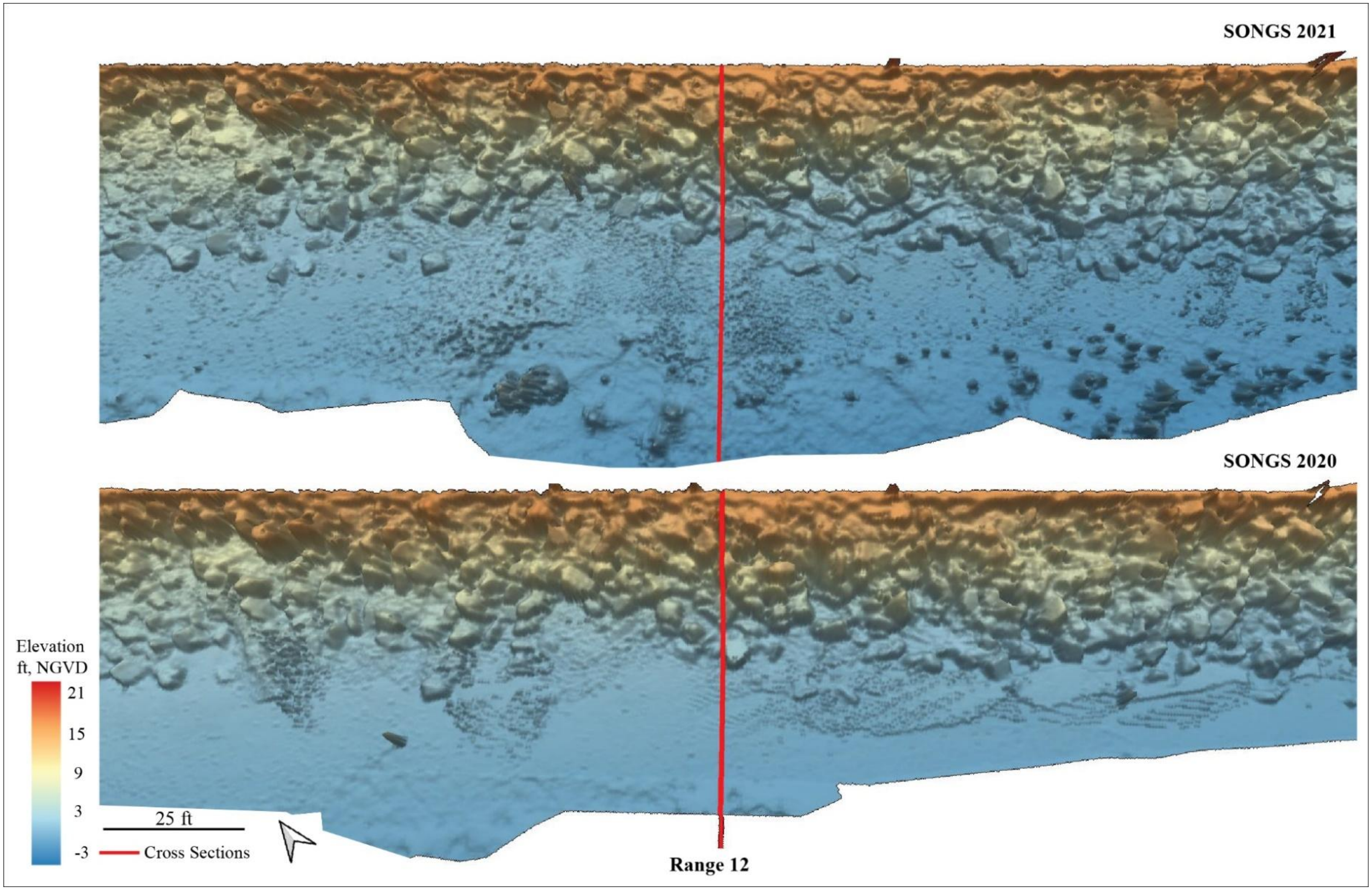

Figure A-13. DEM comparison between 2021 (top) and 2020 (bottom) showing Transect 12 along the SONGS revetment. Notice the increased presence of cobble on the beach along Transect 12 in 2021. There is no noticeable difference in the revetment rocks between the two years.

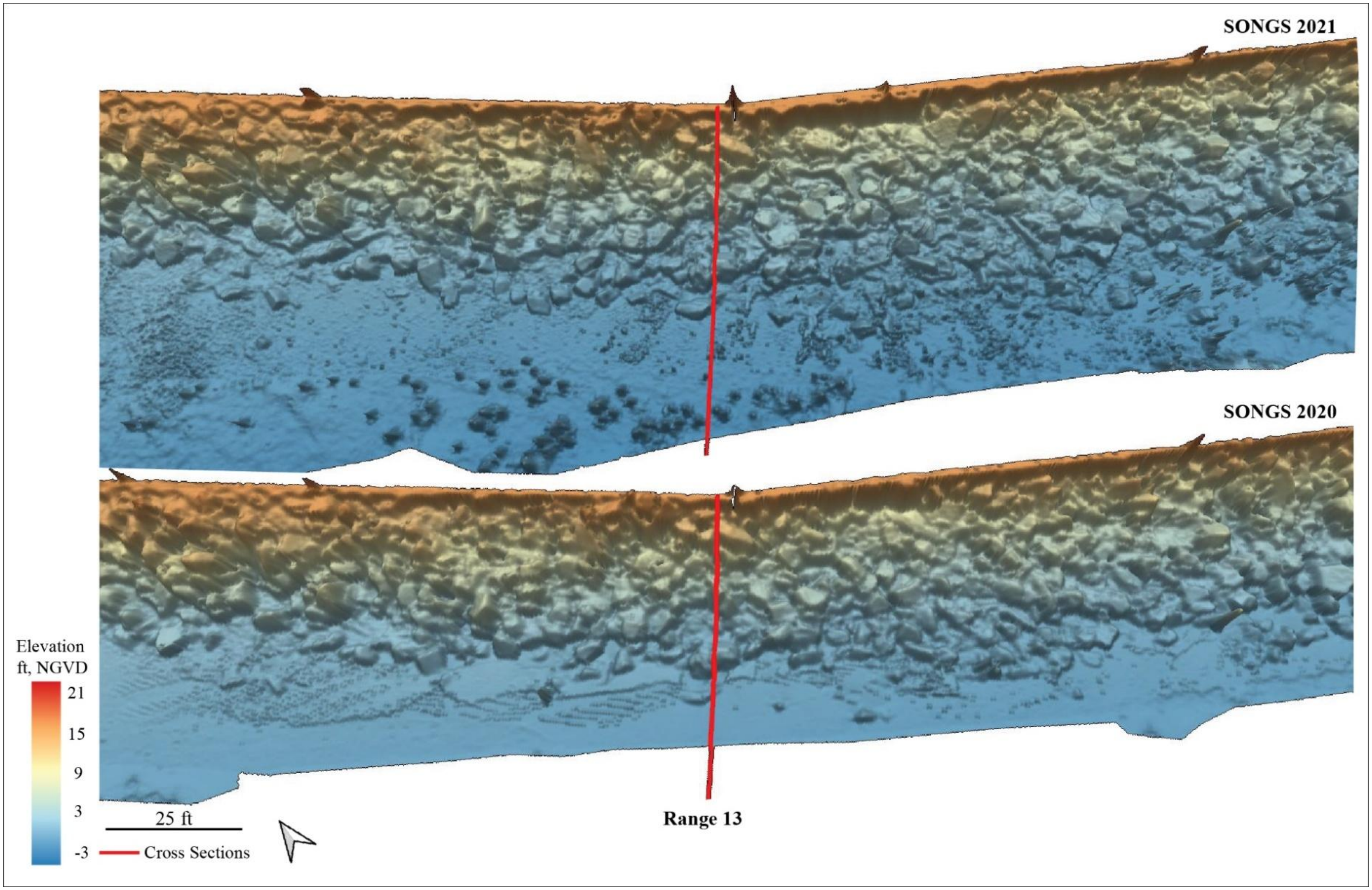

Figure A-14. DEM comparison between 2021 (top) and 2020 (bottom) showing Transect 13 along the SONGS revetment. Notice the slight erosion at the toe of the revetment in 2021. There is no noticeable difference in the revetment rocks between the two years.

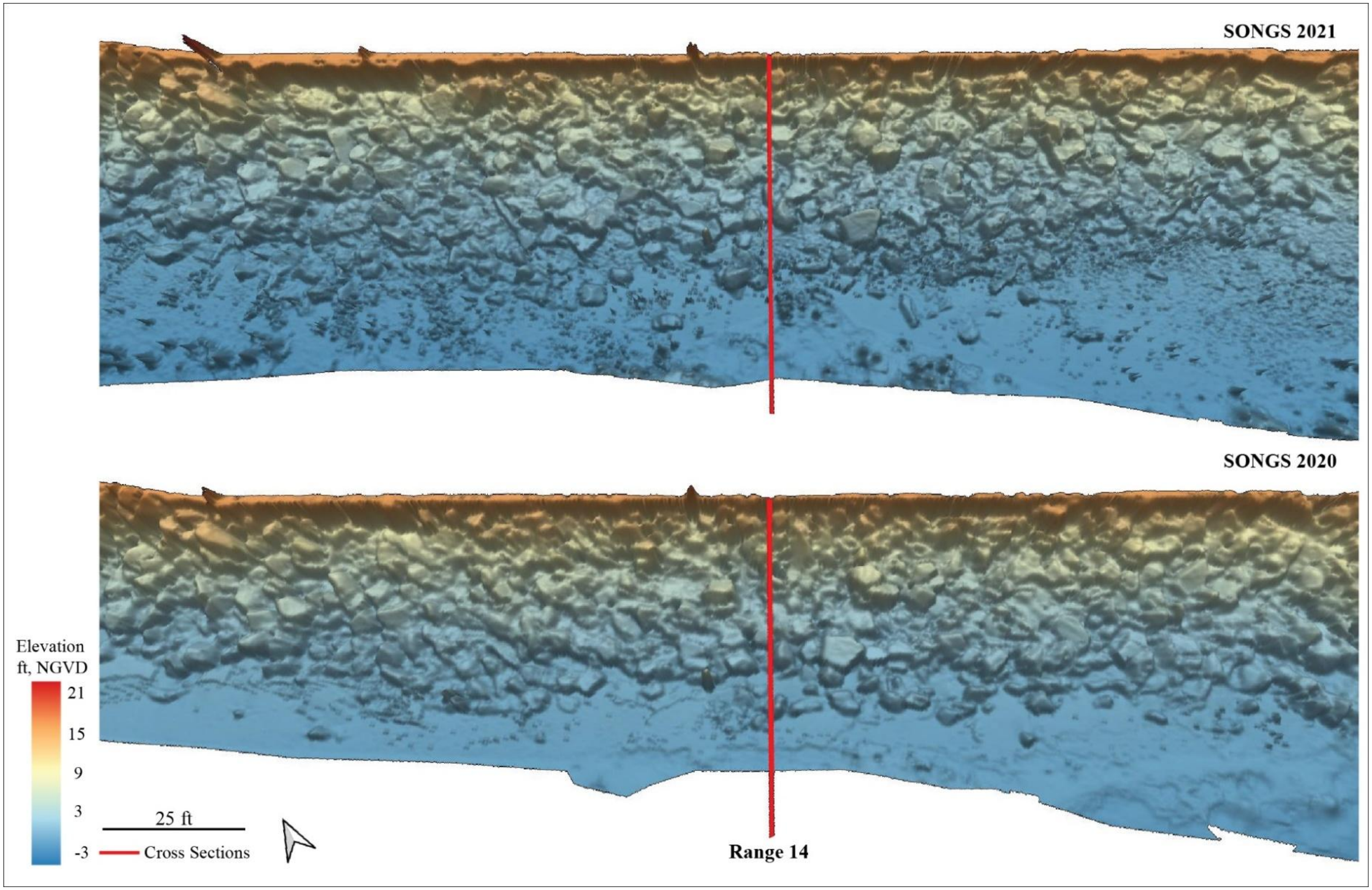

Figure A-15. DEM comparison between 2021 (top) and 2020 (bottom) showing Transect 14 along the SONGS revetment. Notice the increased cobbles, erosion, and movement of some larger rocks at the toe of the revetment in 2021.

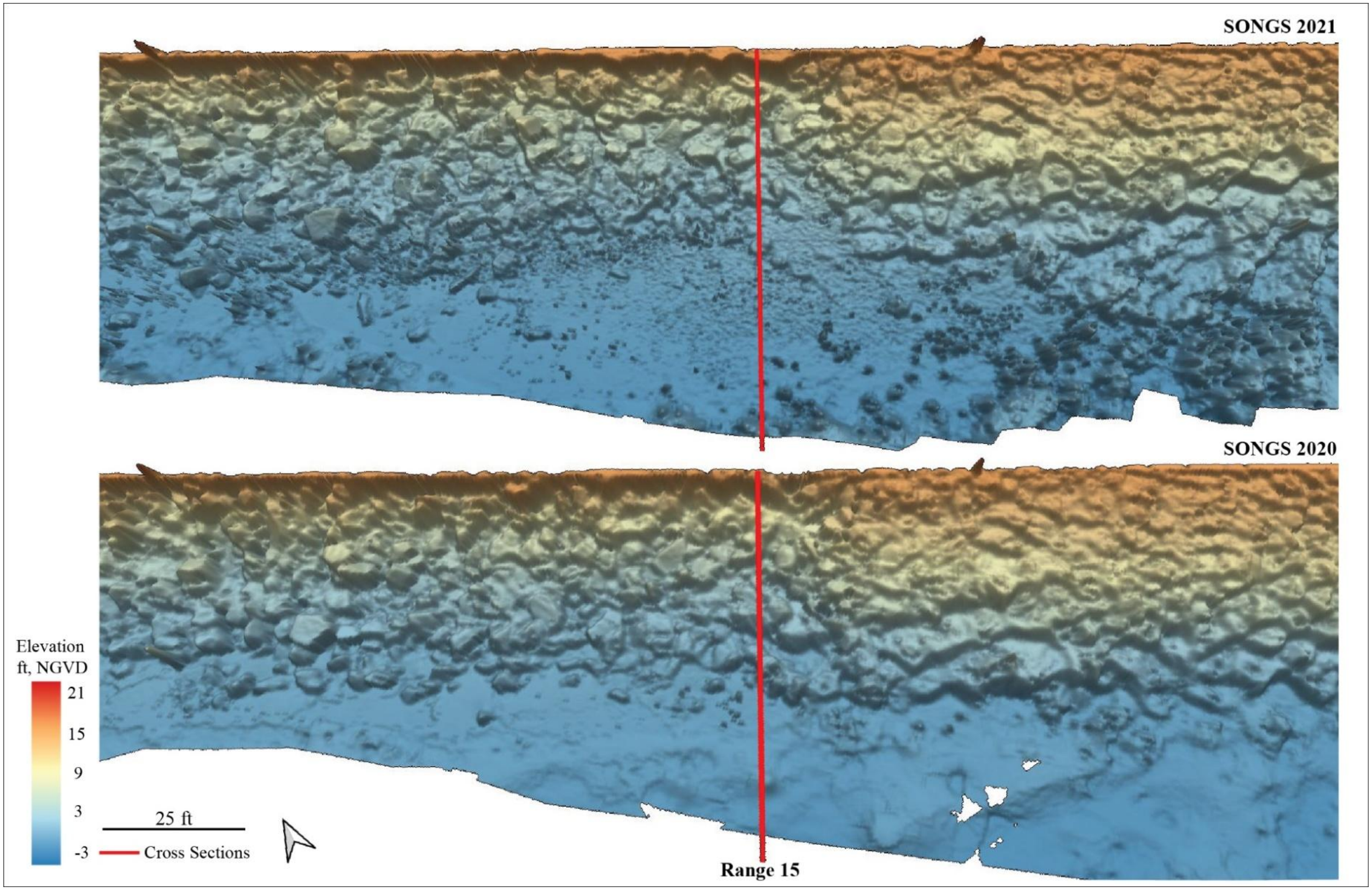

Figure A-16. DEM comparison between 2021 (top) and 2020 (bottom) showing Transect 15 along the SONGS revetment. Notice the increased cobbles and partial coverage of large rocks at the toe of the revetment due to accretion in 2021.

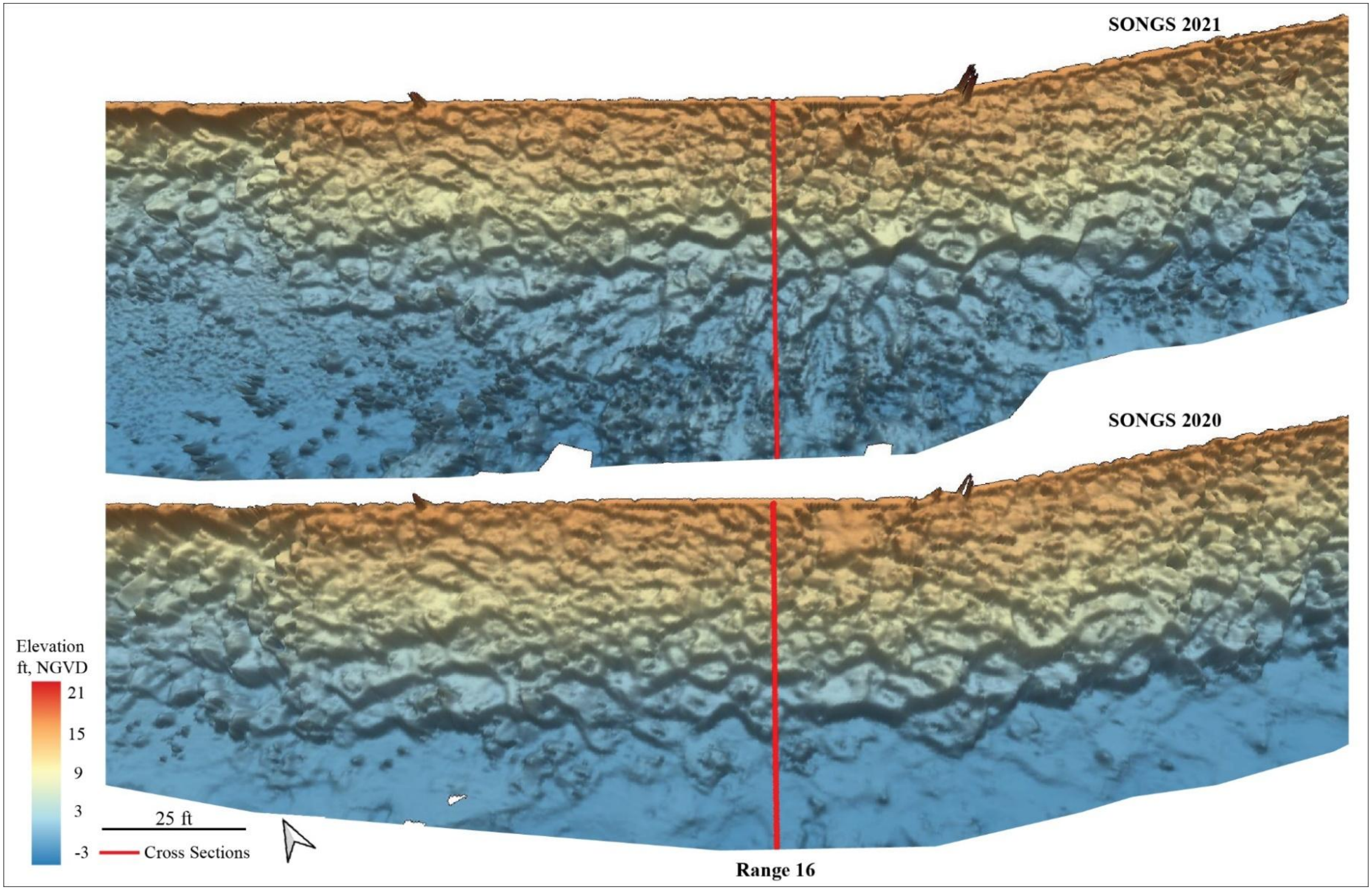

Figure A-17. DEM comparison between 2021 (top) and 2020 (bottom) showing Transect 16 along the SONGS revetment. Notice the increased amount of cobble at the toe of the revetment in 2021.

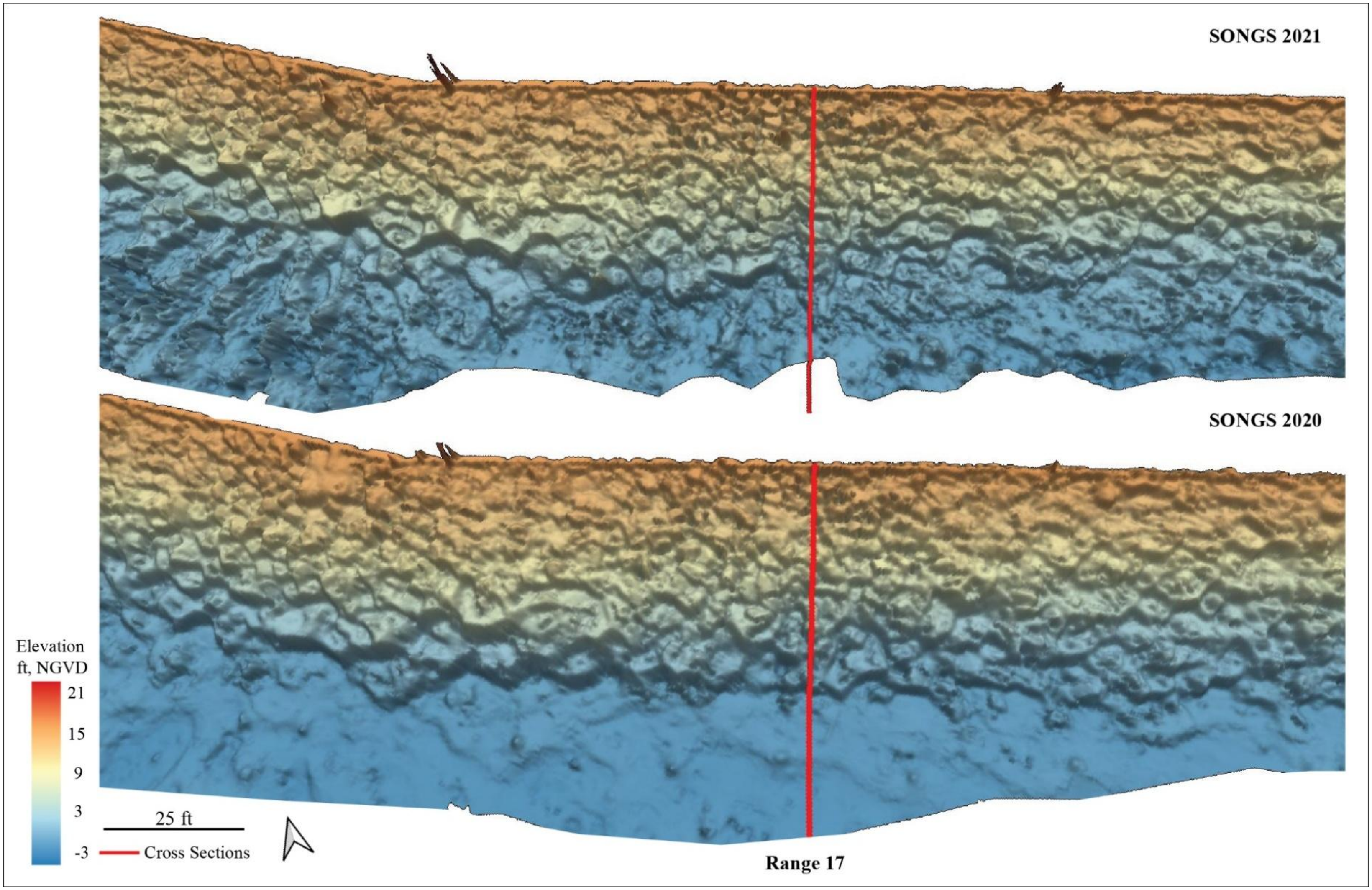

Figure A-18. DEM comparison between 2021 (top) and 2020 (bottom) showing Transect 17 along the SONGS revetment. Notice the increased amount of cobble at the toe of the revetment in 2021.

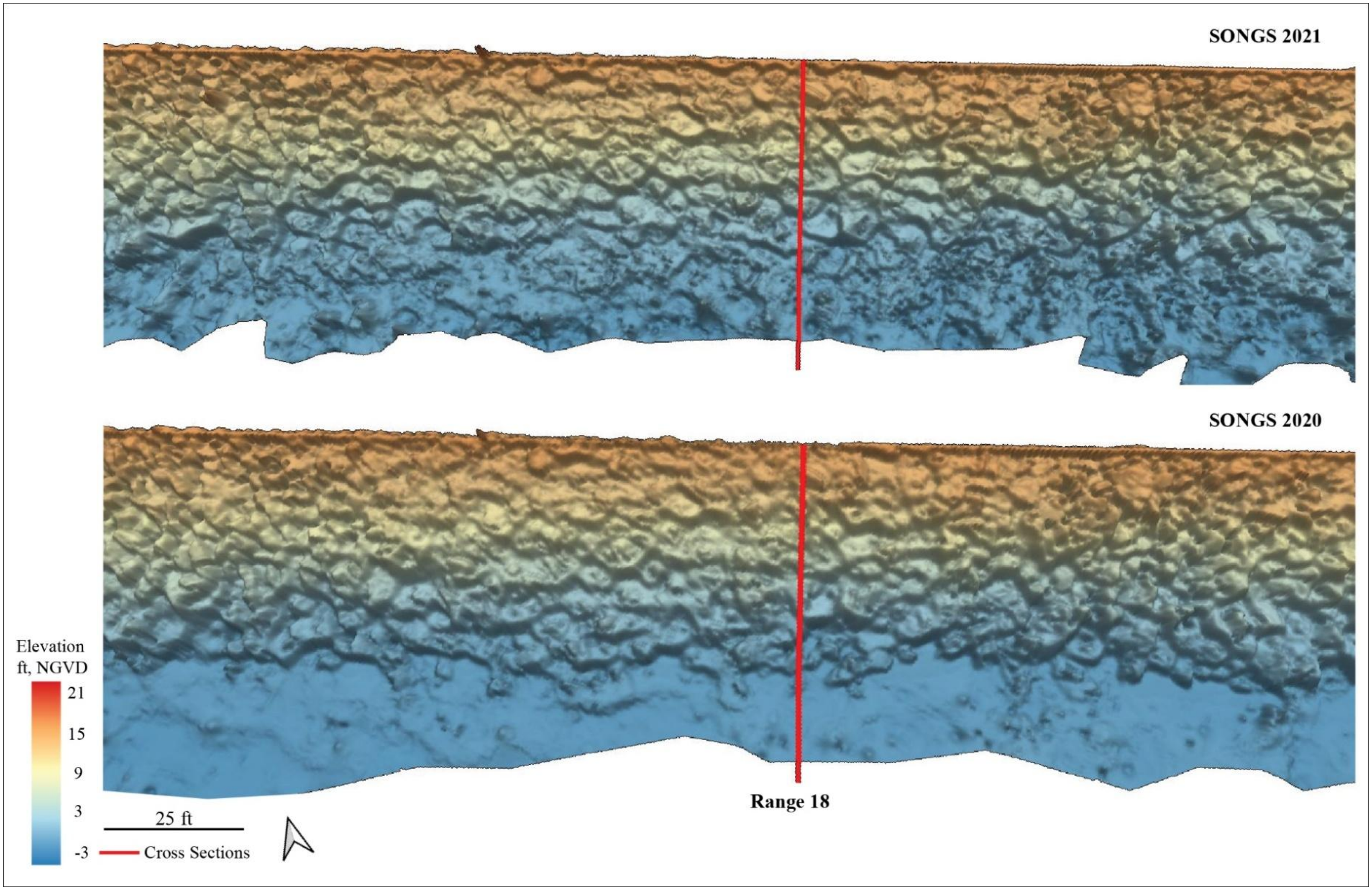

Figure A-19. DEM comparison between 2021 (top) and 2020 (bottom) showing Transect 18 along the SONGS revetment. Notice the increased amount of cobble at the toe of the revetment in 2021.

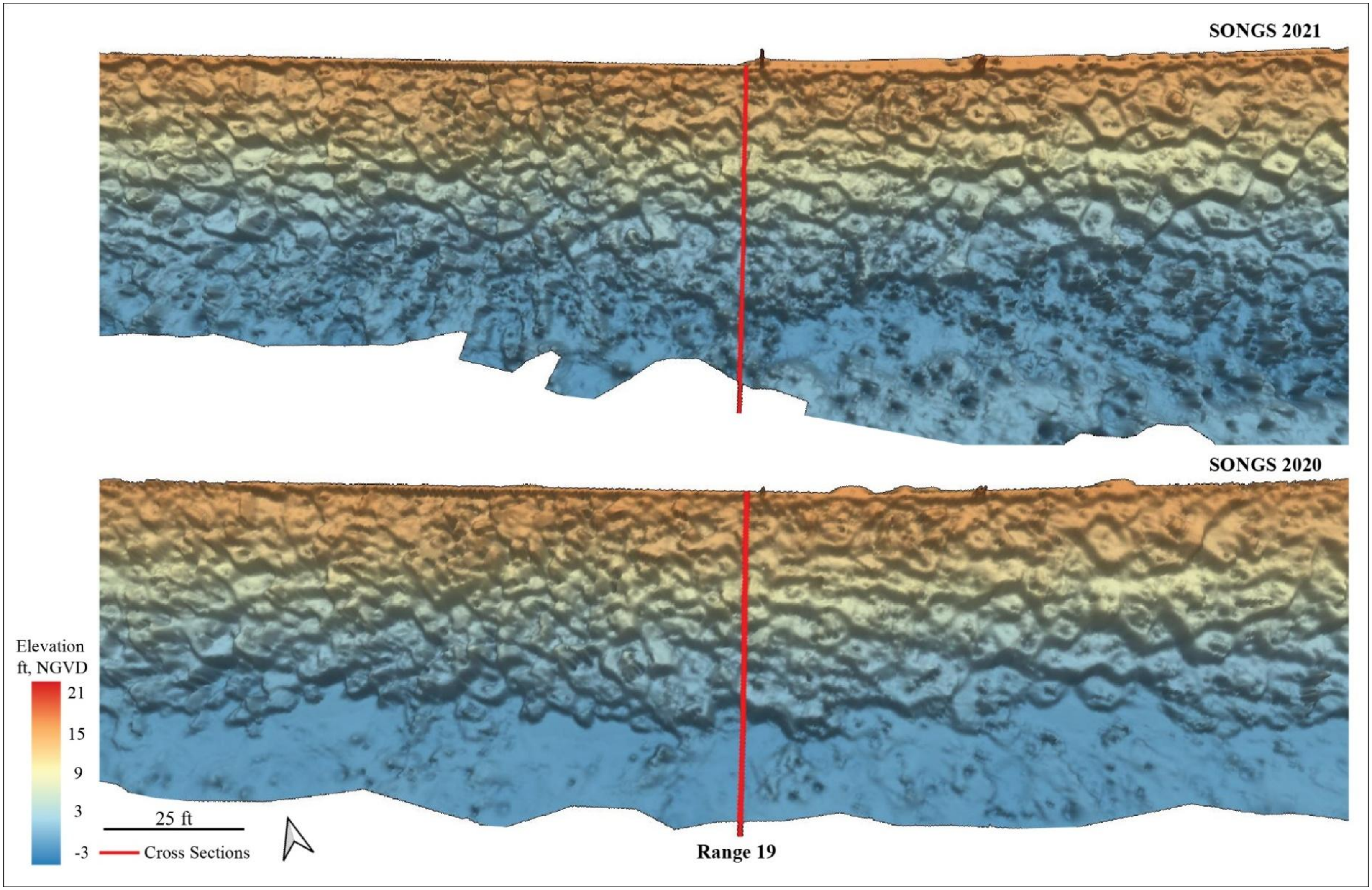

Figure A-20. DEM comparison between 2021 (top) and 2020 (bottom) showing Transect 19 along the SONGS revetment. Notice the increased amount of cobble at the toe of the revetment in 2021.

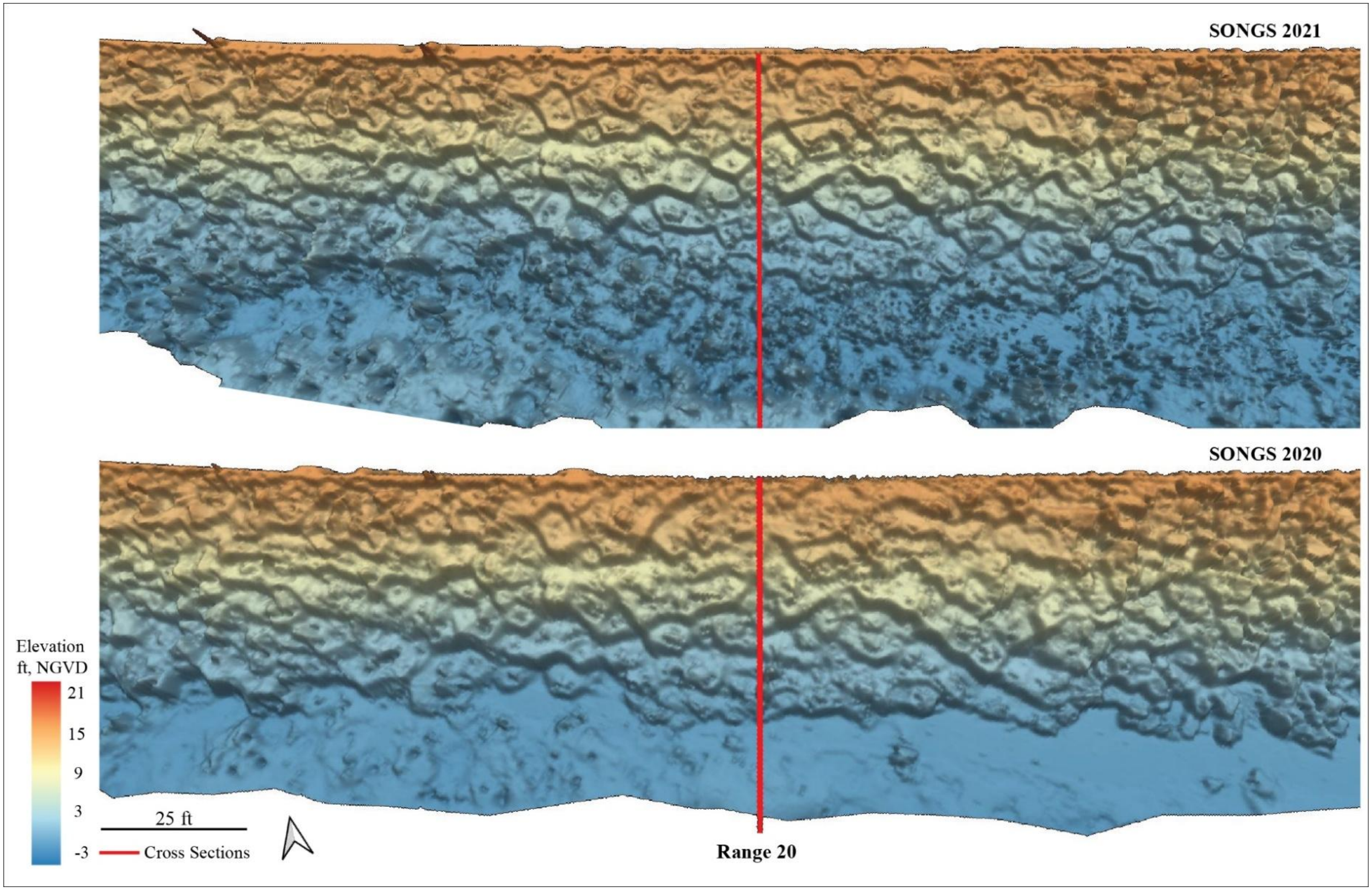

Figure A-21. DEM comparison between 2021 (top) and 2020 (bottom) showing Transect 20 along the SONGS revetment. Notice the increased amount of cobble at the toe of the revetment in 2021.

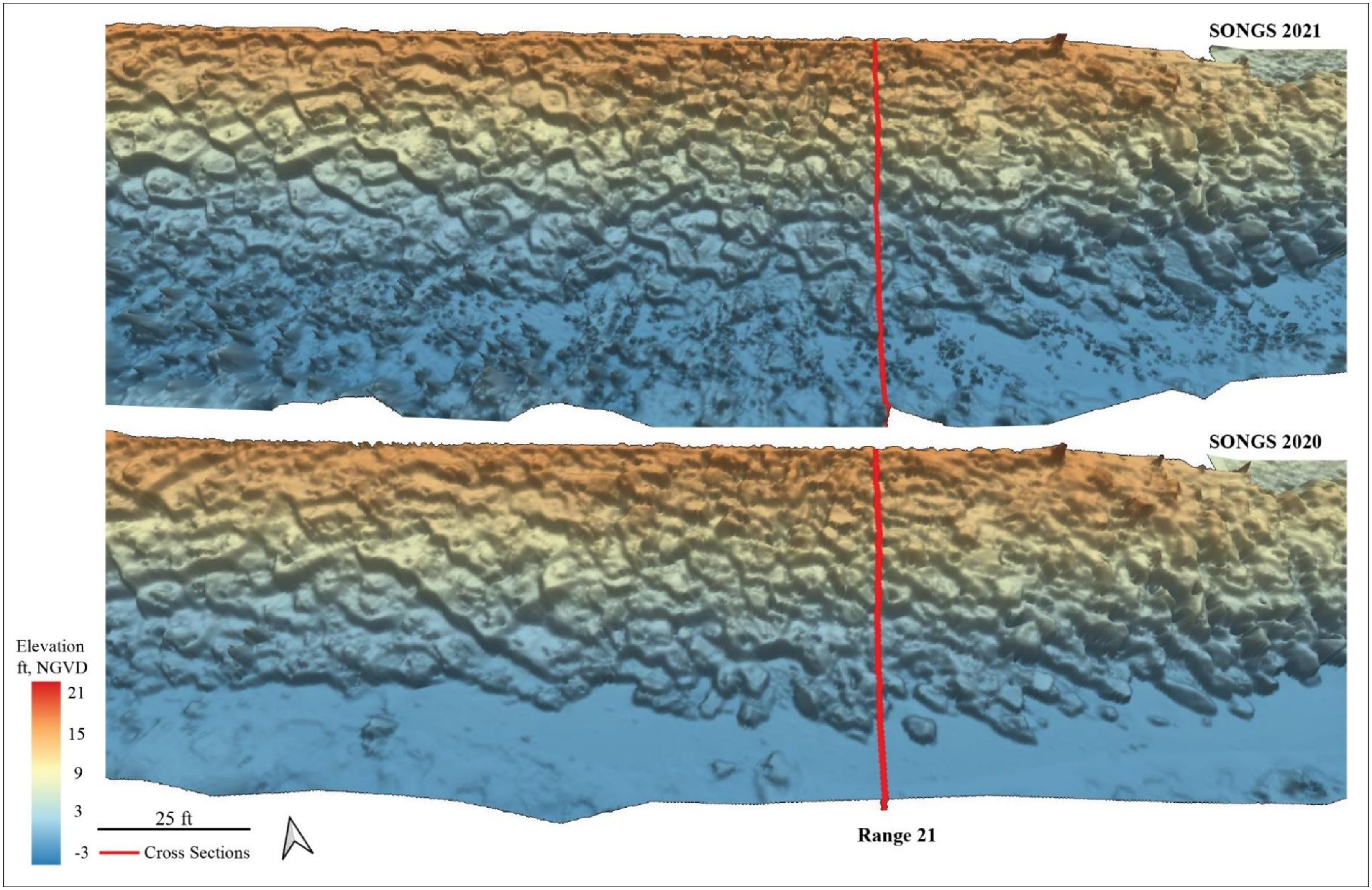

Figure A-22. DEM comparison between 2021 (top) and 2020 (bottom) showing Transect 21 along the SONGS revetment. Notice the increased amount of cobble at the toe of the revetment in 2021.

APPENDIX B

CROSS SECTION ELEVATIONS OF SONGS REVETMENT

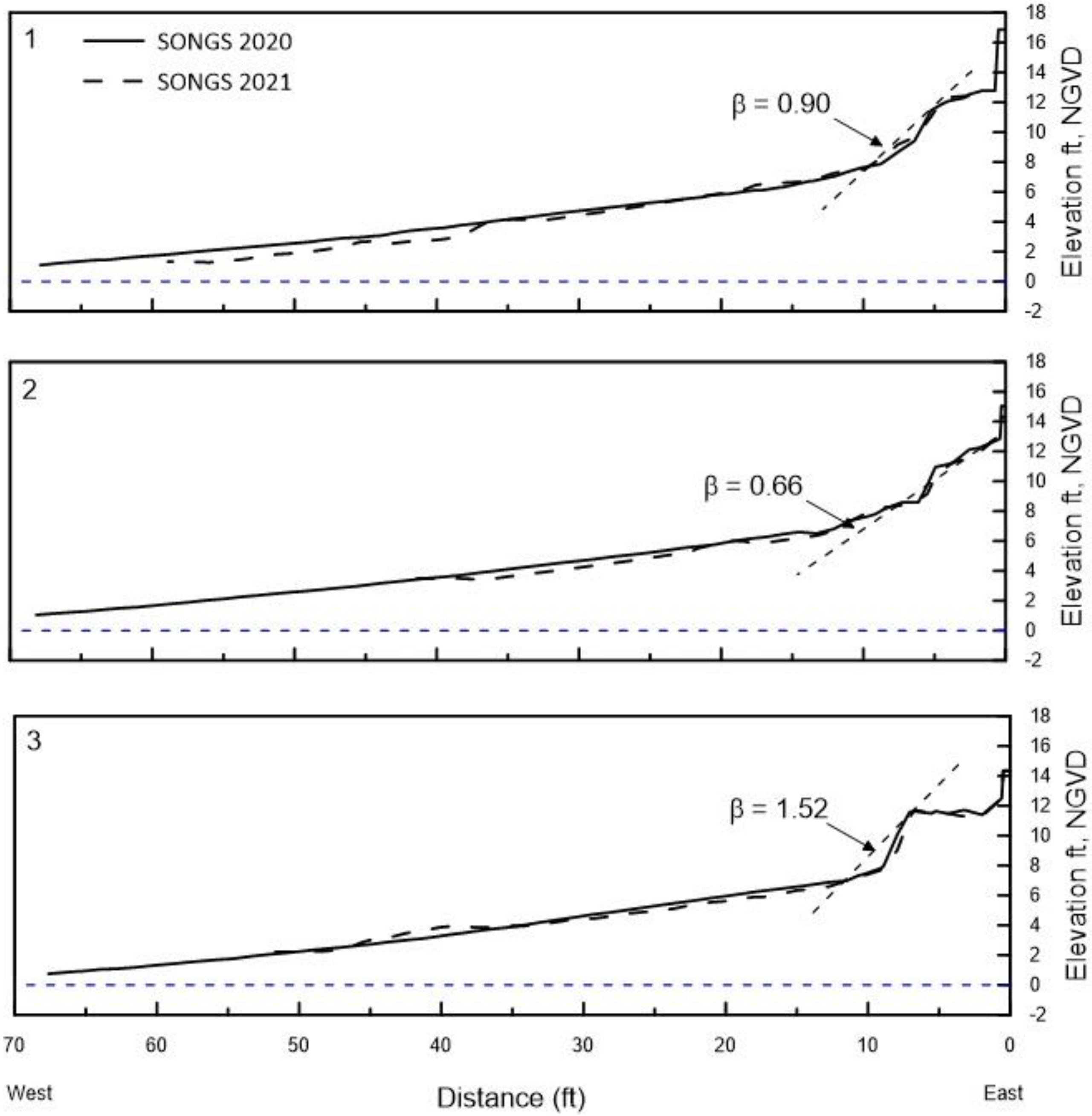

Figure B-1. Cross sections of SONGS revetment along transects 1-3, surveyed on 25 February 2021 and 5 March 2020. β represents the revetment slope.

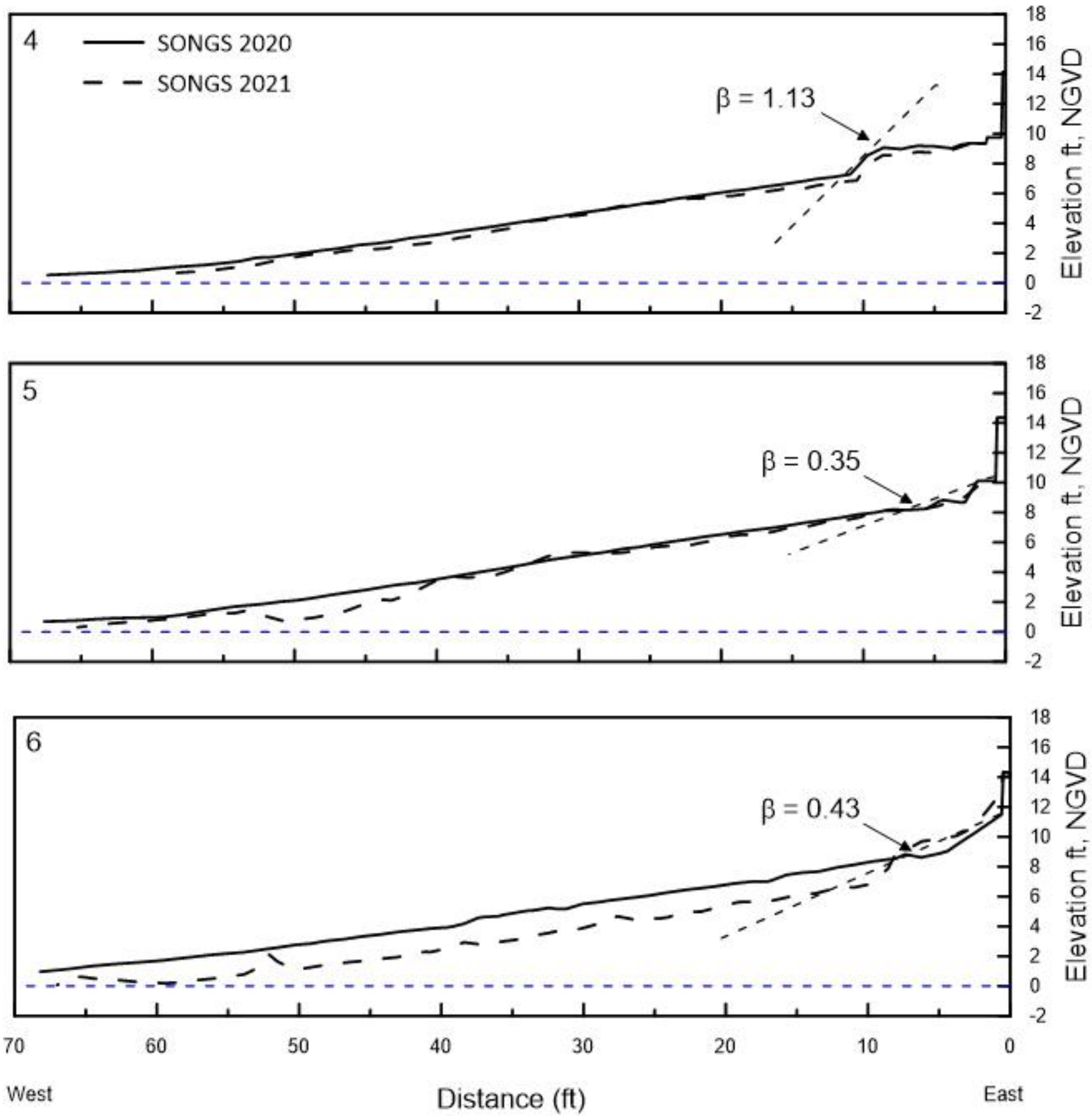

Figure B-2. Cross sections of SONGS revetment along transects 4-6, surveyed on 25 February 2021 and 5 March 2020. β represents the revetment slope.

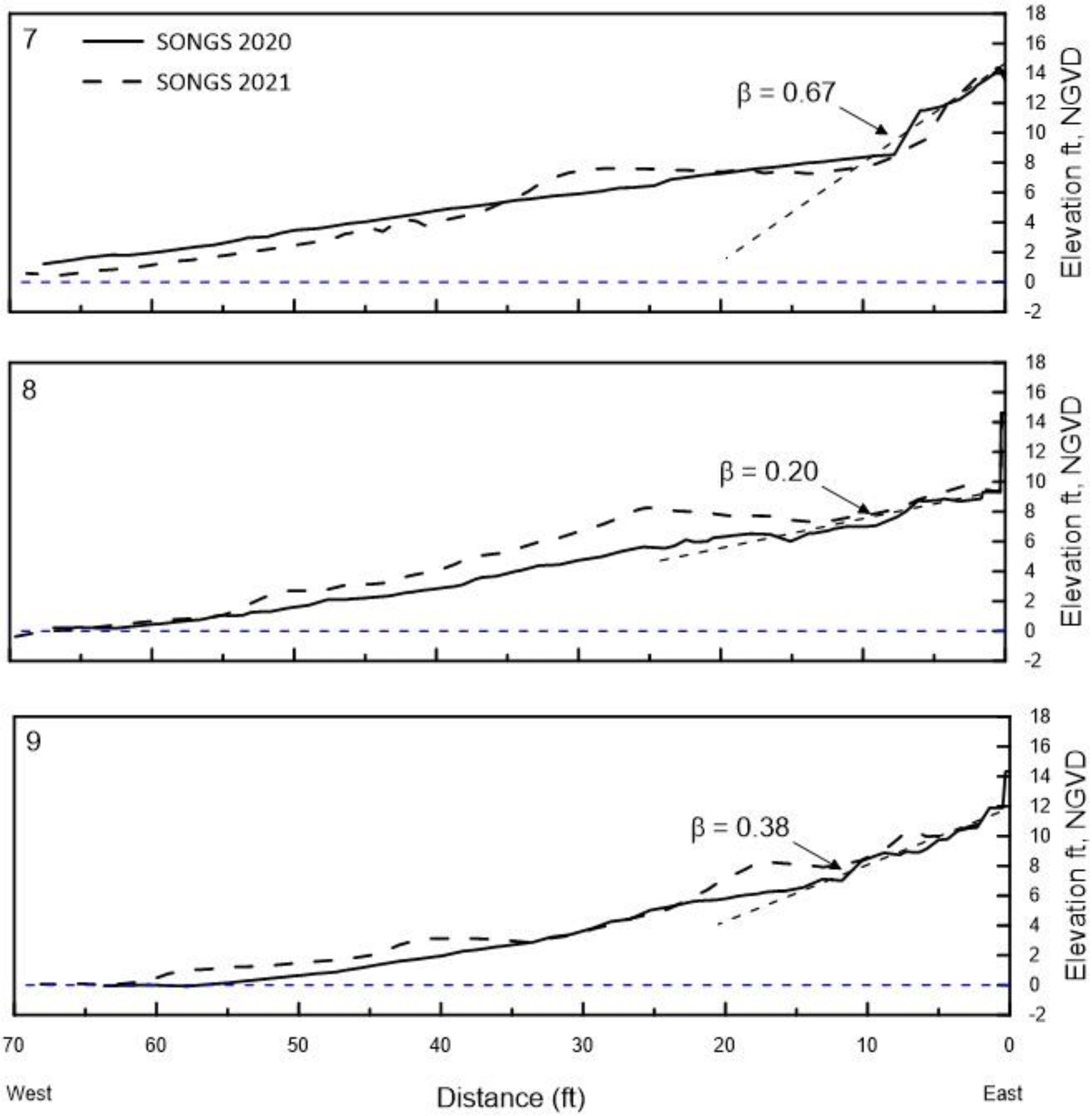

Figure B-3. Cross sections of SONGS revetment along transects 7-9, surveyed on 25 February 2021 and 5 March 2020. β represents the revetment slope.

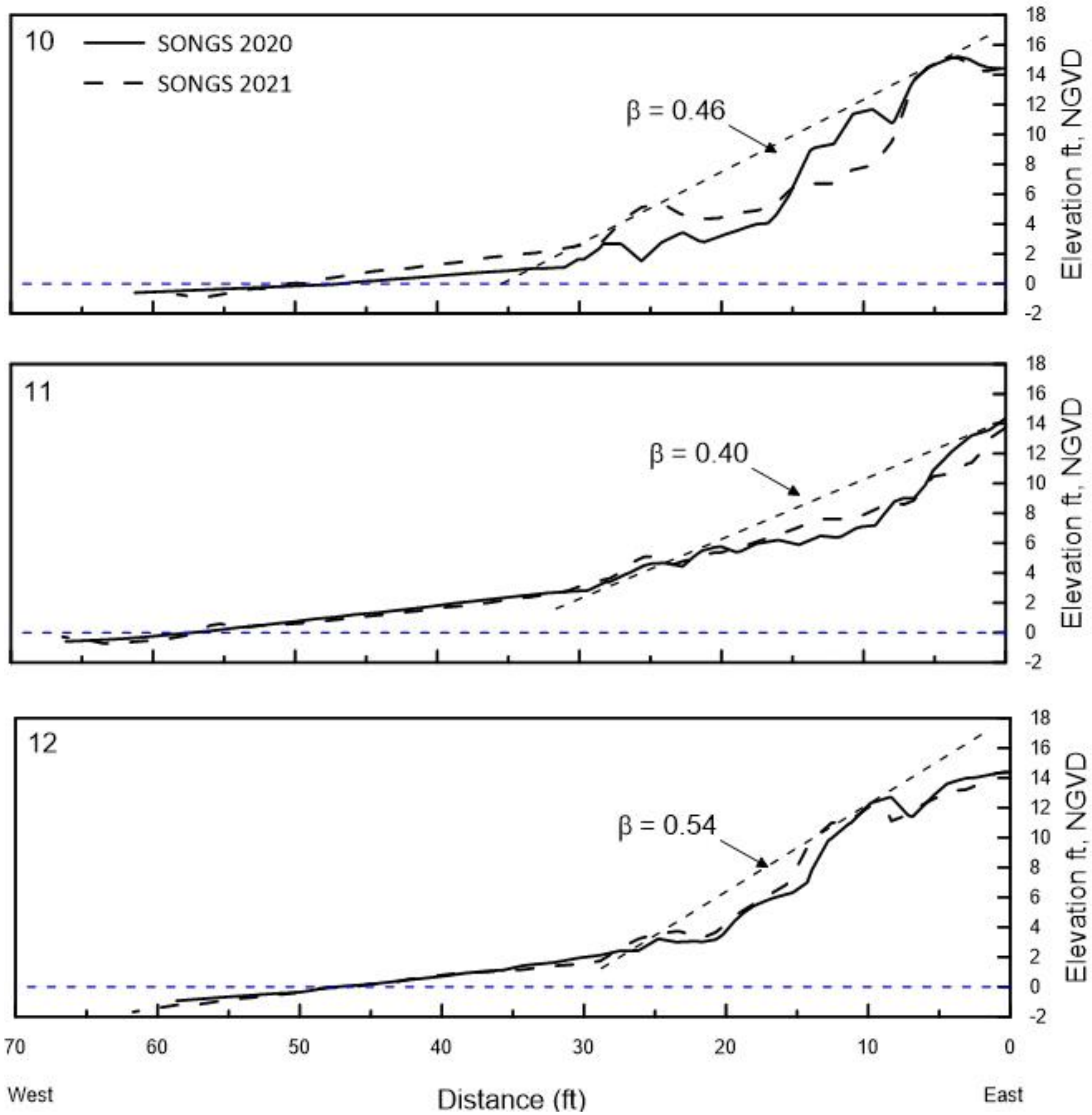

Figure B-4. Cross sections of SONGS revetment along transects 10-12, surveyed on 25 February 2021 and 5 March 2020. β represents the revetment slope.

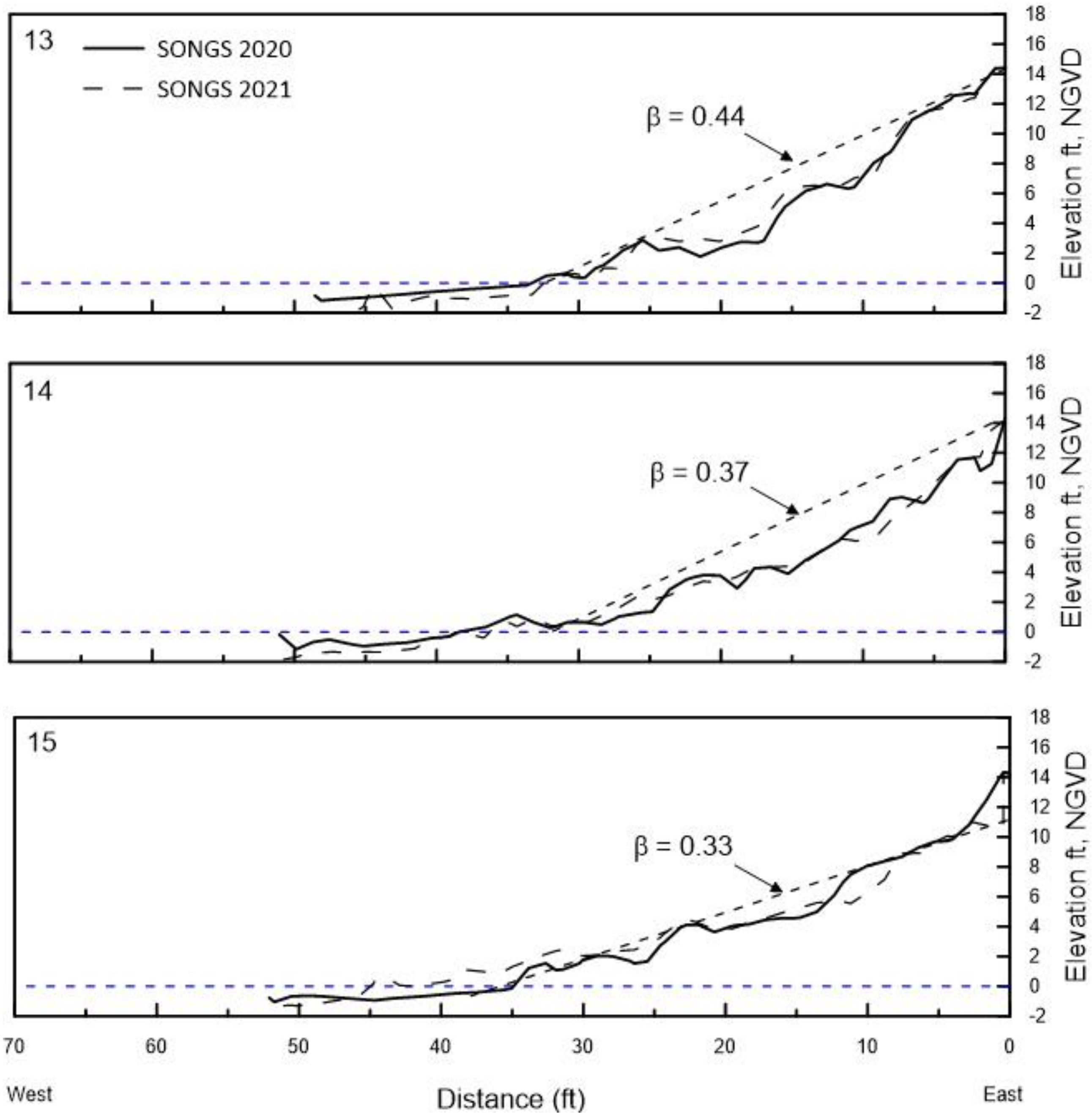

Figure B-5. Cross sections of SONGS revetment along transects 13-15, surveyed on 25 February 2021 and 5 March 2020. β represents the revetment slope.

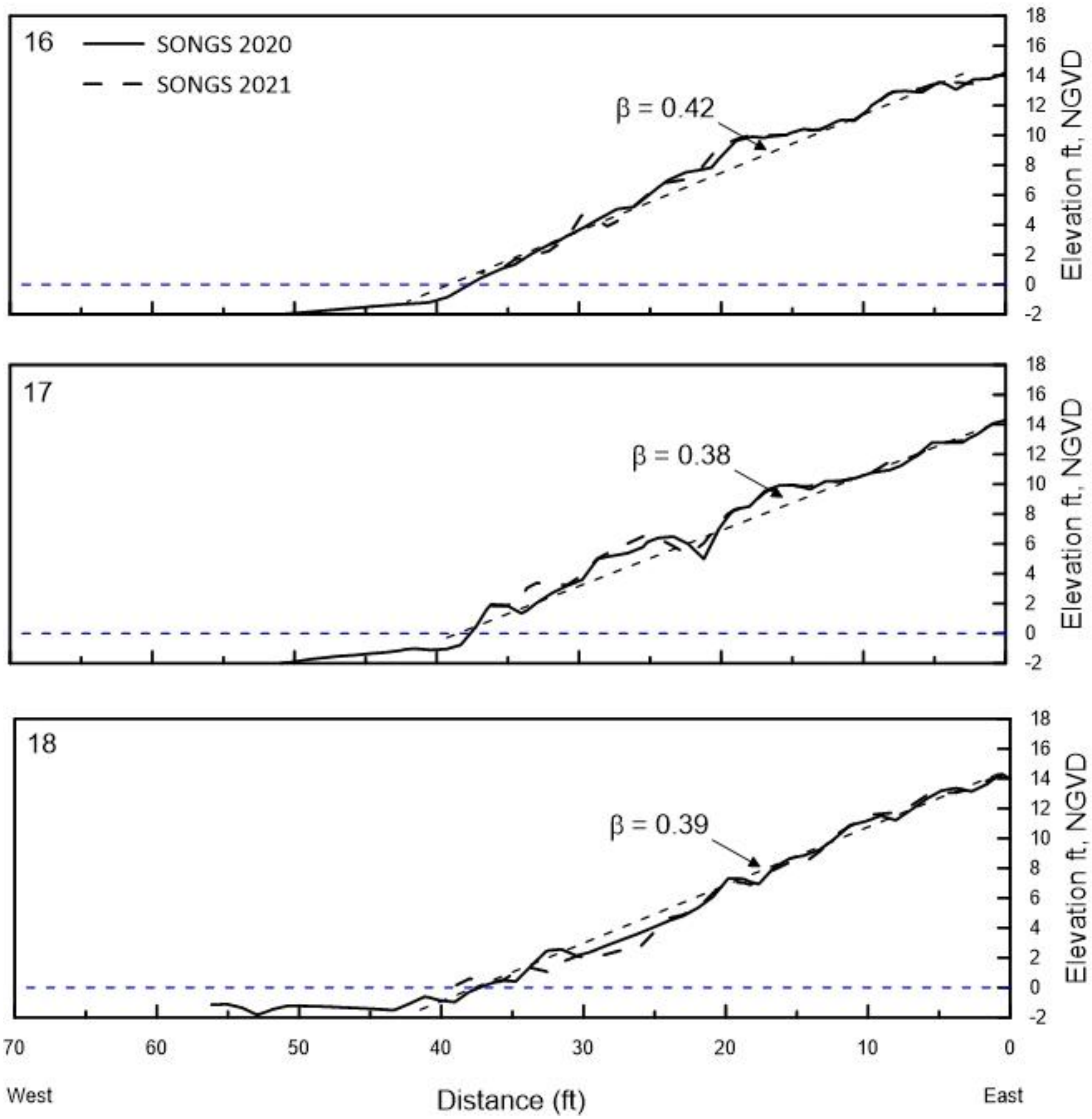

Figure B-6. Cross sections of SONGS revetment along transects 16-18, surveyed on 25 February 2021 and 5 March 2020. β represents the revetment slope.

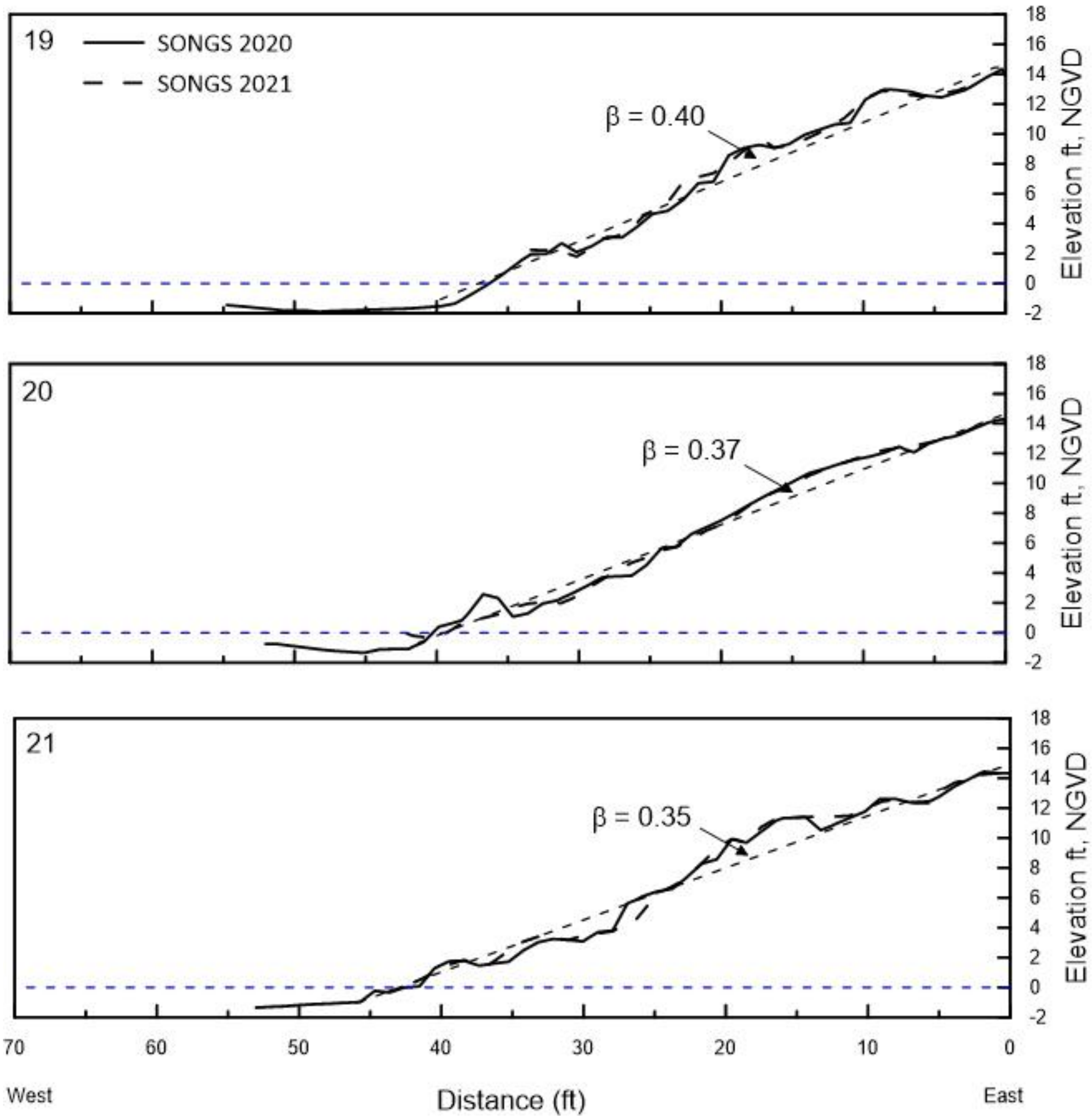

Figure B-7. Cross sections of SONGS revetment along transects 19-21, surveyed on 25 February 2021 and 5 March 2020. β represents the revetment slope.

APPENDIX C

AERIAL PHOTOGRAPHS
NORTH AND SOUTH SONGS, 2003-2020

Photo C-1. Photograph showing revetment covered by sand and fronted by a wide beach at the northern end of SONGS (10 March 2003).

Photo C-2. Photograph showing waves from north swell attacking SONGS revetment at the southern end of SONGS (10 March 2003).

Photo C-3. **Photograph showing waves attacking the revetment and the presence of a sand beach at the northern end of SONGS (26 November 2003).**

Photo C-4. **Photograph showing waves attacking SONGS revetment at the southern end of SONGS (26 November 2003).**

Photo C-5. Photograph showing revetment covered by sand and fronted by a wide beach at the northern end of SONGS (2 August 2006).

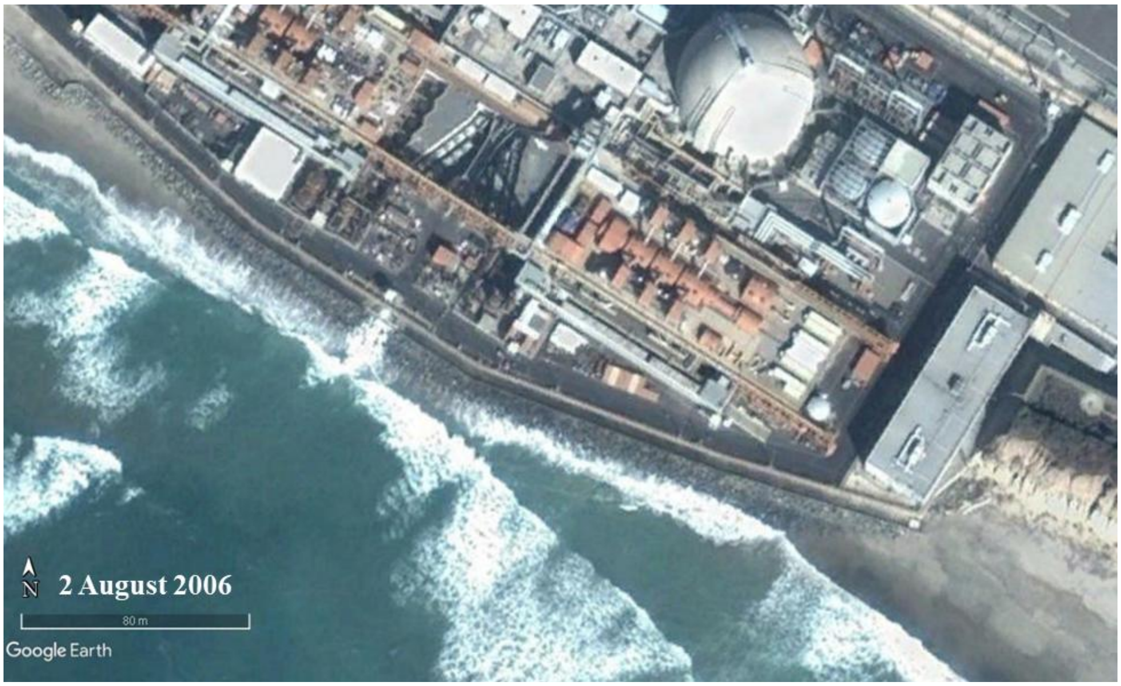

Photo C-6. Photograph showing waves from north swell attacking SONGS revetment at the southern end of SONGS (2 August 2006).

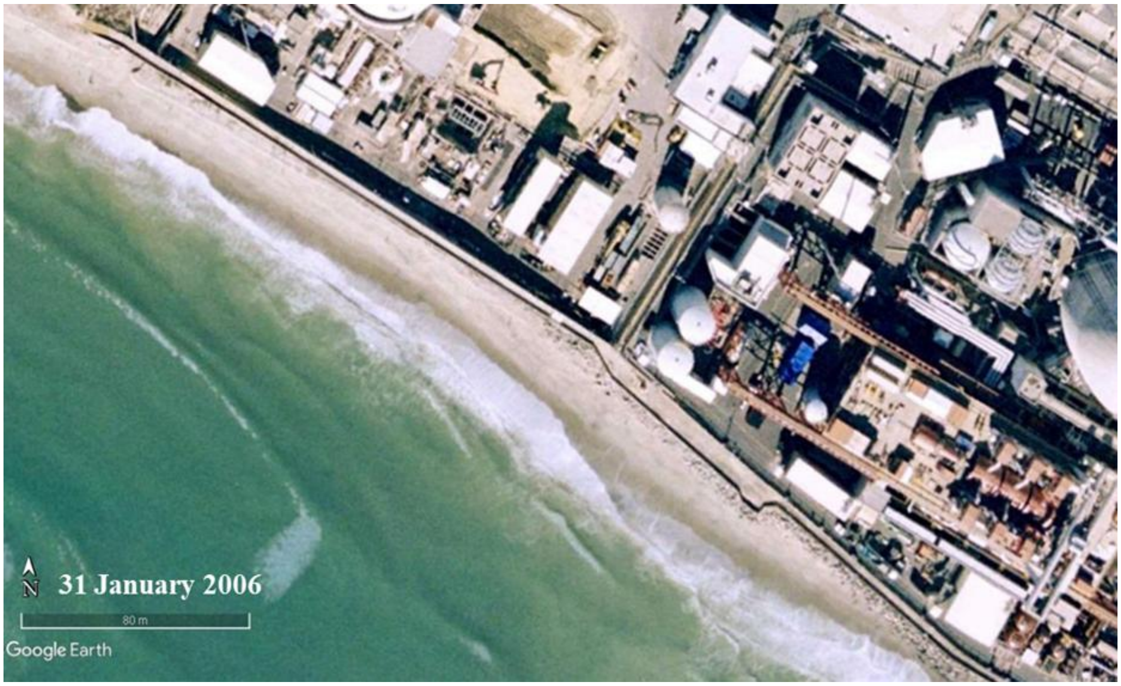

Photo C-7. Photograph showing revetment covered by sand and fronted by a wide beach at the northern end of SONGS (31 January 2006).

Photo C-8. Photograph showing waves from north swell attacking SONGS revetment and refracting towards south at the southern end of SONGS (31 January 2006).

Photo C-9. Photograph showing revetment covered by sand and fronted by a wide beach at the northern end of SONGS (31 January 2008).

Photo C-10. Photograph showing waves attacking SONGS revetment at the southern end of SONGS (31 January 2008).

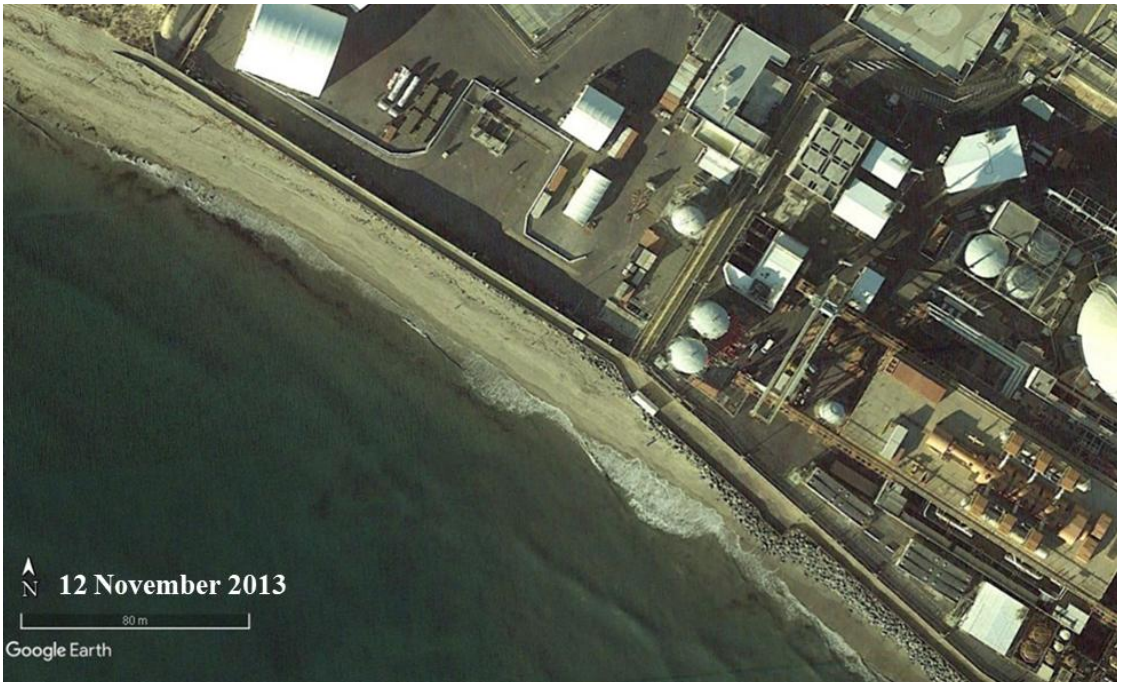

Photo C-11. Photograph showing revetment covered by sand and fronted by a wide beach at the northern end of SONGS (12 November 2013).

Photo C-12. Photograph showing waves attacking SONGS revetment and refracting towards south at the southern end of SONGS (12 November 2013).

Photo C-13. Photograph showing revetment exposed and fronted by a wide beach at the northern end of SONGS (27 April 2014).

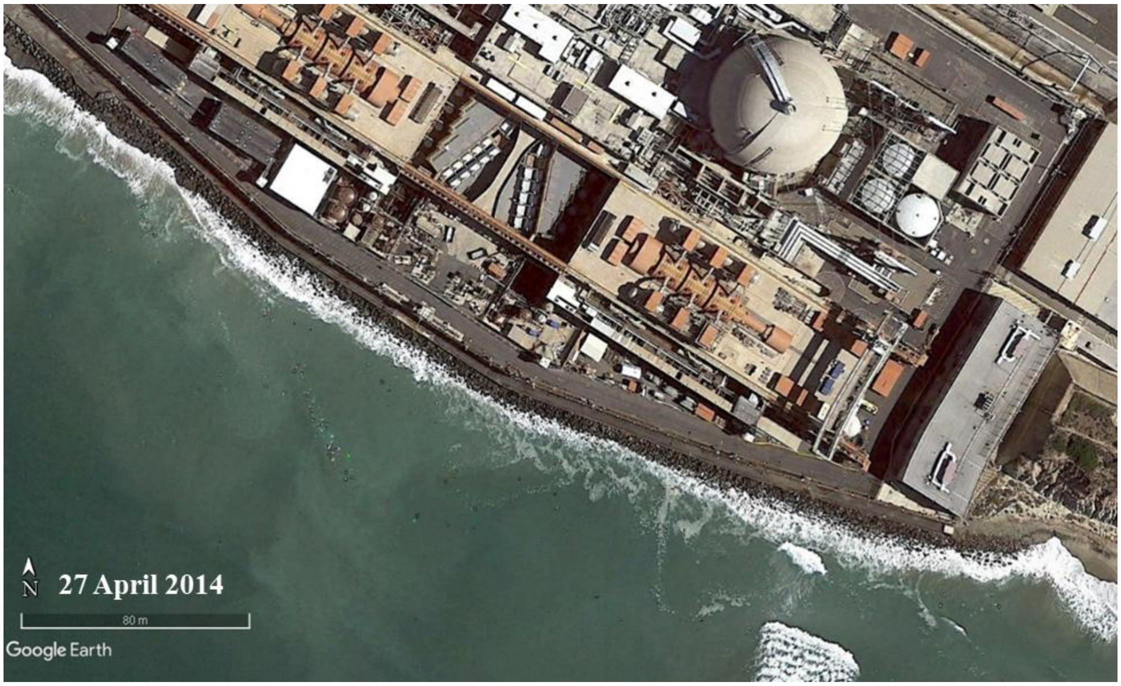

Photo C-14. Photograph showing waves attacking SONGS revetment and refracting towards south at the southern end of SONGS (12 November 2013).

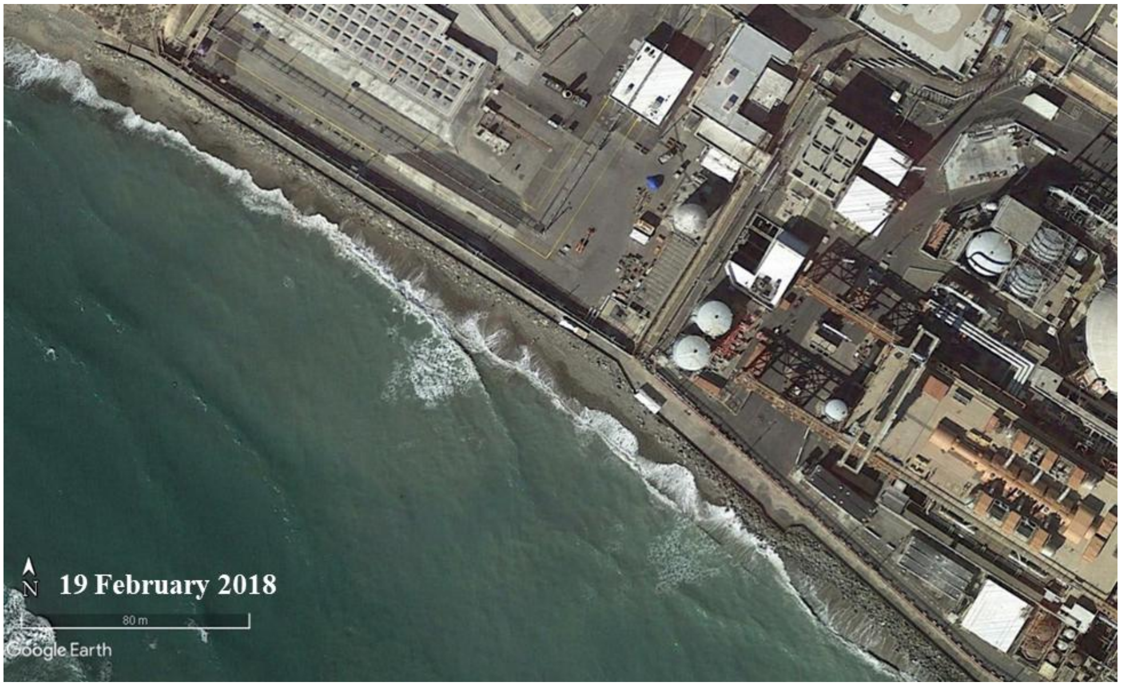

Photo C-15. Photograph showing revetment exposed and fronted by a sand beach at the northern end of SONGS (19 February 2018).

Photo C-16. Photograph showing waves from north swell attacking SONGS revetment and refracting towards south at the southern end of SONGS (19 February 2018).

Photo C-17. Photograph showing revetment exposed and fronted by a wide beach at the northern end of SONGS (24 August 2018).

Photo C-18. Photograph showing waves from north swell attacking SONGS revetment and refracting towards south at the southern end of SONGS (24 August 2018).

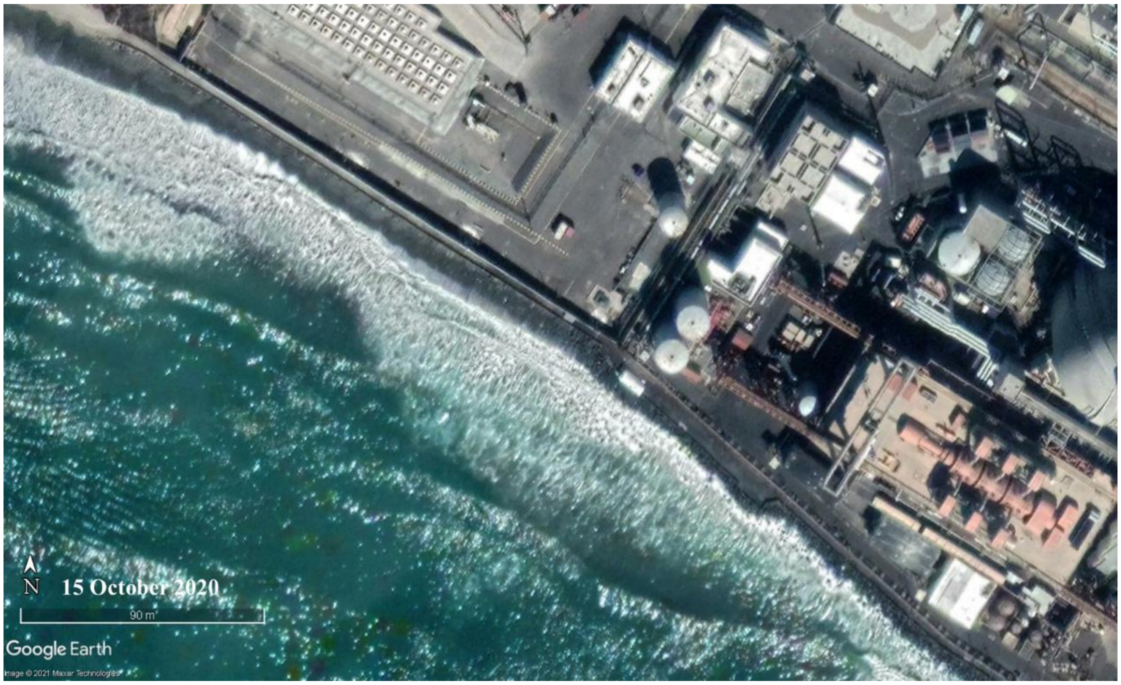

Photo C-19. **Photograph showing revetment exposed and fronted by a wide beach at the northern end of SONGS (15 October 2020).**

Photo C-20. **Photograph showing waves attacking SONGS revetment and refracting towards south at the southern end of SONGS (15 October 2020).**

APPENDIX D

PHOTOGRAPHS FROM 2021 & 2020 SURVEYS

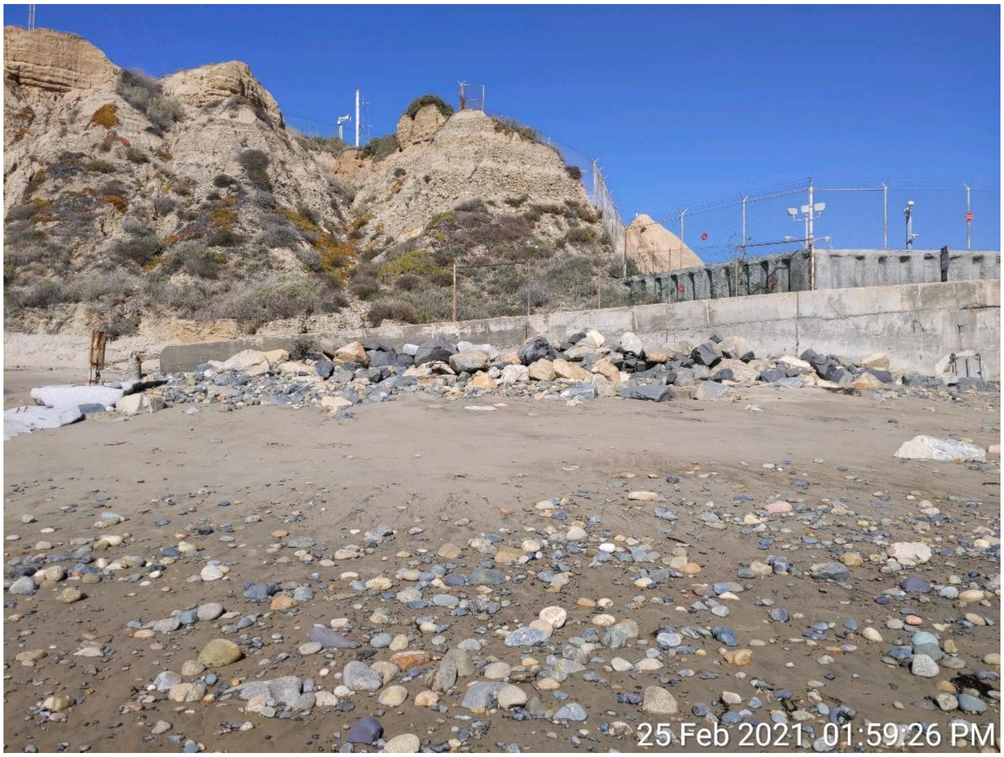

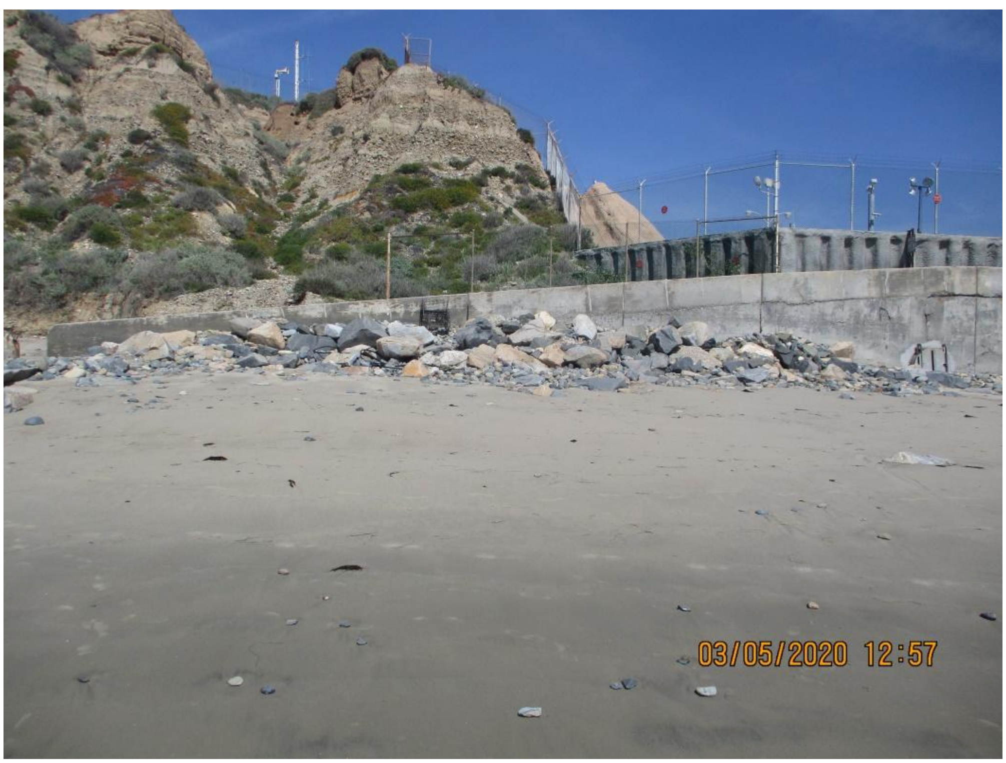

Photo D-1. Photograph for Transect 1 taken on 25 February 2021 (top) and 5 March 2020 (bottom).

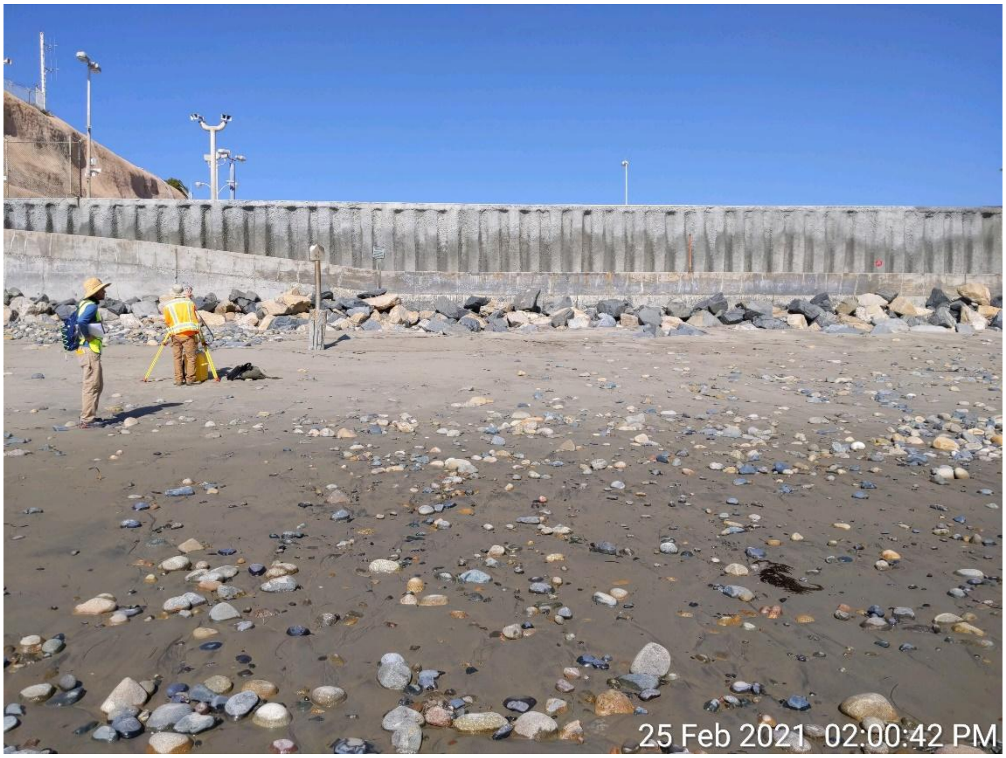

Photo D-2. Photograph for Transect 2 taken on 25 February 2021 (top) and 5 March 2020 (bottom).

Photo D-3. Photograph for Transect 3 taken on 25 February 2021 (top) and 5 March 2020 (bottom).

Photo D-4. Photograph for Transect 4 taken on 25 February 2021 (top) and 5 March 2020 (bottom).

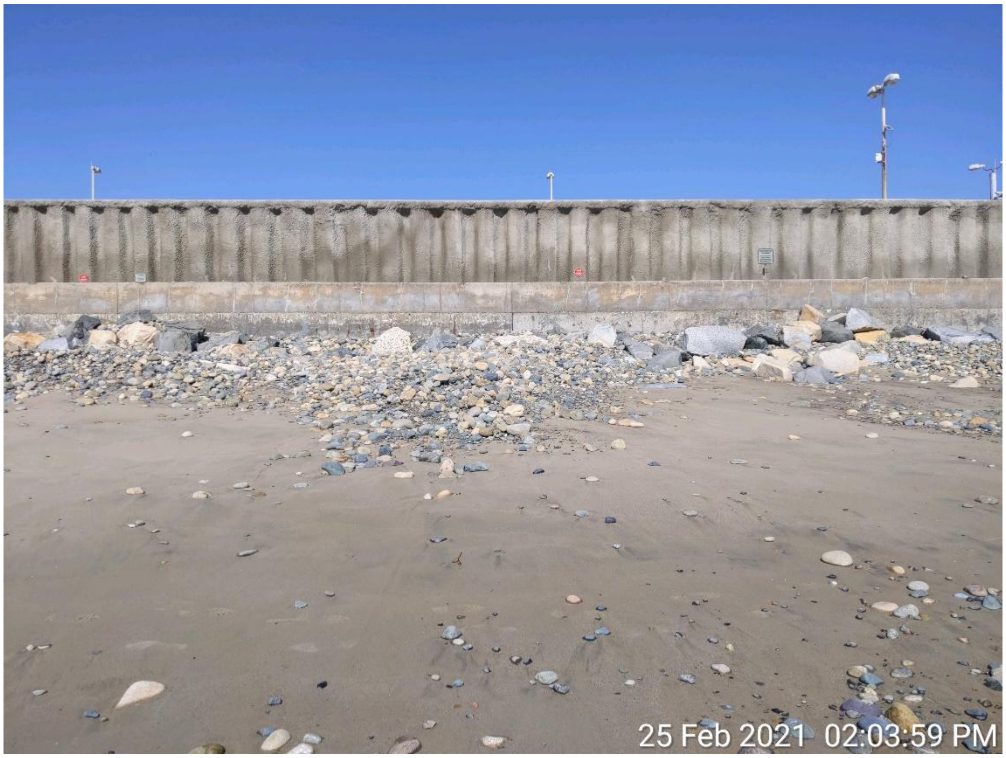

Photo D-5. Photograph for Transect 5 taken on 25 February 2021 (top) and 5 March 2020 (bottom).

Photo D-6. Photograph for Transect 6 taken on 25 February 2021 (top) and 5 March 2020 (bottom).

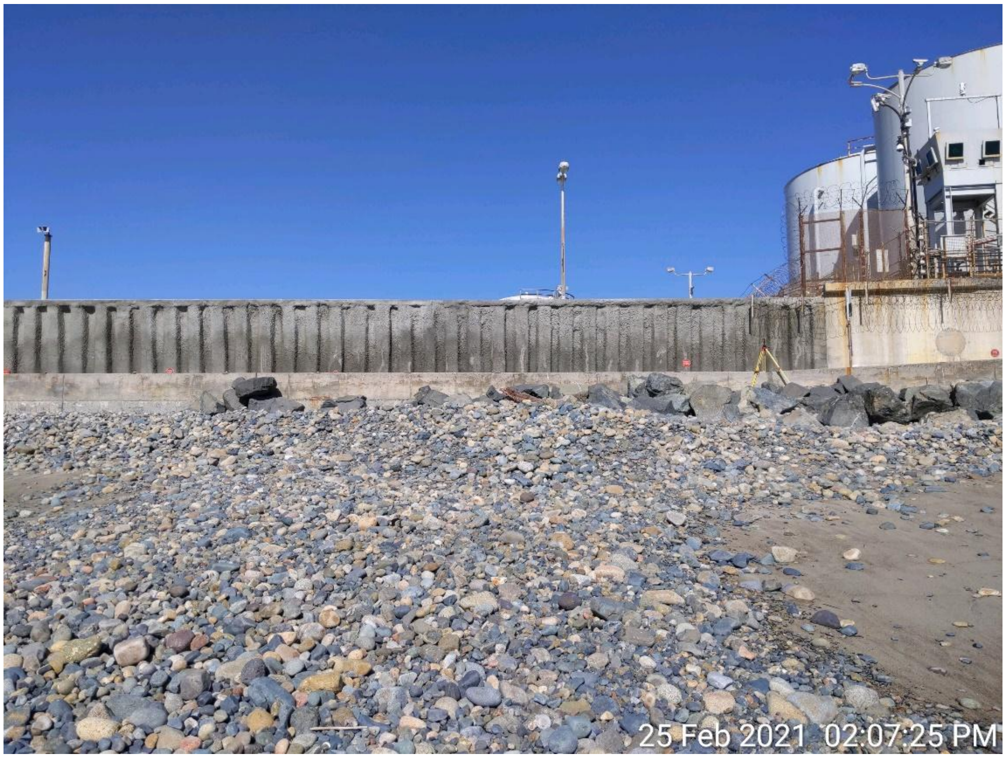

Photo D-7. Photograph for Transect 7 taken on 25 February 2021 (top) and 5 March 2020 (bottom).

Photo D-8. Photograph for Transect 8 taken on 25 February 2021 (top) and 5 March 2020 (bottom).

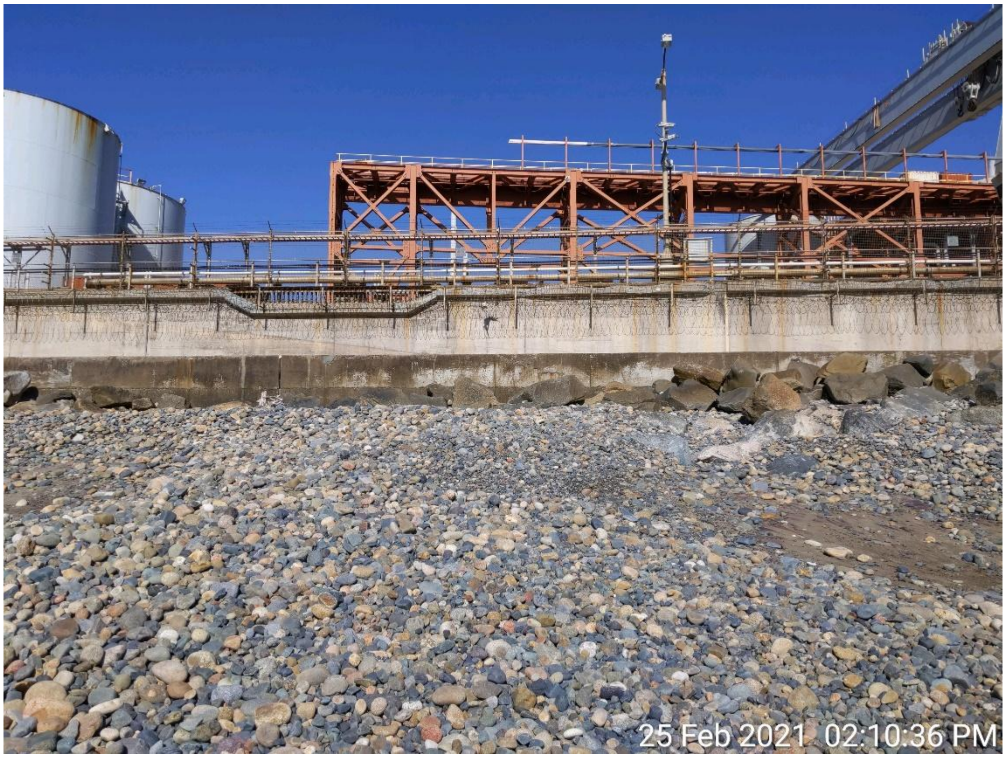

Photo D-9. Photograph for Transect 9 taken on 25 February 2021 (top) and 5 March 2020 (bottom).

Photo D-10. Photograph for Transect 10 taken on 25 February 2021 (top) and 5 March 2020 (bottom).

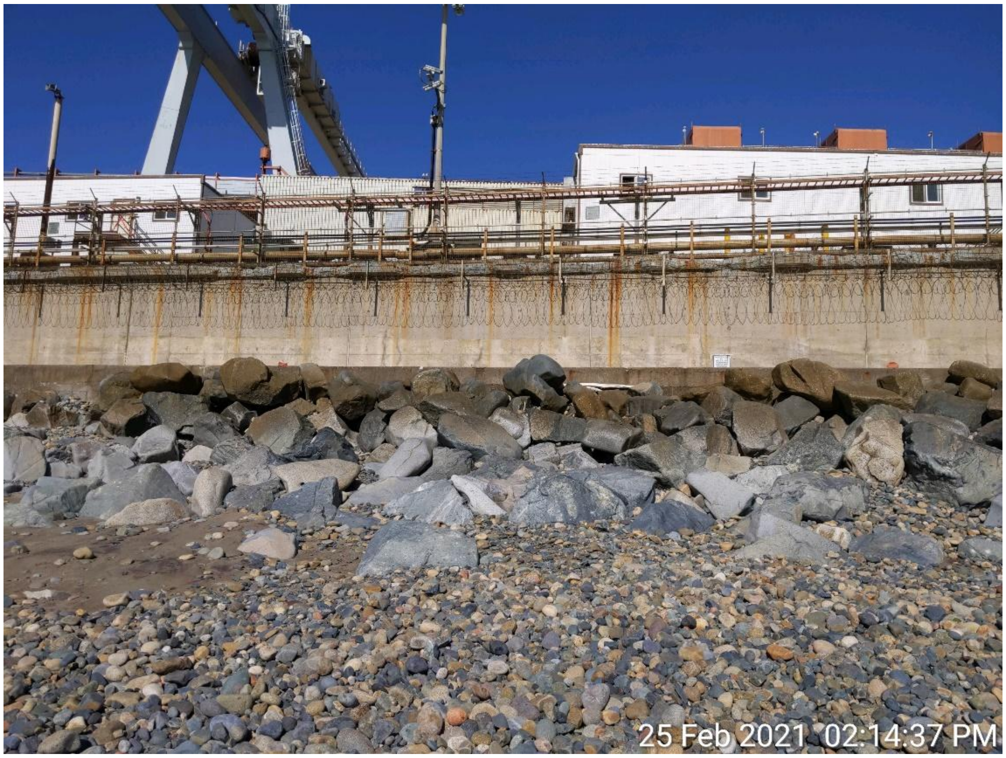

Photo D-11. Photograph for Transect 11 taken on 25 February 2021 (top) and 5 March 2020 (bottom).

Photo D-12. Photograph for Transect 12 taken on 25 February 2021 (top) and 5 March 2020 (bottom).

Photo D-13. Photograph for Transect 13 taken on 25 February 2021 (top) and 5 March 2020 (bottom).

Photo D-14. Photograph for Transect 14 taken on 25 February 2021 (top) and 5 March 2020 (bottom).

Photo D-15. Photograph for Transect 15 taken on 25 February 2021 (top) and 5 March 2020 (bottom).

Photo D-16. Photograph for Transect 16 taken on 25 February 2021 (top) and 5 March 2020 (bottom).

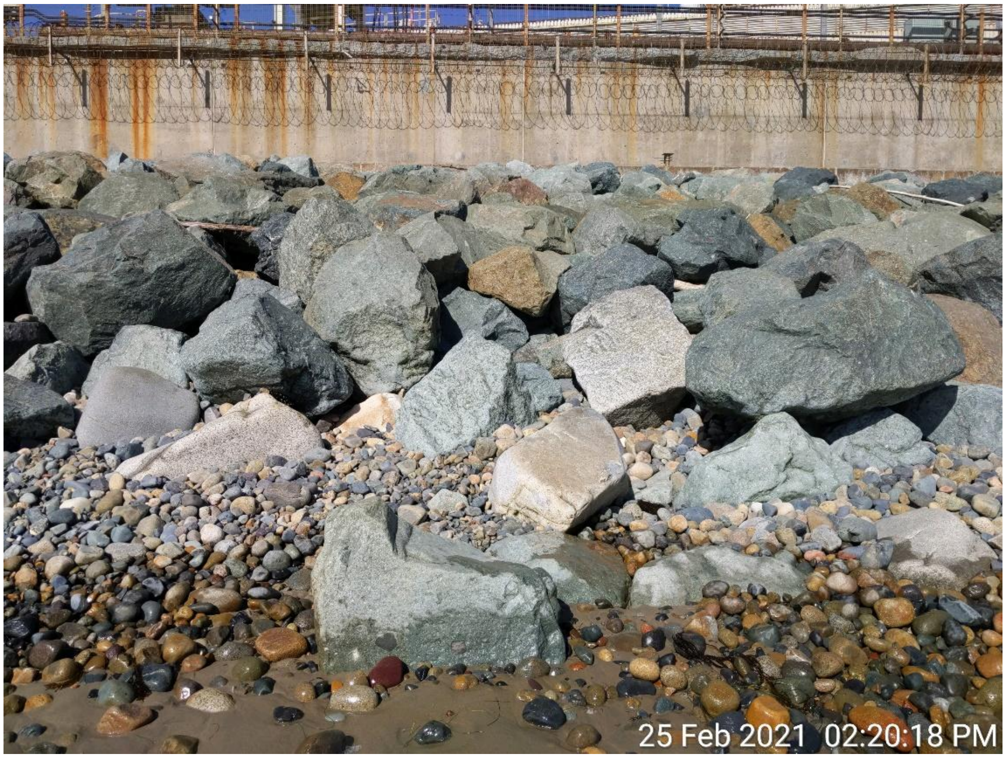

Photo D-17. Photograph for Transect 17 taken on 25 February 2021 (top) and 5 March 2020 (bottom).

Photo D-18. Photograph for Transect 18 taken on 25 February 2021 (top) and 5 March 2020 (bottom).

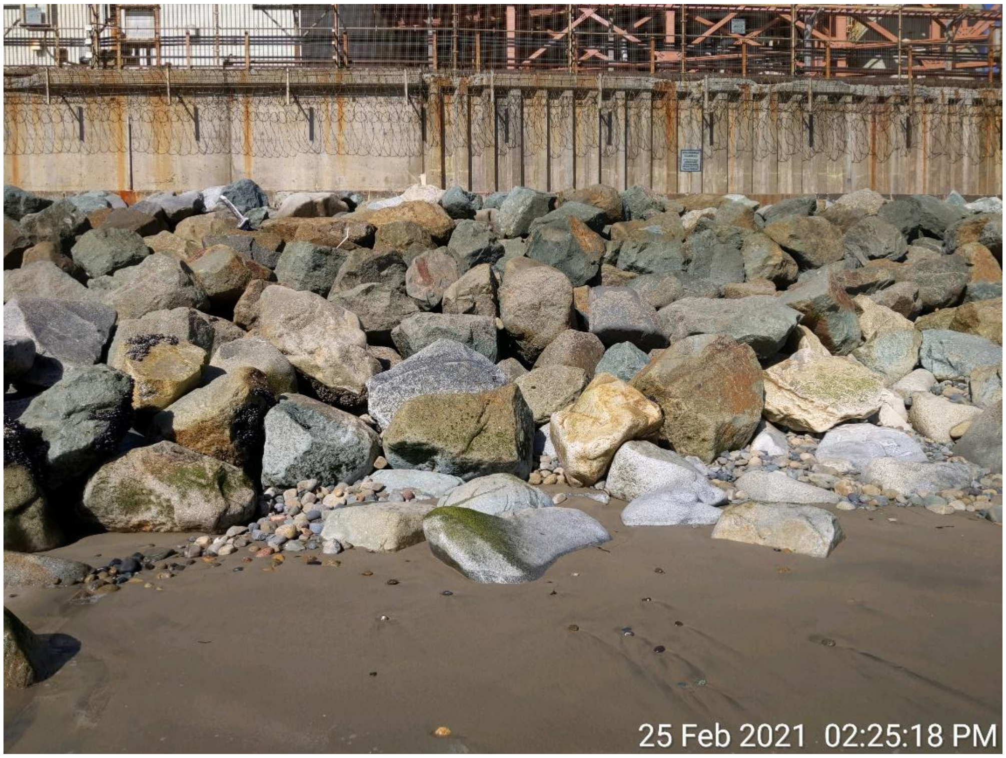

Photo D-19. Photograph for Transect 19 taken on 25 February 2021 (top) and 5 March 2020 (bottom).

Photo D-20. Photograph for Transect 20 taken on 25 February 2021 (top) and 5 March 2020 (bottom).

Photo D-21. Photograph for Transect 21 taken on 25 February 2021 (top) and 5 March 2020 (bottom).

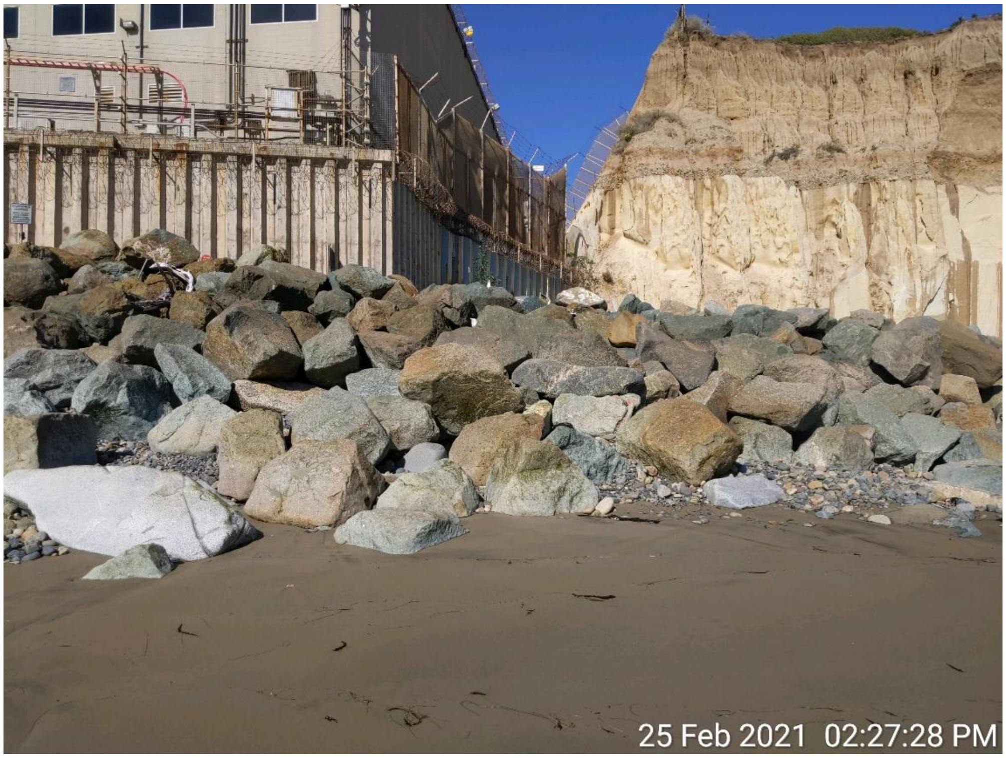

Photo D-22. Photograph showing the start of southern riprap at end of walkway taken on 25 February 2021 (top) and 5 March 2020 (bottom).

Photo D-23. Photograph showing the middle of southern riprap at end of walkway taken on 25 February 2021 (top) and 5 March 2020 (bottom).

Photo D-24. Photograph showing the end of southern riprap at end of walkway taken on 25 February 2021 (top) and 5 March 2020 (bottom).

APPENDIX E

2020 BEACH PROFILE SURVEYS AT SAN ONOFRE

SAN ONOFRE NUCLEAR GENERATING STATION (SONGS) UNITS 2 & 3 DECOMMISSIONING PROJECT
2020 BEACH PROFILE SURVEYS AT SAN ONOFRE

by

M. Hany S. Elwany, Ph.D.
Reinhard E. Flick, Ph.D.
Frederico Scarelli, Ph.D.

Submitted to:

SOUTHERN CALIFORNIA EDISON
2244 Walnut Grove Avenue
Rosemead, CA 91770

COASTAL ENVIRONMENTS, INC.
2166 Avenida de la Playa, Suite E
La Jolla, CA 92037

31 January 2021
CE Reference No. 21-01

TABLE OF CONTENTS

LIST OF APPENDICES

LIST OF TABLES

LIST OF FIGURES

LIST OF PHOTOGRAPHS

2020 BEACH PROFILE SURVEYS AT SAN ONOFRE

1.0 INTRODUCTION

This report summarizes the beach profile survey data collected at San Onofre in 2020 and examines it within the context of recent and historical beach profile data. The goals of this report are to address the recent characteristics of the beach nearby the San Onofre Nuclear Generating Station (SONGS), and to define the short- and long-term erosion and accretion patterns of the beach.

Recent beach characteristics are defined by the 2017, 2018, 2019, and 2020 beach measurements, which were carried out quarterly. These measurements capture the beach configuration corresponding to the autumn, winter, spring, and summer seasons, as well as continuing erosion or accretion trends. Additionally, each year the winter and summer beach profile surveys were extended to cover the offshore portion of the beach up to -40 ft water depth. The results of each survey have been presented in reports by Coastal Environments, Inc. (Coastal Environments [CE], 2017, 2018, 2019, 2020b). The longer-term beach change patterns are characterized by comparing the beach widths from these recent surveys to comparable measurements from 1985-1993. The earliest directly comparable data were taken in May 1985, just after the sand release of the SONGS Units 2 and 3 laydown pad (Flick and Wanetick, 1989), and from 1990-1993 (Elwany et al., 1994), 2000 (CE, 2000), and 2016 (CE, 2016).

Data for this study comes from the 16 surveys carried out from March 2017 through October 2020 (Table 1-1). Each survey covered seven profiles (Figure 1-1). Beach profile measurements generally extended to 12 ft below mean sea level (MSL). Two offshore profiles each year extended to 40 ft water depth using a boat-mounted fathometer. Profile elevations are plotted relative to the National Geodetic Vertical Datum 1929 (NGVD), which is 0.44 ft below MSL.

Section 2 of this report presents an overview of the data and how it was collected. In Section 3, the results of the 2020 beach profile surveys at SONGS are presented. The characteristics of SONGS beach profiles and how they relate to typical Southern California beaches are discussed in Section 4. Beach width changes and shoreline trends are discussed in Sections 5 and 6, respectively. Section 7 utilizes the available historical information to better understand beach width fluctuations over a longer time scale and shoreline changes at San Onofre. The conclusions and recommendations are detailed in Section 8. Appendix A shows the nearshore beach profiles carried out in summer and winter for 2017 through 2020. Appendix B presents photographs taken at San Onofre Beach during each survey in 2020, as well as the location of newly established benchmarks.

Table 1-1. Surveys at San Onofre, 2017-2020.

Survey Number	Date	Season
1	01Mar17	Winter
2	19May17	Spring
3	16Aug17	Summer
4	02Nov17	Autumn
5	23Jan18	Winter
6	29May18	Spring
7	22Aug18	Summer
8	18Nov18	Autumn
9	04Mar19	Winter
10	23Apr19	Spring
11	25Jun19	Summer
12	14Oct19	Autumn
13	05Feb20	Winter
14	15May20	Spring
15	17Jul20	Summer
16	27Oct20	Autumn

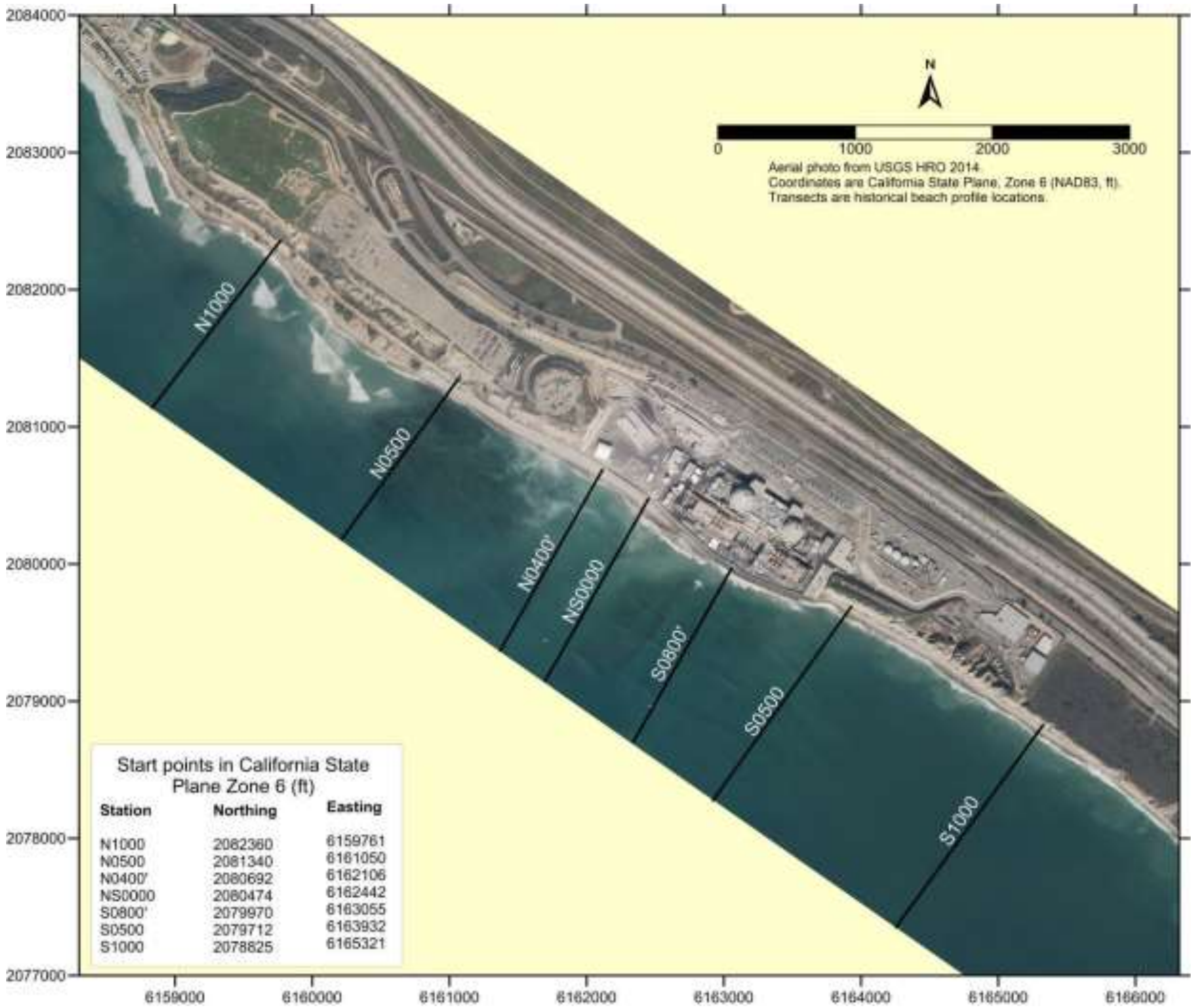

Figure 1-1. Locations of beach profiles surveyed at SONGS.

2.0 SURVEY METHOD

The beach and surf zone were surveyed using a total station (Sokkia SET-610), data logger (Spectra Precision Ranger), and survey rod. The rod holder carries a prism target at the top of a fixed-length pole that reflects an infrared beam sent from the total station. The instrument measures the slant angle and horizontal and vertical distances to the target with an accuracy of approximately 4-6 cm. A handheld electronic field data logger calculates the relative coordinates and elevation using permanent local benchmarks and stores the results. Figure 2-1 illustrates the survey method.

The offshore portions of the profiles were acquired with a digital acoustic echo sounder operated from a 27-ft shallow-draft survey vessel. A Differential Global Positioning System (DGPS) receiver was used to determine the position of each sounding. To improve the accuracy of each position, differential corrections transmitted in real time from U.S. Coast Guard (USCG) beacons were utilized. All systems were interfaced to a laptop computer using the HYDROpro survey package.

At each survey range, the boat traveled from the offshore limit to the surf zone guided by a DGPS navigation system. Soundings were acquired on a near-continuous basis (approximately four to five per second). Vessel positions were recorded at 1-second intervals and merged with the soundings using HYDROpro bathymetric survey software. The calibration of the echo sounder was checked at the beginning and end of each survey session using a standard “bar check” procedure. The merged plots from the 2020 nearshore and offshore profile surveys are presented in Section 3.

All distance measurements on a survey line are made relative to the first reading taken on the starting point of that profile. Starting points were placed as close as practical to the edge or face of the sea cliff. Efforts were made to position the profile starting points used for recent surveys (2017 through 2020) at the same location as those used for all surveys conducted from 1985 to 1993. This enables us to compare the results of the latest surveys with previous data (Flick and Wanetick, 1989; Waldorf, 1989; Elwany et al., 1992, and 1993). The recent survey lines are oriented perpendicular to the mean shoreline using approximately the same fixed bearings as before. The locations of the beach profiles are shown in Figure 1-1.

The horizontal coordinates of the profile starting points were determined by DGPS, and the elevations of these points were determined based on existing benchmarks near SONGS. Figure 2-2 shows the benchmark locations, and Table 2-1 gives their horizontal coordinates and elevations. Table 2-2 gives the horizontal coordinates and elevations of the starting points and the alignment (degrees) of each profile. In January 2020, 11 new benchmarks (BM02 through BM12) were created at SONGS. Photographs displaying these new benchmarks and the surveyed beach profiles are shown in Appendix B.

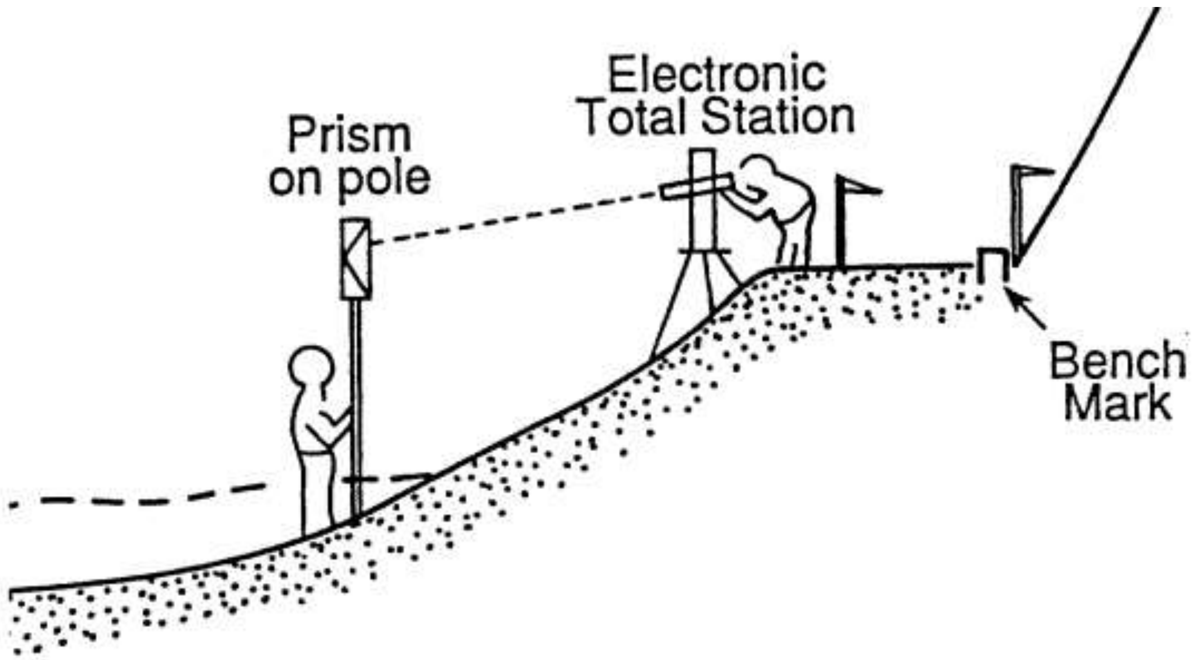

Figure 2-1. Schematic illustration of the beach profile survey method.

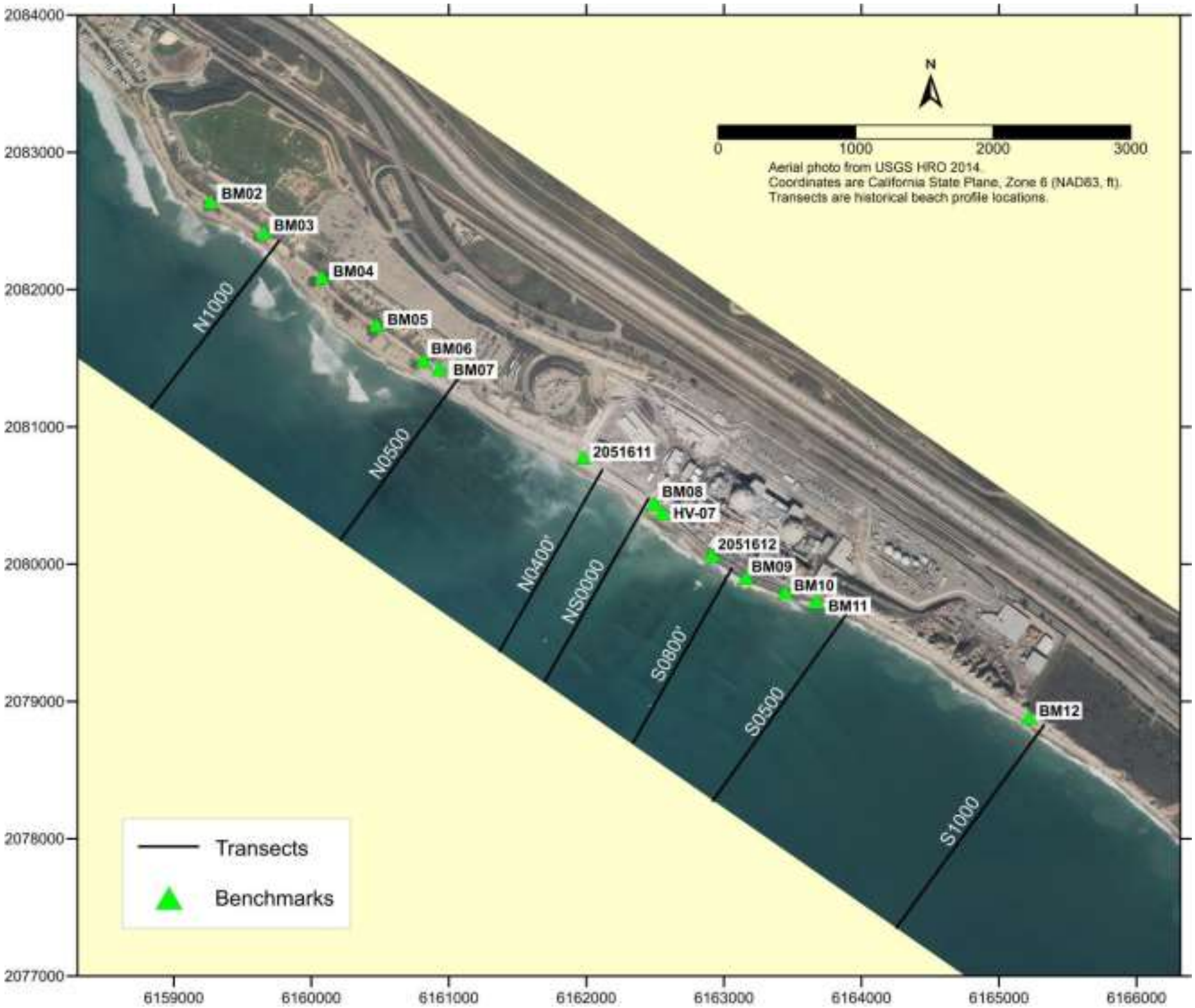

Figure 2-2. Locations of benchmarks at SONGS indicated by green triangular symbols.

Table 2-1. Locations and elevations of benchmarks.

Benchmark	California State Plane Coordinates, Zone 6 (ft), NAD 83		Elevation (ft) NGVD 29
	Easting	Northing	
SO1530	6158825.91[a]	2083254.09[a]	17.69
BM02	6159268.34	2082644.35	13.21
BM03	6159653.531	2082419.132	13.072
BM04	6160076.956	2082089.165	16.383
BM05	6160474.686	2081742.329	12.407
BM06	6160816.546	2081485.969	11.542
BM07	6160931.48	2081424.959	19.522
2051611	6161974.95	2080779.78	16.81
BM08	6162490.544	2080441.441	14.298
HV-07	6162550.71	2080377.00	11.47
2051612	6162911.73	2080065.75	11.23
BM09	6163158.671	2079901.588	14.08
BM10	6163444.986	2079797.431	11.065
BM11	6163671.964	2079729.024	11.226
BM12	6165219.354	2078883.841	14.258

[a] = Horizontal coordinates determined by GPS.

Table 2-2. Beach profile start point coordinates, elevations, and alignments.

Range	California State Plane Coordinates, Zone 6 (ft), NAD 83		Elevation, NGVD (ft)	Magnetic Heading
	Northing	Easting		
N1000	2082359.92	6159761.45	17.69	205
N0500	2081339.99	6161050.00	15.87	203.5
N0400’	2080691.70	6162106.26	14.32	197
NS0000	2080473.91	6162441.66	14.42	197
S0800’	2079969.71	6163054.98	14.33	197
S0500	2079711.68	6163931.78	varies	203
S1000	2078824.56	6165320.87	varies	203.5

3.0 2020 BEACH PROFILE SURVEY RESULTS

Nearshore beach profiles are performed quarterly along seven profiles at San Onofre (N1000, N0500, N0400’, NS0000, S0800’, S0500, and S1000). The 2020 beach profile surveys took place on February 5, May 15, July 17, and October 27, 2020. Figures 3-1 through 3-7 compare the four 2020 nearshore surveys with the October 2019 survey. As described in Section 2, offshore surveys extending to 40 ft water depth are also performed twice each year in spring and fall in order to represent the winter and summer beach profiles respectively. Figures 3-8 through 3-14 display a comparison of the beach profile surveys conducted on May 15 and October 27, 2020.

Similar figures comparing the nearshore surveys for the years 2017, 2018, and 2019 can be found in the report *2017-2019 Beach Profile Surveys at San Onofre* (CE, 2020a). Appendix A compares the summer and winter nearshore surveys for 2017-2020 in order to observe the seasonal fluctuations at SONGS in recent years.

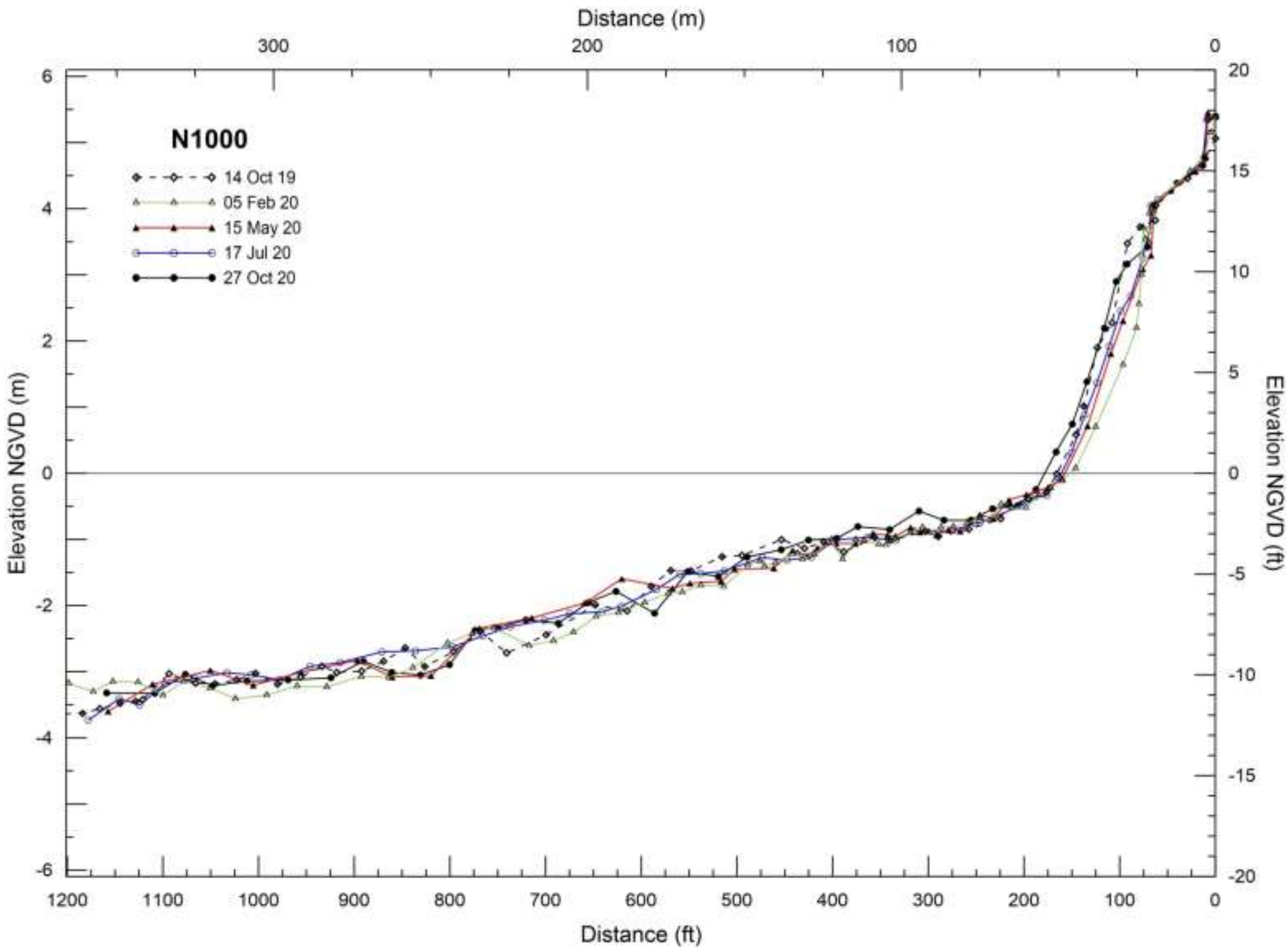

Figure 3-1. 2020 nearshore beach profile surveys of N1000.

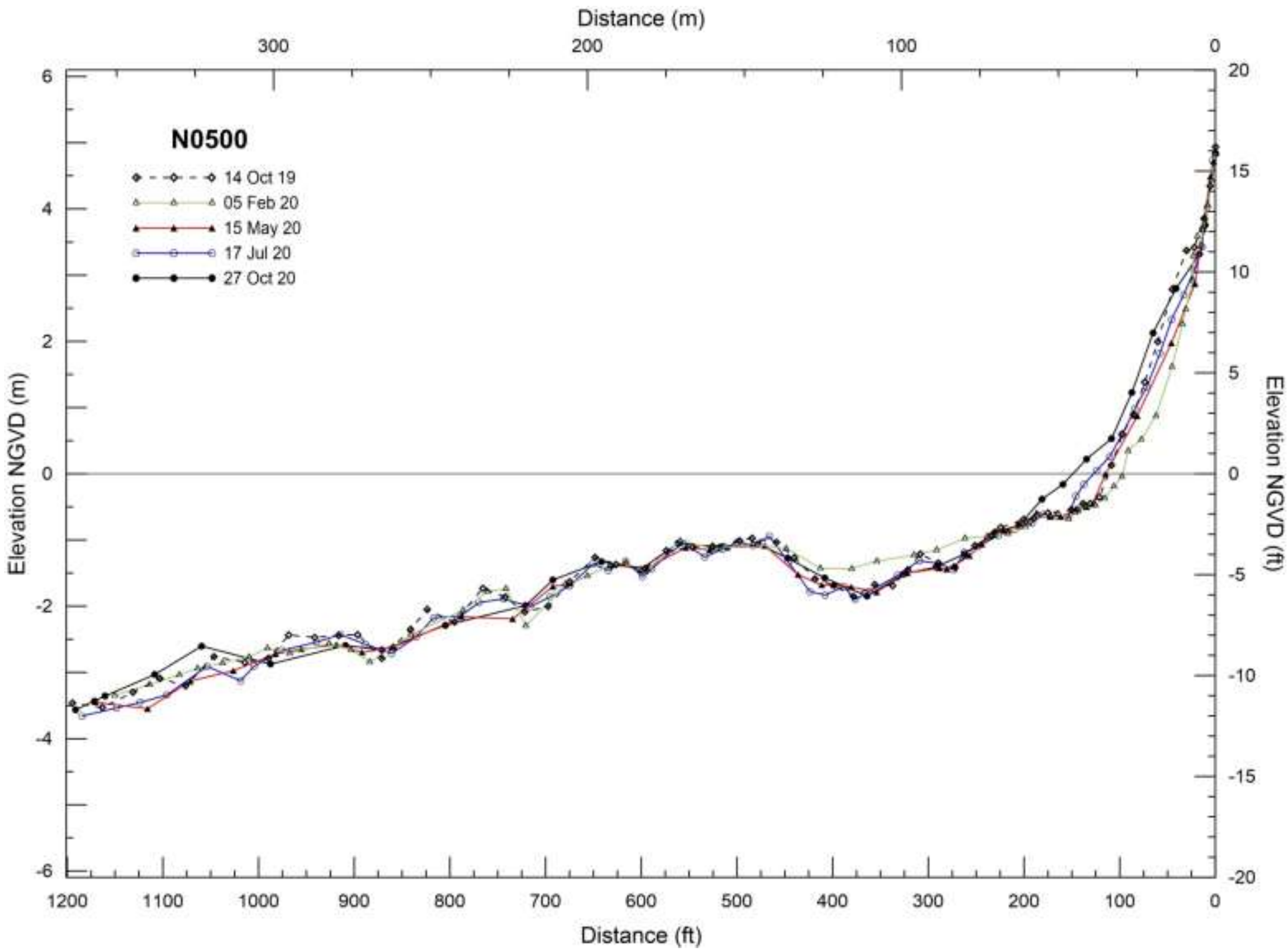

Figure 3-2. 2020 nearshore beach profile surveys of N0500.

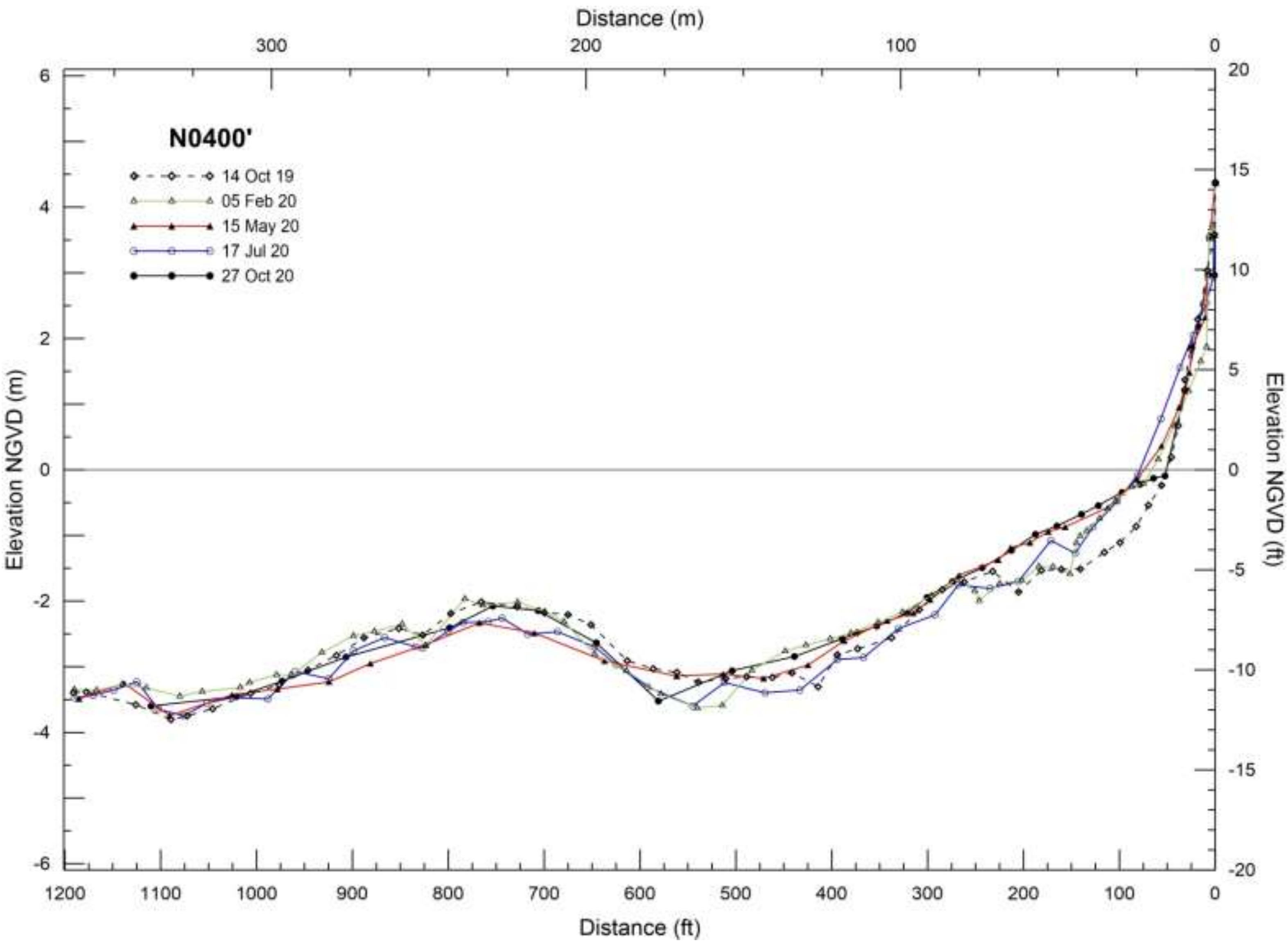

Figure 3-3. 2020 nearshore beach profile surveys of N0400'.

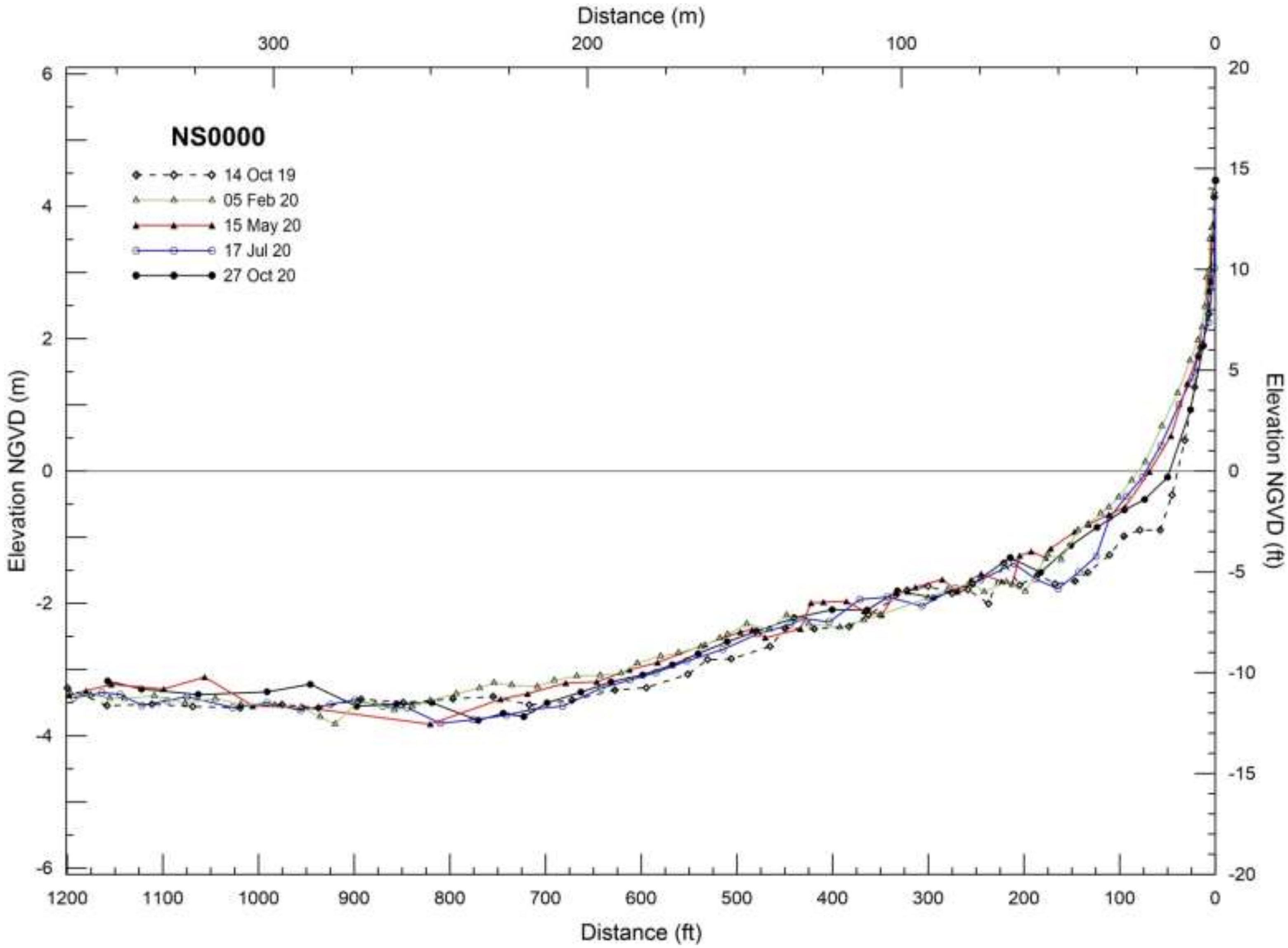

Figure 3-4. 2020 nearshore beach profile surveys of NS0000.

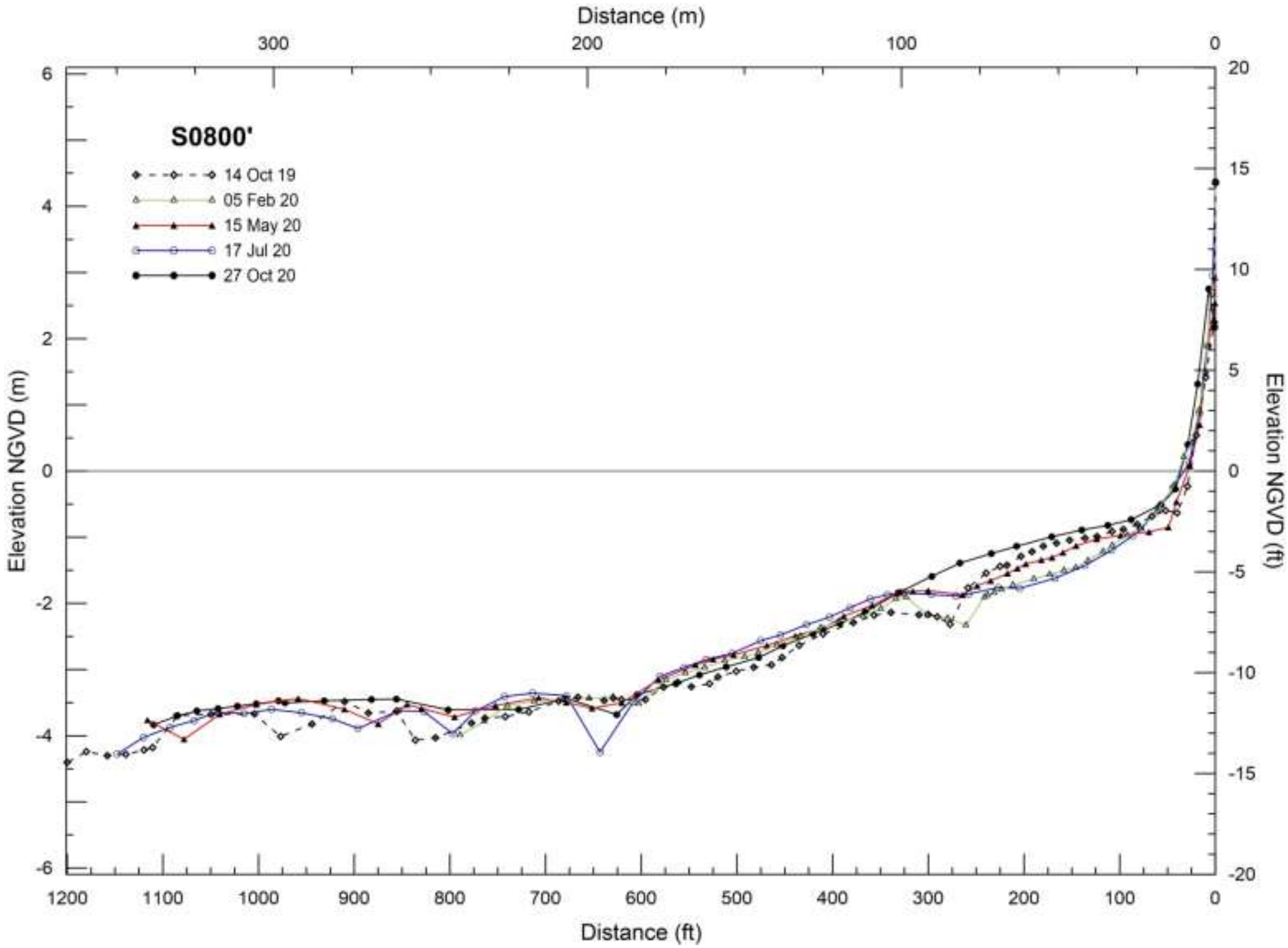

Figure 3-5. 2020 nearshore beach profile surveys of S0800'.

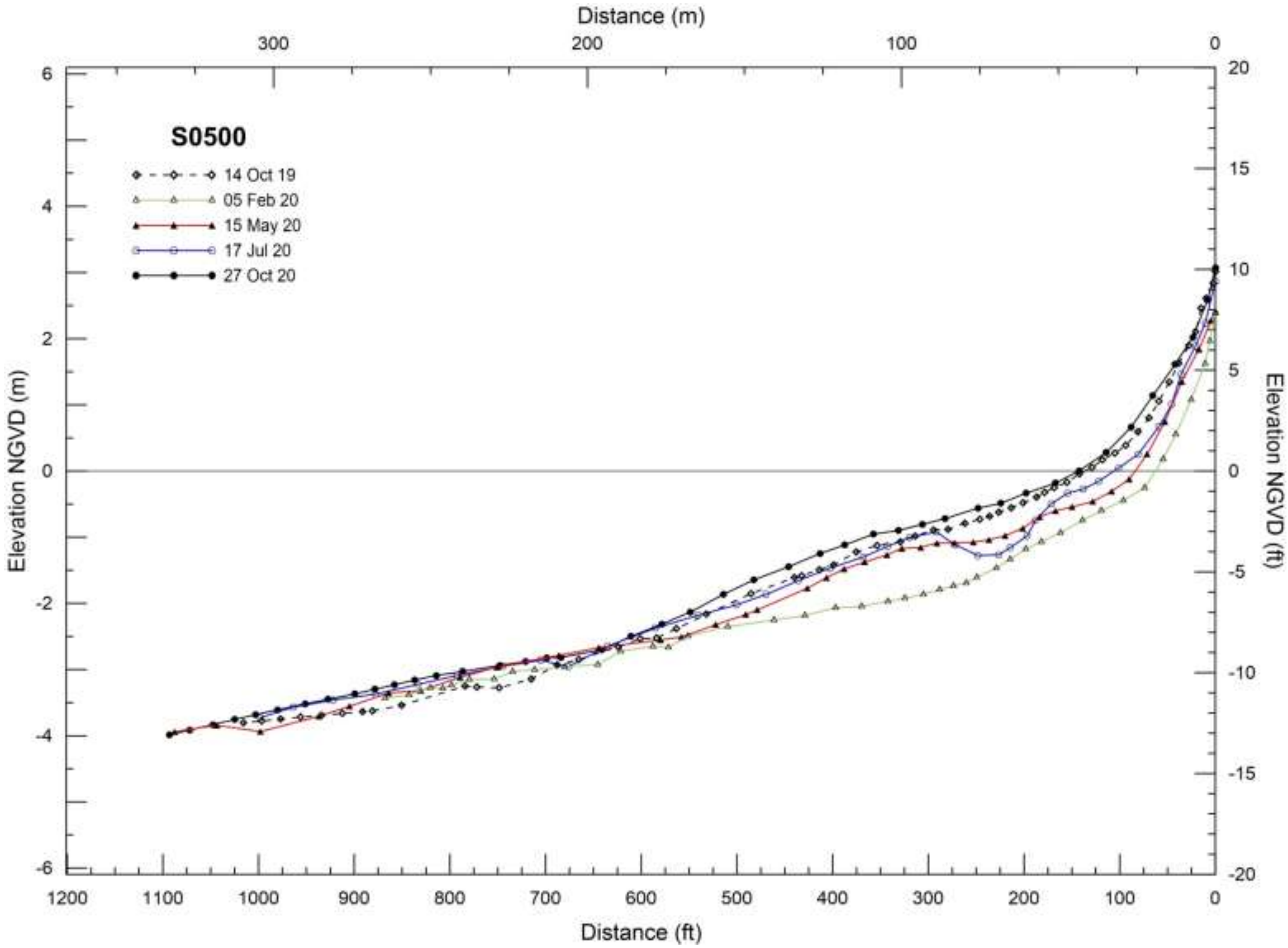

Figure 3-6. 2020 nearshore beach profile surveys of S0500.

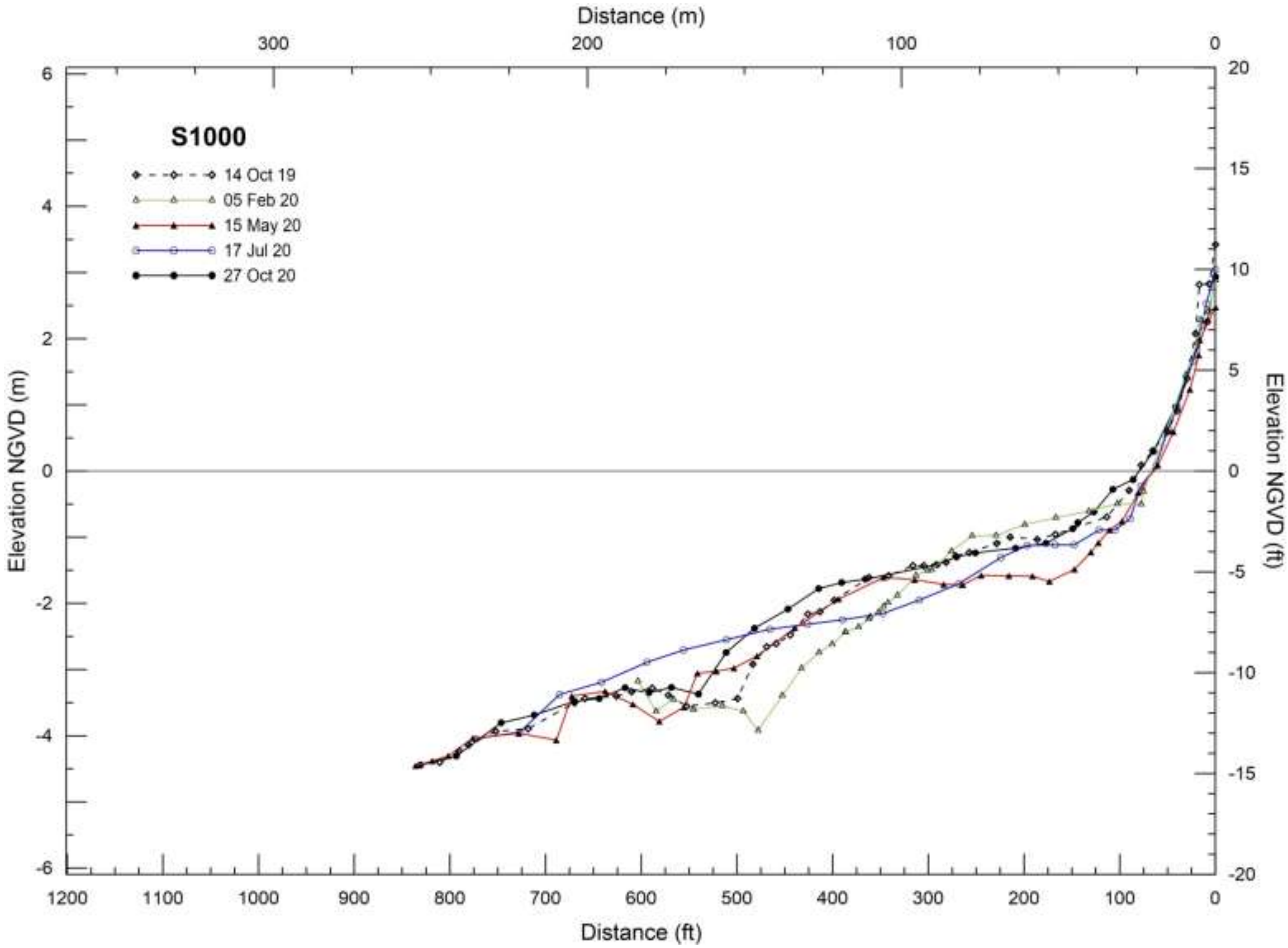

Figure 3-7. 2020 nearshore beach profile surveys of S1000.

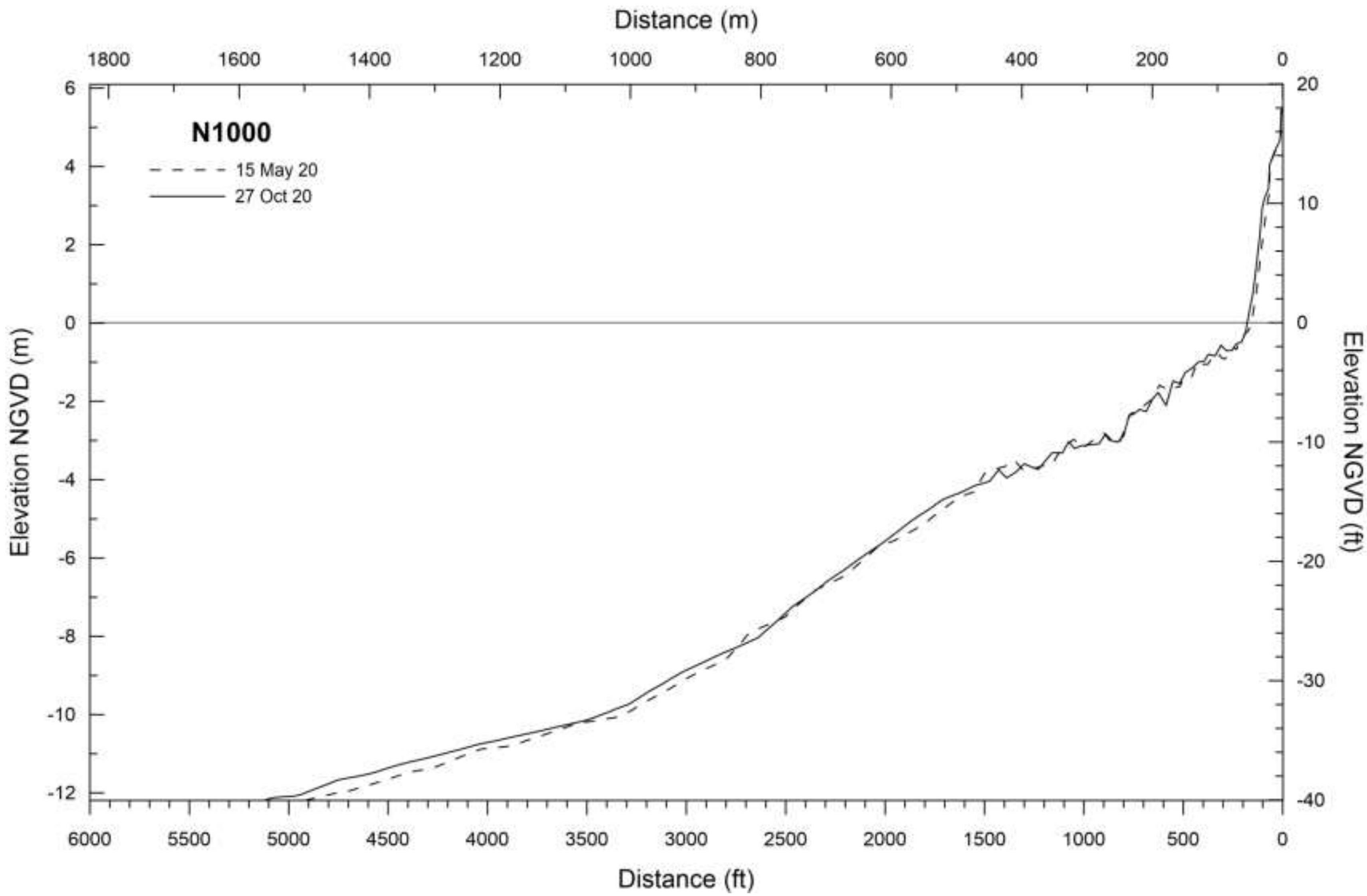

Figure 3-8. 2020 offshore beach profile surveys of N1000.

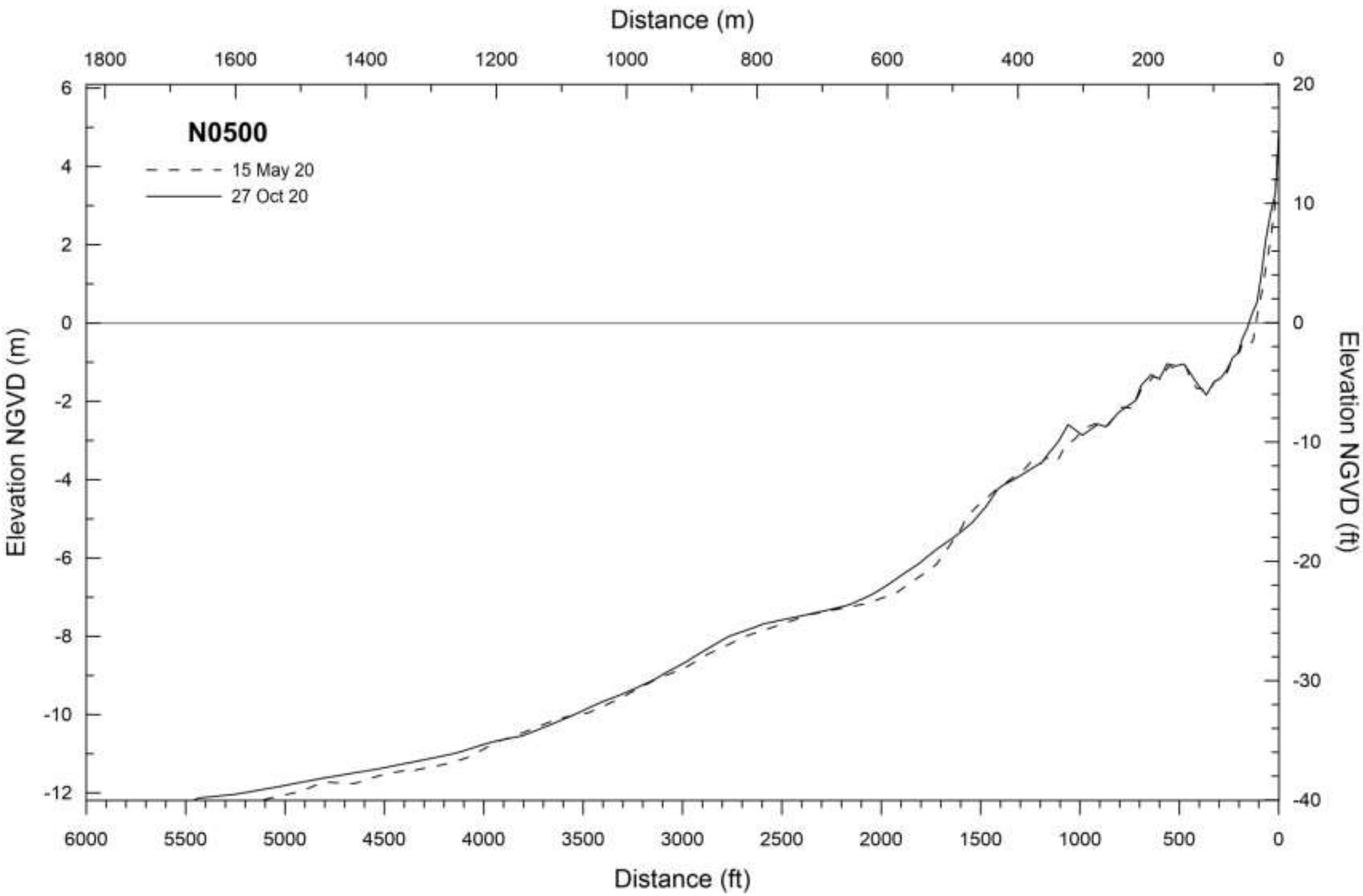

Figure 3-9. 2020 offshore beach profile surveys of N0500.

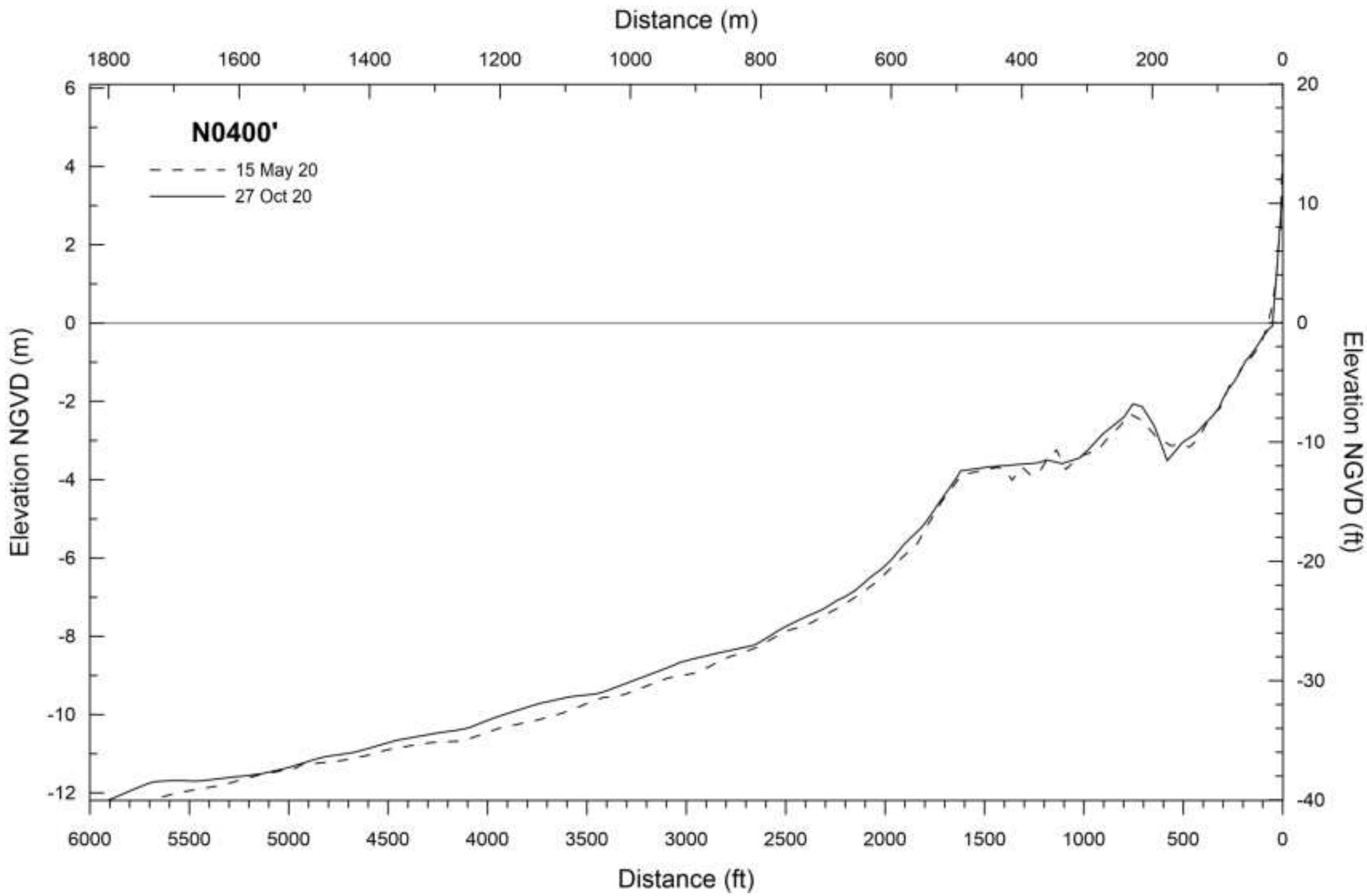

Figure 3-10. 2020 offshore beach profile surveys of N0400'.

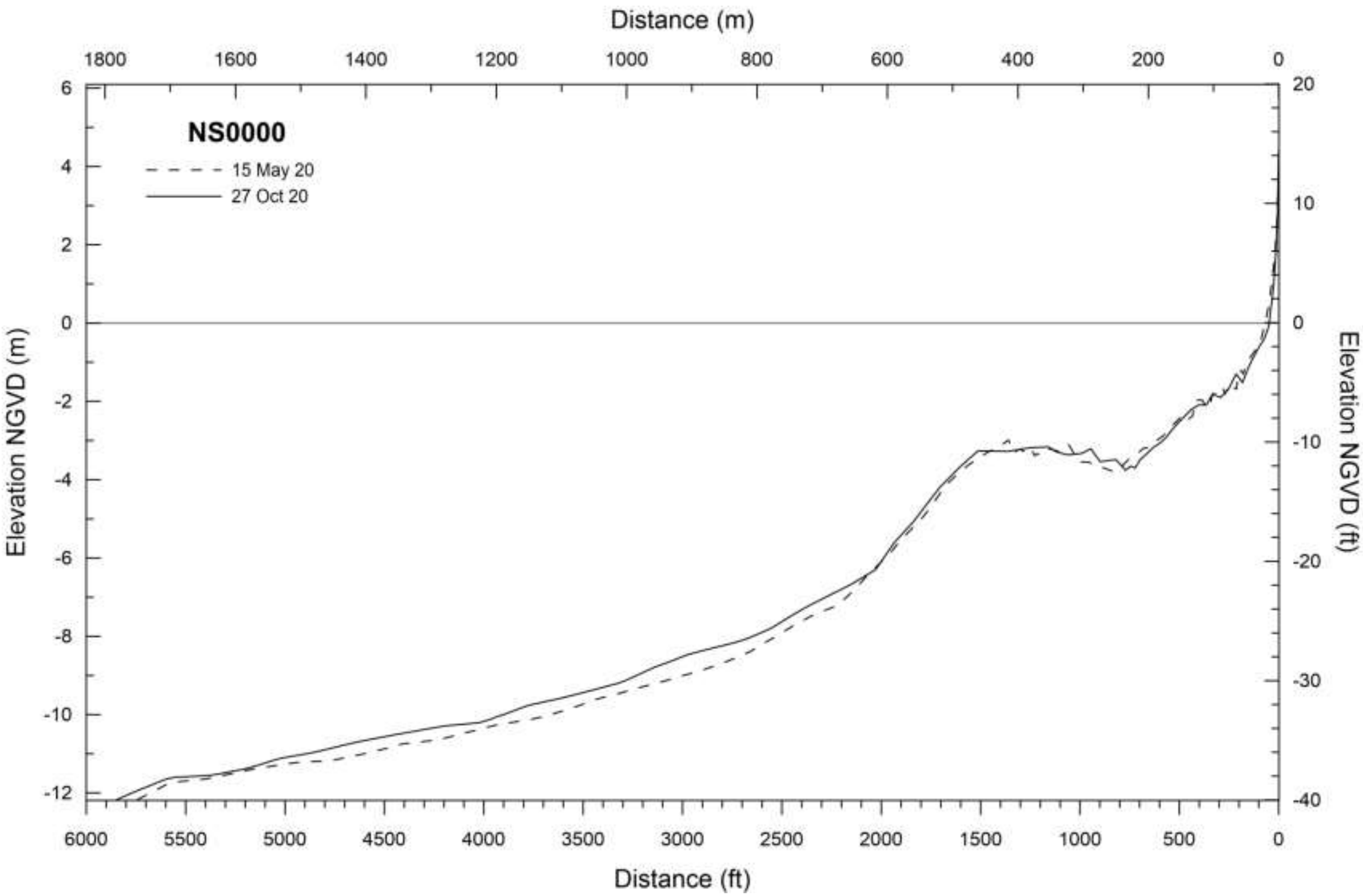

Figure 3-11. 2020 offshore beach profile surveys of NS0000.

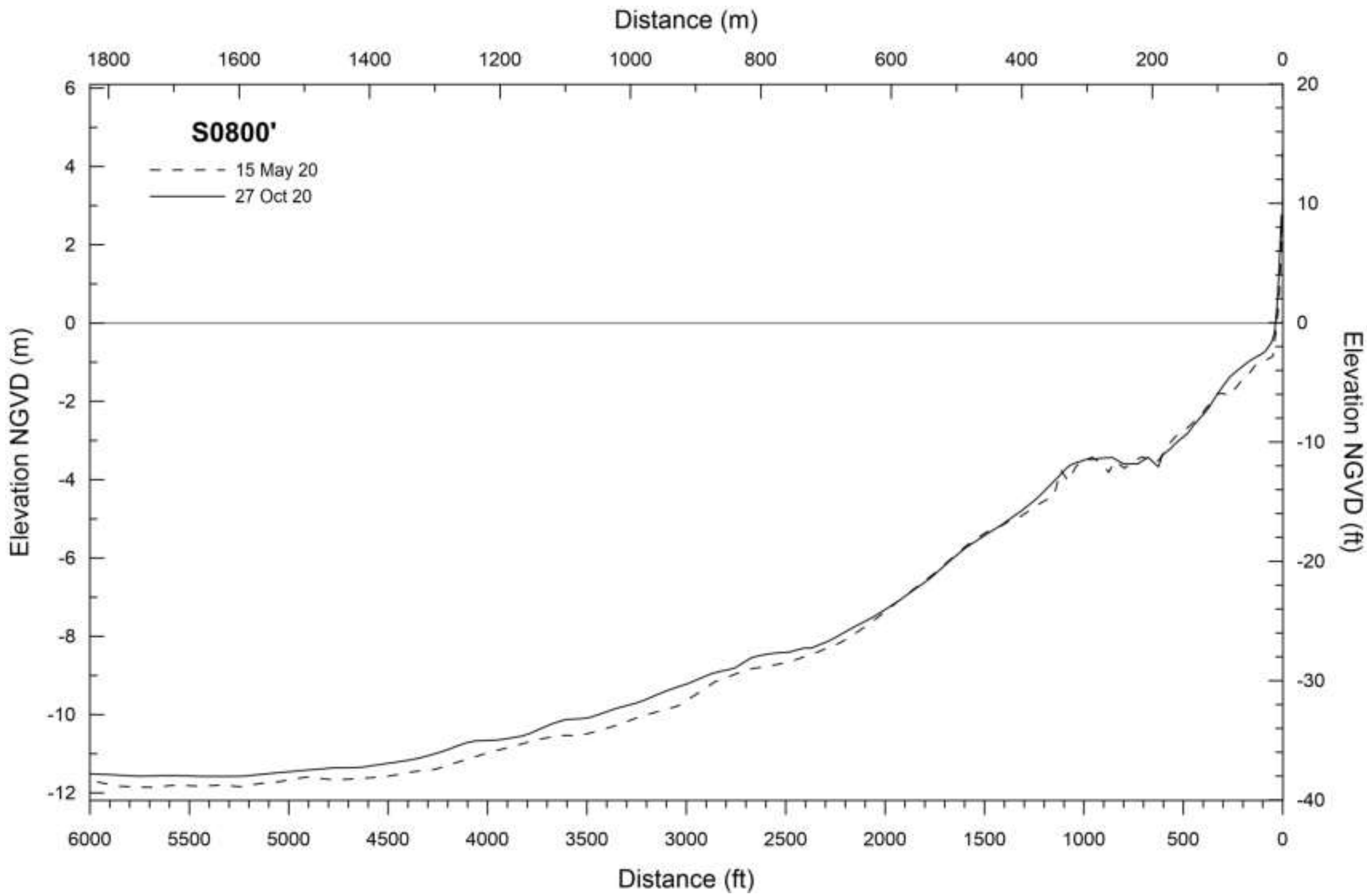

Figure 3-12. 2020 offshore beach profile surveys of S0800'.

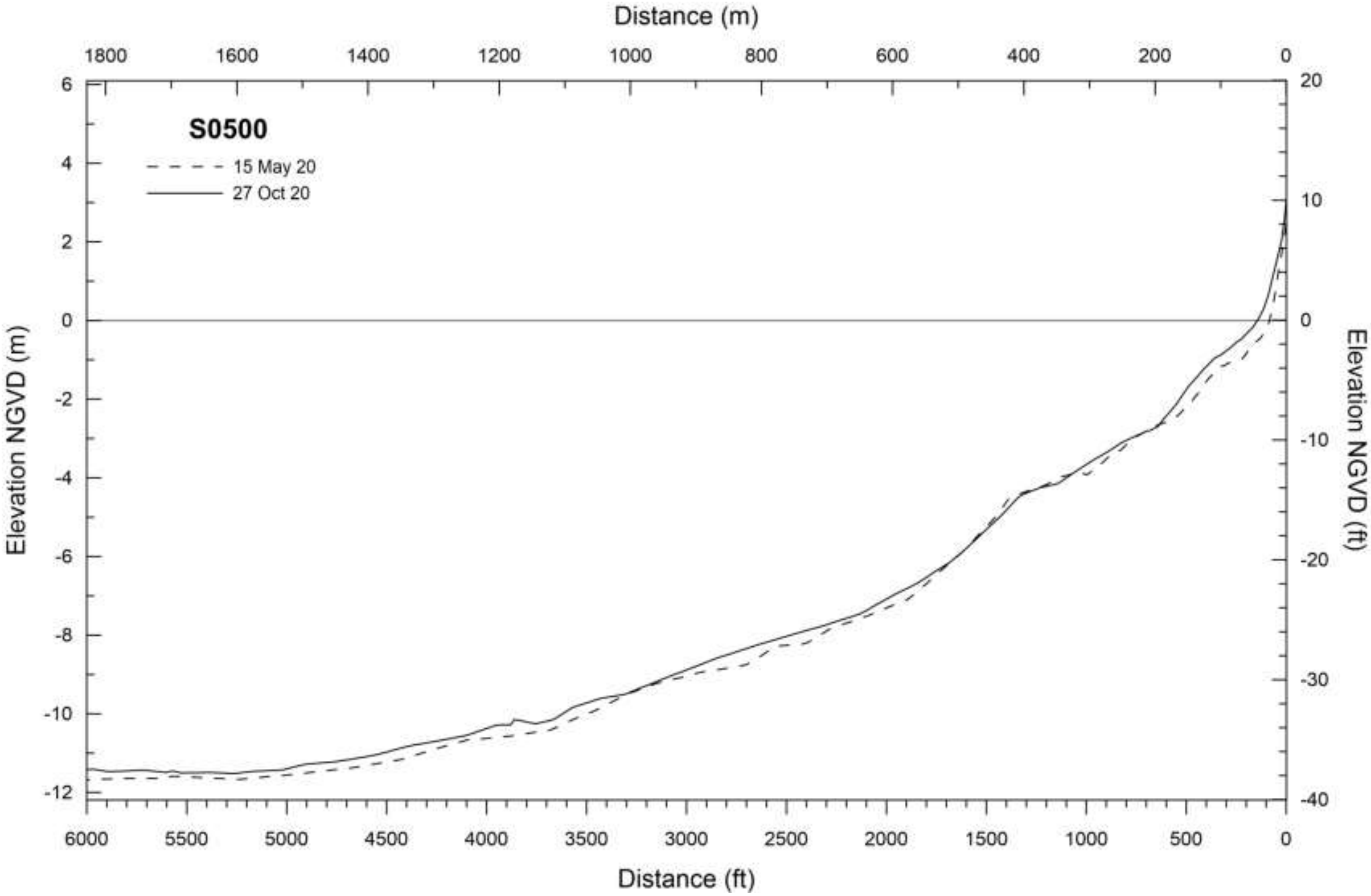

Figure 3-13. 2020 offshore beach profile surveys of S0500.

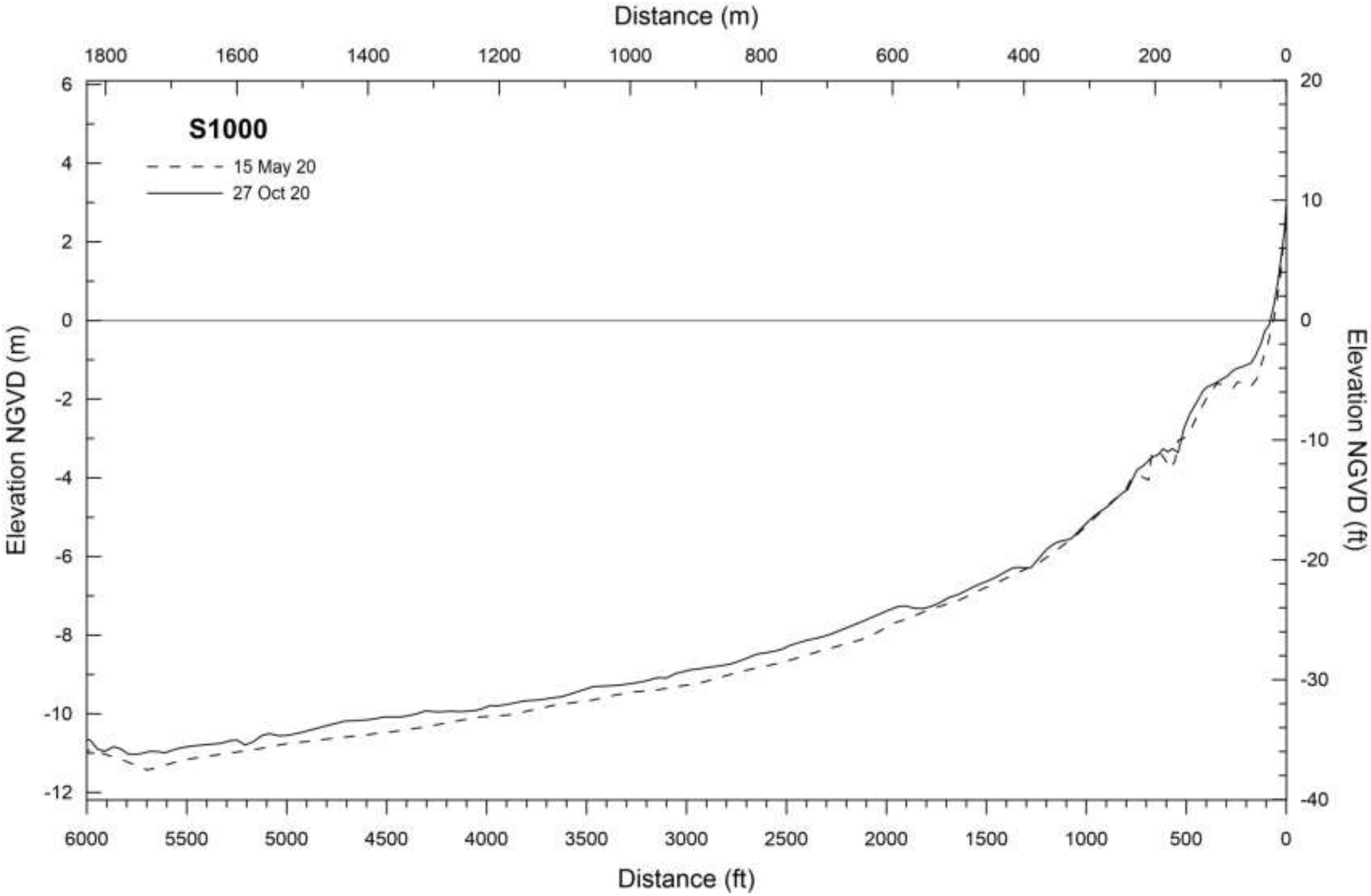

Figure 3-14. 2020 offshore beach profile surveys of S1000.

4.0 BEACH PROFILE CHARACTERISTICS

The beach profiles at San Onofre have much in common with other typical Southern California beaches (Figure 4-1). The characteristics of San Onofre beaches are discussed in detail in *Coastal Analysis for End-State Planning of SONGS, Phase 1* (Elwany et al., 2016). A brief description is given below.

The beaches at San Onofre consist of a relatively thin veneer of medium to coarse sand backed by a sea cliff of varying height. In most places, cobble and bedrock underlay the beach sands at various depths. These depths can vary from zero, where the sand cover is stripped, to several meters where there is an adequate supply of sand to cover the bedrock or the cobble layer.

The subaerial portion of the beach profile extends from the cliff face (or sea wall) to the mean water line. It is distinguished by a narrow to medium width, relatively flat berm, and a moderately steep beach face slope. The berm height and the slope of the beach face both depend on sand grain size and wave climate. The subaerial beach width is defined as the distance from the cliff face (or seawall) to 0 ft NGVD.

The beach berm may contain one or more storm scarps. These are erosional features resulting from large waves that remove sand and cobbles from the beach face and transport them offshore. This represents the normal summer to winter erosion sequence that progressively narrows the berm width and flattens the beach slope. The sand moved offshore often forms into one or more bars, generally in depths less than 10 ft, but seaward of the low tide terrace. The bars act as reservoirs for the sand that is returned to the shore face during the winter to summer accretion phase, coinciding with milder seasonal wave conditions.

The beach berm both in front of, and north and south of SONGS, contain a large amount of cobbles in comparison to many Southern California beaches. These cobble layers are typically covered with sand during the summer and become exposed during winter due to the changing wave climate. The thickness and position of this cobble berm also changes throughout the year and over time (Appendix B pictures).

Berm heights at San Onofre average about 10 ft , and foreshore slopes are about 1:7, vertical to horizontal, or about 8°. Both are fairly uniform longshore. The lack of a winter berm has been common at the sea wall in front of SONGS during the past few years. Lack of sand and occasional high wave activity have resulted in some displacement and settling of the rock riprap, which provides toe protection to the SONGS beach access walkway retaining wall.

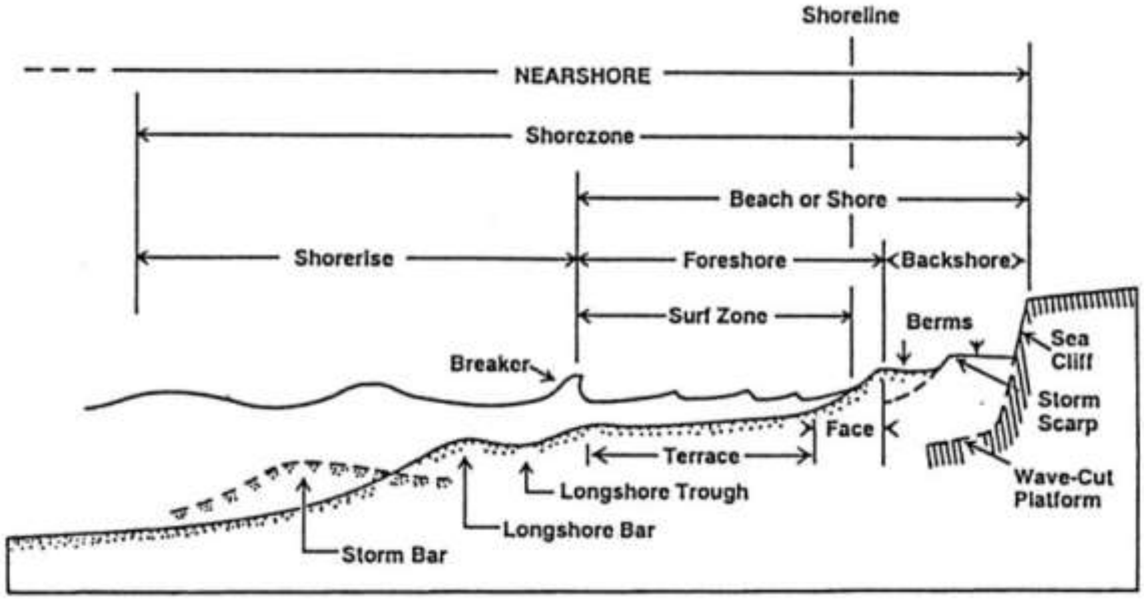

Figure 4-1. Typical Southern California beach profile (Inman, 1980).

5.0 BEACH WIDTH CHANGES FROM 2017 THROUGH 2020

Beach width changes from 2017 through 2020 at seven profiles from N1000 to S1000 are illustrated in Figures 5-1a and 5-1b. The beach width for each survey was computed as the distance from the respective profile's starting point to the intersection of the beach and 0 ft NGVD. Table 5-1 summarizes the beach width observations at each profile for the 16 surveys conducted between March 2017 and October 2020.

Table 5-2 gives the yearly mean beach widths for each profile during this time period. Overall, the northern profiles (N1000 and N0500) consistently display the widest beaches at San Onofre, followed by the profiles south of the power plant (S0500 and S1000). The profiles directly in front of SONGS regularly display the narrowest beaches along all surveyed profiles. The seasonal cycles of these profiles are discussed further in Section 6.

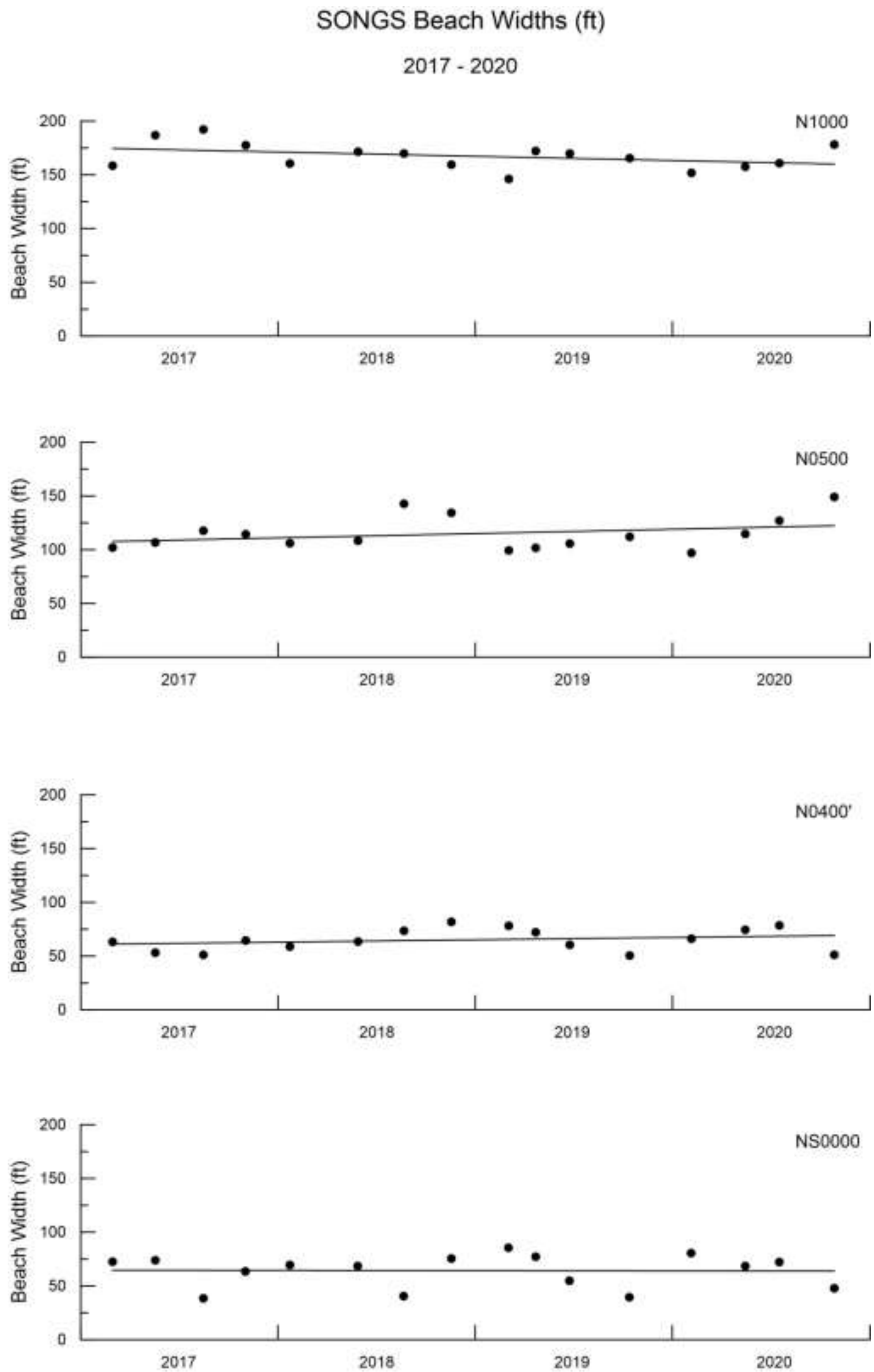

Figure 5-1a. Beach width changes at San Onofre at N1000 – NS0000.

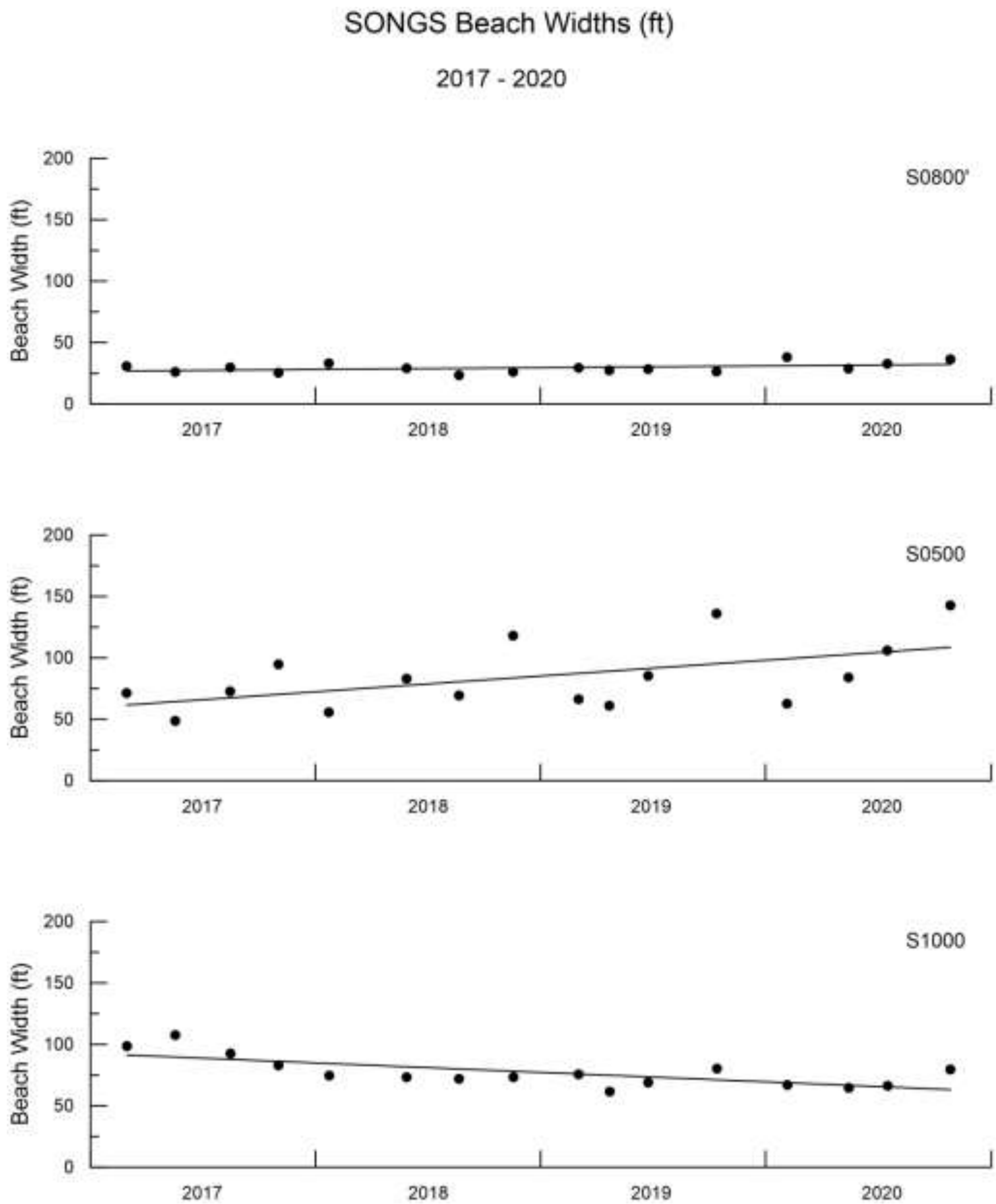

Figure 5-1b. Beach width changes at San Onofre at S0800' – S1000.

Table 5-1. Beach widths (ft) at San Onofre profiles (2017-2020).

Survey Date	Profile						
	N1000	**N0500**	**N0400'**	**NS0000**	**S0800'**	**S0500**	**S1000**
01Mar17	158.6	102.0	63.4	72.4	30.8	71.4	98.6
19May17	187.0	106.5	53.0	74.0	26.1	48.6	107.8
16Aug17	192.1	117.7	51.2	38.4	29.9	72.7	92.7
02Nov17	177.4	114.3	64.4	63.6	25.5	94.6	82.8
23Jan18	160.4	106.1	58.8	69.5	33.0	55.7	74.6
29May18	171.4	108.3	63.5	68.4	29.3	83.1	73.3
22Aug18	169.8	142.6	73.6	40.6	23.4	69.2	72.1
18Nov18	159.3	134.4	82.0	75.5	26.0	118.2	73.4
04Mar19	146.3	99.2	78.1	85.5	29.5	66.3	75.5
23Apr19	172.3	101.8	72.3	77.4	27.5	61.0	61.6
25Jun19	169.9	105.7	60.6	54.9	28.4	85.4	69.0
14Oct19	165.3	112.0	50.4	39.5	26.5	136.2	80.3
05Feb20	151.9	96.9	66.3	80.4	38.2	62.8	67.1
15May20	157.3	114.6	74.4	68.5	28.8	83.9	64.5
17Jul20	160.7	127.2	78.7	72.3	32.9	105.9	66.3
27Oct20	178.4	149.0	51.0	47.8	36.4	142.7	79.7
Max	192.1	149.0	82.0	85.5	38.2	142.7	107.8
Min	146.3	96.9	50.4	38.4	23.4	48.6	61.6
Mean	167.4	114.9	65.1	64.3	29.5	84.9	77.5
Std. Dev	12.4	15.6	10.6	15.3	4.0	28.0	12.8

Table 5-2. Yearly mean beach widths (ft).

Survey Year	Profile						
	N1000	**N0500**	**N0400'**	**NS0000**	**S0800'**	**S0500**	**S1000**
2017	178.8	110.1	58.0	62.1	28.1	71.8	95.5
2018	165.2	122.8	69.5	63.5	27.9	81.5	73.3
2019	163.5	104.7	65.3	64.3	28.0	87.2	71.6
2020	162.1	121.9	67.6	67.3	34.1	98.8	69.4
Mean	167.4	114.9	65.1	64.3	29.5	84.9	77.5

6.0 ESTIMATION OF SHORELINE TRENDS AND SEASONAL CYCLES

The shoreline changes at various profiles consist of two components. The first is the seasonal cycle, which is superimposed on the second component: the long-term trend in the beach width. The long-term trends are due to the processes that affect beach width on longer time scales, such as changing wave climates or sand supply changes.

The beach profile data from March 2017 through October 2020 have been used to separate trends in shoreline changes from the yearly seasonal cycle in order to obtain quantitative estimates for the two parameters. The shoreline data from the 16 surveys were regressed against date, and a straight line was fitted to the entire data set (Figures 5-1a and 5-1b). The slope of this line gives the trend and rate (ft/year) of change of the beach width.

These regression values were then used to determine the seasonal shoreline changes. The expected beach width value obtained via linear regression was subtracted from the measured values for each survey date between March 2017 and October 2020. By removing this slope and "detrending" the measured data, the seasonal shoreline cycle for each SONGS profile was determined (Figures 6-1a and 6-1b). The estimate of yearly beach width changes at San Onofre are presented in Table 6-1. These values were determined by taking the difference between the minimum and maximum beach widths for each year. Profile S0500 displays the greatest seasonal shoreline change, while profile S0800' shows the least change. The average annual fluctuation at San Onofre is about 27.9 ft.

Seasonal trends were also evaluated by examining average beach widths by time of year. Table 6-2 displays the average beach width during winter and summer for each year between 2017 and 2020. The winter values were determined by averaging the beach widths measured between January and May of that year, while the summer values averaged beach widths measured between June and November. Table 6-3 shows the overall mean winter and summer beach widths between the years 2017-2020, with summer beaches being on average wider than the winter beaches at SONGS.

In a typical year, southern Californian beaches are widest in the fall, before high-energy winter storms move sediment offshore. Interestingly, the seasonal cycle at NS0000, and to a lesser extend N0400', seems to be reversed, in that the beaches are narrower toward the end of summer and widen throughout the winter. This pattern is reflected graphically in Figure 6-1 and quantitatively in Tables 6-2 and 6-3.

Table 6-4 gives the estimates of the observed long-term trends in beach width for 2017 through 2020. Statistical tests were carried out on trends and p-values are presented in Table 6-4. The trend is significantly different from zero on those ranges with p-value < 0.05. The maximum observed trend is an accretion rate of 12.8 ft/year along profile S0500. The only other profile with a statistically significant rate of change during this time period is S1000, which displays an erosional trend of -7.7 ft/yr.

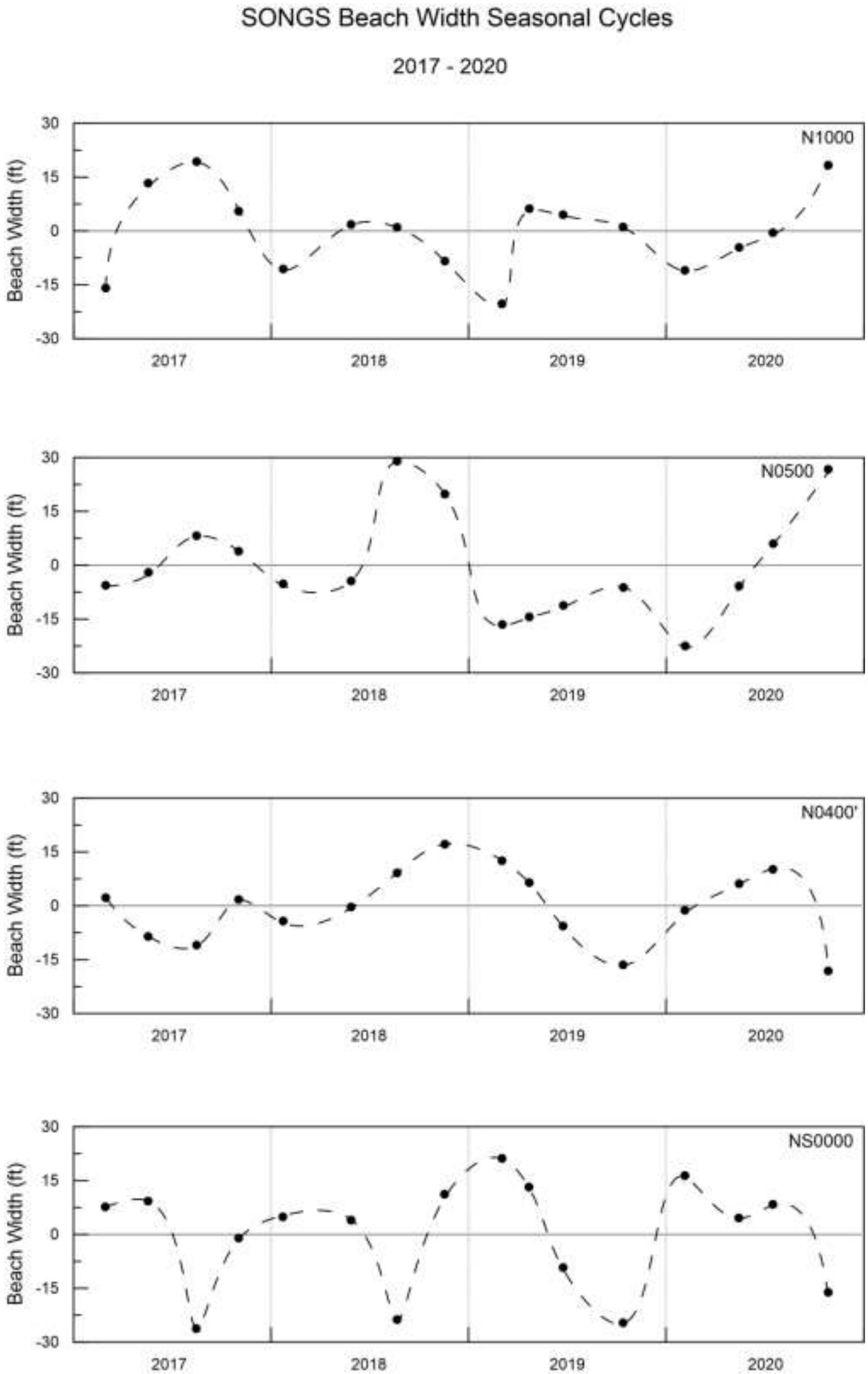

Figure 6-1a. SONGS beach width seasonal cycles at N1000–NS0000 (2017-2020).

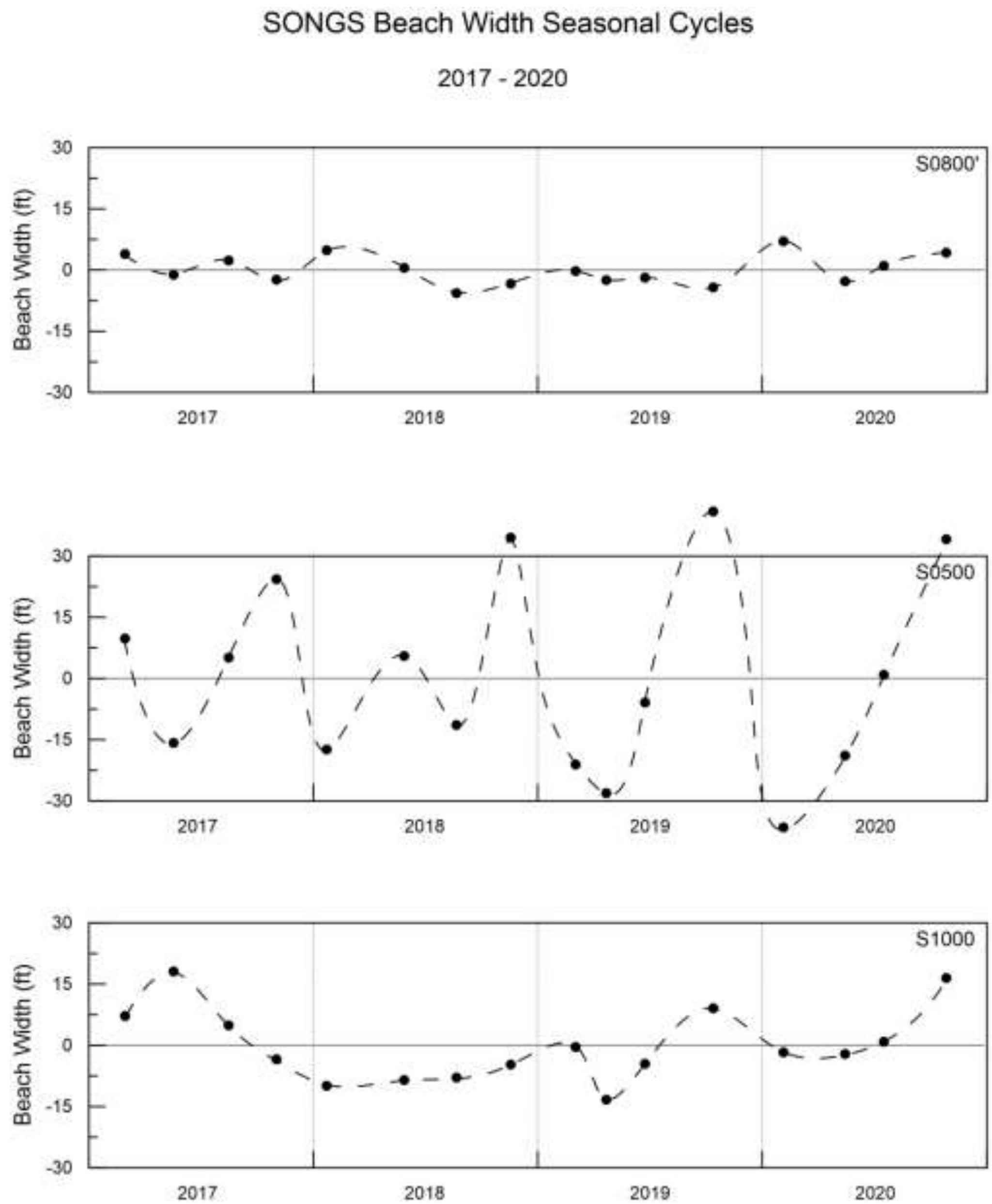

Figure 6-1b. SONGS beach width seasonal cycles at S0800'–S1000 (2017-2020).

Table 6-1. Annual beach width changes at San Onofre.

Profile	Annual Beach Width Change (ft)				Mean
	2017	2018	2019	2020	
N1000	35.30	12.41	26.51	29.33	25.89
N0500	13.88	34.19	10.37	49.18	26.90
N0400’	13.24	21.41	29.06	28.23	22.99
NS0000	35.52	34.93	45.84	32.45	37.18
S0800’	6.27	10.46	3.98	9.76	7.62
S0500	40.20	51.91	68.99	70.61	57.93
S1000	21.46	5.10	22.35	18.68	16.90

Table 6-2. Average beach widths (ft) by season at San Onofre.

Profile	2017		2018		2019		2020	
	Winter[a]	Summer[b]	Winter[a]	Summer[b]	Winter[a]	Summer[b]	Winter[a]	Summer[b]
N1000	172.8	184.7	165.9	164.6	159.3	167.6	154.6	169.5
N0500	104.2	116.0	107.2	138.5	100.5	108.9	105.8	138.1
N0400'	58.2	57.8	61.2	77.8	75.2	55.5	70.3	64.9
NS0000	73.2	51.0	69.0	58.1	81.4	47.2	74.5	60.1
S0800'	28.4	27.7	31.1	24.7	28.5	27.4	33.5	34.7
S0500	60.0	83.6	69.4	93.7	63.7	110.8	73.4	124.3
S1000	103.2	87.8	73.9	72.7	68.6	74.6	65.8	73.0

[a] = averaged beach width values between January and May.
[b] = averaged beach width values between June and November

Table 6-3. Average seasonal beach widths (ft) for March 2017 – October 2020.

Profile	Winter	Summer
N1000	163.1	171.6
N0500	104.4	125.3
N0400'	66.2	64.0
NS0000	74.5	54.1
S0800'	30.4	28.6
S0500	66.6	103.1
S1000	77.9	77.0

Table 6-4. Linear regression analysis of beach width, March 2017 – October 2020.

Profile	Rate of Change (ft/yr)	Intercept (ft)	p-value[a]	Trend
N1000	-3.96	175.2	0.1546	Slight erosion[a]
N0500	4.01	107.0	0.2604	Slight accretion[a]
N0400'	2.18	60.8	0.3682	Slight accretion[a]
NS0000	-0.24	64.8	0.9453	Slight erosion[a]
S0800'	1.46	26.6	0.1015	Slight erosion[a]
S0500	12.84	59.5	0.0331	Accretion[b]
S1000	-7.70	92.6	0.0023	Erosion[b]

[a] = p-values > 0.05 indicate a statistically non-significant trend (i.e., trend is not different from zero).
[b] = p-values < 0.05 indicate a statistically significant trend (i.e., trend is not equal to zero).

7.0 BEACH PROFILES AND WIDTH FROM 1964 THROUGH 2020

The available beach profile data at San Onofre from 1945 through 1998 were used in evaluating the observed changes from 2017 through 2020. There are large gaps in the beach profile data sets where no beach surveys were carried out, but the available information is useful to better understand beach width fluctuations over a long time scale. Beach width is controlled by waves, sediment supply, beach site location and surroundings, and the beach nearshore and offshore bathymetry.

7.1 BEACH PROFILE HISTORY

Figure 7-1 shows the benchmarks used for historical profiles, in comparison to beach width determined from photographs over time. The earliest beach profile data (1945-1949) for the area were collected by Shepard (1950a, b) at four range lines, three of which are shown in Figure 7-1. The benchmarks for these three surveys are noted as “Crescent” (farthest upcoast), “Fence” (about 4,000 ft [1,200 m] upcoast of Unit 1), and “Surf” (about 660 feet [200 m] upcoast of Unit 1). Shepard’s original survey notes are available in the Scripps Institution of Oceanography (SIO) archives, but efforts to reconstruct the profiles were unsuccessful.

The first set of beach profiles associated with Unit 1 construction was taken on May 15, 1964 and represents the San Onofre State Beach area before the influence of any construction activity, which began in June 1964. A second set of profiles was taken on July 13, 1964, which would also have been before construction activity had any effect. Note that Figure 7-1 also shows the location of the Unit 1 laydown pad (the hatched area), which was in existence from 1964 through 1966. The last set of profiles recorded in this phase of beach measurement, taken on October 29-30, 1970, represents the beach well after the disappearance of the pad’s influence.

The next beach profile study began in 1974 as part of the oceanographic monitoring program for the construction of Units 2 and 3. Benchmarks “B1,” “B3,” “B5,” “B6,” and the remote “B7” (the triangles in Figure 7-1) were established at the beginning of construction for Units 2 and 3. The May 3, 1974 set of profiles represents the “pre-construction beach” in this series. The “B1” line, which is nearest the 1964-1971 “A” line, is shown in Figure 7-1. SCE land survey teams performed these profile surveys, which extend to a depth of -2 to -6 ft (-0.6 to -1.8 m) mean lower low water (MLLW). These profile lines were monitored monthly from 1974 through early 1979.

The larger Units 2 and 3 laydown pad (shown in Figure 7-1, to the right [south] of the Unit 1 pad) was in existence from 1974 through early 1985. The beach profiling work started again in 1985 after the laydown pad had been removed and the sand behind it had been released. The first set of these measurements was taken in May 1985, and this phase of the beach measurement program concluded in September 1987, with nine sets of profiles recorded. An additional survey was carried out by Waldorf (1989) in January 1989. Wading depth profiles were measured every 500 m along the beach, from -6,600 ft (-2,000 m) (north) to +9,900 ft (+3,000 m) (south). These survey lines reached to about -1.5 ft (-0.45 m) depth (MLLW) in the surf zone. The benchmarks for these surveys along the bottom of the cliff face are represented in Figure 7-1 as dots along the beach.

The beach profiling work carried out by CE was started in 1991 and continued through February 1994. Additional surveys were performed along the 1985-1989 range lines at 1650-ft (500 m) intervals (Elwany et al., 1992, 1993, 1994). Up to 14 profile lines were surveyed on a quarterly basis. The locations of these ranges are shown in Figure 7-2. Additional beach profile surveys were carried out by CE in 2000 and 2016 on the same ranges.

7.2 BEACH WIDTH DATA

Massive beach widening at San Onofre was associated with the SONGS construction activity that stretched over 20 years from 1964, when Unit 1 was started, to late 1984, when Units 2 and 3 were completed. Over 1 million cubic meters of sand were placed on the beach while constructing the two temporary laydown pads needed for equipment staging and workspace (Flick and Wanetick, 1989). These laydown pads extended about 70 m seaward of the present-day seawall; even this modest width sufficiently interrupted the longshore transport of sand to widen and stabilize the beaches for several kilometers up-coast.

Most pertinent to this study were the data that documented changes at San Onofre State Beach through the time of construction of Units 1, 2, and 3, and the data gathered after the 1985 removal of the Unit 2 and Unit 3 laydown pad. The SONGS beach surveys showed how the local beach responded to the massive input of sand from construction activities (1985-2000), and also provided pre-construction beach conditions. The pre-construction beach width is shown in Figure 7-3.

The post-1985 beach profile data shown in Figure 7-4 documents the return to a narrower state of the beach after completion of construction. Figure 7-5 displays beach width data from 1964-2000, which documents the beach widening due to the placement of the laydown pads and the subsequent beach narrowing back to its natural configuration. A comparison of the 2000 and 2016 beach profiles at NS0000 is shown in Figure 7-6, which further displays the long-term erosional trend seen after construction activities at SONGS.

Figure 7-7 shows the beach widths measured at N1000, N0500, NS0000, S0500, and S1000 during the time periods of 1990-1993 and 2017-2020. The solid line is the mean of beach width for the referenced periods. The dotted lines cover the period where no long-term measurements were carried out. Table 7-1 displays these mean beach widths.

The change in mean beach widths between these two time periods (1990-1993 and 2017-2020) was evaluated with a two-tailed t-test, and the resulting p-values for all transects were less than 0.01 (Table 7-1). This indicates that all profiles displayed a statistically significant erosional trend (p-value < 0.05) between these two time periods. The long-term average erosion rate at San Onofre beach is between 2.3 and 4.3 ft/year.

The beach at San Onofre State Beach, which extends 1 km north and south from SONGS, has retreated considerably and subsequently has caused the cliffs to retreat by about 1.34 ft/year (Hapke & Reed, 2007) due to wave action. Table 7-2 gives the estimated average winter-summer seasonal cycle for the beach width data collected during 1990-1993 (34.5 ft) and 2017-2020 (27.9 ft).

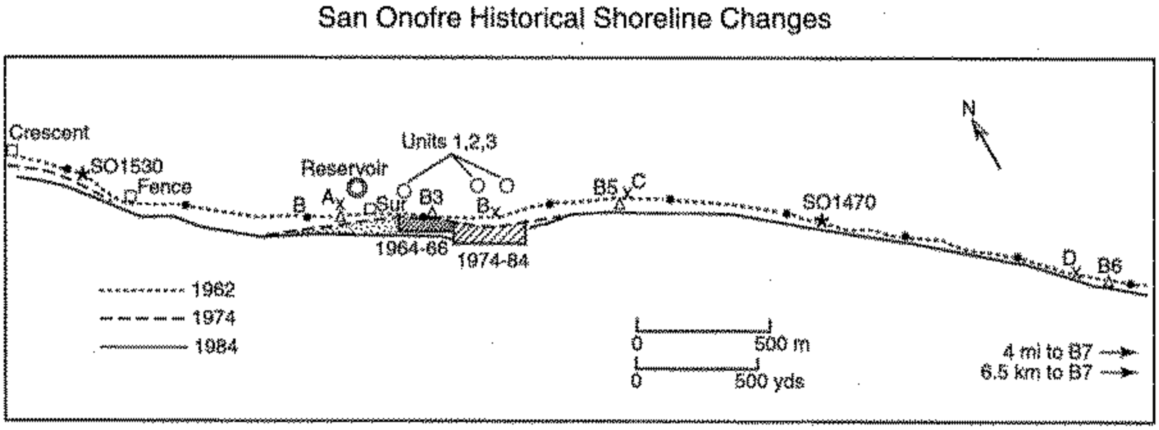

Figure 7-1. **SONGS area historical shoreline changes, laydown pad locations (bracketed hatch marks labeled 1964-66 are for Unit 1; those labeled 1974-84 are for Units 2 and 3), and fillet beach (stippled). The shorelines in this figure are an approximation of MHHW traced from photographs for 1962, 1974, 1984. The fillet beach is a salient, perimeter beach. Benchmark designations for early profiles: Crescent, Fence, and Surf, 1940s; A-D, 1984-86; B1-B7, 1974-85. Flick et al. (2010).**

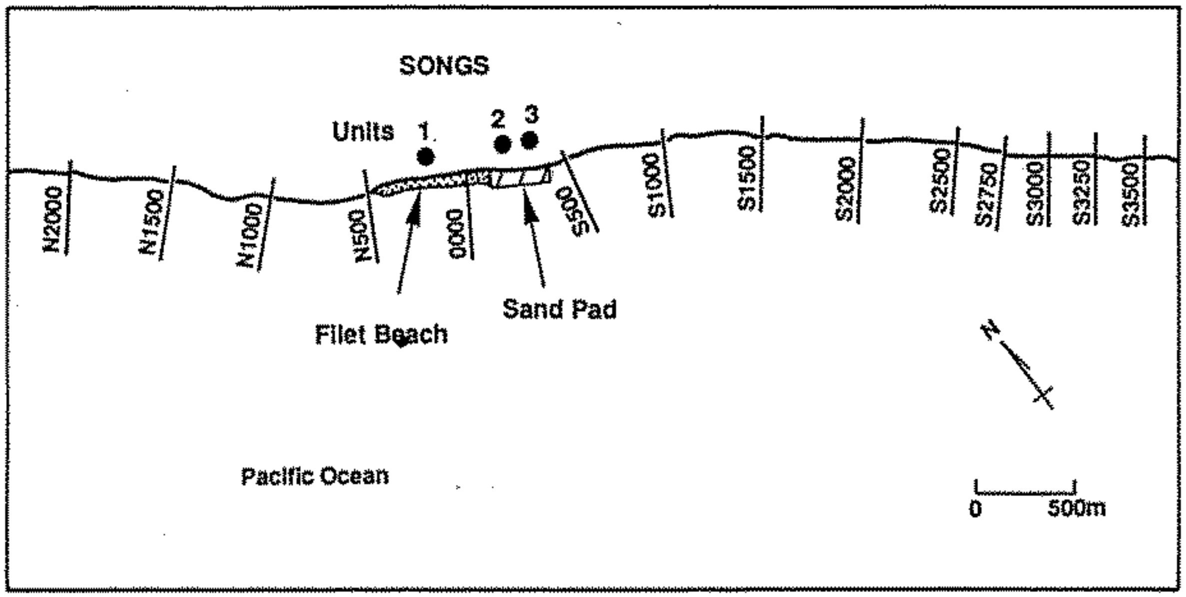

Figure 7-2. Beach profile range lines at San Onofre, 1990-1993.

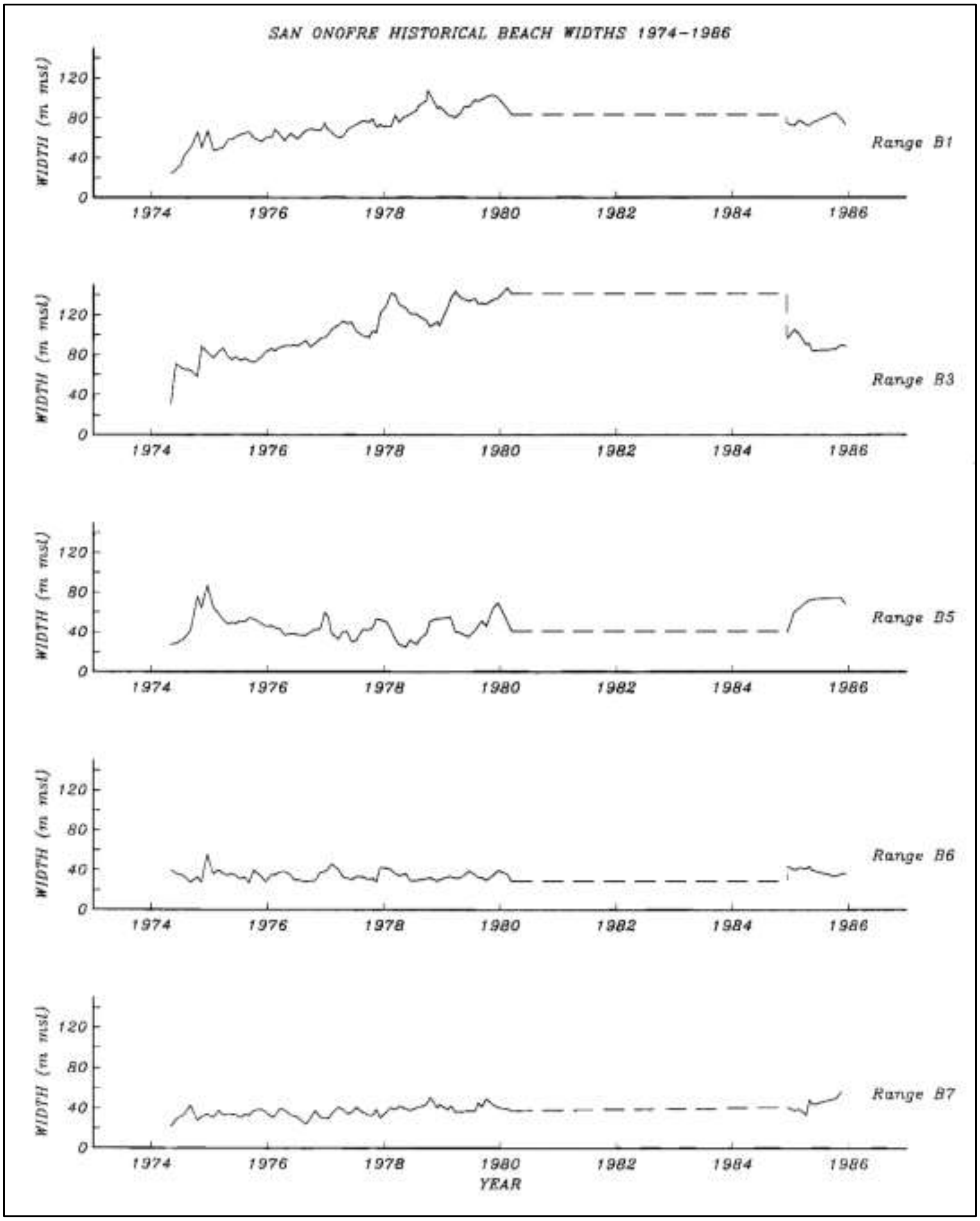

Figure 7-3. Beach-width time histories around the time of Units 2 and 3 construction. Broken lines show time of missing data.

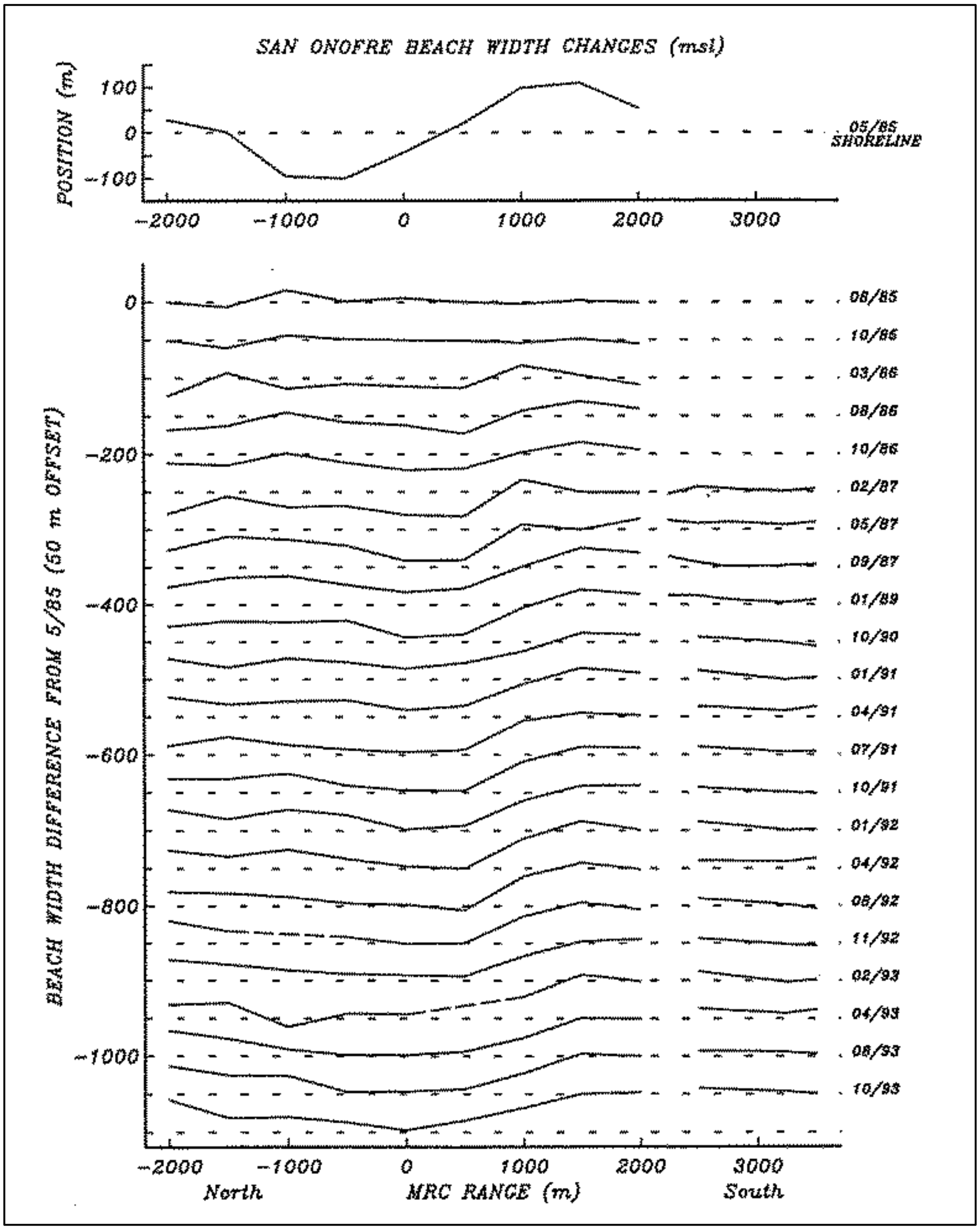

Figure 7-4. Time history of beach-width changes at San Onofre after removal of Units 2 and 3 laydown pad. Changes for dates (month/year) at right relative to May 1985 survey (top panel). Numbers on left axis are dummy values to position lines vertically; each line is plotted relative to the dotted line, which represents the May 1985 survey.

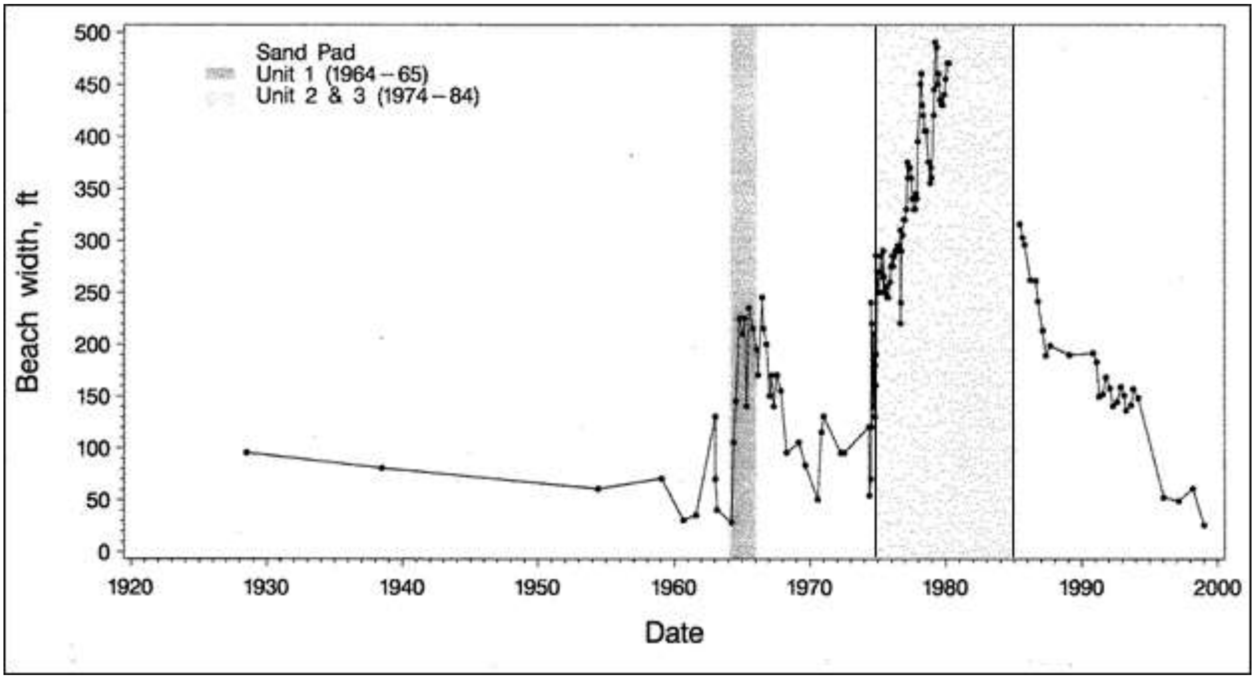

Figure 7-5. Historical beach width adjacent to Unit 1, 1928-2000. Shaded columns show periods when laydown pads were present.

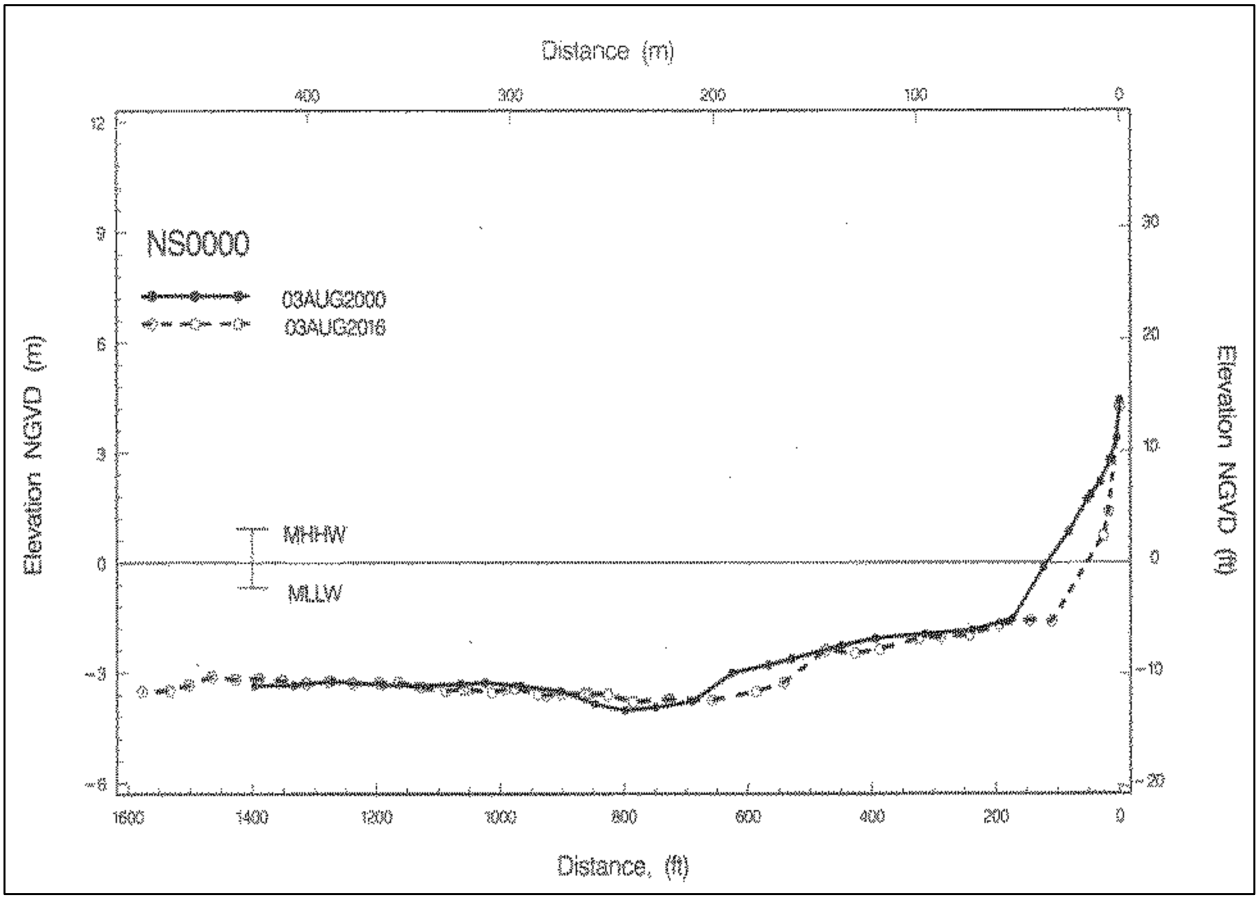

Figure 7-6. Beach profiles at NS0000, years 2000 and 2016.

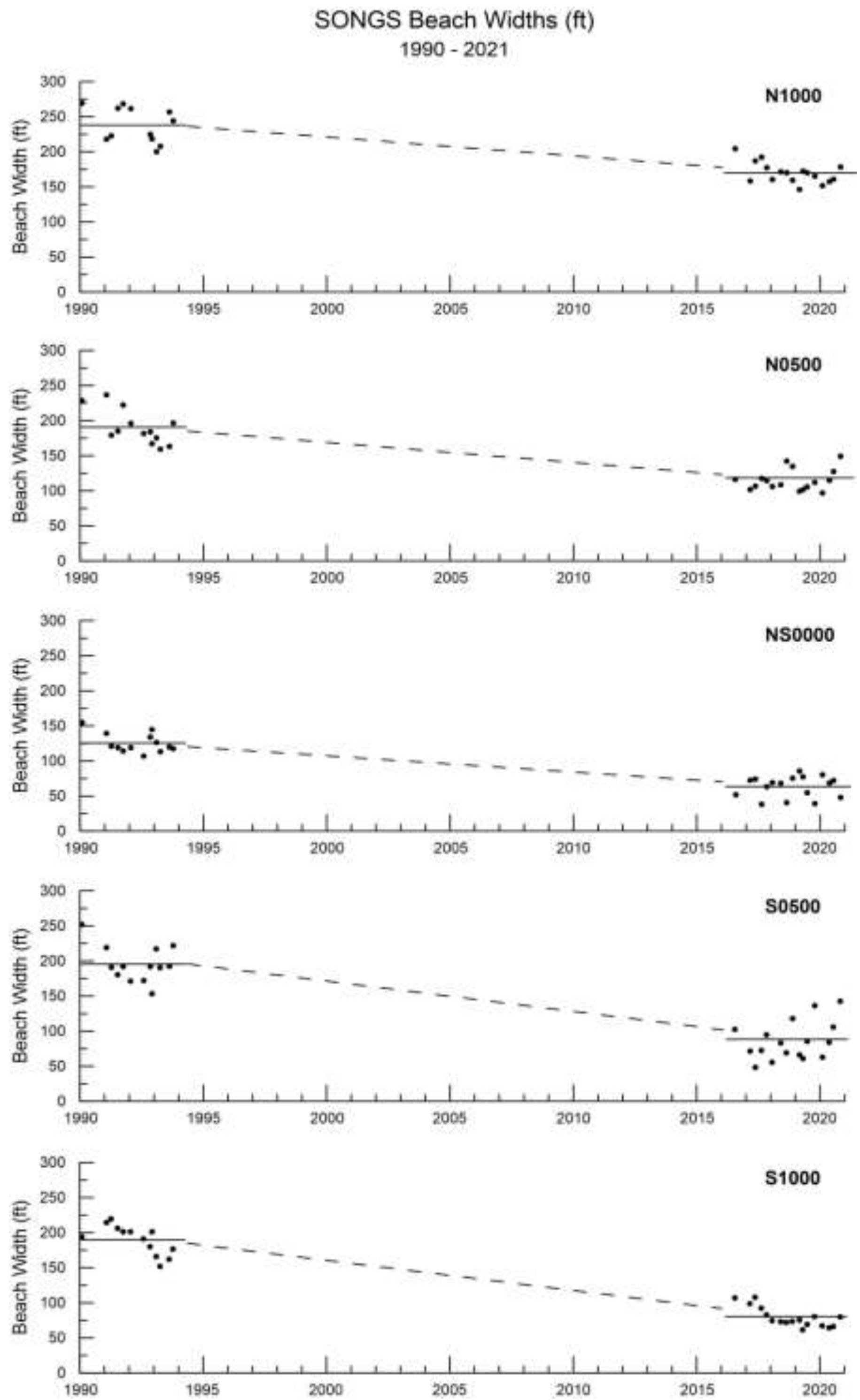

Figure 7-7. Beach width measured between 1990 through 1993 and between 2016 through 2020. Solid lines are the mean of beach width for the referenced periods and dotted lines cover the period where no long-term measurements were carried out.

Table 7-1. Mean beach widths (ft) at San Onofre, 1990-1993 vs 2017-2020

Profile	1990-1993		2017-2020		Difference in mean	p-value
	Mean	Std. Dev	Mean	Std. Dev		
N1000	237.9	25.1	167.4	12.4	70.5	2.09E-07
N0500	190.4	25.0	114.9	15.6	75.5	1.19E-08
NS0000	125.4	13.9	64.3	15.3	61.1	1.02E-11
S0500	195.8	26.0	84.9	28.0	110.9	2.64E-11
S1000	189.8	20.9	77.5	12.8	112.3	6.05E-13

Table 7-2. Estimates of seasonal beach widths changes at San Onofre (ft).

Survey Period	Profiles					
	N1000	N0500	NS0000	S0500	S1000	Mean
1990-1993	51.6	38.8	23.9	36.2	30.2	34.5
2017-2020	25.9	26.9	37.2	57.9	16.9	27.9

8.0 CONCLUSIONS AND RECOMMENDATIONS

Construction activities at SONGS over the 20-year period from 1965 to 1984 resulted in substantial increases in beach width adjacent to and north of the plant. These increases were primarily a result of the large quantities of excavated sand being placed on the beach and the Unit 1 and Units 2 and 3 laydown pad structures that served to retain the fill. Since the removal of the Units 2 and 3 laydown pad in 1985, the beaches adjacent to and north of SONGS have experienced dramatic narrowing and returned to their pre-construction configuration (Figures 7-4 and 7-5).

Generally, San Onofre Beach retreats moderately by a rate of about 2-4 ft/year. In the period between 1993 and 2020, this is due to limited sand supply from the surrounding creeks and rivers. Since the end of the last wet period in 1998, sediment flows from the surrounding waterways have been considerably reduced.

In the long term, the heavily used beach access and parking at San Onofre State Beach just north of SONGS is likely to suffer sustained erosion as this area continues to return to its more natural, pre-construction beach width. Because of the heavy use and intense public interest in this area, continued monitoring should take place. The information gathered will be very valuable to guide any future decisions concerning management options.

The amplitude of the seasonal cycles in beach width is distinguishable from the net advance or retreat. The average annual cycle varied from 28 to 35 ft (Section 7).

The changes of the beach width and profile are controlled by the waves, sand supply, topography of the site (presence of headland and coastal protection structures), and nearshore and offshore bathymetry. In Southern California, the presence of the offshore islands, the complex bathymetry offshore, and the presence of cobbles and/or bedrocks in the nearshore can cause a single, straight beach to experience various beach width changes along different stretches of the same beach. Monitoring the beaches continues to be a good tool to understand and manage these changes.

The beach profile surveys and photography programs sponsored by SCE since 1964 have provided valuable information and understanding of the response at San Onofre to beach filling and the construction of stabilizing structures. This insight will be valuable as sea level rise accelerates in the future.

9.0 REFERENCES

CDIP, 1992. *Coastal Data Information Program, Multi-Year Report: Vol. I, 1975-1991*. Scripps Institution of Oceanography, SIO Ref. No. 91-32. 295 pp. and 2 appendices.

Coastal Environments, 2000. *SONGS Unit 1 Deconstruction Marine Impacts Study, Phase I.* Unpublished report submitted to Southern California Edison Company, 24 January 2000, CE Ref. No. 2000-03, 44 pp. plus 2 appendices.

Coastal Environments, 2017. San Onofre Nuclear Generating Station, November 2-3, 2017 Beach Profiles, San Onofre, California, Data Report. Submitted to Southern California Edison, 7 November 2017. CE Ref. No. 17-22, 7 pp. + 2 appendices

Coastal Environments, 2018. San Onofre Nuclear Generating Station, November 18-21, 2018 Beach Profiles, San Onofre, California, Data Report. Submitted to Southern California Edison, 27 November 2018, CE Ref. No. 18-16, 7 pp. + 2 appendices.

Coastal Environments, 2019. San Onofre Nuclear Generating Station, October 14, 2019 Beach Profiles, San Onofre, California, Data Report. Submitted to Southern California Edison, 30 October 2019, CE Ref. No. 19-33, 7 pp. + 2 appendices.

Coastal Environments, 2020a. San Onofre Nuclear Generating Station (SONGS) Unites 2 & 3 Decommissioning Project, 2017-2019 Beach Profile Surveys at San Onofre. Submitted to Southern California Edison, 17 February 2020, CE Ref. No. 20-03, 41 pp. + 6 appendices.

Coastal Environments, 2020b. San Onofre Nuclear Generating Station, October 27, 2020 Beach Profiles, San Onofre, California, Data Report. Submitted to Southern California Edison, 09 November 2020, CE Ref. No. 20-30, 7 pp. + 2 appendices.

Crosby, S.C., B. D. Cornuelle, W.C. O'Reilly, and R. T. Guza , 2017. Assimilating global wave model predictions and deep-water wave observations in nearshore swell predictions, *Jour. Atmos. and Oceanic Tech*., 34(8), 1823-1836.

Elwany, M. H. S., and R. E Flick, 1992. *1991 Beach Profile Survey at San Onofre*. Unpub. Report, Southern California Edison Co., CE Ref. No. 92-1. 24 pp. and 1 appendix.

Elwany, H., R. Flick, W. Waldorf, and J. Wanetick, 1993. *1992 Beach Profile Survey at San Onofre*. Report submitted to Southern California Edison Co., 20 April 1993, CE Ref. No. 93-7. 26 pp. and appendices.

Elwany, H., R. Flick, and Samia Aijaz, 1994. *1993 Beach Profile Survey at San Onofre*. Final Report submitted to Southern California Edison Co., 1 July 1994, CE Ref. No. 94-7. 32 pp. and 2 appendices.

Elwany, H., R.E. Flick, and A.D. Young, 2016. *Coastal Analysis for End-State Planning of San Onofre Nuclear Generating Station*, *Phase 1.* Report prepared for Southern California Edison by Coastal Environments, La Jolla, CA, CE Reference No. 16-26, 151 pp.

Flick, R.E., and J.R. Wanetick, 1989. *San Onofre Beach Study*. Unpublished report submitted to Southern California Edison Co., Rosemead, CA, October 1989, SIO Ref. No 89-20. 26 pp. and 25 figures.

Flick, R., J.R. Wanetick, M.H. Elwany, R.S. Grove, and B.W. Waldorf, 2010. Beach changes from construction of San Onofre Nuclear Generating Station, 1964-1989. Shore & Beach, 78(4): 12-25.

Hapke, C.J. and D. Reid, 2007. *National Assessment of Shoreline Change, Part 4: Historical Coastal Cliff Retreat along the California Coast.* USGS Report 2007-1133.

Inman, D.L., 1980. Man's Impact on the California Coast Zone. Report submitted to State of California, The resources Agency, Department of Boating & Waterways, p. 18.

Pawka, S.S., 1982. *Wave directional characteristics on a partially sheltered coast*. Ph.D. dissertation, University of California, San Diego, 246 pp.

U.S. Army Corps of Engineers, 1986. *Southern California Coastal Processes Data Summary*. CCSTWS 86-1, Corps of Engineers, Los Angeles District, Los Angeles, CA. 572 pp.

Waldorf, B.W., 1989. *Beach Profiles in the Vicinity of the San Onofre Nuclear Generating Station*. Unpublished data report submitted to Southern California Edison Company. 5 pp. and appendices.

APPENDIX A

NEARSHORE SUMMER AND WINTER BEACH PROFILES FOR 2017-2020

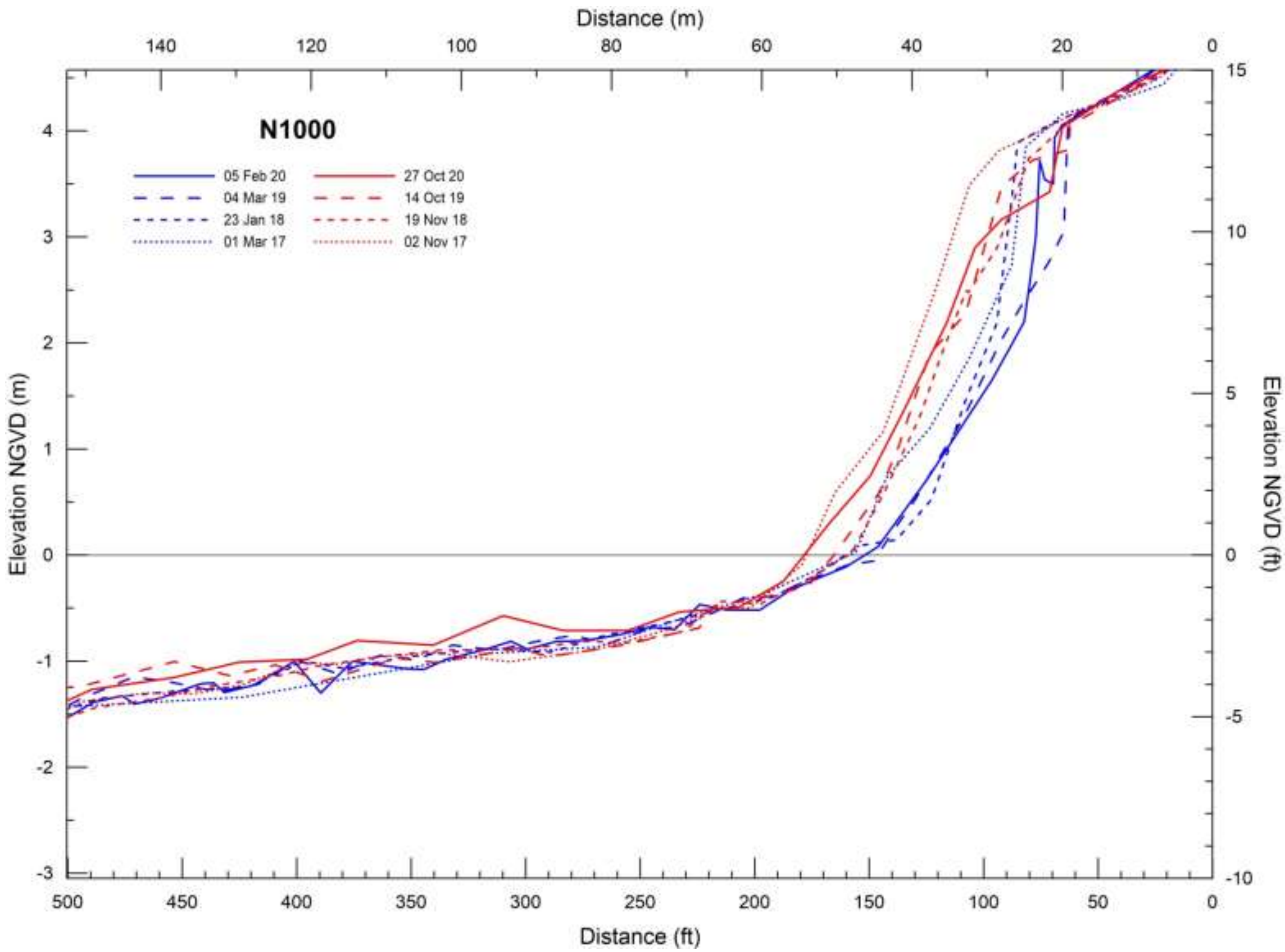

Figure A-1. Nearshore beach profile surveys taken in winter (blue) and summer (red) for N1000.

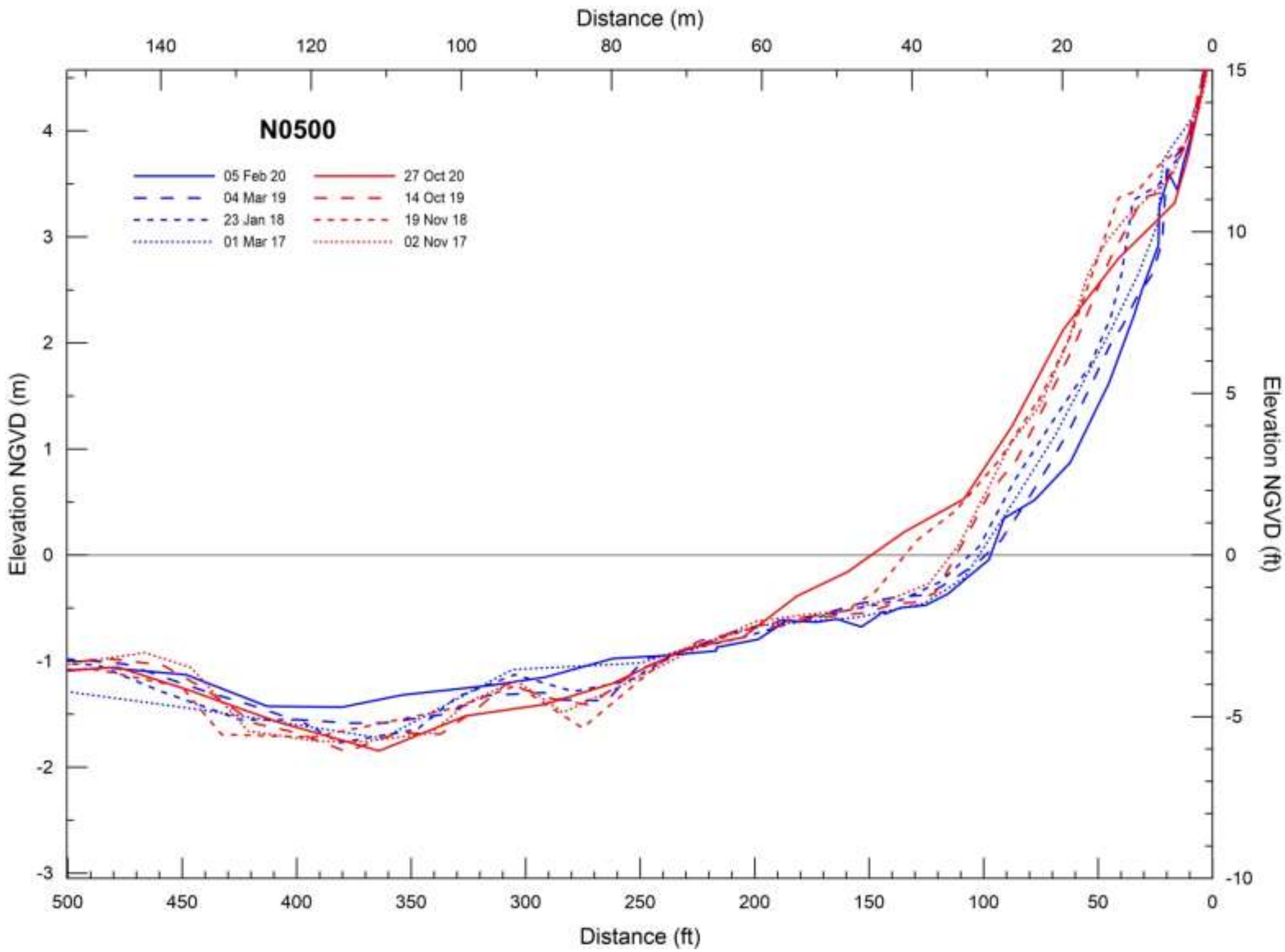

Figure A-2. Nearshore beach profile surveys taken in winter (blue) and summer (red) for N0500.

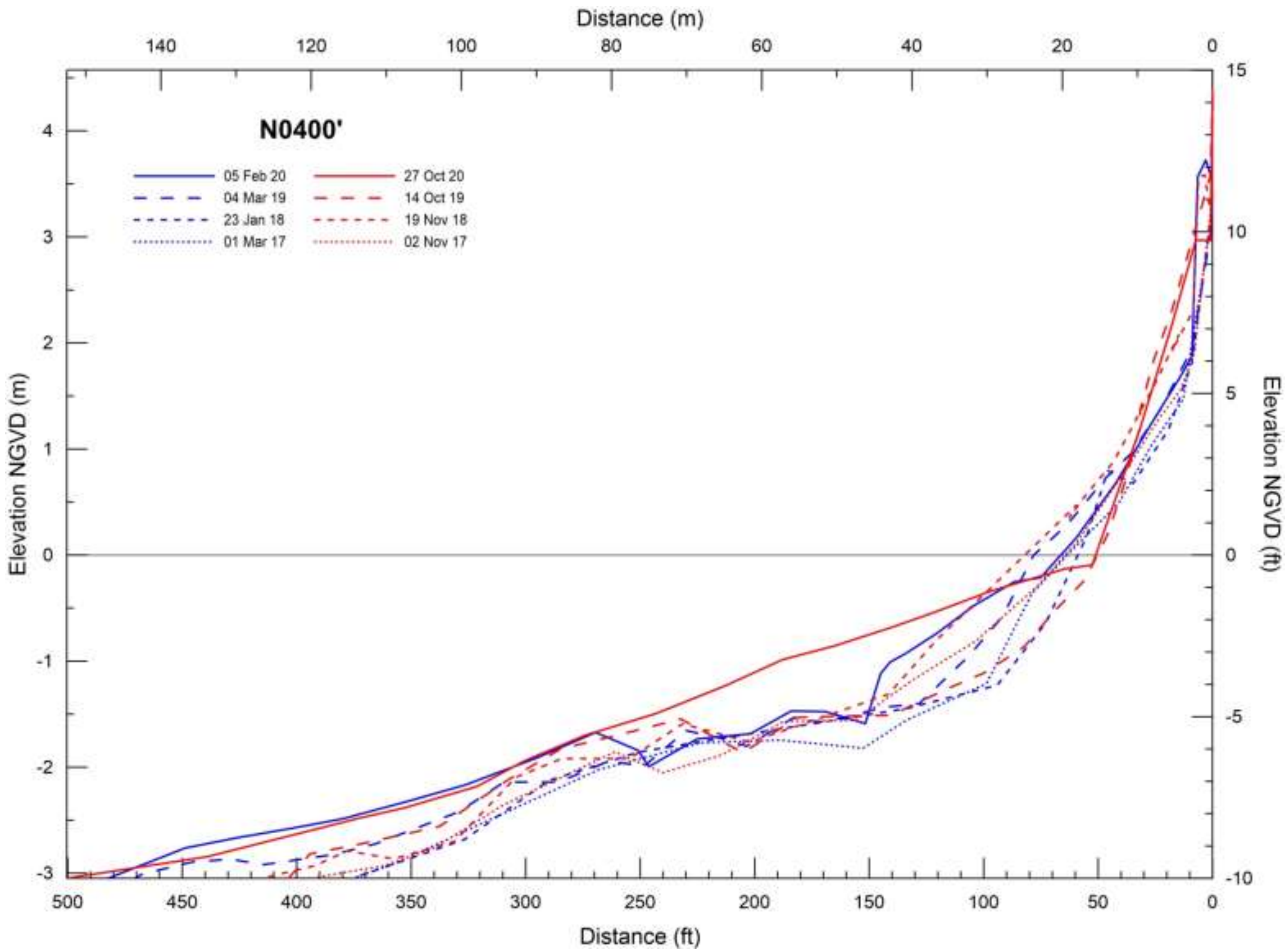

Figure A-3. Nearshore beach profile surveys taken in winter (blue) and summer (red) for N0400'.

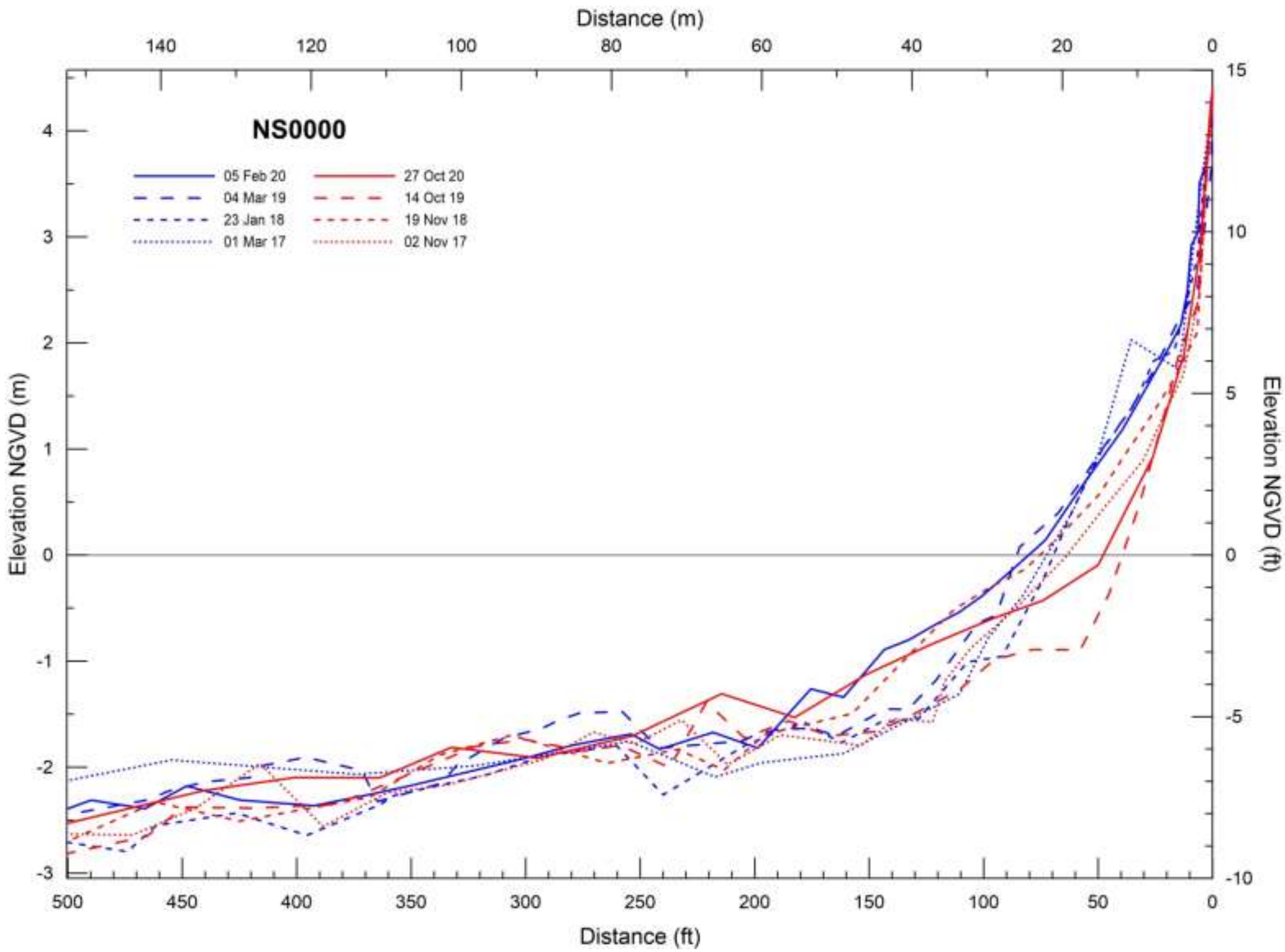

Figure A-4. Nearshore beach profile surveys taken in winter (blue) and summer (red) for NS0000.

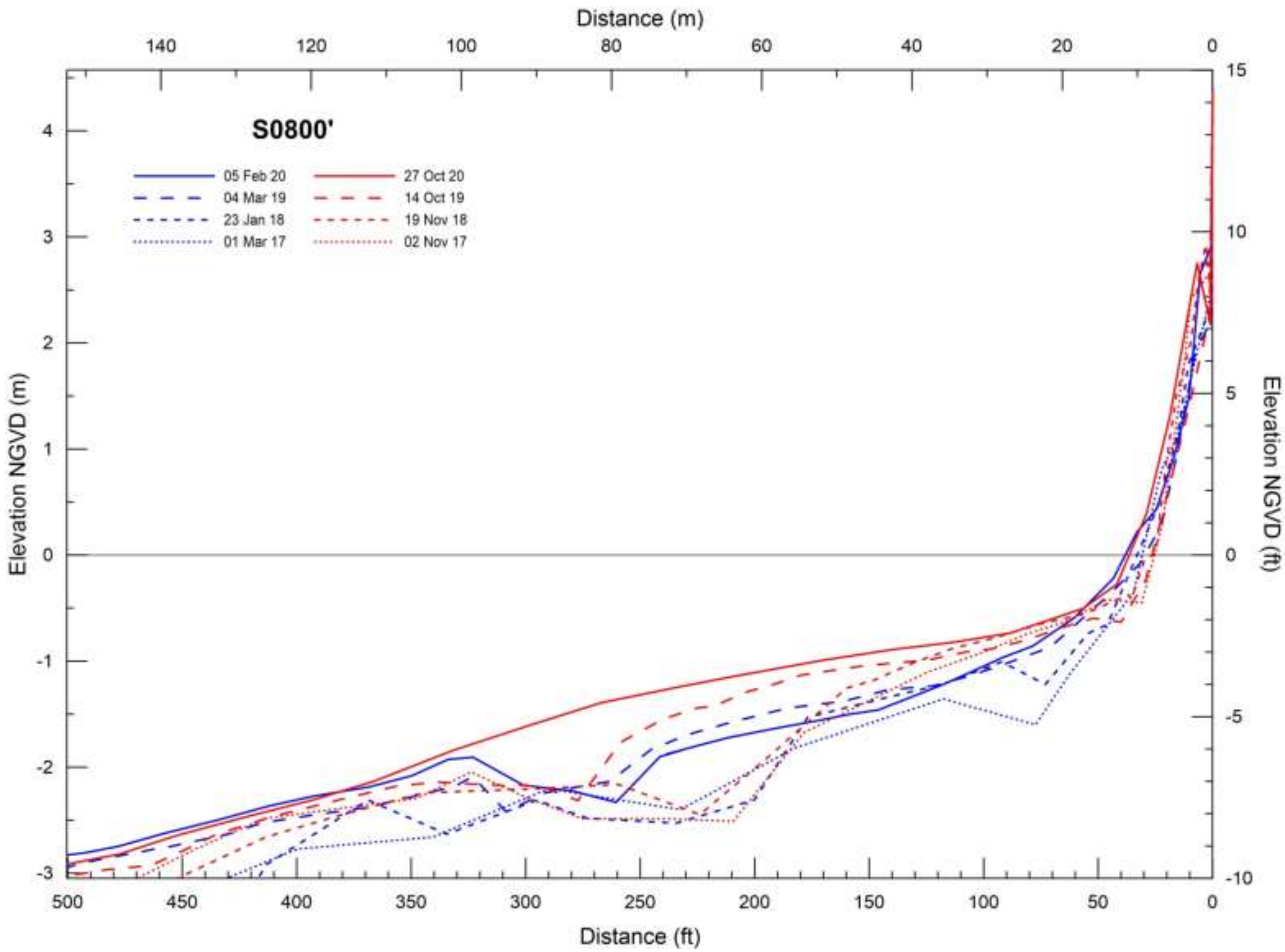

Figure A-5. Nearshore beach profile surveys taken in winter (blue) and summer (red) for S0800'.

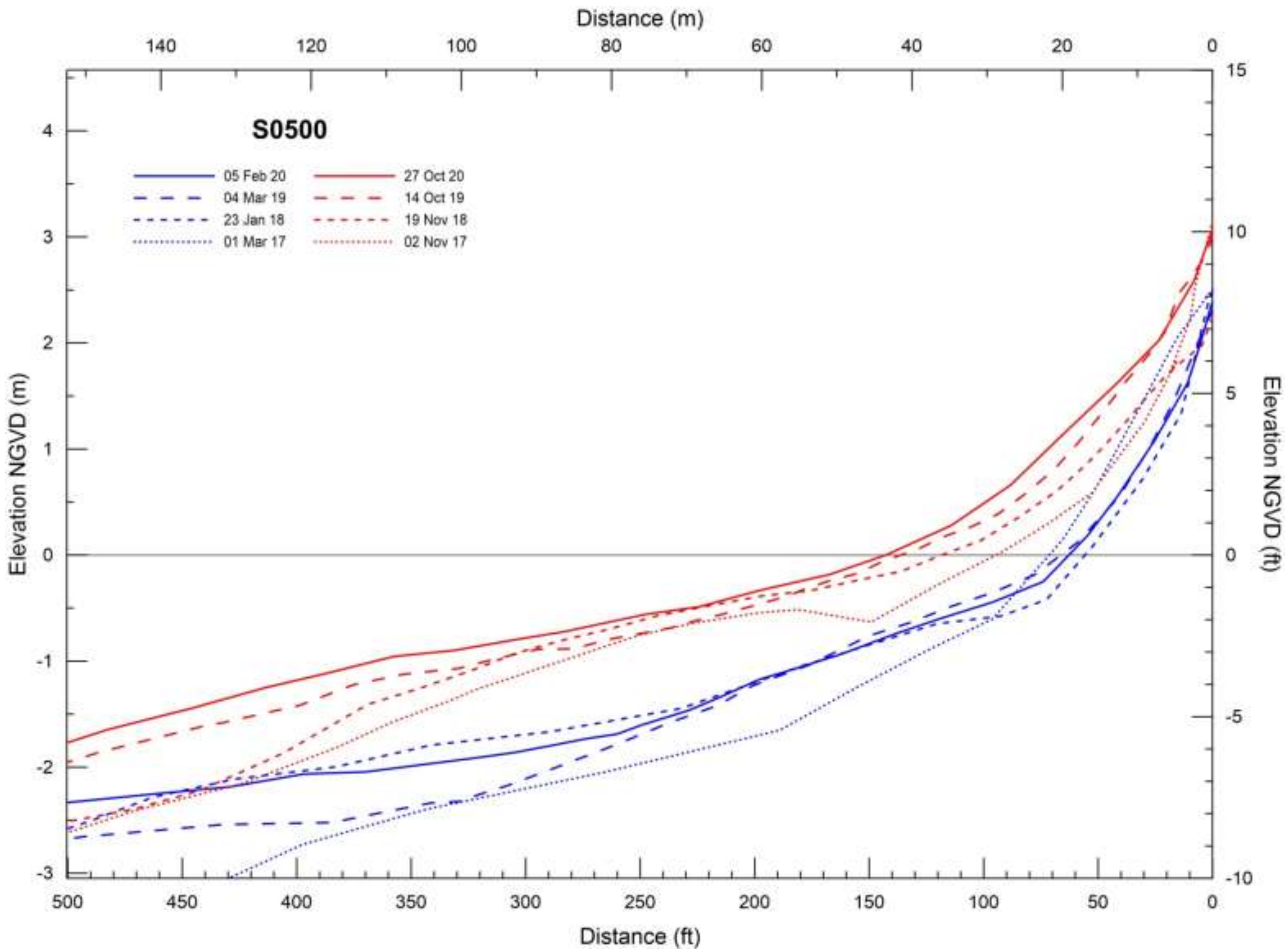

Figure A-6. Nearshore beach profile surveys taken in winter (blue) and summer (red) for S0500.

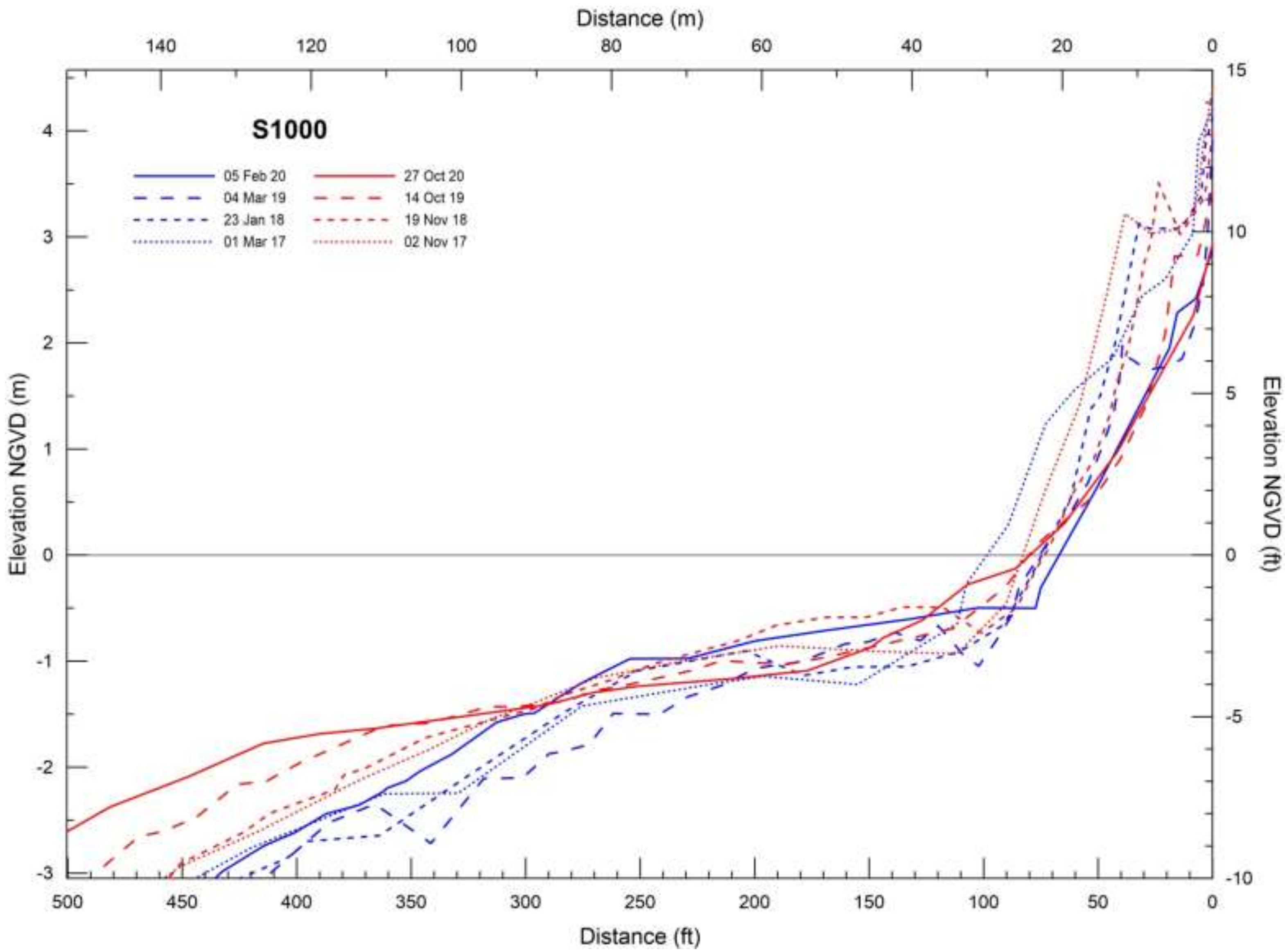

Figure A-7. Nearshore beach profile surveys taken in winter (blue) and summer (red) for S1000.

APPENDIX B

PHOTOGRAPHS OF SAN ONOFRE BEACH AND NEW SURVEY BENCHMARKS TAKEN IN 2020

Photo B-1. Photographs taken in February (top left), May (top right), July (bottom left), and October 2020 (bottom right) looking north from range N1000.

Photo B-2. Photographs taken in February (top left), May (top right), July (bottom left), and October 2020 (bottom right) looking south from range N1000.

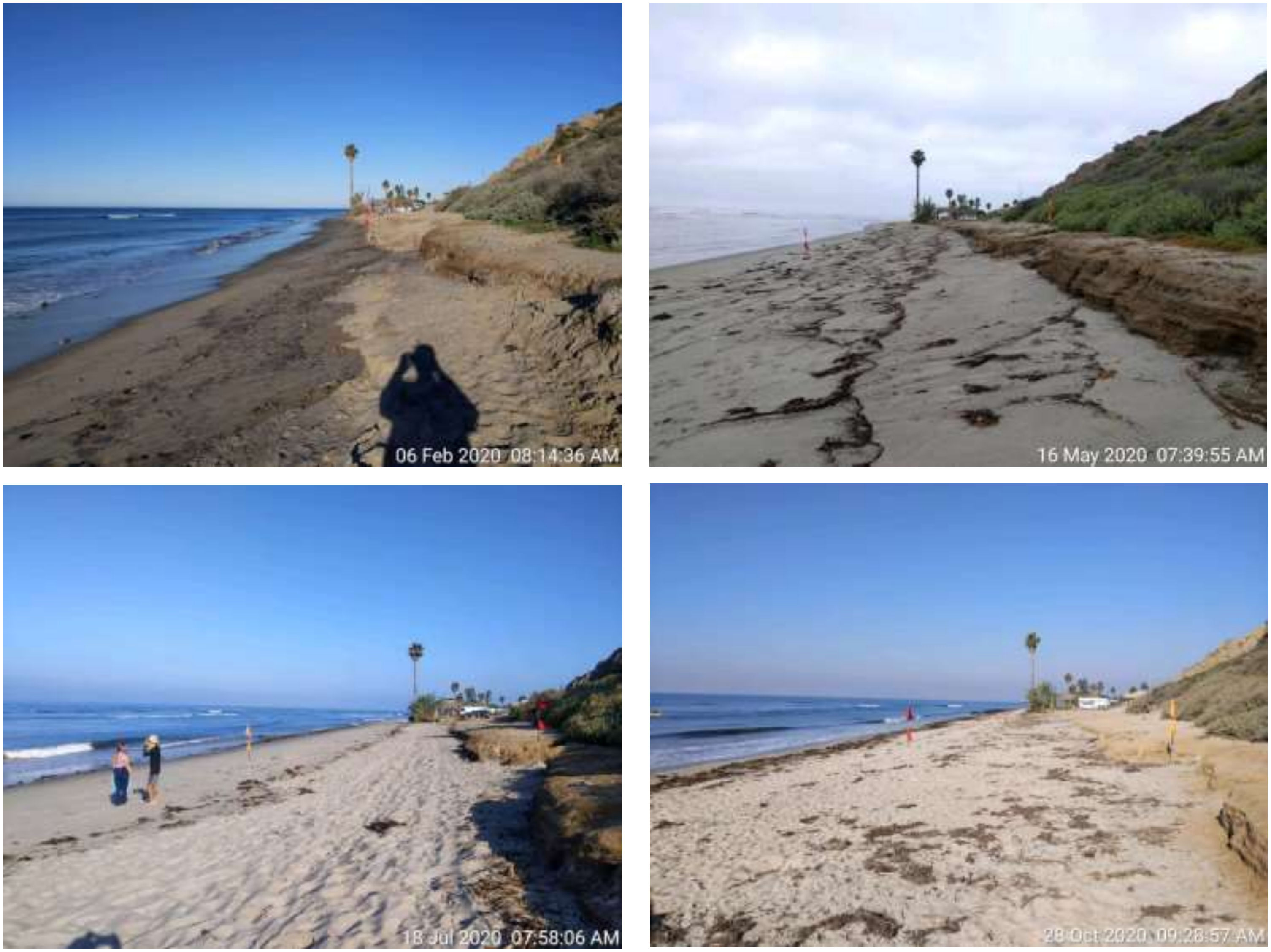

Photo B-3. Photographs taken in February (top left), May (top right), July (bottom left), and October 2020 (bottom right) looking north from range N0500.

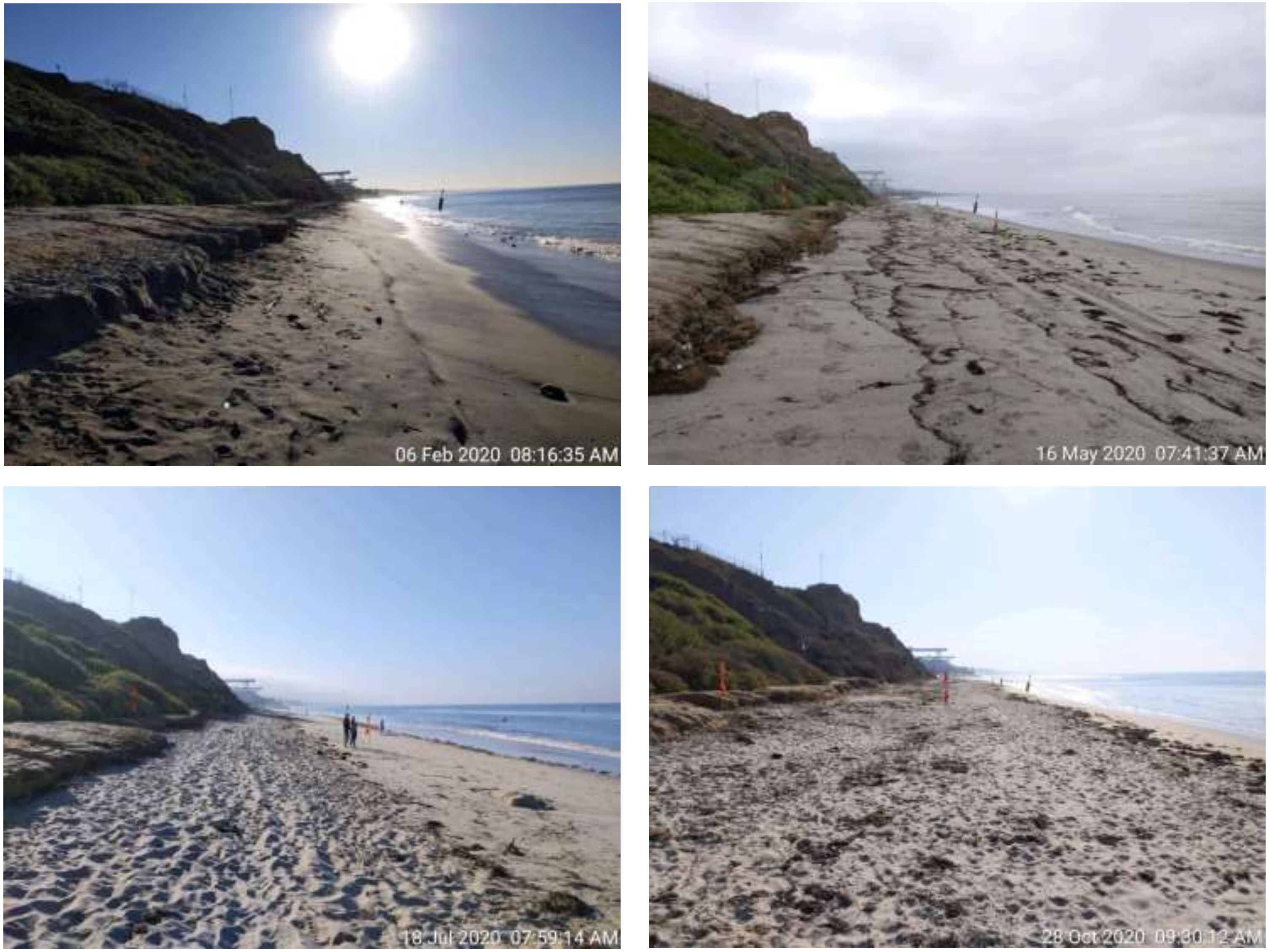

Photo B-4. Photographs taken in February (top left), May (top right), July (bottom left), and October 2020 (bottom right) looking south from range N0500.

Photo B-5. Photographs taken in February (top left), May (top right), and October 2020 (bottom) looking north from range N0400'.

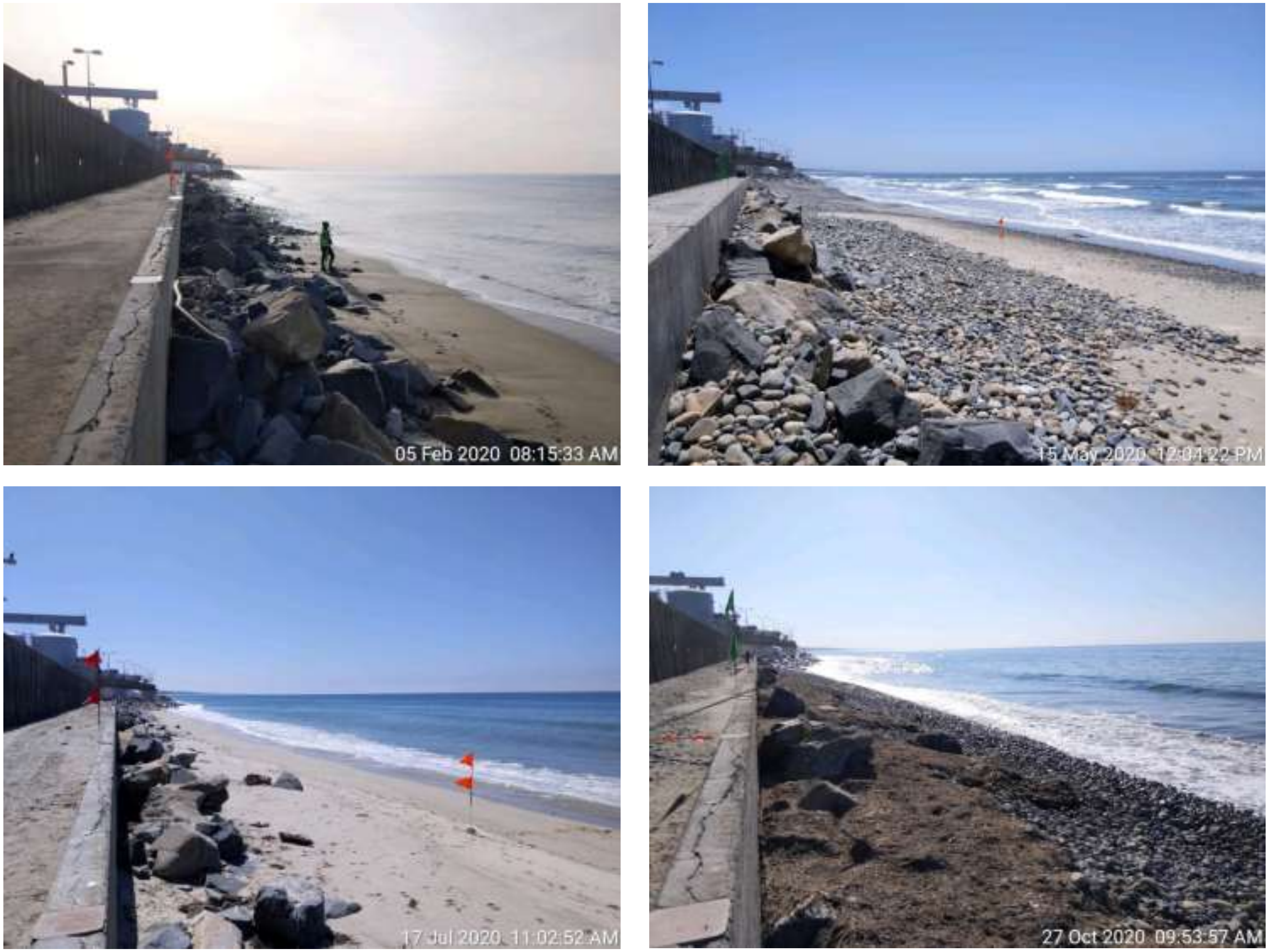

Photo B-6. Photographs taken in February (top left), May (top right), July (bottom left), and October 2020 (bottom right) looking south from range N0400'.

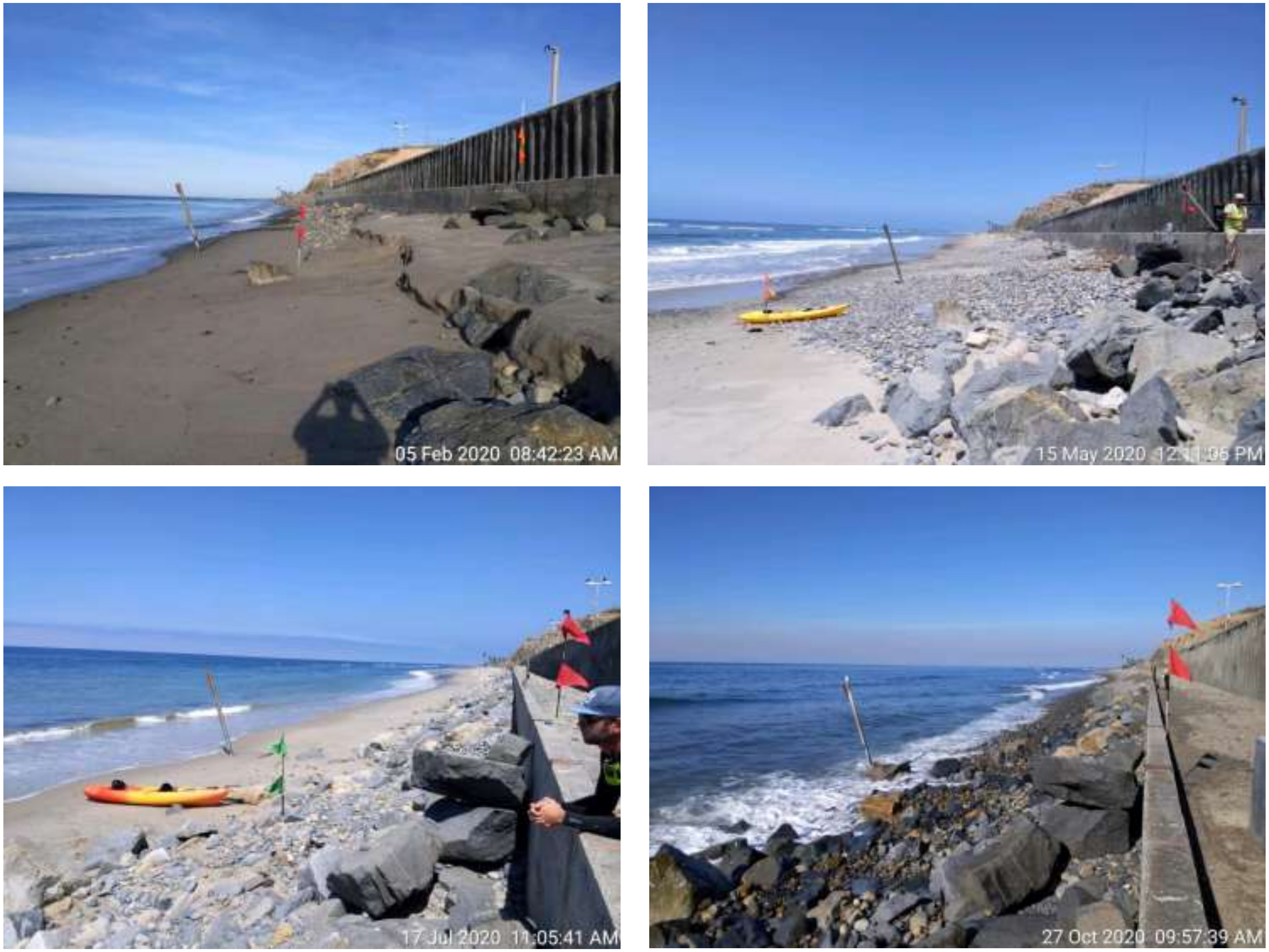

Photo B-7. Photographs taken in February (top left), May (top right), July (bottom left), and October 2020 (bottom right) looking north from range NS0000.

Photo B-8. Photographs taken in February (top left), May (top right), July (bottom left), and October 2020 (bottom right) looking south from range NS0000.

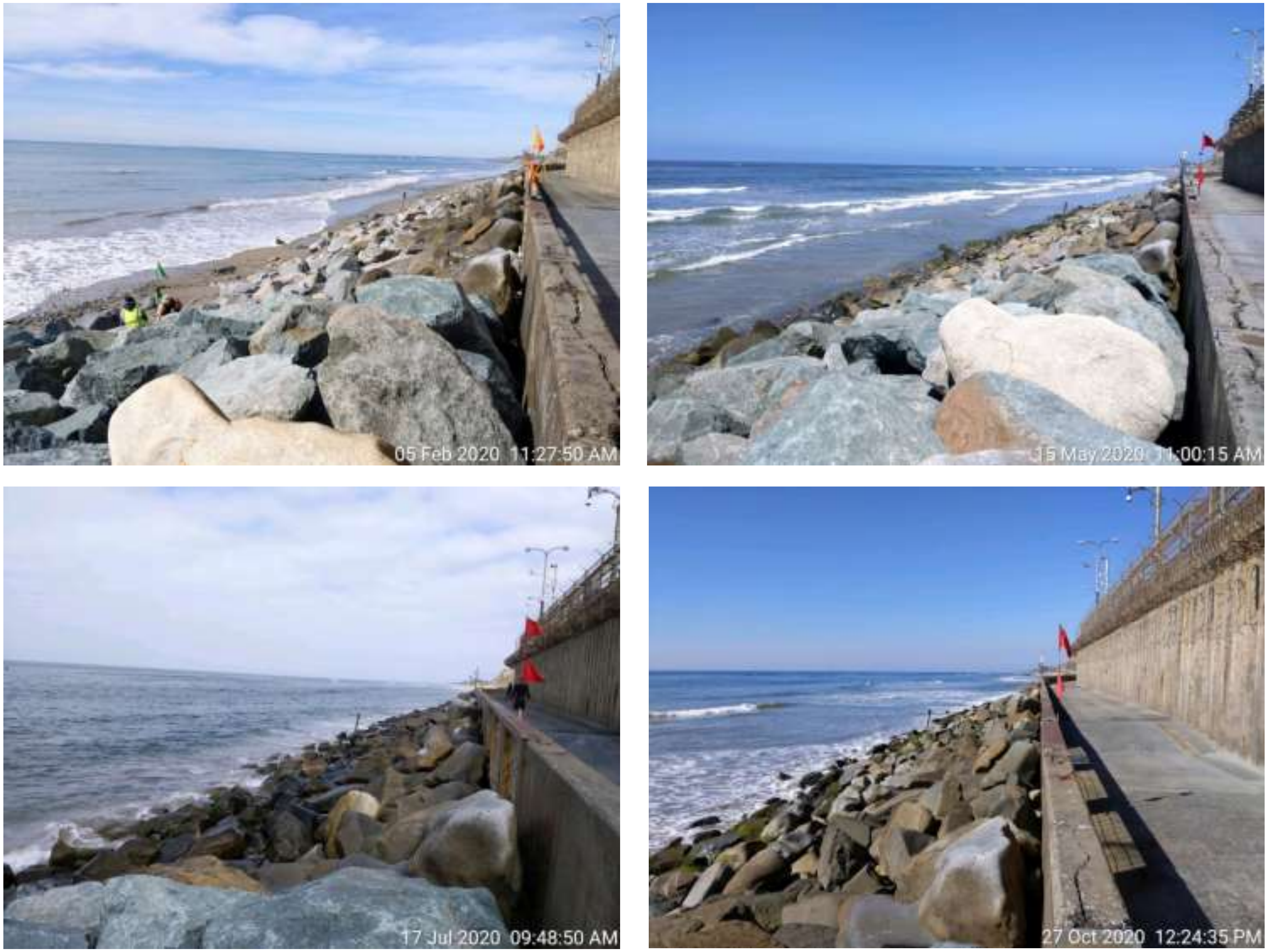

Photo B-9. Photographs taken in February (top left), May (top right), July (bottom left), and October 2020 (bottom right) looking north from range S0800'.

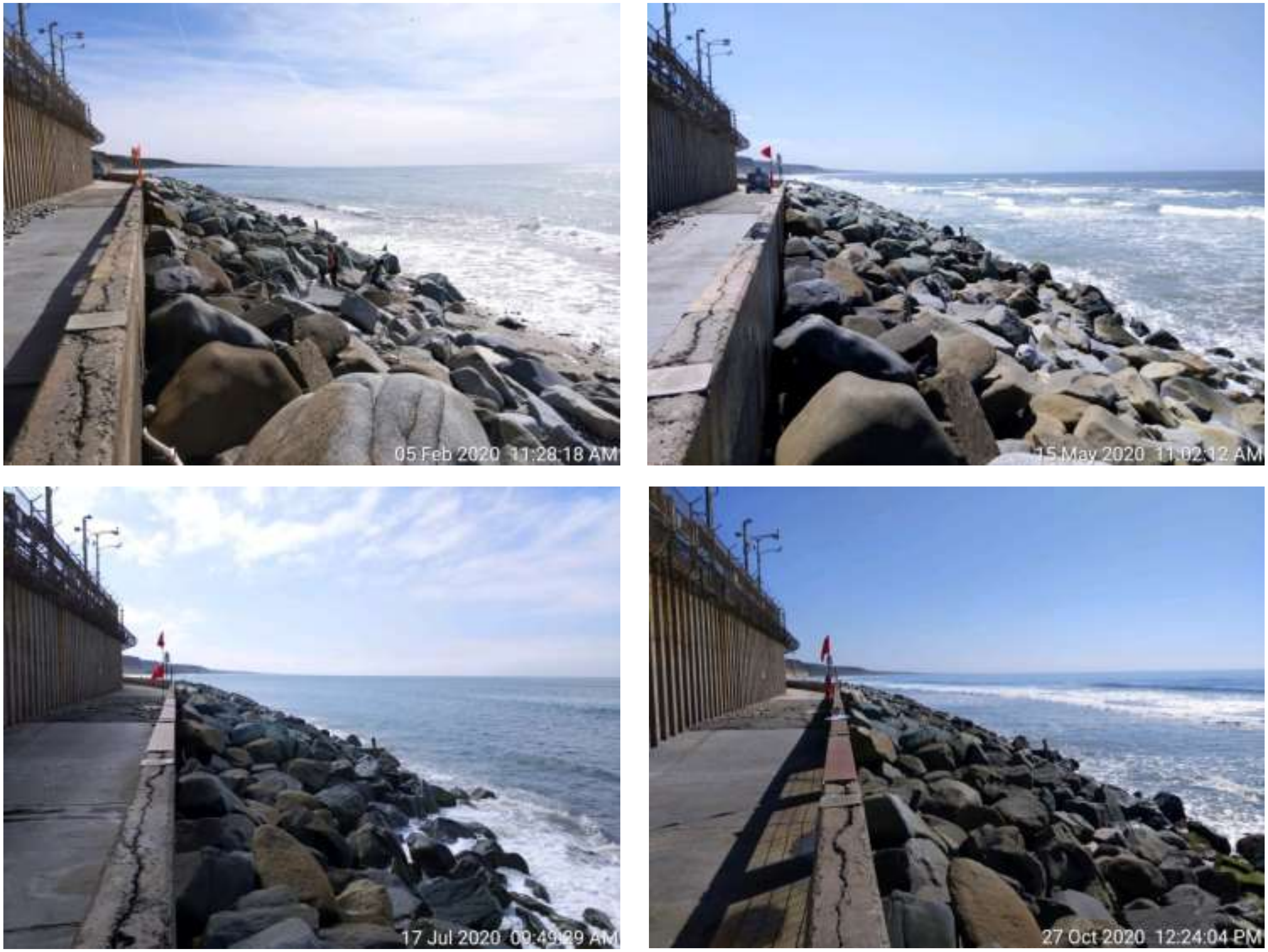

Photo B-10. Photographs taken in February (top left), May (top right), July (bottom left), and October 2020 (bottom right) looking south from range S0800'.

Photo B-11. Photographs taken in February (top left), May (top right), July (bottom left), and October 2020 (bottom right) looking north from range S0500.

Photo B-12. Photographs taken in February (top left), May (top right), July (bottom left), and October 2020 (bottom right) looking south from range S0500.

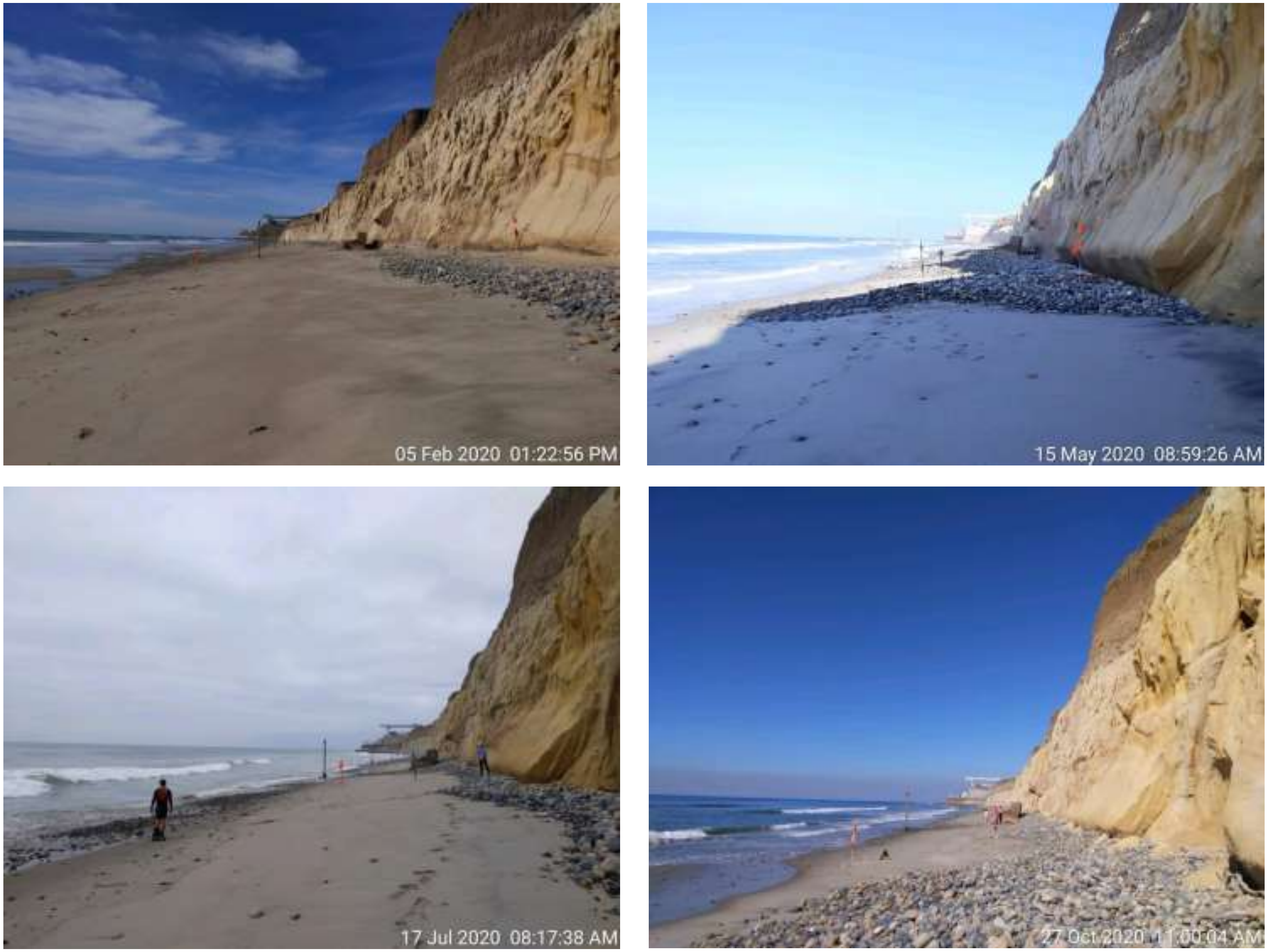

Photo B-13. Photographs taken in February (top left), May (top right), July (bottom left), and October 2020 (bottom right) looking north from range S1000.

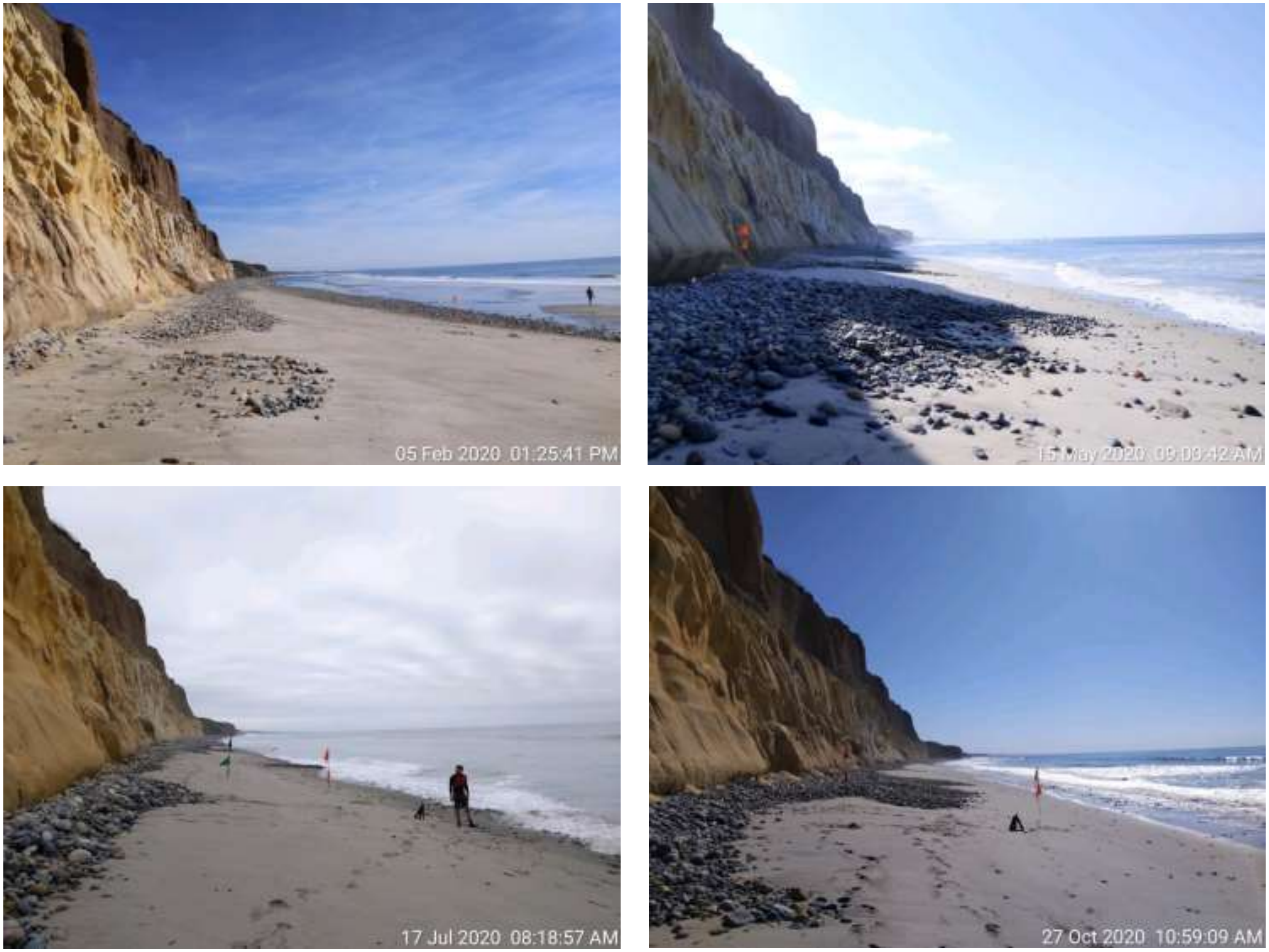

Photo B-14. Photographs taken in February (top left), May (top right), July (bottom left), and October 2020 (bottom right) looking south from range S1000.

Photo B-15. Benchmark BM04, created on 21 January 2020, is located on the SW corner of Bathroom 4 in the San Onofre State Beach parking lot.

Photo B-16. Benchmark BM02, created on 21 January 2020, is located on the SW corner of Bathroom 2 in the San Onofre State Beach parking lot. Benchmarks BM02 through BM06 are all marked by a scribed X on the concrete foundation.

Photo B-17. **Benchmark BM07, created on 21 January 2020, is located on the NE corner of a concrete structure located south of the San Onofre State Beach parking lot and north of transect N0500.**

Photo B-18. **Benchmark BM08, created on 21 January 2020, is marked by a scribed X and located just south of transect NS0000 on top of the seawall.**

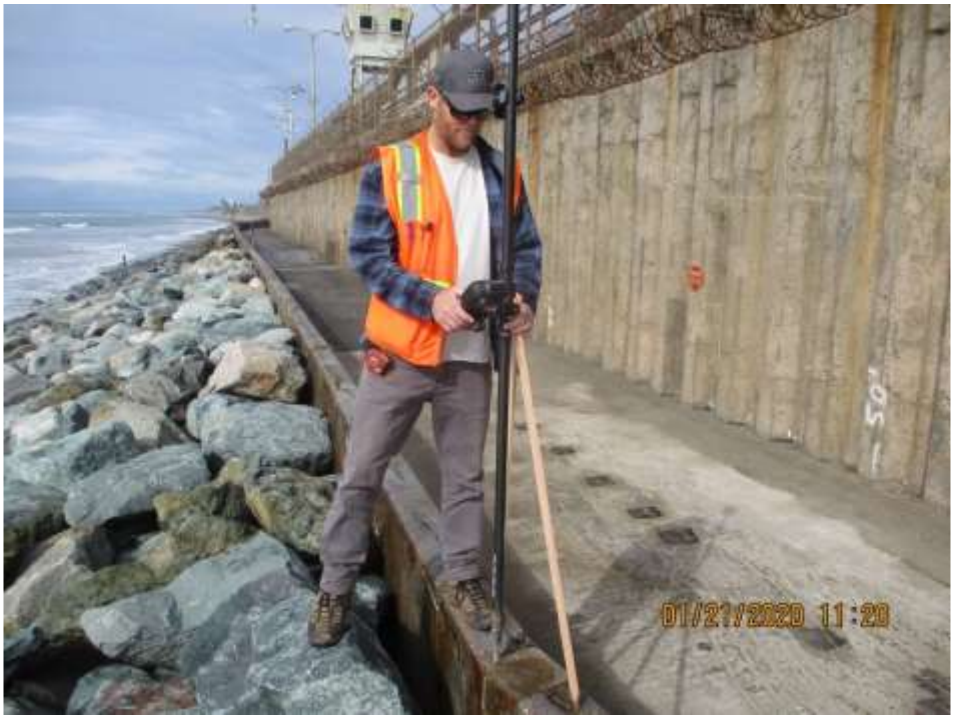

Photo B-19. Benchmark BM09, created on 21 January 2020, is located on top of the seawall, just south of transect S0800'.

Photo B-20. Benchmark BM10, created on 21 January 2020, is marked by a metal screw and washer and is located on the walkway south of transect S0800'. This benchmark has replaced benchmark 2051613.

Photo B-21. Benchmark BM11, created on 21 January 2020, is located on top of the concrete blocks at the southern end of the SONGS walkway.

Photo B-22. Benchmark BM12, created on 21 January 2020, is located on top of the concrete drainage structure located just north of transect S1000.

APPENDIX F

2020 GROUNDWATER LEVEL AT SAN ONOFRE

2020 GROUNDWATER LEVELS AT SAN ONOFRE NUCLEAR GENERATING STATION, SAN ONOFRE, CALIFORNIA

Prepared by

Coastal Environments, Inc.
2166 Avenida de la Playa, Suite E
La Jolla, CA 92037

Prepared for

Southern California Edison Company
2244 Walnut Grove Avenue
Rosemead, CA 91770

08 March 2021
CE Reference No. 21-05

TABLE OF CONTENTS

LIST OF APPENDICES

LIST OF FIGURES

LIST OF TABLES

2020 GROUNDWATER LEVELS AT SAN ONOFRE NUCLEAR GENERATING STATION,

SAN ONOFRE, CALIFORNIA

1.0 INTRODUCTION

This report has been compiled per Special Provision 14 (b) in the California State Lands Commission Lease No. PRC 6785.1 for the use, maintenance, and decommissioning of exiting offshore improvements associated with the San Onofre Nuclear Generating Station (SONGS). Lease Provision 14 (b) requires, as part of compliance with applicable provisions or standards addressing sea-level rise that may be required or adopted by local, state or federal agencies related to and affecting the lease premises, that the Lessee provide an annual summary including quarterly groundwater elevation data collected from onsite monitoring wells.

In accordance with this requirement, this report compares the quarterly groundwater elevation data from the 16 wells located within SONGS against coastal tide data to observe any correlation between elevation values. Data for both groundwater and tidal elevations span from February to November 2020.

At coastal discharge boundaries, freshwater and saltwater are typically slow to mix; the less-dense freshwater remains at the top of the water table, riding above the denser saltwater wedge which extends below the land. Closer to the shoreline, however, daily tidal changes can result in a short-term mixing of water sources and can directly raise or lower the water table. San Onofre exemplifies one of these shallow coastal aquifers where tidal effects on groundwater levels have been noted in 2020 groundwater measurements.

Section 2 of this report describes the sources and uses of the SONGS groundwater well and tidal data, as well as how this data was organized to obtain discernable results. Section 3 presents these results both graphically and in table format, while Section 4 discusses these results and the relationship between groundwater elevation, daily tides, and sea level rise (SLR) at SONGS. Ultimately, this report finds that projected groundwater elevations in 2050 are lower than the Independent Spent Fuel Storage Installation (ISFSI) support foundation by 1.54 and 0.74 ft. for a medium-high and extreme risk aversion scenario, respectively (Section 3).

2.0 ANALYSIS METHODS

Groundwater and well data for the year 2020 was provided by Southern California Edison (SCE) and compared against tidal data gathered by Coastal Environments (CE). These include quarterly data from SCE Groundwater Protection Initiative (GPI) wells and other wells where data is collected semiannually or annually. ISFSI pad cross-sections were also provided by SCE. Figures 2-1 and 2-2 show the locations of the sampled wells at SONGS. Individual wells were measured 1 or 4 times within the calendar year. Data provided for the 16 wells located within SONGS included: date and time of sample, ground surface elevation of well, measured water depth, and groundwater elevation.

Groundwater elevations were determined by measuring the wells' water depth, defined as the distance from a well's ground surface to its water level. This value was then subtracted from the known ground surface elevation of each well to determine groundwater elevations. Elevation data are presented in NGVD29 (National Geodetic Vertical Datum, 1929) for this report. Unlike MLLW (Mean Lower Low Water) datum values which vary between tidal epochs, NGVD29 datum values remains fixed. Additionally, NGVD29 lies closer to Mean High Water (MHW) than MLLW, making NGVD29 more useful for representing current sea levels and SLR. Elevation values can be converted between datums by subtracting 2.60 ft. from MLLW (Epoch 1941-1959) to get the elevation in NGVD29. Appendix A presents the groundwater measurements for the 16 wells in both datums.

To better examine groundwater trends, each of the 16 wells was assigned to one of three groups based on their elevation and location within SONGS. Group 1 includes wells NIA-1, NIA-2, NIA-3, NIA-4, NIA-5, NIA-6, NIA-7, NIA-10, and NIA-11. This clustered group of wells occupies the lowest ground surface elevation and is located between the shoreline and North Industrial Area (Unit 1 remnants and ISFSI). Group 2 includes wells PA-1, PA-2, PA-3, and PA-4, which are at middling ground surface elevations and located between Unit 2/3 structures and the shoreline. Group 3 includes the remaining wells OCA-1, OCA-2, and OCA-3, which have the highest ground surface elevations and lie farthest from the shoreline.

Figure 2-1. Locations of SONGS groundwater wells.

Figure 2-2. Locations of Group 1 (NIA) SONGS groundwater wells.

3.0 RESULTS

Table 3-1 displays the pertinent groundwater well elevation data for all measured samples, as well as the corresponding tidal data. Table 3-2 shows the mean groundwater elevations for each well group. Mean elevations were also calculated for individual wells that were measured more than once in 2020. Standard deviation values were not calculated for wells measured only once during 2020.

Figures 3-1 through 3-3 graphically show the groundwater elevations for each well plotted against the measured daily maximum and minimum tide elevations for 2020. Each figure displays well measurements from one of the three well groups; this allows for a visual comparison of groundwater elevations for wells within similar areas of SONGS.

The Group 1 wells are located just west of the Unit 1 remnants and ISFSI pads and their ground surface elevations vary from 11.19 to 13.46 ft. The 2020 groundwater elevation at these wells varies from 1.95 to 3.06 ft. (Table 3-1) and the mean groundwater elevation for these 9 wells is 2.73 ft. (Table 3-2). Due to their location within SONGS, Group 1 data were used to determine the distance between groundwater levels and the Holtec UMAX ISFSI support foundation in 2050, where the projections of SLR according to the Ocean Protection Council (OPC) is 2 ft. for a medium-high risk aversion scenario and 2.8 ft. for the H++ extreme risk scenario. Figure 3-4 shows these 2050 sea level projections, along with the 2020 groundwater elevations, in comparison to the ISFSI pad. The H++ scenario groundwater elevation for 2050 is 5.23 ft. and is lower than the bottom of the Holtec UMAX ISFSI support foundation (5.97 ft., NGVD) by 0.74 ft. The CCC scenario groundwater elevation for 2050 is 4.43 ft., NGVD and is 1.54 ft. lower than the bottom of the ISFSI support foundation. Figure 3-5 is similar to Figure 3-4 but the elevation values are referenced to MLLW (Epoch 1941-1959).

Table 3-1. SONGS groundwater well sample data.

Well Group	Well Description	Sample Date	Sample Time	Surface Ground Elevation (NGVD29, ft)	Groundwater Elevation (NGVD29, ft)	Ocean Tide Level (NGVD29, ft)
Group 1	NIA-1	2-Mar-20	9:08	11.19	3.06	-0.68
		6-May-20	8:55	11.19	2.61	2.61
		3-Sep-20	8:25	11.19	2.35	1.00
		28-Oct-20	10:24	11.19	2.86	1.85
	NIA-2	27-Feb-20	9:16	12.80	2.54	1.43
		30-Apr-20	8:41	12.80	1.95	-1.41
		8-Sep-20	10:13	12.80	2.91	1.75
		29-Oct-20	9:13	12.80	2.97	3.01
	NIA-3	7-May-20	8:12	11.25	2.33	1.24
	NIA-4	14-May-20	8:27	11.58	2.27	-1.01
	NIA-5	13-May-20	8:14	12.08	2.17	-1.77
	NIA-6	14-May-20	10:22	11.59	1.97	-1.95
	NIA-7	13-May-20	10:04	12.14	2.12	-2.16
	NIA-10	11-May-20	10:23	13.46	2.20	-1.15
	NIA-11	11-May-20	8:35	13.46	2.22	-2.52
Group 2	PA-1	9-Mar-20	9:40	26.21	2.49	4.20
		3-Jun-20	8:38	26.21	1.87	1.93
		29-Jul-20	9:00	26.21	1.88	0.53
		12-Oct-20	8:31	26.21	1.95	1.92
	PA-2	9-Mar-20	13:06	26.91	2.02	0.01
		3-Jun-20	11:23	26.91	1.24	0.11
		29-Jul-20	11:16	26.91	0.99	-0.11
		12-Oct-20	10:54	26.91	1.39	0.67
	PA-3	20-Mar-20	10:37	26.72	1.24	0.87
		10-Jun-20	8:35	26.72	1.52	-2.48
		19-Aug-20	12:50	26.72	1.56	1.48
		14-Oct-20	10:37	26.72	1.30	1.57
	PA-4	20-Mar-20	8:18	26.34	2.57	2.82
		11-Jun-20	8:36	26.34	-0.02	-2.20
		20-Aug-20	8:46	26.34	1.22	1.22
		15-Oct-20	8:27	26.34	2.72	3.56

Table 3-1 (cont). SONGS groundwater well sample data.

Well Group	Well Description	Sample Date	Sample Time	Surface Ground Elevation (NGVD29, ft)	Groundwater Elevation (NGVD 29, ft)	Ocean Tide Level (NGVD29, ft)
Group 3	OCA-1	13-Feb-20	9:03	45.09	3.71	0.70
		29-Apr-20	8:48	45.09	3.62	-1.89
		2-Sep-20	9:29	45.09	4.06	2.23
		4-Nov-20	14:27	45.09	3.97	0.06
	OCA-2	10-Feb-20	11:40	113.79	4.02	2.81
		27-Apr-20	9:53	113.79	3.43	-0.99
		31-Aug-20	11:37	113.79	4.04	1.46
		26-Oct-20	10:18	113.79	4.05	1.24
	OCA-3	6-Feb-20	10:55	103.10	2.94	-0.51
		23-Apr-20	8:38	103.10	2.11	0.89
		24-Aug-20	10:20	103.10	2.50	0.97
		22-Oct-20	10:00	103.10	2.92	1.66

Table 3-2. Mean SONGS groundwater elevations.

Well Group	Well Description	Surface Ground Elevation (NGVD29, ft)	Mean Groundwater Level (NGVD29, ft)		Standard Deviation (ft)	
			Well	Group	Well	Group
Group 1	NIA-1	11.19	2.72	2.43	0.31	0.37
	NIA-2	12.80	2.59		0.47	
	NIA-3	11.25	2.33		N/A	
	NIA-4	11.58	2.27		N/A	
	NIA-5	12.08	2.17		N/A	
	NIA-6	11.59	1.97		N/A	
	NIA-7	12.14	2.12		N/A	
	NIA-10	13.46	2.20		N/A	
	NIA-11	13.46	2.22		N/A	
Group 2	PA-1	26.21	2.05	1.62	0.30	0.68
	PA-2	26.91	1.41		0.44	
	PA-3	26.72	1.41		0.16	
	PA-4	26.34	1.62		1.29	
Group 3	OCA-1	45.09	3.84	3.45	0.21	0.67
	OCA-2	113.79	3.89		0.30	
	OCA-3	103.10	2.62		0.39	

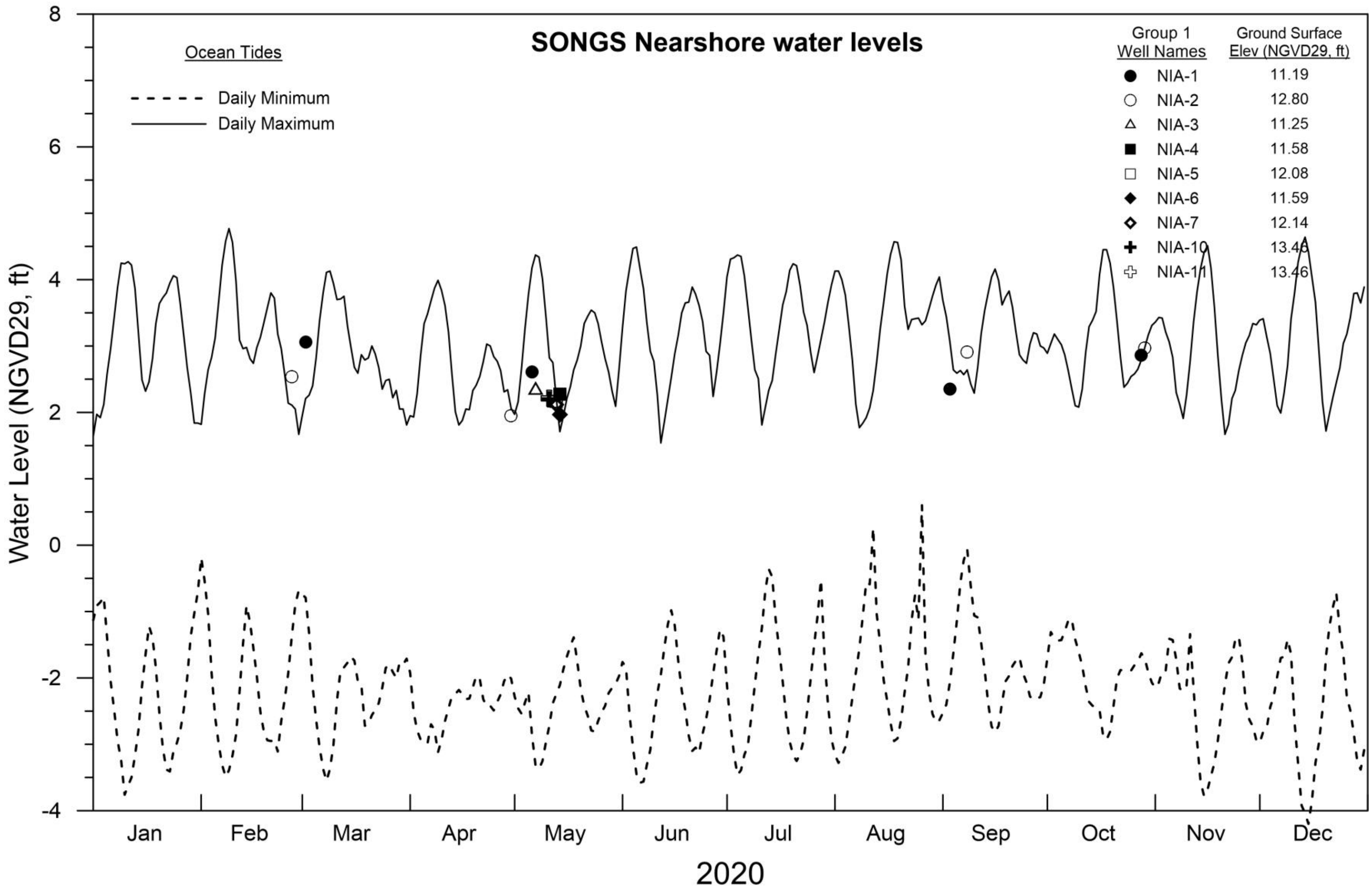

Figure 3-1. Groundwater elevation of Group 1 (NIA) SONGS wells and daily tides for 2020.

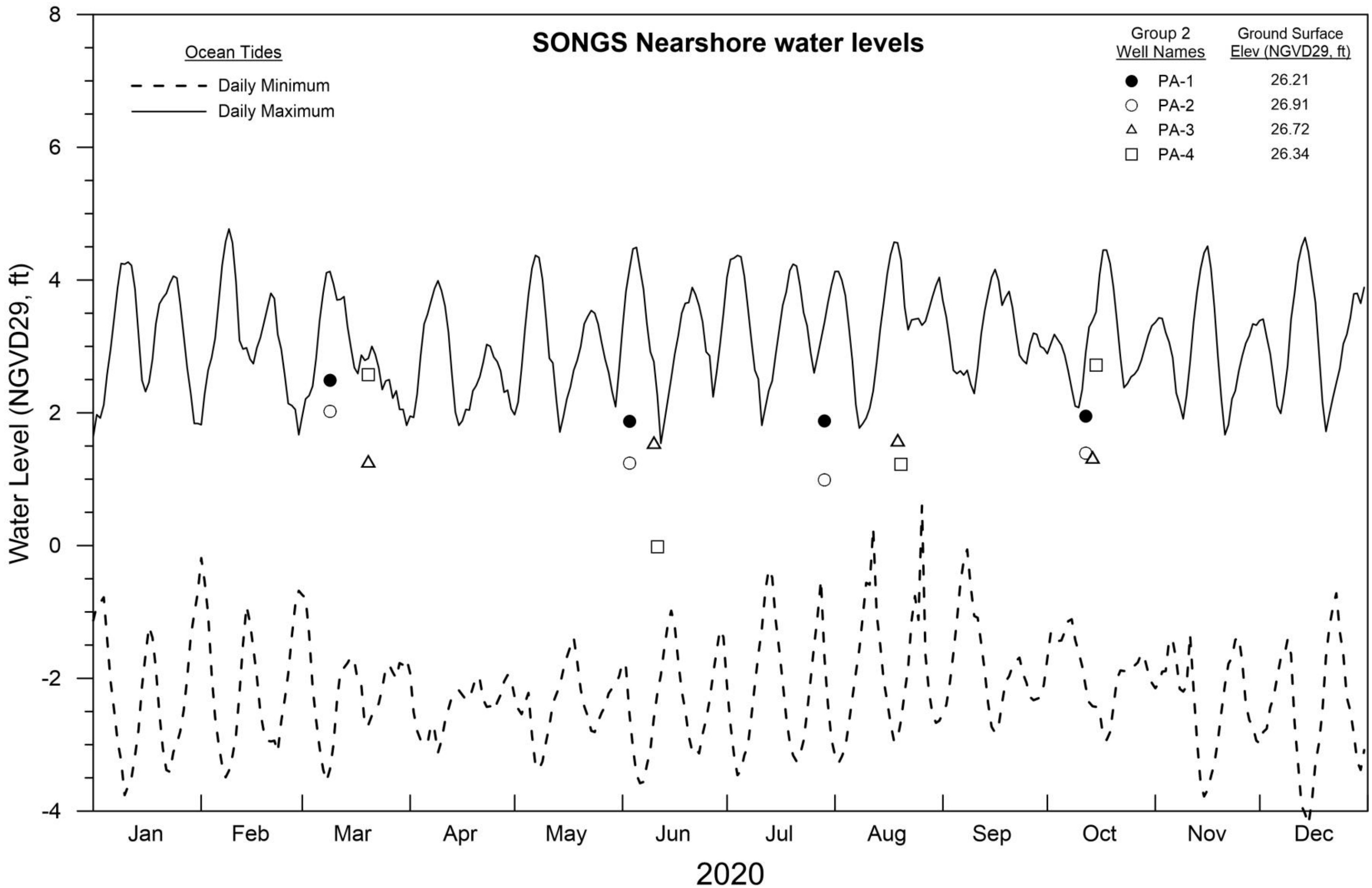

Figure 3-2. Groundwater elevation of Group 2 (PA) SONGS wells and daily tides for 2020.

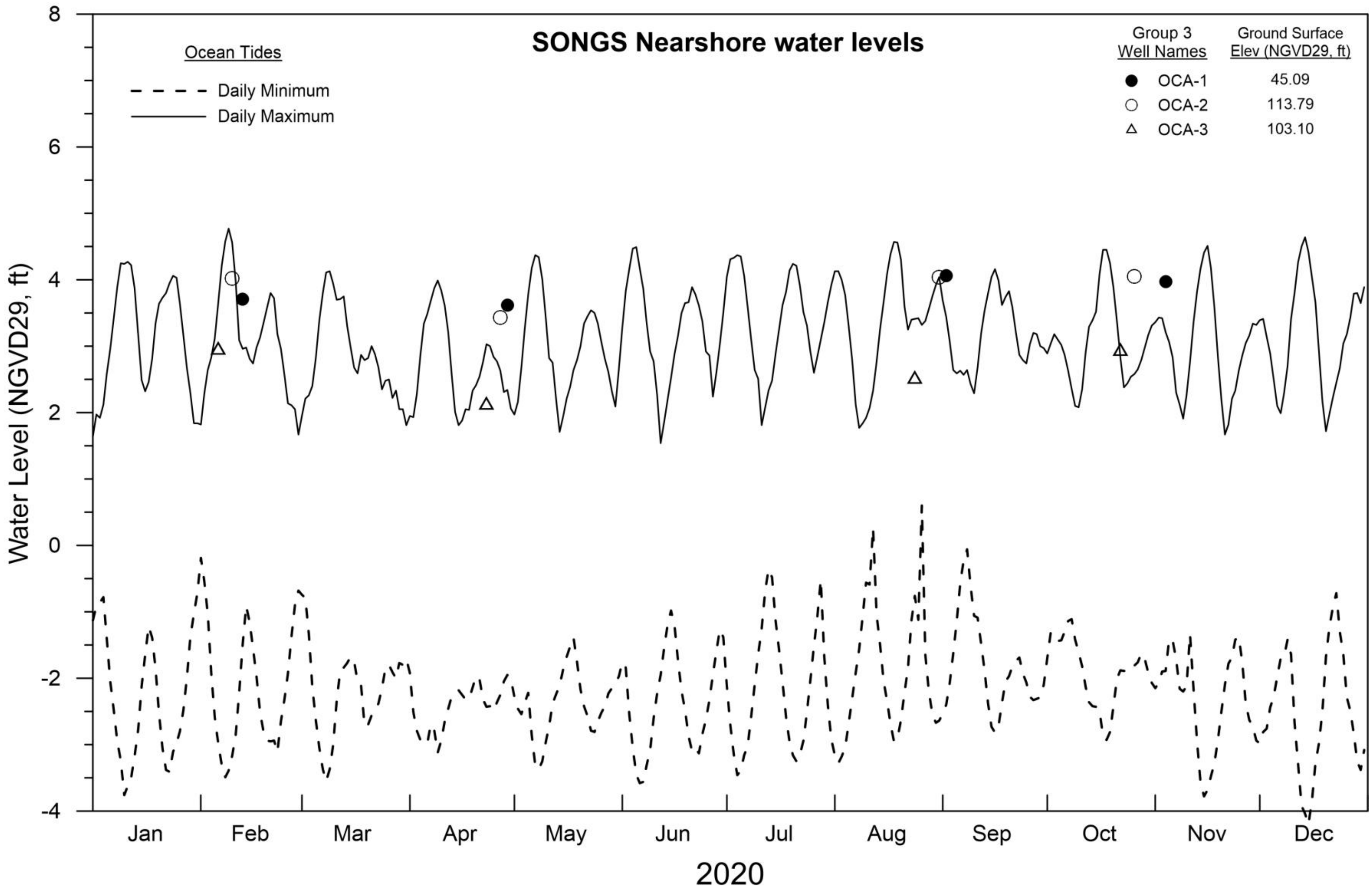

Figure 3-3. Groundwater elevation of Group 3 (OCA) SONGS wells and daily tides for 2020.

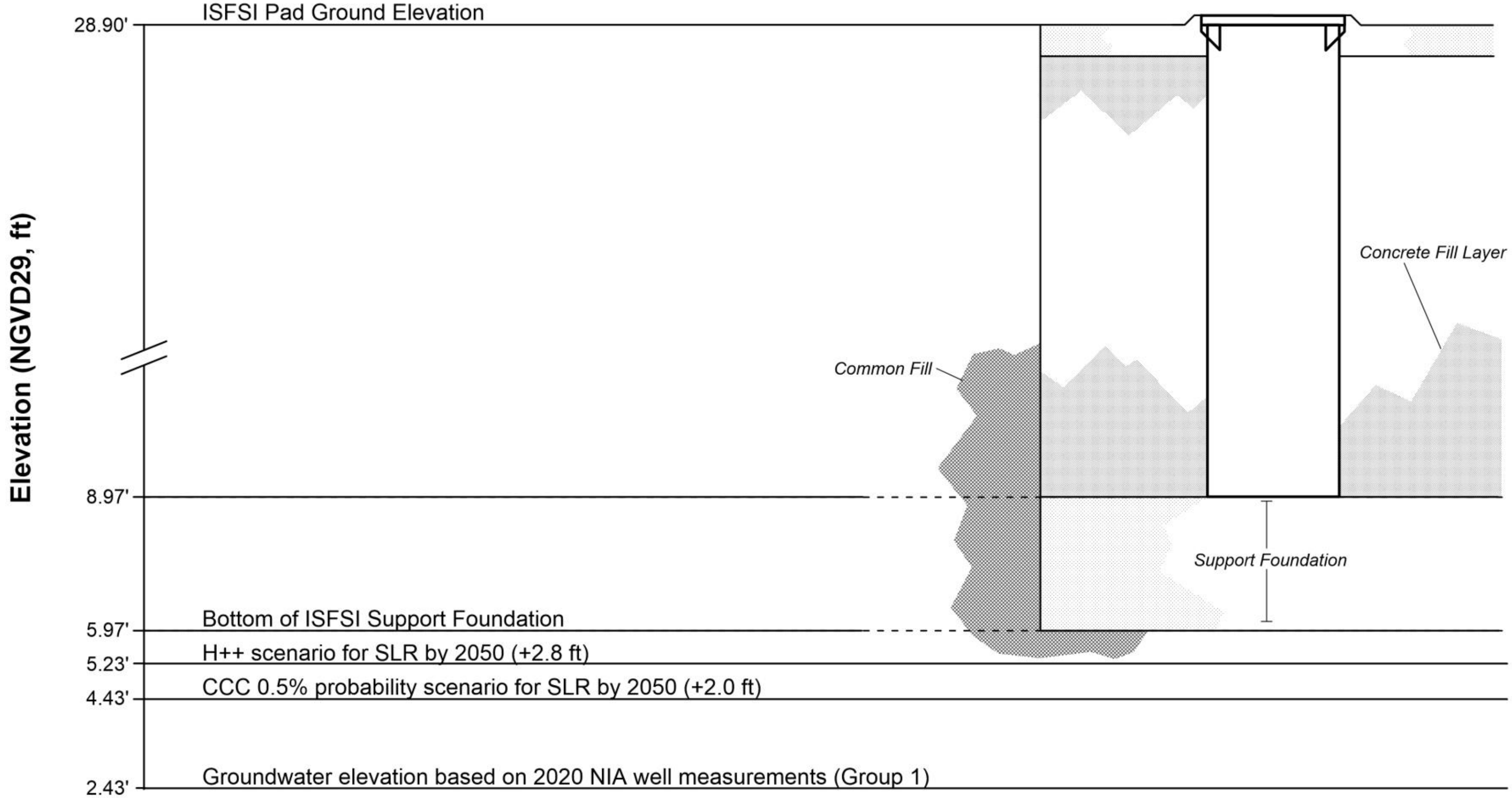

Figure 3-4. Groundwater elevations (NGVD29) in 2020 and 2050 based on the CCC and H+++ SLR projections (OPC, 2018).

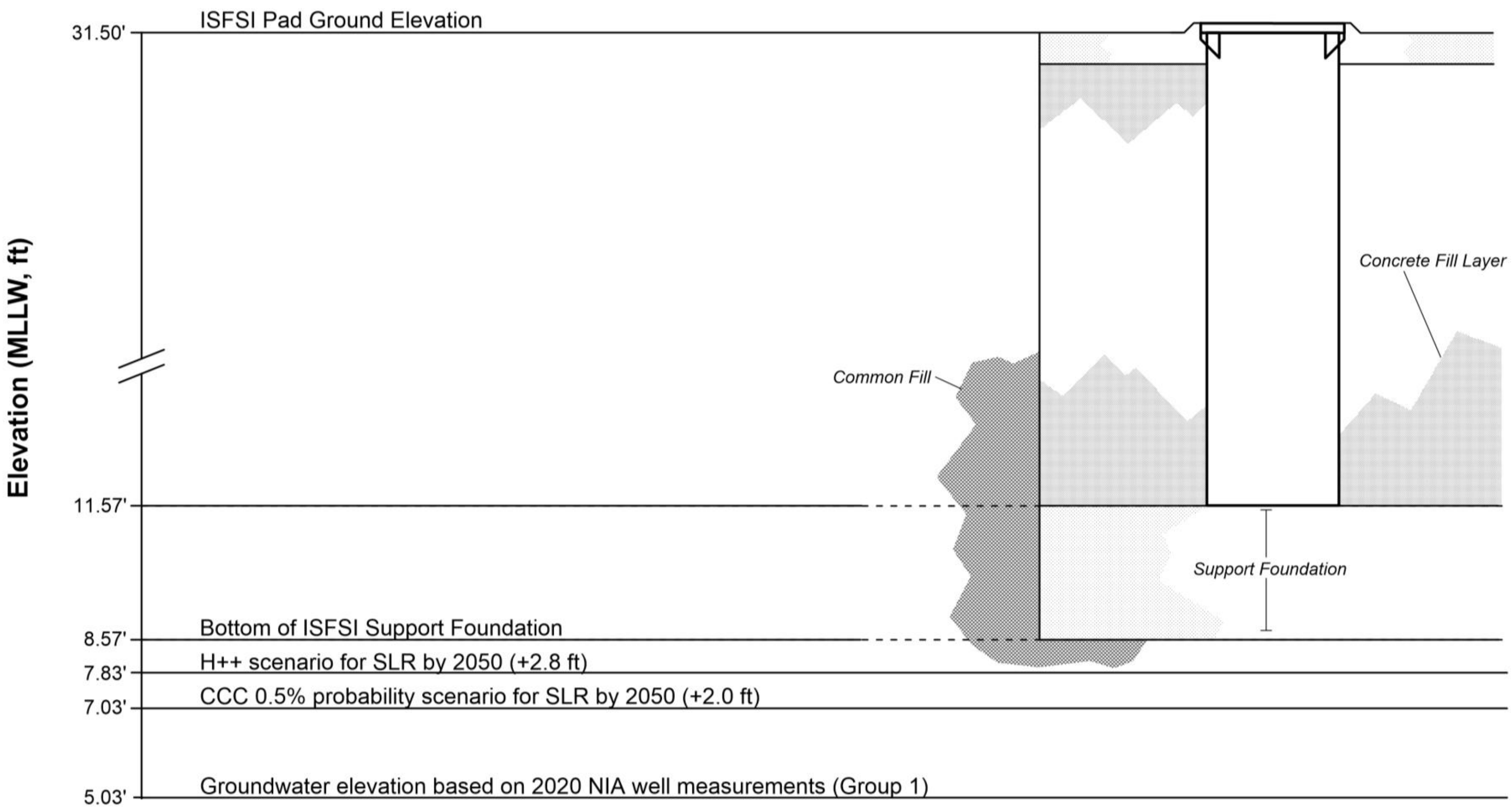

Figure 3-5. Groundwater elevations (MLLW, Epoch 1941-1959) in 2020 and 2050 based on the CCC and H++ SLR projections (OPC, 2018).

4.0 CONCLUSIONS

On average, Group 1 and Group 2 wells, located closer to shoreline, have lower mean groundwater levels that closely match the mean high water level at the ocean (approximately 2.31 ft., NGVD29). Group 3 wells are located at higher elevations and their groundwater elevations are higher than Groups 1 and 2.

Group 1 wells were selected to estimate groundwater elevations underneath the ISFSI pads. Because Group 1 wells are located closest to the ISFSI pads, their mean groundwater elevation provides a good estimate for groundwater elevations at the ISFSI. The OPC has several scenarios for how high sea levels will rise by 2050 (OPC, 2018). As sea levels rise, groundwater levels will increase in about the same value. Therefore, 2 ft. rise in sea level by 2050 correlates to 2 ft. or less rises in groundwater elevation by 2050 at SONGS.

As shown in Figure 3-4, the highest H++ projected groundwater elevation scenario is 5.23 ft., NGVD and rests 0.74 ft. below the Holtec UMAX ISFSI (ISFSI) support foundation in 2050. The medium-high risk aversion CCC scenario has a 0.5% probability of SLR meeting or exceeding a +2 ft. projection; this scenario puts groundwater elevations at SONGS 1.54 ft. below the Holtec UMAX ISFSI support foundation in 2050. It should also be pointed out that the upper surface support foundation is 3 ft. above the bottom surface of the ISFSI support foundation (i.e., the support foundation pad is 3 ft. thick), minimizing any chance that the groundwater will contact the Cavity Enclosure Containers (CECs) in which the spent nuclear fuel is stored.

5.0 REFERENCES

California Coastal Commission, 2015, updated 2018. *California Coastal Commission Sea Level Rise Policy Guidance, Interpretive Guidelines for Addressing Sea Level Rise in Local Coastal Programs and Coastal Development Permits,* California Coastal Commission, San Francisco, CA, 307 pp.

Ocean Protection Council, 2018. *State of California Sea-Level Rise Guidance, 2018 Update*, Sacramento, CA: California Natural Resources Agency, 84 pp. http://www.opc.ca.gov/updating-californias-sea-level-rise-guidance/

APPENDIX A

GROUNDWATER AND TIDAL DATA
2020

Table A-1. SONGS groundwater well and ocean tide elevation data.

Well Group	Well Description	Sample Date	Quarter	Sample Time	Measured Water Depth (ft.)	Ground Surface Elevation (MLLW, ft.)	Groundwater Elevation (MLLW, ft.)	Ground Surface Elevation (NGVD29, ft.)	Groundwater Elevation (NGVD29, ft.)	Ocean Tide Level (MLLW, ft.)*	Ocean Tide Level (NGVD29, ft.)	Tide
Group 1	NIA-1	2-Mar-20	Q1	9:08	8.13	13.791	5.66	11.19	3.06	1.61	-0.68	mean, falling
		6-May-20	Q2	8:55	8.58	13.791	5.21	11.19	2.61	4.90	2.61	spring, rising
		3-Sep-20	Q3	8:25	8.84	13.791	4.95	11.19	2.35	3.29	1.00	mean, rising
		28-Oct-20	Q4	10:24	8.33	13.791	5.46	11.19	2.86	4.14	1.85	mean, falling
	NIA-2	27-Feb-20	Q1	9:16	10.26	15.397	5.14	12.80	2.54	3.72	1.43	mean, rising
		30-Apr-20	Q2	8:41	10.85	15.397	4.55	12.80	1.95	0.88	-1.41	spring, falling
		8-Sep-20	Q3	10:13	9.89	15.397	5.51	12.80	2.91	4.04	1.75	neap, rising
		29-Oct-20	Q4	9:13	9.83	15.397	5.57	12.80	2.97	5.30	3.01	mean, falling
	NIA-3	7-May-20	Q2	8:12	8.92	13.853	4.93	11.25	2.33	3.53	1.24	spring, rising
	NIA-4	14-May-20	Q2	8:27	9.31	14.184	4.87	11.58	2.27	1.28	-1.01	mean, falling
	NIA-5	13-May-20	Q2	8:14	9.91	14.675	4.77	12.08	2.17	0.52	-1.77	mean, falling
	NIA-6	14-May-20	Q2	10:22	9.62	14.189	4.57	11.59	1.97	0.35	-1.95	mean, falling
	NIA-7	13-May-20	Q2	10:04	10.02	14.737	4.72	12.14	2.12	0.13	-2.16	mean, rising
	NIA-10	11-May-20	Q2	10:23	11.26	16.058	4.80	13.46	2.20	1.15	-1.15	mean, rising
	NIA-11	11-May-20	Q2	8:35	11.24	16.056	4.82	13.46	2.22	-0.23	-2.52	mean, rising
Group 2	PA-1	9-Mar-20	Q1	9:40	23.72	28.81	5.09	26.21	2.49	6.49	4.20	spring, falling
		3-Jun-20	Q2	8:38	24.34	28.81	4.47	26.21	1.87	4.22	1.93	mean, falling
		29-Jul-20	Q3	9:00	24.33	28.81	4.48	26.21	1.88	2.82	0.53	neap, falling
		12-Oct-20	Q4	8:31	24.26	28.81	4.55	26.21	1.95	4.21	1.92	mean, falling
	PA-2	9-Mar-20	Q1	13:06	24.89	29.51	4.62	26.91	2.02	2.30	0.01	spring, falling
		3-Jun-20	Q2	11:23	25.67	29.51	3.84	26.91	1.24	2.40	0.11	mean, falling
		29-Jul-20	Q3	11:16	25.92	29.51	3.59	26.91	0.99	2.18	-0.11	mean, rising
		12-Oct-20	Q4	10:54	25.52	29.51	3.99	26.91	1.39	2.96	0.67	mean, falling
	PA-3	20-Mar-20	Q1	10:37	25.48	29.32	3.84	26.72	1.24	3.16	0.87	spring, falling
		10-Jun-20	Q2	8:35	25.20	29.32	4.12	26.72	1.52	-0.19	-2.48	mean, rising
		19-Aug-20	Q3	12:50	25.16	29.32	4.16	26.72	1.56	3.77	1.48	mean, falling
		14-Oct-20	Q4	10:37	25.42	29.32	3.90	26.72	1.30	3.86	1.57	spring, falling
	PA-4	20-Mar-20	Q1	8:18	23.77	28.94	5.17	26.34	2.57	5.11	2.82	spring, falling
		11-Jun-20	Q2	8:36	26.36	28.94	2.58	26.34	-0.02	0.09	-2.20	mean, falling
		20-Aug-20	Q3	8:46	25.12	28.94	3.82	26.34	1.22	3.51	1.22	spring, rising
		15-Oct-20	Q4	8:27	23.62	28.94	5.32	26.34	2.72	5.85	3.56	spring, rising

* = Tidal Datum Epoch (1983-2001)

Table A-1 (cont). SONGS groundwater well and ocean tide elevation data.

Well Group	Well Description	Sample Date	Quarter	Sample Time	Measured Water Depth (ft.)	Ground Surface Elevation (MLLW, ft.)	Groundwater Elevation (MLLW, ft.)	Ground Surface Elevation (NGVD29, ft.)	Groundwater Elevation (NGVD29, ft.)	Ocean Tide Level (MLLW, ft.)*	Ocean Tide Level (NGVD29, ft.)	Tide
Group 3	OCA-1	13-Feb-20	Q1	9:03	41.38	47.69	6.31	45.09	3.71	2.99	0.70	mean, rising
		29-Apr-20	Q2	8:48	41.47	47.69	6.22	45.09	3.62	0.40	-1.89	spring, falling
		2-Sep-20	Q3	9:29	41.03	47.69	6.66	45.09	4.06	4.52	2.23	mean, rising
		4-Nov-20	Q4	14:27	41.12	47.69	6.57	45.09	3.97	2.35	0.06	mean, falling
	OCA-2	10-Feb-20	Q1	11:40	109.77	116.39	6.62	113.79	4.02	5.10	2.81	spring, falling
		27-Apr-20	Q2	9:53	110.36	116.39	6.03	113.79	3.43	1.31	-0.99	spring, rising
		31-Aug-20	Q3	11:37	109.75	116.39	6.64	113.79	4.04	3.75	1.46	mean, falling
		26-Oct-20	Q4	10:18	109.74	116.39	6.65	113.79	4.05	3.53	1.24	mean, falling
	OCA-3	6-Feb-20	Q1	10:55	100.16	105.7	5.54	103.10	2.94	1.78	-0.51	spring, falling
		23-Apr-20	Q2	8:38	100.99	105.7	4.71	103.10	2.11	3.18	0.89	spring, rising
		24-Aug-20	Q3	10:20	100.60	105.7	5.10	103.10	2.50	3.26	0.97	mean, rising
		22-Oct-20	Q4	10:00	100.18	105.7	5.52	103.10	2.92	3.95	1.66	neap, rising

* = Tidal Datum Epoch (1983-2001)